

Biomedical engineering in the reconstruction of the cardiovascular and skeletal systems

Roman Major

r.major@imim.pl

Institute of Metallurgy and Materials Science, Reymonta 24, 30-059 Krakow, Poland

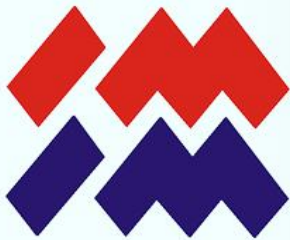


<https://www.youtube.com/watch?v=QONVYTPjZbI>



Topics

- 1.) Eugenika i jej wpływ na losy świata
- 2.) Ewolucja mechanicznych zastawek serca
- 3.) Odpowiedź na pytanie „co było pierwsze jajko czy kura?”
- 4.) Wytyczne etyki w poborze narządów
- 5.) Rozwój anestezji w historii medycyny i problem korozji implantów.
- 6.) Holograficzne techniki obrazowania w medycynie

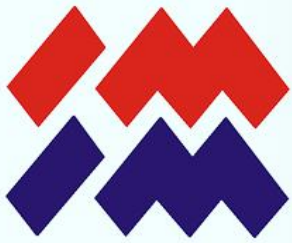


Biomaterial is any substance other than the drug either a combination of natural or synthetic substances, which can be used in any period, and which task is to supplement or replacement of organ tissues or parts or fulfill their function.

[European Society for Biomaterials]

Biocompatibility is the ability to properly preserve the material in contact with the tissue in a particular application

[\[Biomaterials Science An Introduction to Materials in Medicine-
ELSEVIER 2004 Academic Press\]](#)



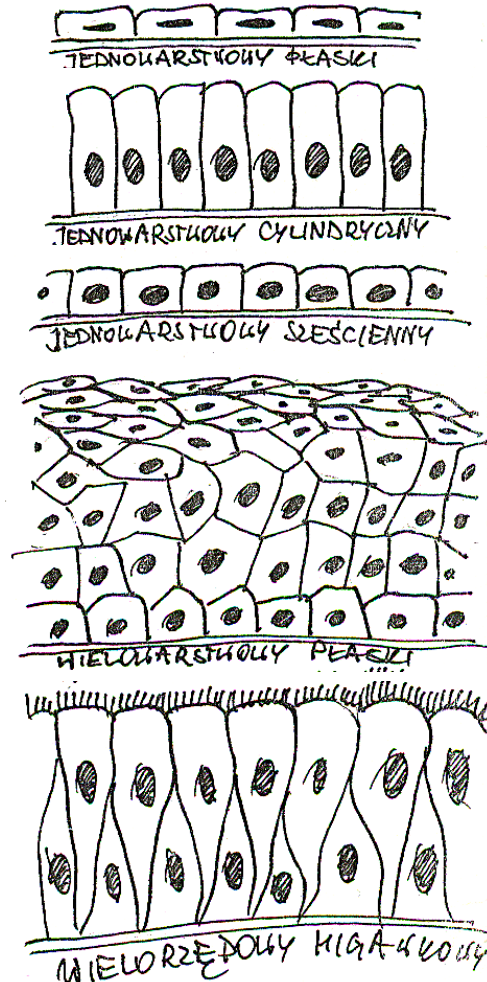
Part 1

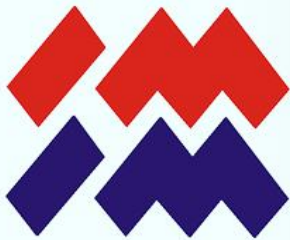
Introduction to the human anatomy

Types of human tissue

Tissue

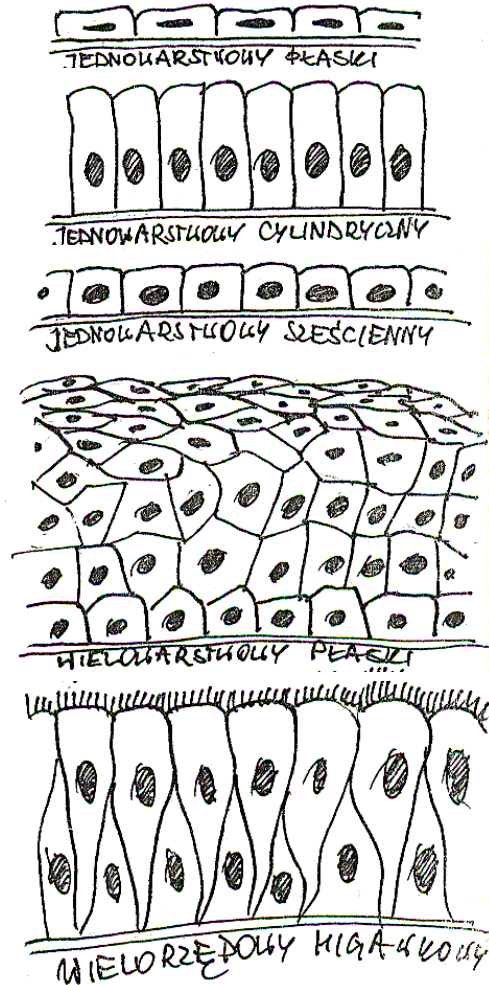
- Epithelial (Nabłonkowa)
- Connective (Łączna)
- Muscular (mięśniowa)
- Nervous (nerwowa)

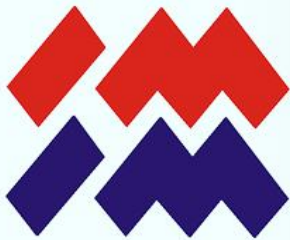




Epithelial tissue

Functions:
protective-cover
resorption
secretory
barrier
sensual





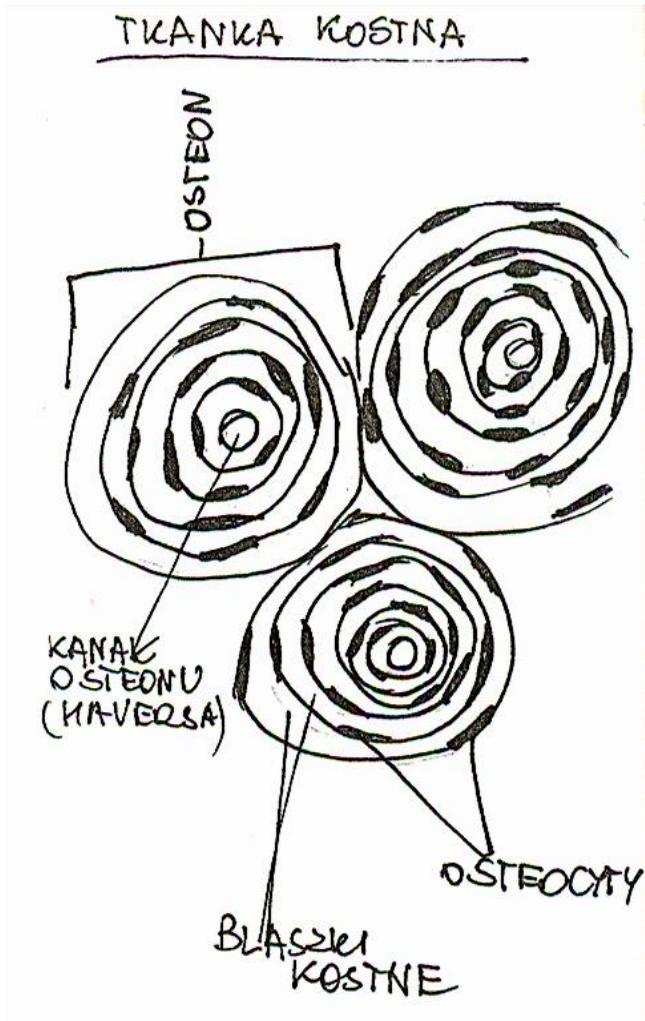
Connective tissue

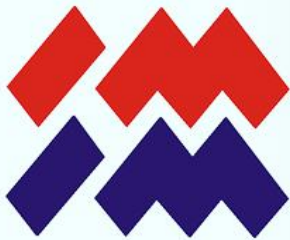
Epithelial (Nabłonkowa)

→ Connective (Łączna)

Muscular (mięśniowa)

Nervous (nerwowa)

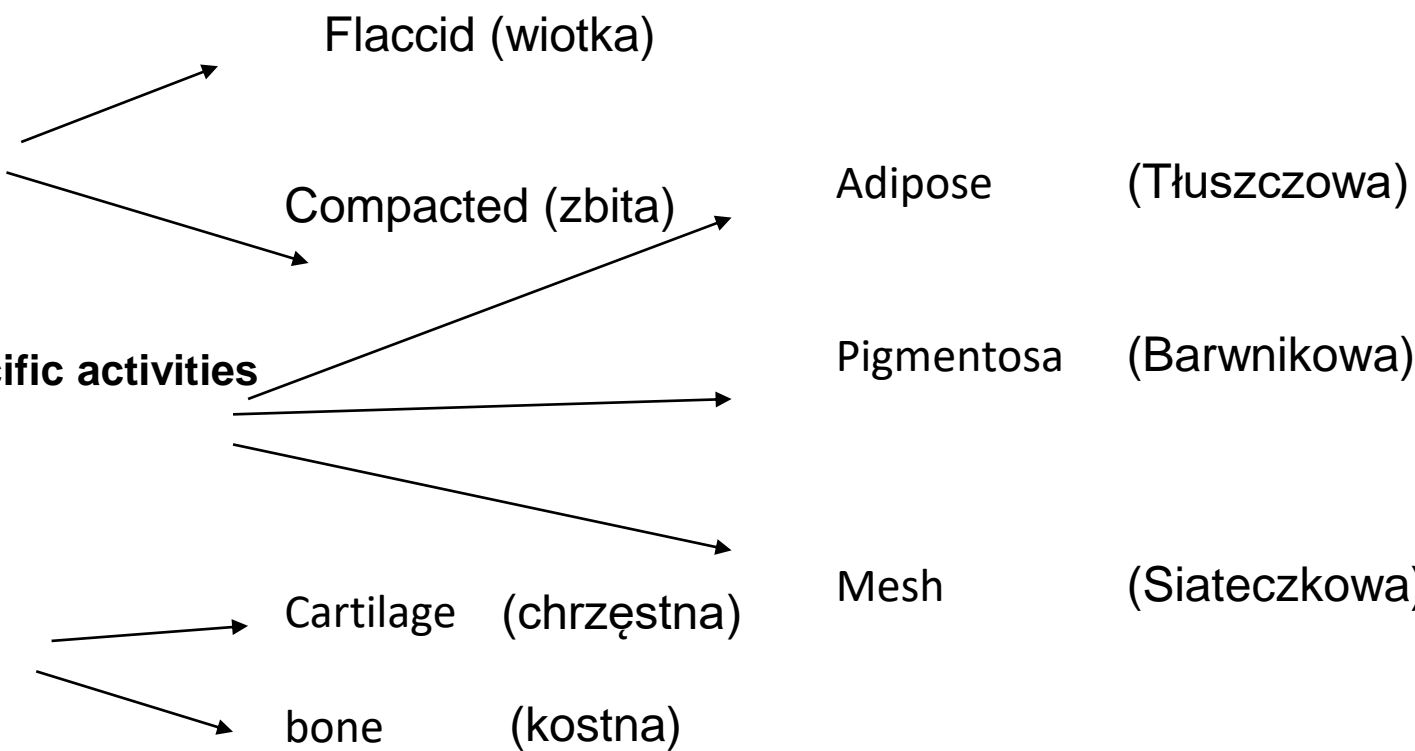




Connective tissue

Types:

-Connective



-Skeletal

Tissue

Epithelial (Nabłonkowa)

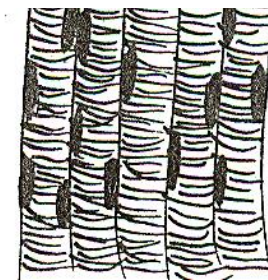
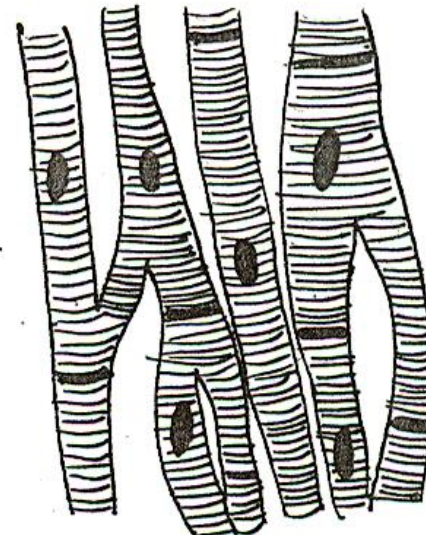
Connective (Łączna)

→ Muscular (mięśniowa)

Nervous (nerwowa)

MIESNIÓWKA CIĄDCA

MIESIĘ SERCOWY



Tissue

Epithelial (Nabłonkowa)

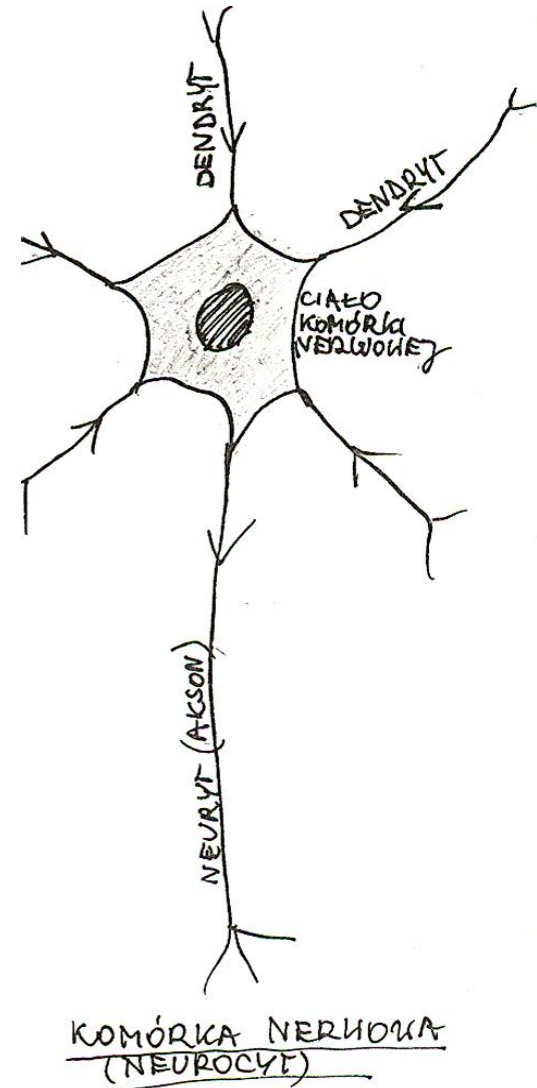
Connective (Łączna)

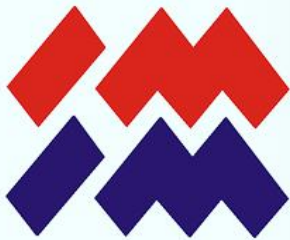
Muscular (mięśniowa)

→ Nervous (nerwowa)

Action potentials (MOV)

Neuron

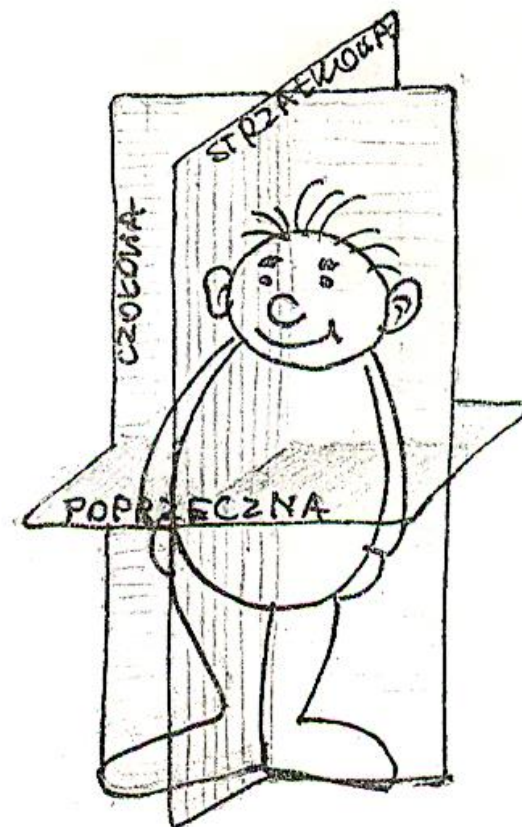


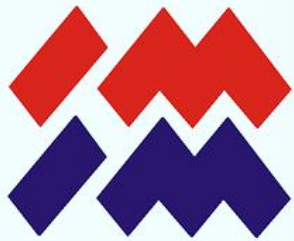


Organ systems

Kostno- stawowy
Mięśniowy
Naczyniowy
Pokarmowy
Oddechowy
Moczowy
Płciowy
Nerwowy
Powłoka wspólna

Główne osie i płaszczyzny ciała





Part 2

Introduction to the human anatomy

Cardiovascular system



Cardiovascular system

Heart (cor)

Naczynia krwionośne Blood vessels

Tętnice krażenia dużego

Large circulation arteries

Żły krażenia dużego

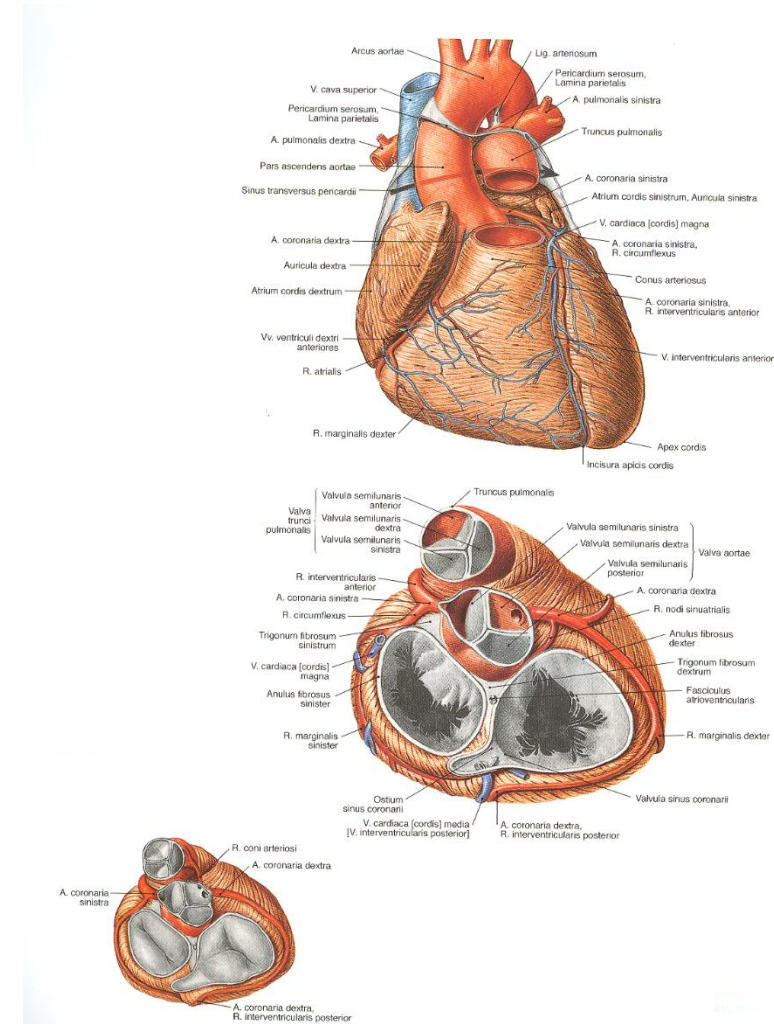
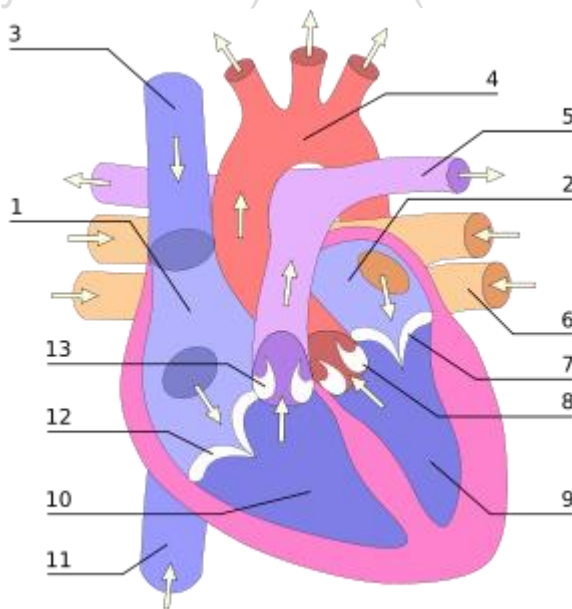
Veins of the large circulation

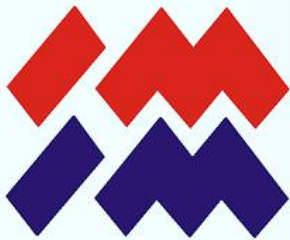
Naczynia chłonne

Lymph vessels

Krażenie małe
(czynnościowe)

Small circulation
(functional)





Cardiovascular system

Heart (cor)

Naczynia krwionośne Blood vessels

Tętnice krażenia dużego

Large circulation arteries

Żły krażenia dużego

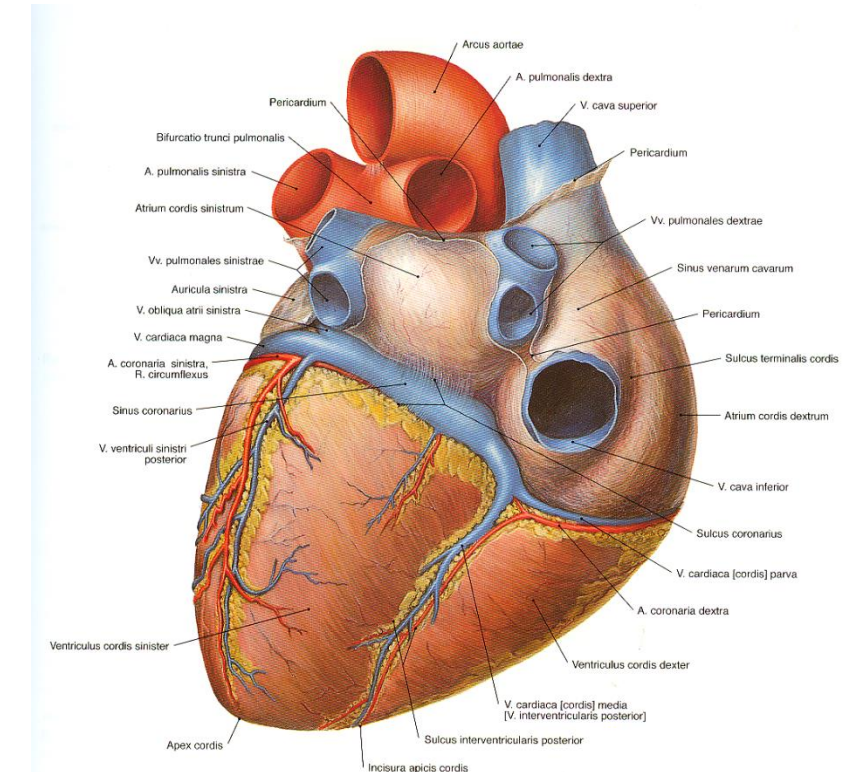
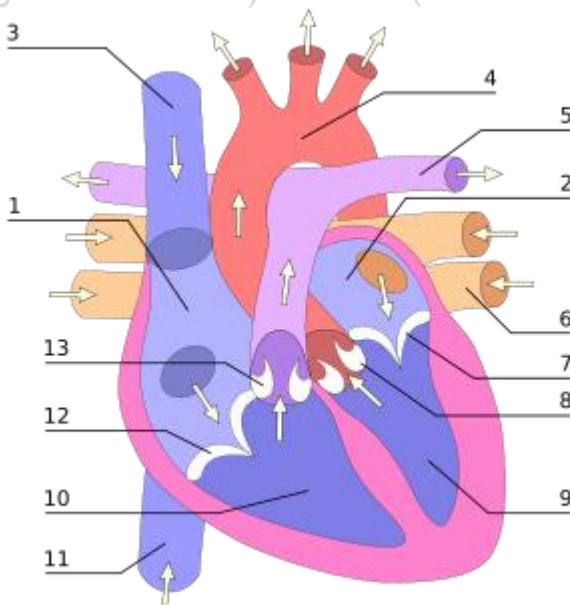
Veins of the large circulation

Naczynia chłonne

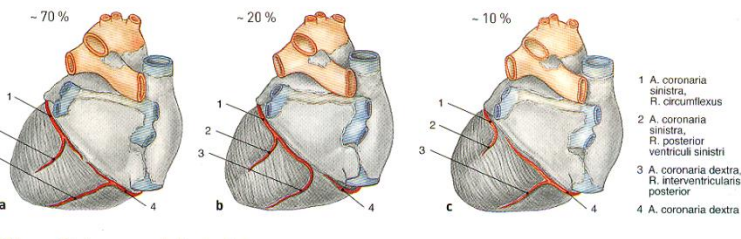
Lymph vessels

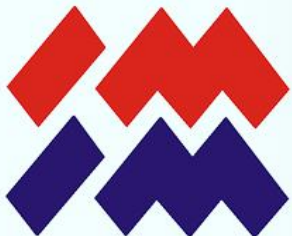
Krażenie małe
(czynnościowe)

Small circulation
(functional)



Ryc. 894 Żły serca, vv. cordis.





Cardiovascular system

Naczynia krwionośne Blood vessels

Tętnice krążenia dużego

Large circulation arteries

Żły krążenia dużego

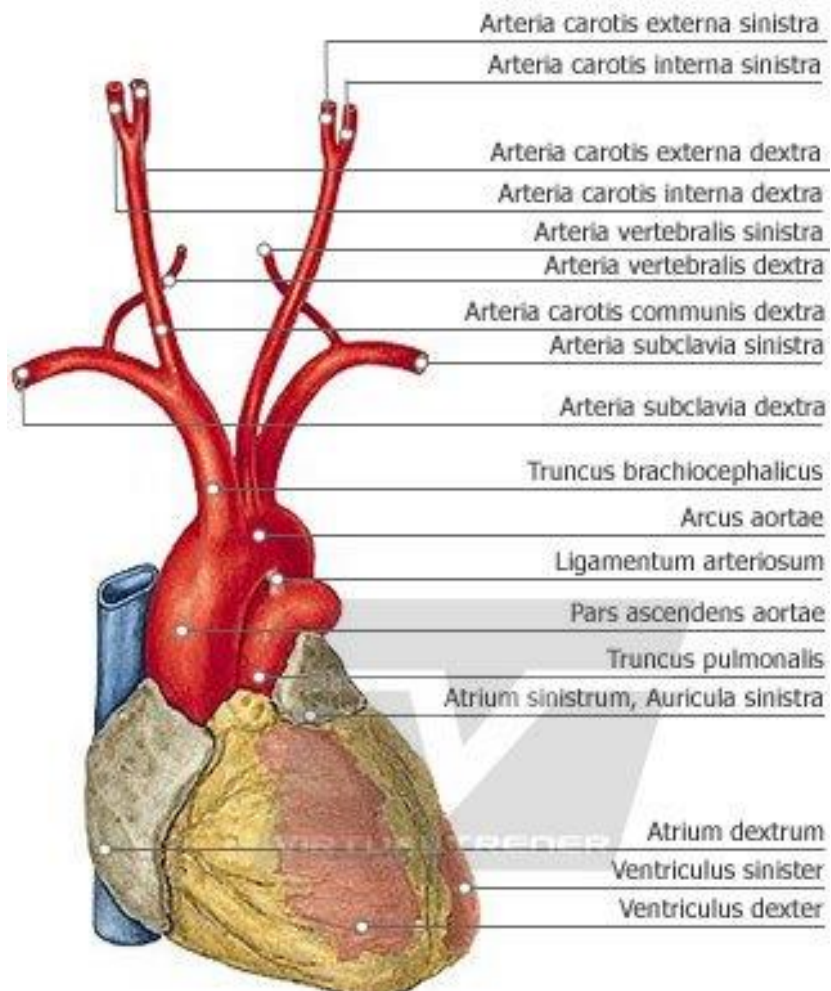
Veins of the large circulation

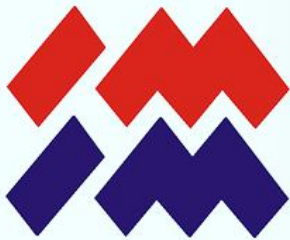
Naczynia chłonne

Krążenie małe
(czynnościowe)

Lymph vessels

Small circulation
(functional)





Biomaterials

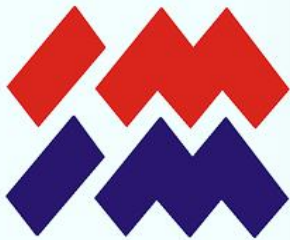
Polymers

Metals

Ceramic (carbides, ceramic glass and glass)

Natural materials (greens and animal)

Composite materials (silica reinforced silicone rubber, carbon fibers,
hydroxyapatite particle- reinforced poly (lactic acid))



Dedicated materials

Biodegradable polymers

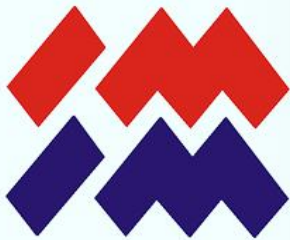
Bioactive ceramics

Celuloze

Pyrolityc carbon

Modified materials, surfaces preventing clots

Natural tissues and polymers combined with living cells



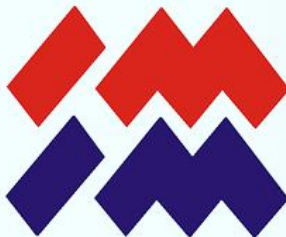
Implant- definition

Implant- wszelkie przyrządy medyczne wykonywane z jednego lub więcej Biomateriałów, które mogą być umieszczone wewnętrz organizmu, jak również częściowo lub całkowicie pod powierzchnią nabłonka i które mogą pozostać przez dłuższy okres w organizmie

Implant chirurgiczny- używany jest w kontekście umieszczenia go w zamierzonym miejscu w procedurze chirurgicznej. Istnieją także implanty wprowadzane innym sposobem. Do nich zalicza się igły, dreny, saczki itp.

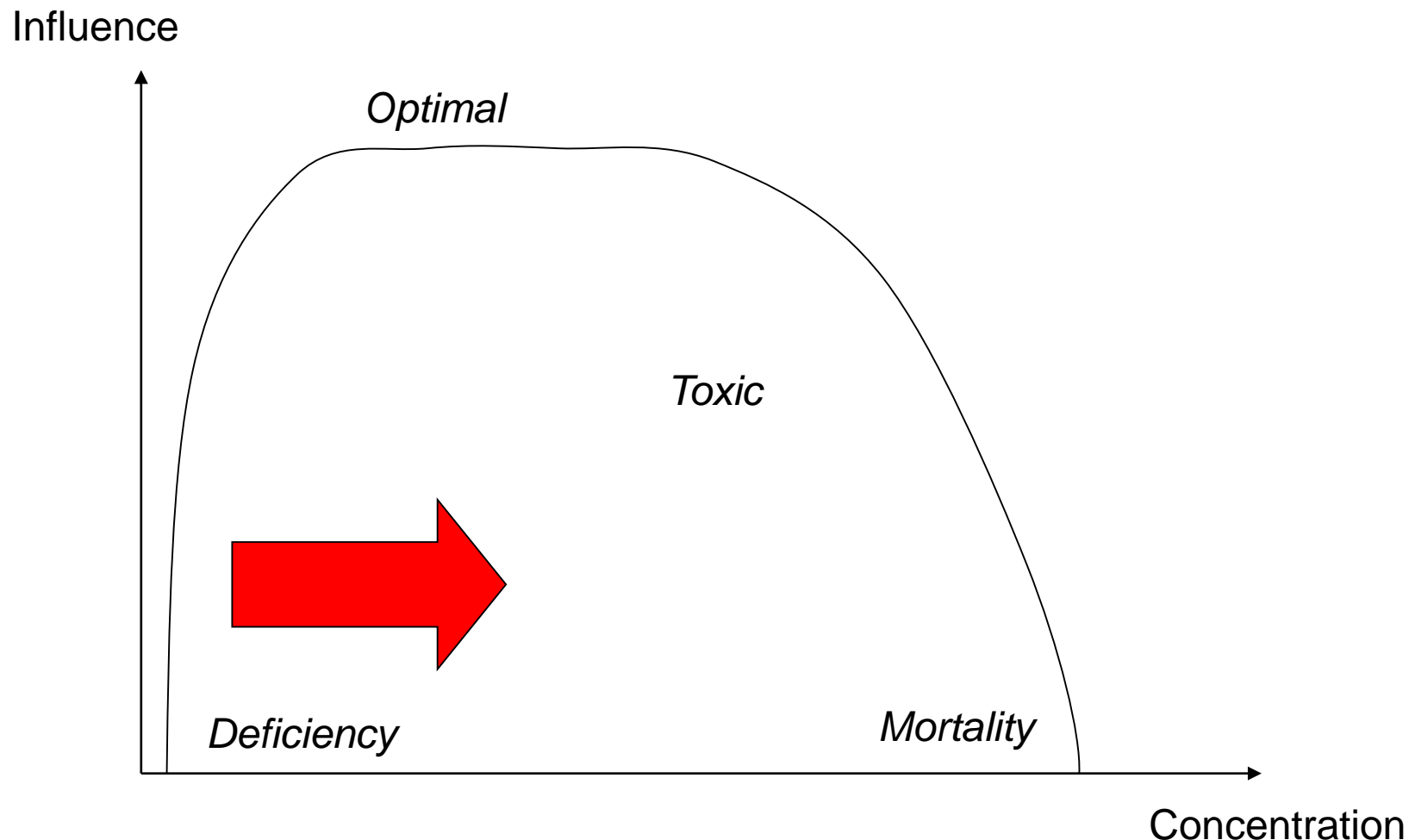
Proteza implantowa- (proteza wewnętrzna lub endoproteza)- przyrząd, który fizycznie zastępuje organ lub tkankę. W odróżnieniu, bioproteza stanowi implantowaną protezę wykonaną w całości lub częściowo z tkanek dawcy

Sztuczny organ- materiał medyczny, który zastępuje w całości lub częściowo funkcje jednego z głównych organów ciała. Sztuczne organy zastępują funkcje organów chorych, częściowo w nieanatomiczny sposób



Implant- influence

Implants- the concentration of elements influence on the reactions of vital processes





Mo:

Deficiency

- tooth brush
- bone crumbling
- disorders in the functioning of the gonads

Excess

- difference of enzyme diffusion through cell membranes
- allergic reactions

Me: biochemical reactions and conversion of vitamin C

Deficiency

- disturbances in the development of bones and genital organs

Excess

- respiratory tract irritation and pneumonia
- OSN

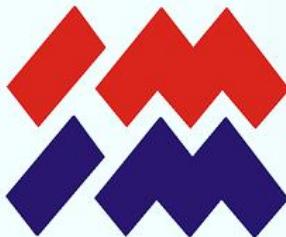
Ti: in the spleen, liver and kidneys

Deficiency

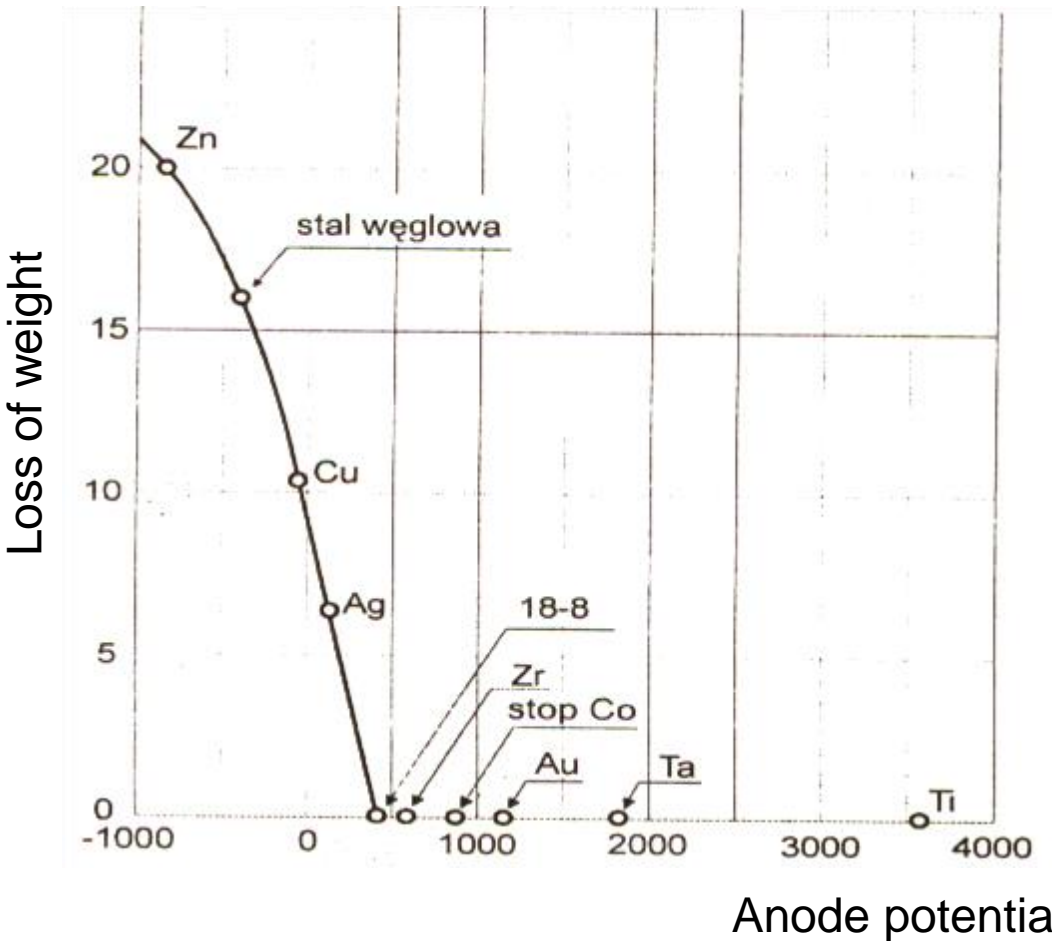
-inert

Excess

- allergy or peri-implant reaction in inter-implantology as evidenced by the presence of macrophages and T-lymphocytes



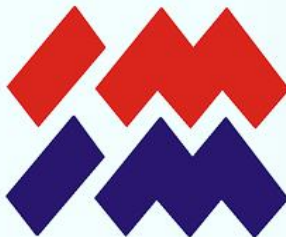
Implants- corrosion



Division of corrosive reactions

- quiet
- acute
- discreet

[Frank E., Zitter H.: Metallische Implantate in der Knochenchirurgie. Wien-New York, Springer Verlag 1977]
[Clarke E. G. C., Hickman J.: J. Bone Jt. Surg. 35-A, 1953]



Implants- layers

- AIM**
- **Biofunction (friction resistance)**
 - **Diffusion barriers (increase of corrosion resistance)**
 - **Improvement of osseointegration (ceramic bioactive layers)**

Types

- diffusion layers of titanium compounds
- diamond layers (NCD, DLC)
- hydroxyapatite coatings
- composite layers - new

Deposition methods

- methods using plasma, photons, ions:
- PDT processes - Plasma Diffusion Treatment
- RFCVD - Radio Frequency Chemical Vapor Deposition
- MWCVD - Microwave CVD
- PLD - Pulsed Laser Deposition
- the sol-gel method



Part 2.1

Executed projects

Cardiovascular system



Heart support

„My great desire to create a Polish Artificial Heart finally fully fulfills...”

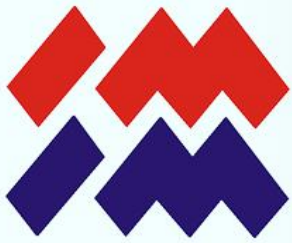
prof. Zbigniew Religa

„POLISH ARTIFICIAL HEART” Medicine

Modern technology



https://www.youtube.com/watch?v=7QFhxfVF7SA&list=PLMkpKh2ylbEa9OThOL0F6vQC_aKmHvgs8



„Moje wielkie pragnienie stworzenia polskiego sztucznego serca nareszcie w pełni się urzeczywistnia. Usilne starania o otoczenie tego przedsięwzięcia opieką państwa, uwieńczone uchwaleniem Wieloletniego Programu "Polskie Sztuczne Serce", uważam za ogromny sukces. Bardzo się z tego cieszę iżyczę powodzenia wszystkim, którzy zaangażowani są w realizację prac".

https://www.youtube.com/watch?v=71_E3Hh2Jqg

prof. Zbigniew Religa



Heart support

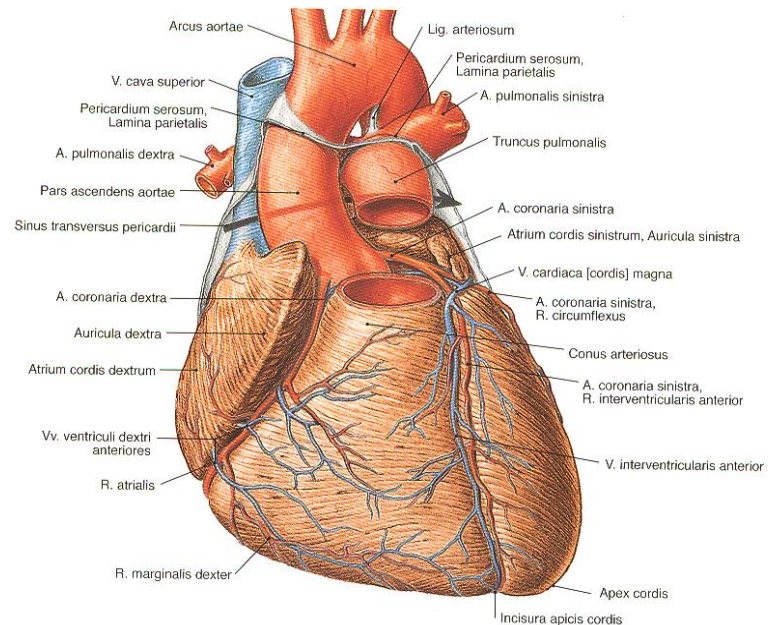
DIVISION BY SUPPORT TIME

Short-term

- An acute heart failure with a good prognosis of regeneration
- An infirmity with an uncertain prognosis for further treatment

Permanent support

- chronic heart failure disqualifying for transplantation
- cardiomyopathy

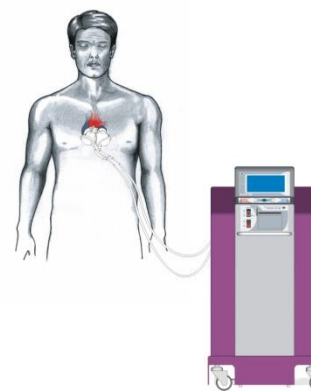
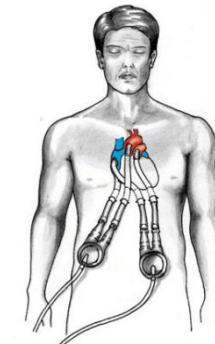




Heart support

DIVISION BY TYPE OF FAILURE

- Acute failure
- Long-term failure
- Patients with cardiomyopathy





Heart support

More than 40 teams from 35 scientific and research institutions, clinical centers and professional entities producing elements of heart prostheses participated in the implementation of the Program.

As part of 5 projects, 17 research tasks and 12 implementation tasks, covering over 200 stages, were implemented.

I STRATEGIC GOAL

Developed families of Polish heart prostheses, with a completely implantable permanent heart prosthesis as a final element

II STRATEGIC GOAL

Clinical development of the use of Polish heart prostheses in the treatment of patients with critical heart failure

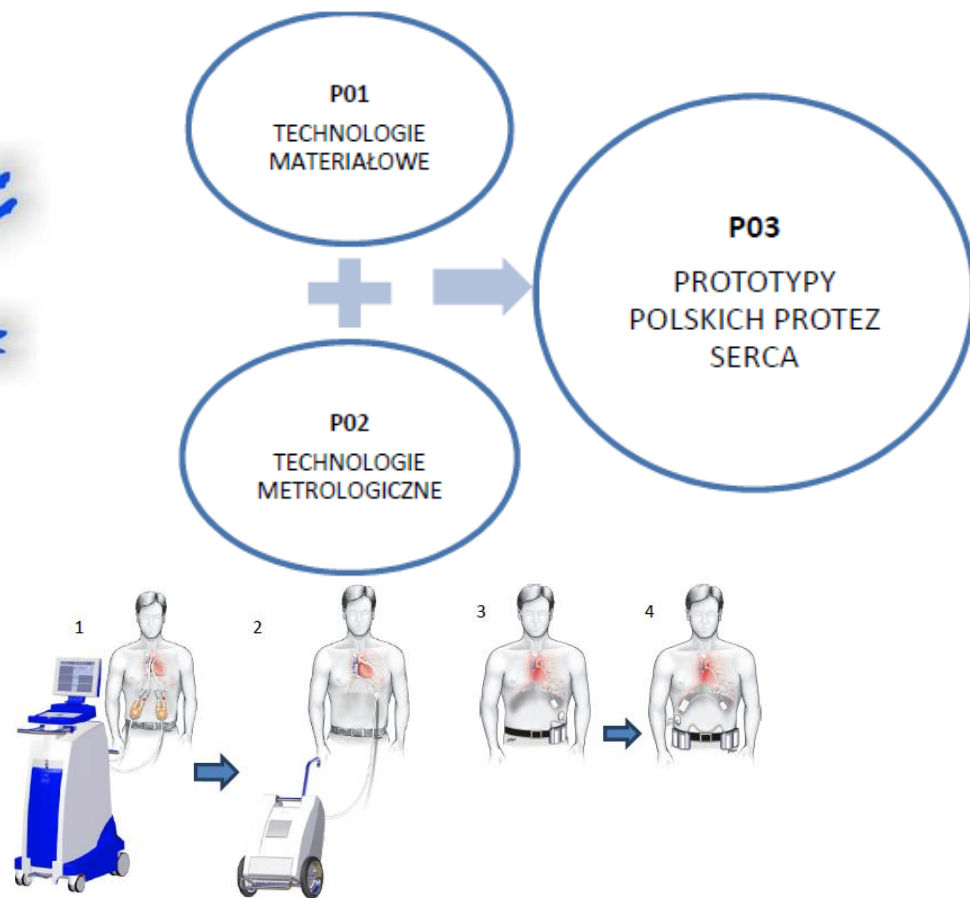
III STRATEGIC GOAL

Creation of a highly specialized scientific and technological platform for the purpose of conducting comprehensive research and development in the field of heart prostheses



Heart support

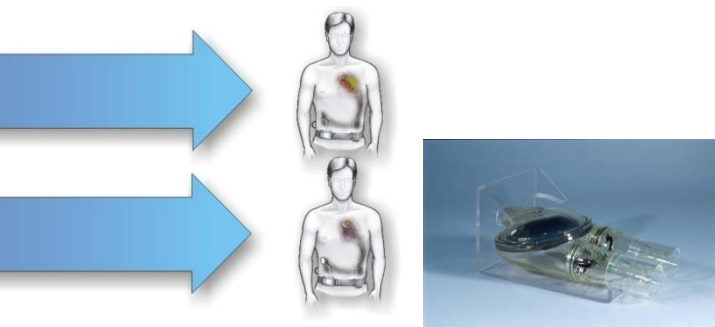
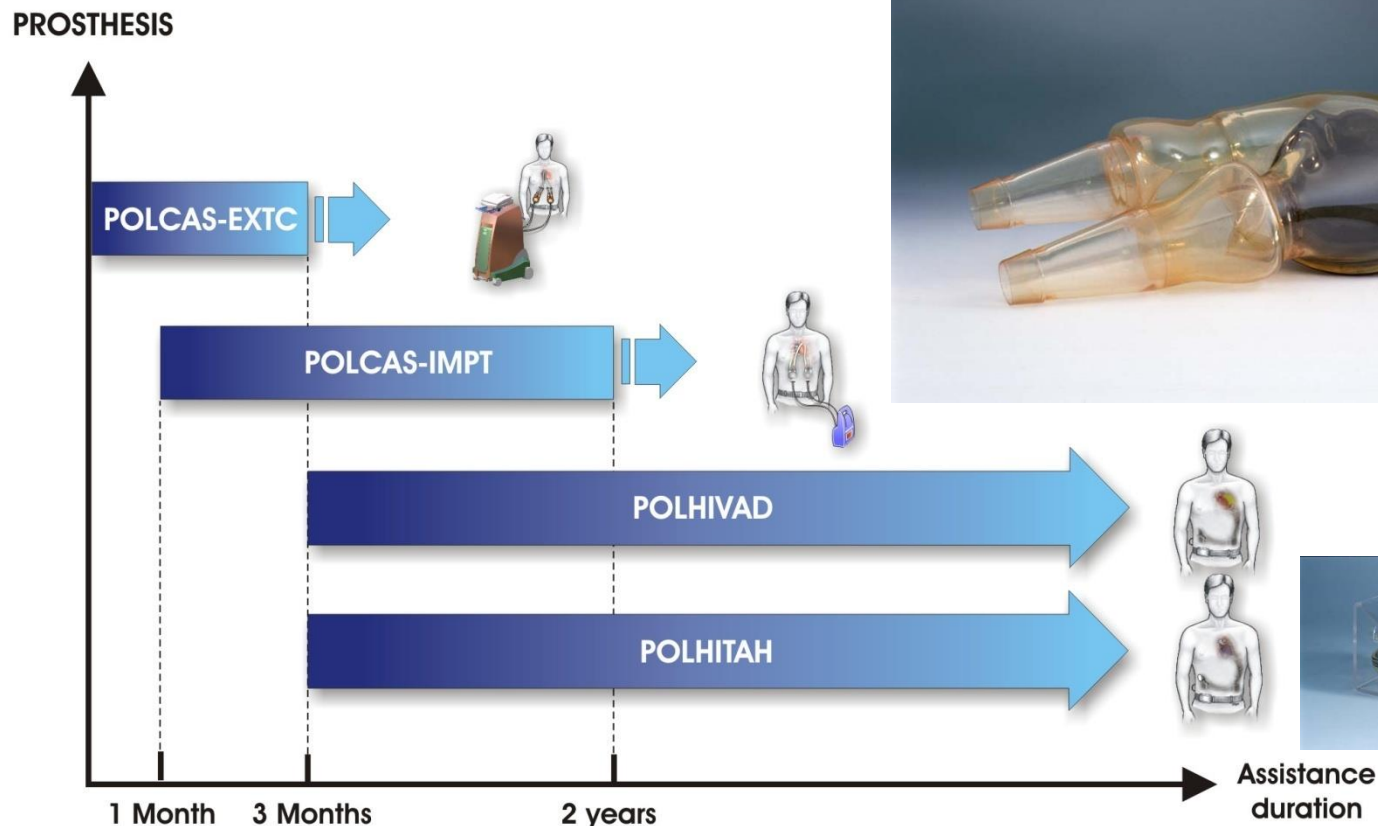
Effects of the program





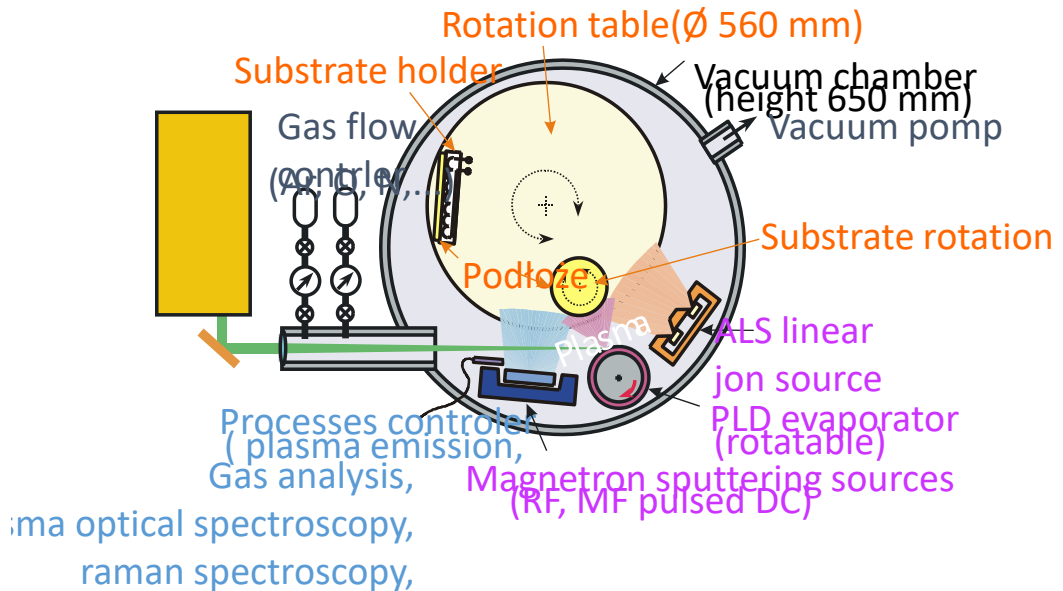
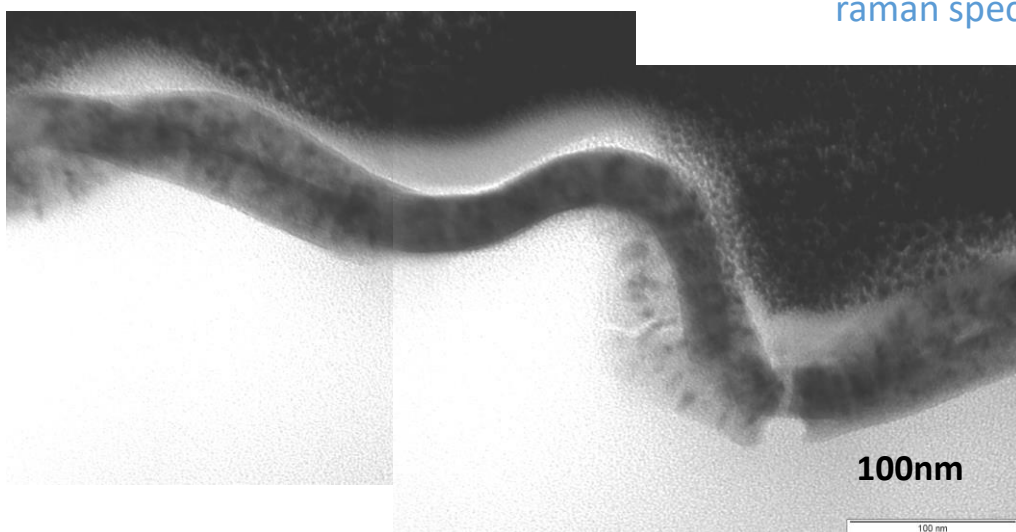
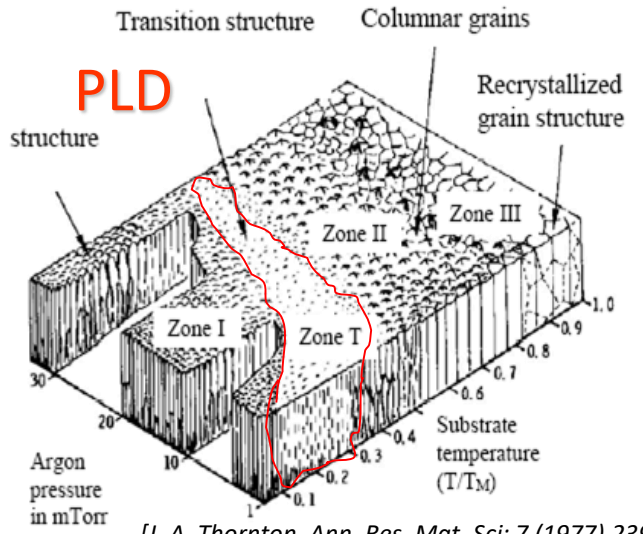
Heart support

System POLVAD





Heart support



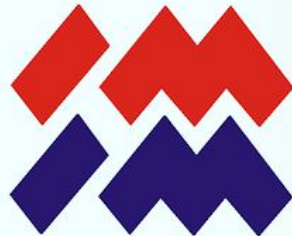
Main assumptions

Good adhesion

Biocompatibility

Lack of substrate degradation

TiN, TiO, Si-DLC, Ti(C,N), DLC

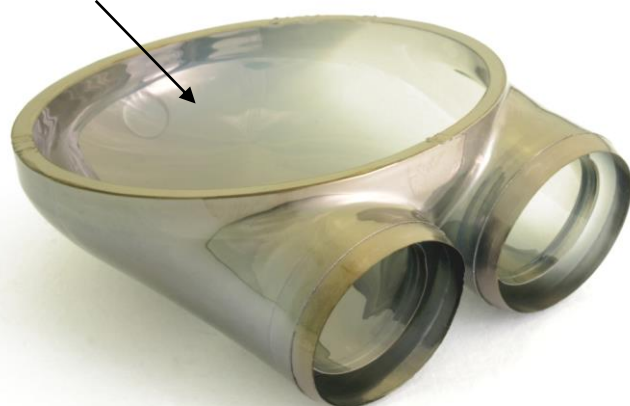


Heart support

Membrane



Chamber



The goal of the work is the reduction of life-threatening thrombo-emboli formation in heart assist systems by a new material design

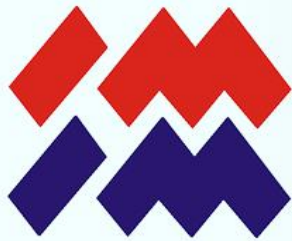
Valve



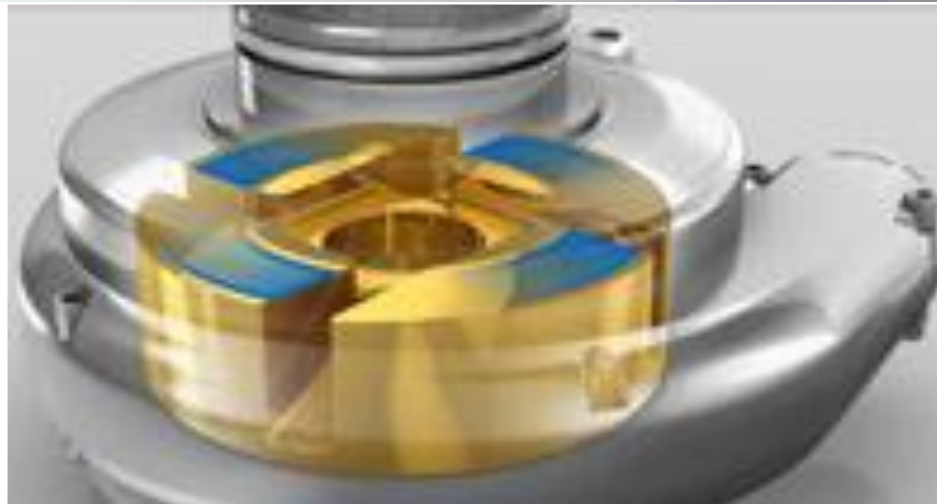


Heart support





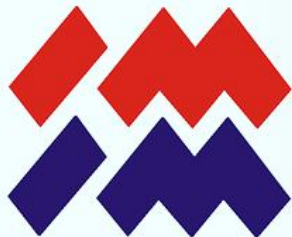
Heart support



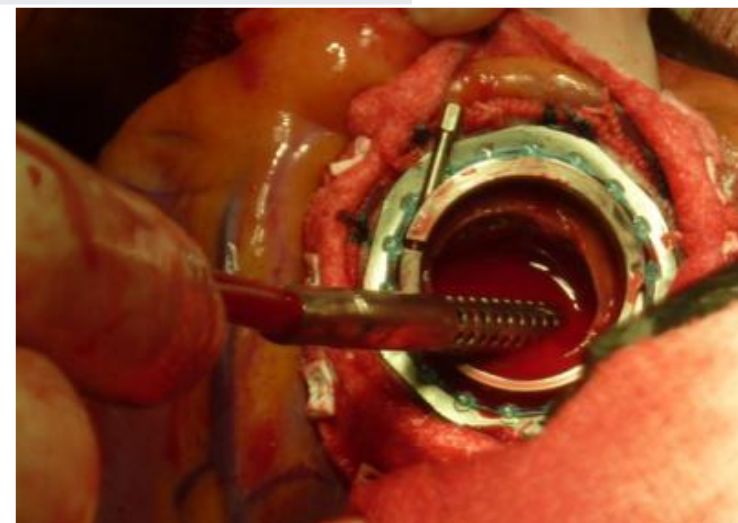
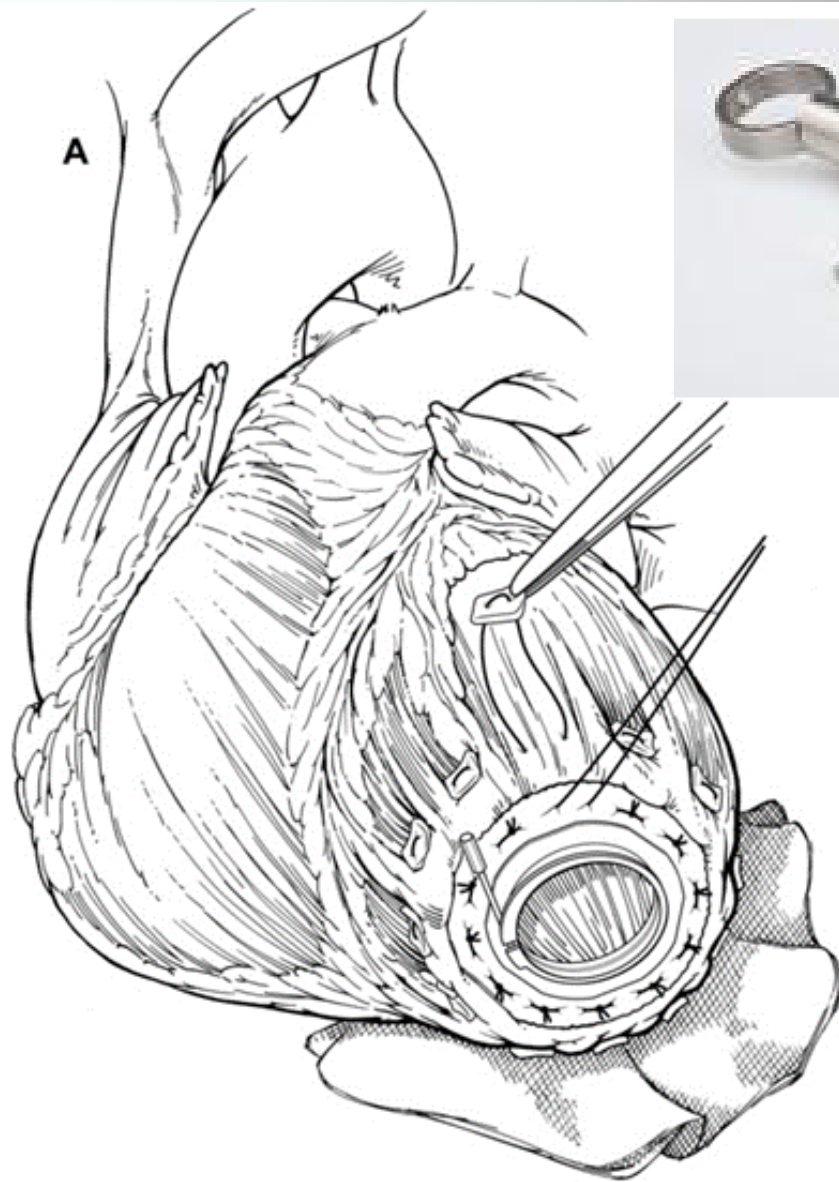


Heart support



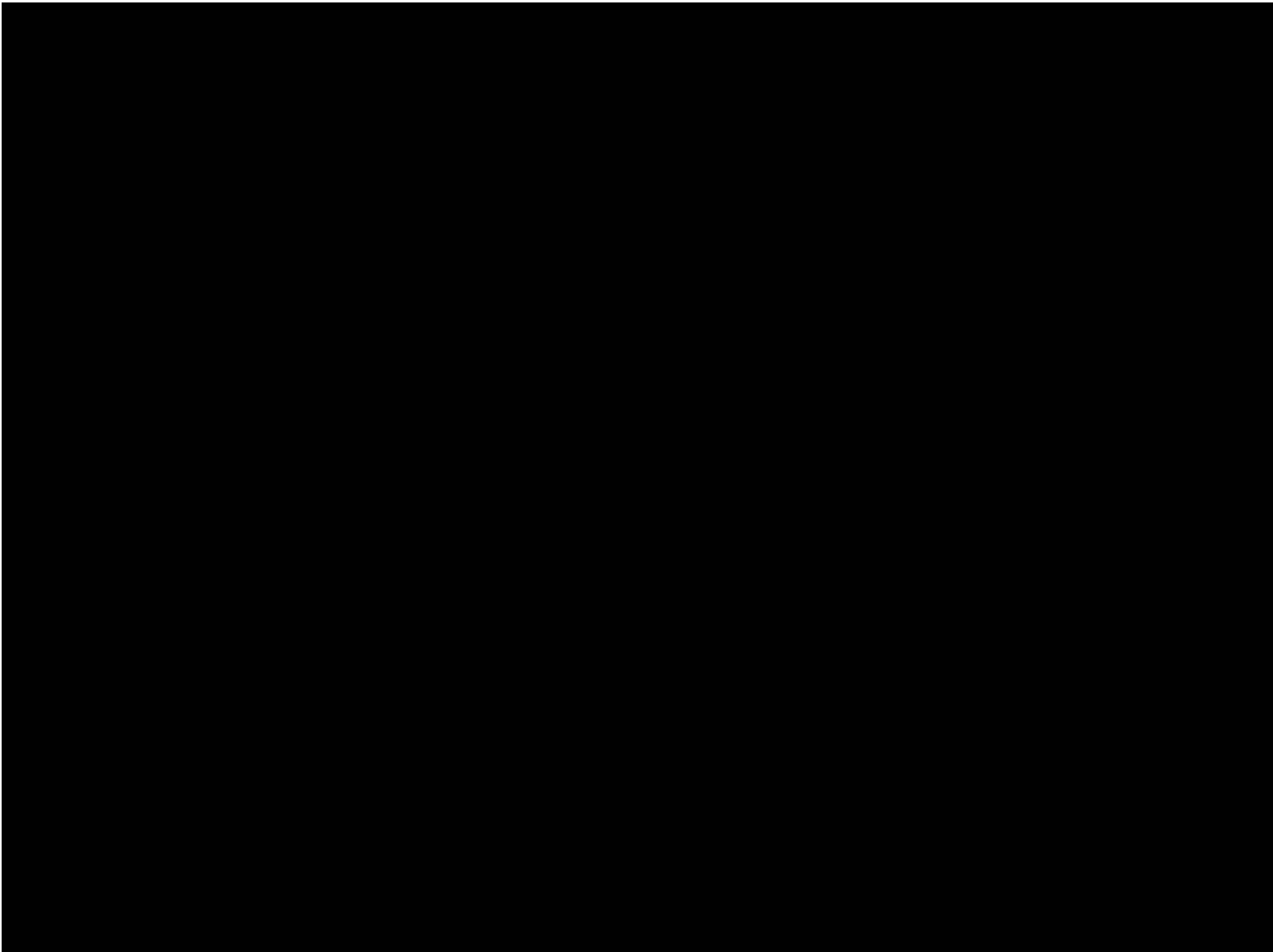


Heart support





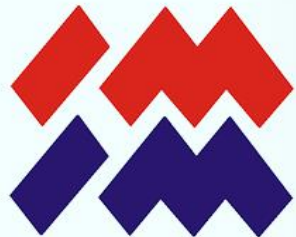
Heart support





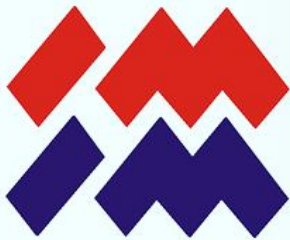
Material engineering mission in regenerative cardiac surgery





- Confokal Modul LSM 5 Exciter, two canals, RGB
- Laser HeNe 633nm 5mW
- Laser HeNe 543nm 1mW
- Laser argon 458/488/514nm, 25mW
- Laser diodowy V 405nm
- Main Beam Splitter turret PASCAL
- Software ZEN 2008 LSM 5 EXCITER
- Light division system (405, 458, 488, 514, 543 nm)
- Filtr BP 505-530
- Filtr BP 505-600
- Filtr BP 530-600
- Filtr BP 560-615
- Filtr LP 420
- Filtr BP 420-480
- System ECU LSM 5 EXCITER
- Moduł DIC I/0,9 z polaryzatorem
- Transmited light detector T-PMT LSM 710





Polish Artificial Heart



Nishe like structure

2014/13/B/ST8/04287
NCN



Silent heart mechanical valve

M-ERA.NET

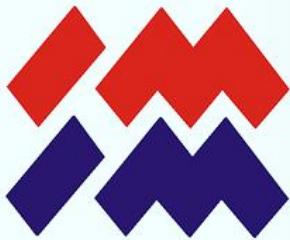
Nonthrombogenic metal-polymer composites with adaptable micro and macro flexibility for next generation heart valves in artificial heart devices

Tissue precursor

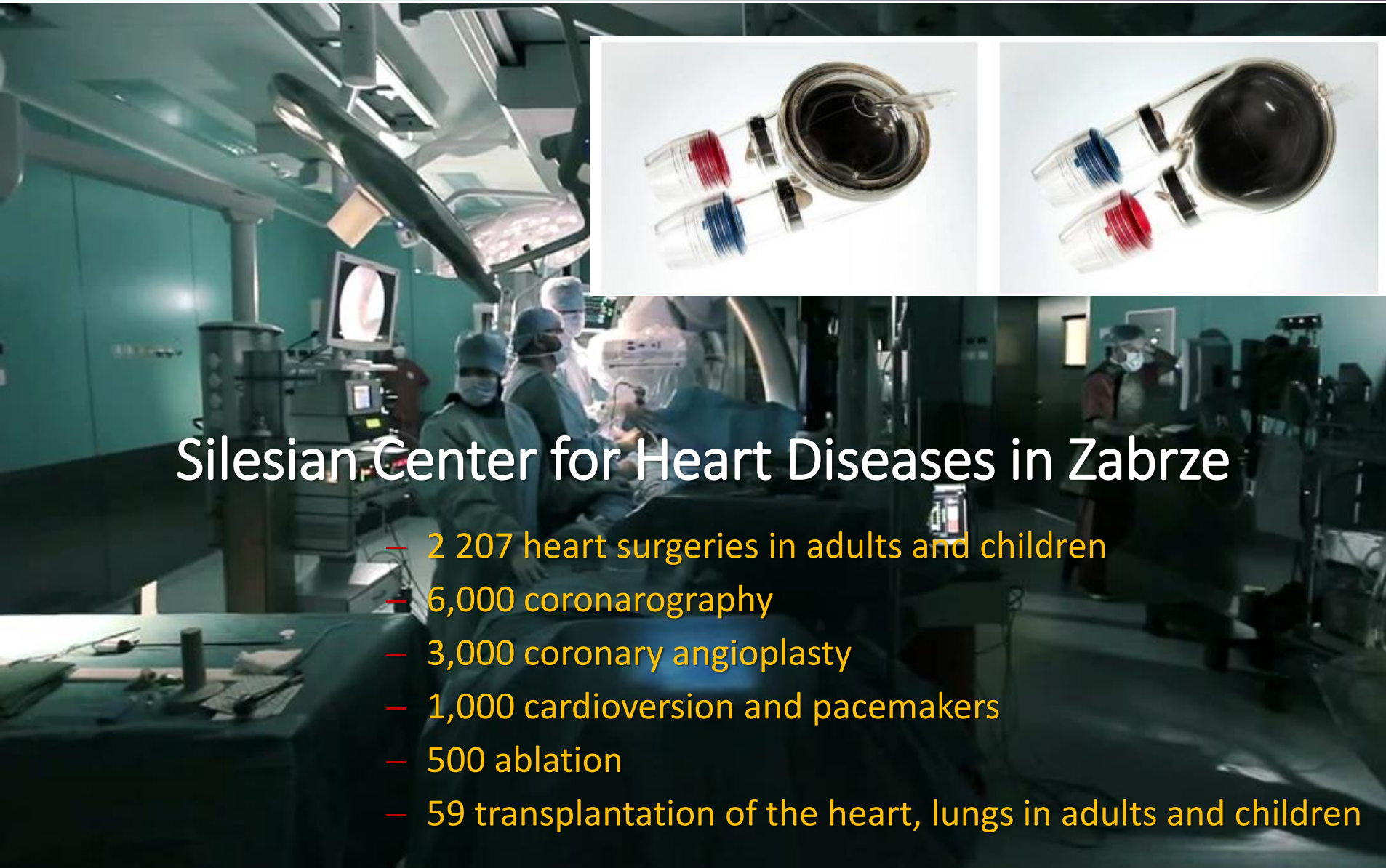
2011/03/D/ST8/04103
NCN

Bioactive heart valve

Program for Applied
Research, Medical and
Pharmaceutical Science



Deplanted chambers

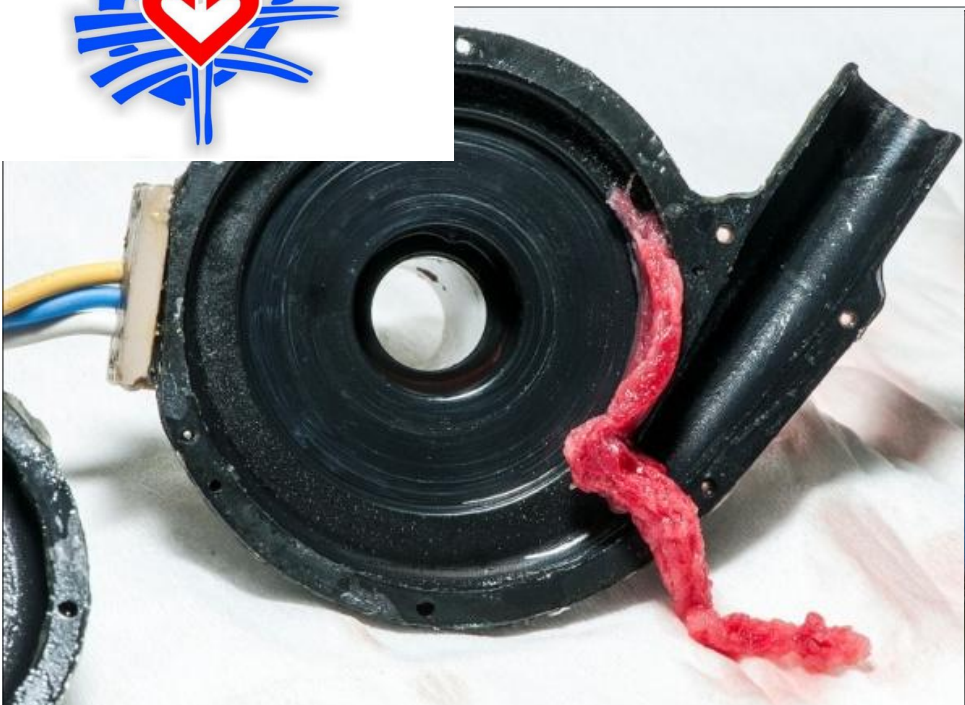


Silesian Center for Heart Diseases in Zabrze

- 2 207 heart surgeries in adults and children
- 6,000 coronary angiography
- 3,000 coronary angioplasty
- 1,000 cardioversion and pacemakers
- 500 ablation
- 59 transplantation of the heart, lungs in adults and children

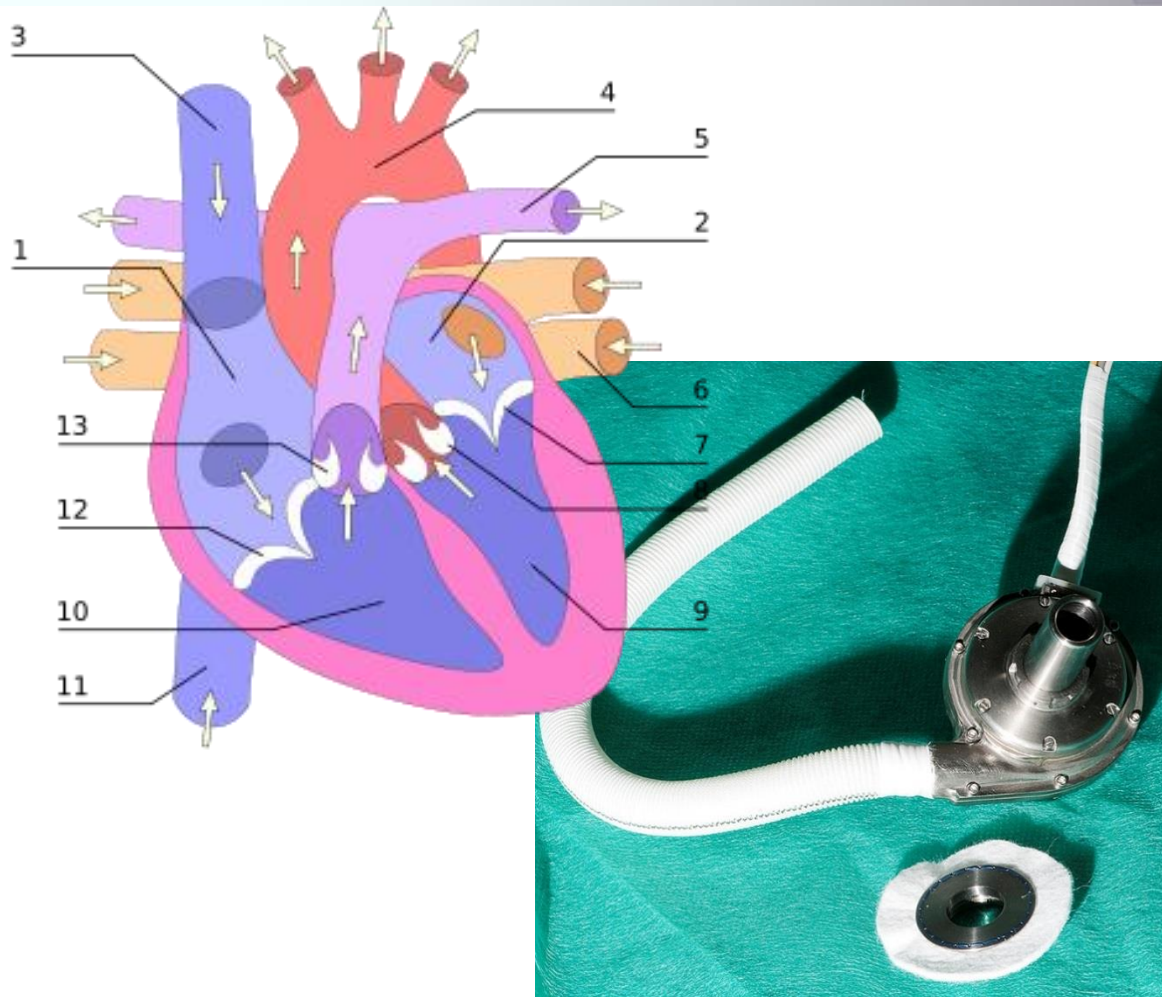


Deplanted chambers



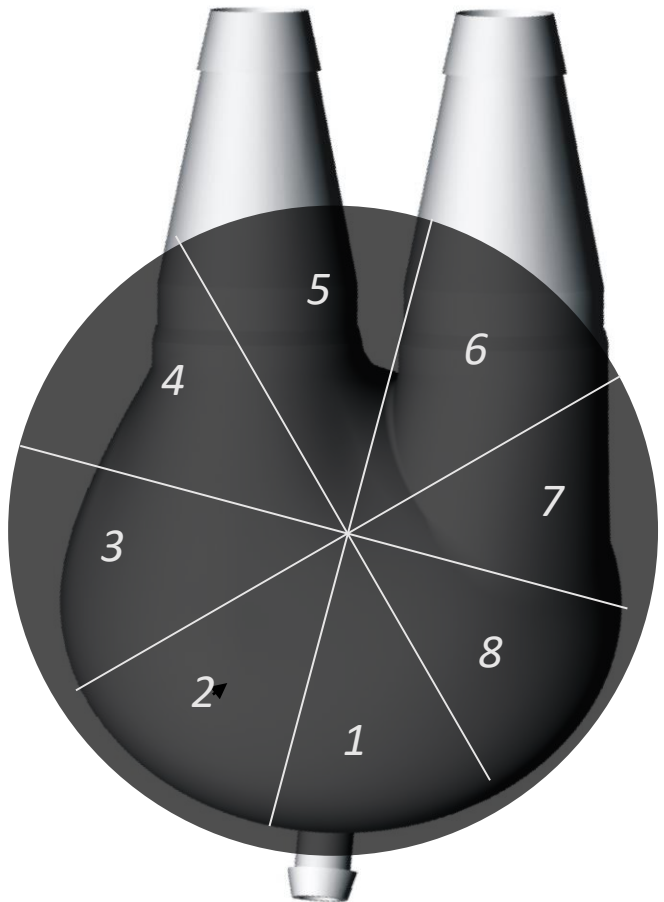


Deplanted chambers



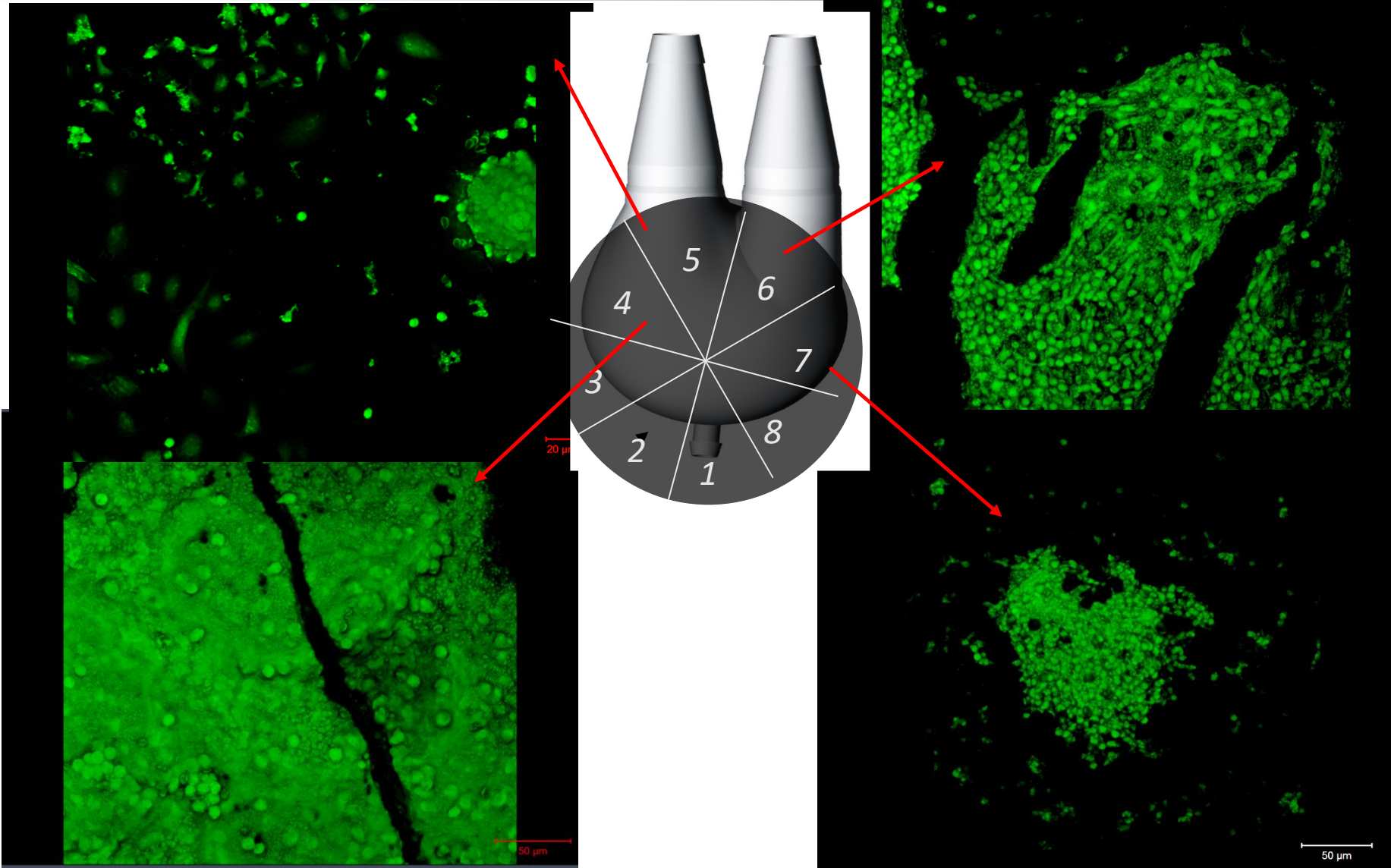


Deplanted chambers



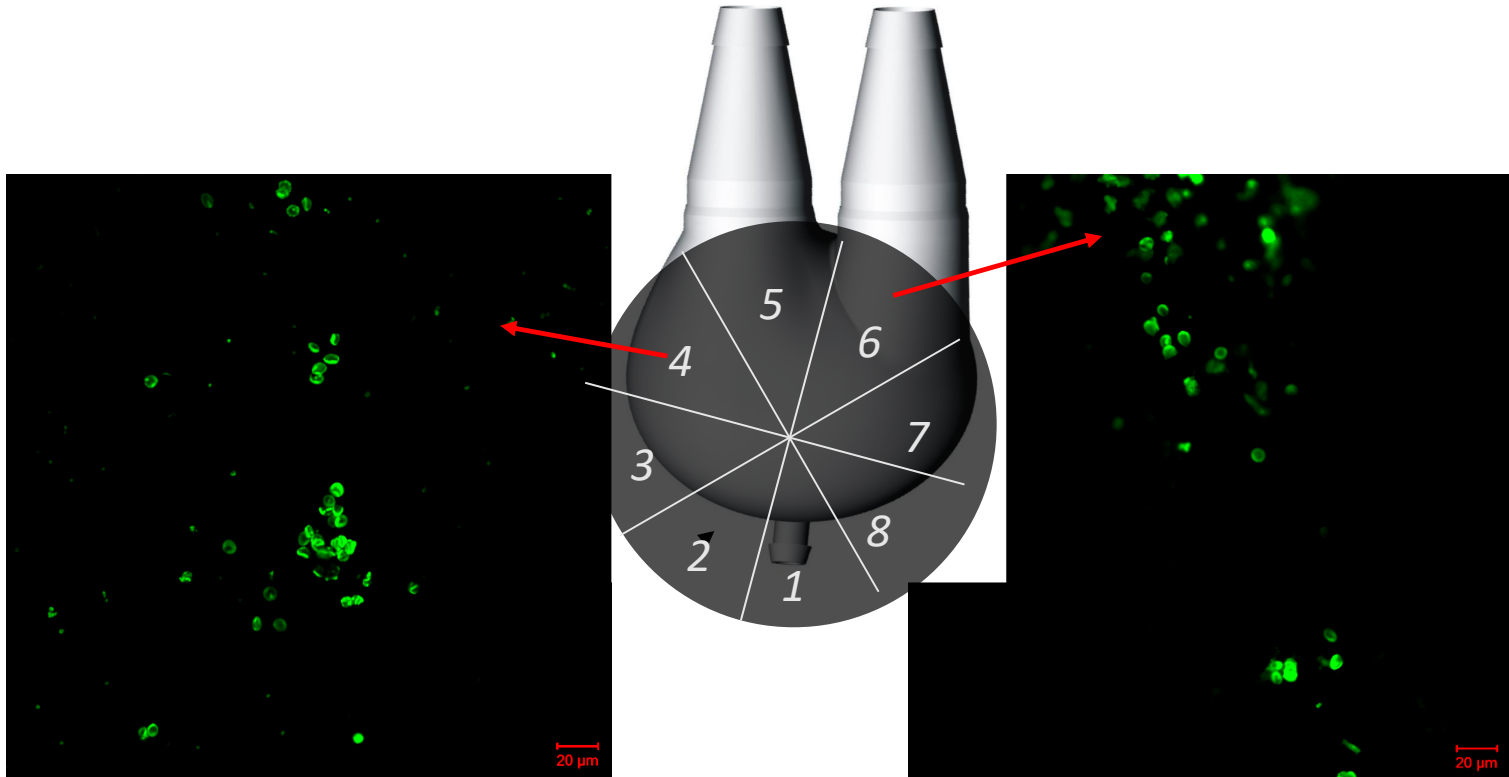


Deplanted chambers



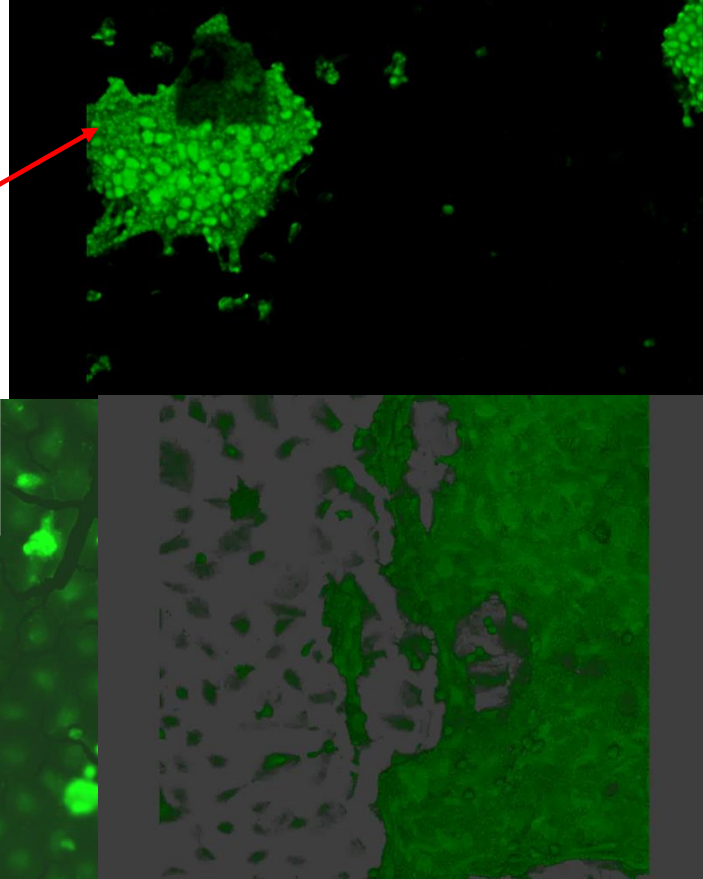
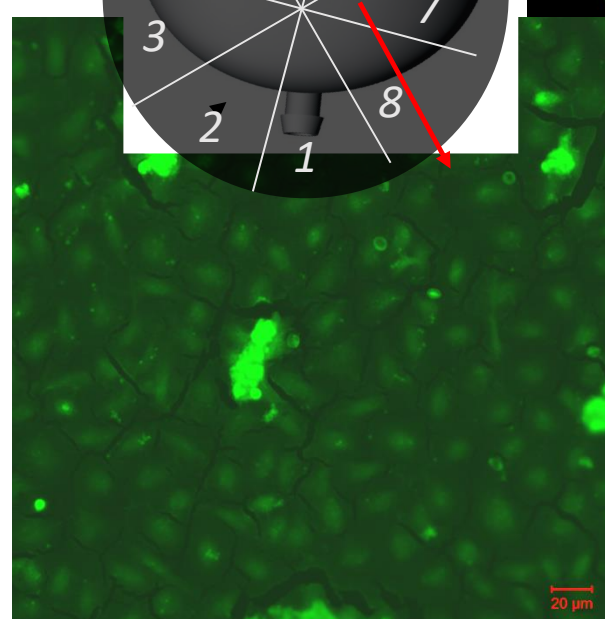
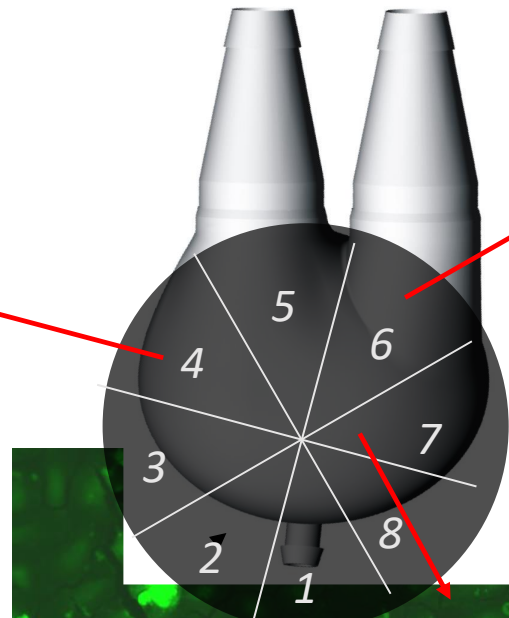
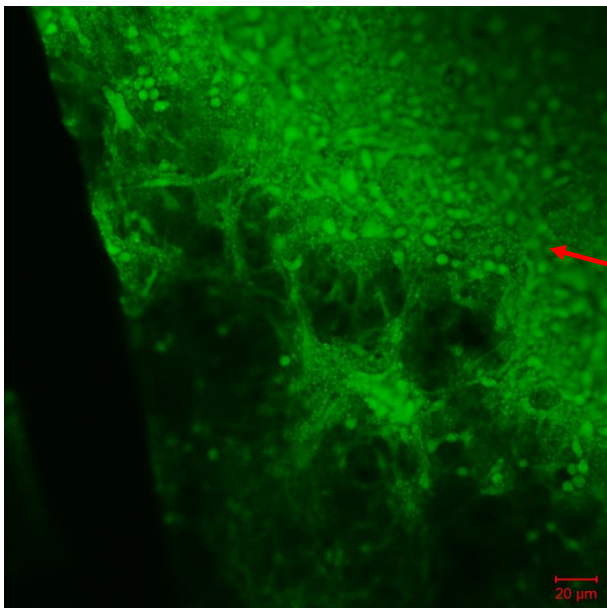


Deplanted chambers



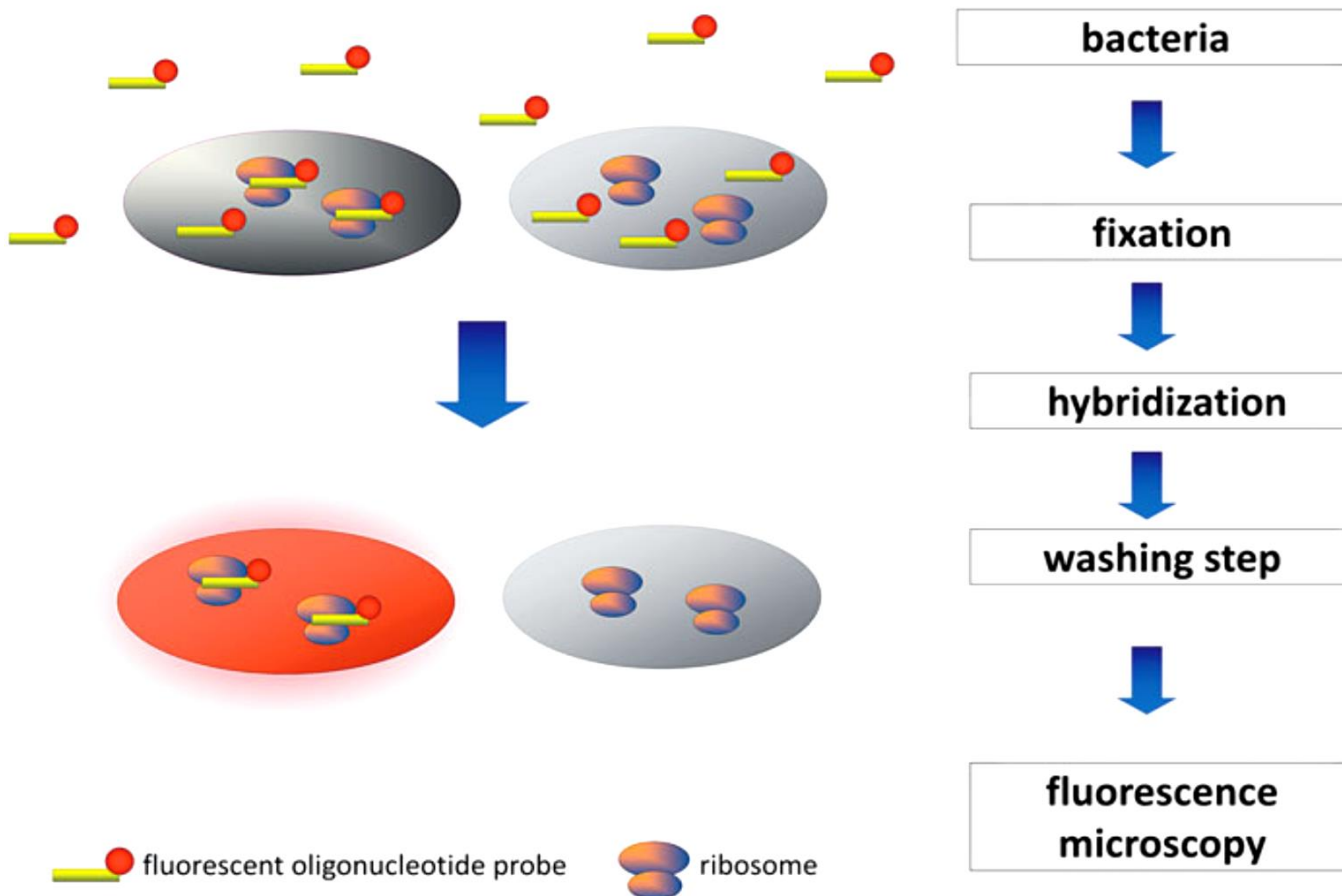


Deplanted chambers





Deplanted chambers





Deplanted chambers

PACJENT NR 1

Patient: male aged 46, assisted due to left ventricular failure and developing in failure. Supported by two chambers from 4.07.2018. He underwent a neurological incident during the treatment, a small-blood hemorrhagic stroke. Currently, the patient is rehabilitating, being physically active, and the symptoms of stroke persisting.

No Antibiotics have been used throughout the heart support process. The antibiotic is only perioperatively. Patient treated with anticoagulants.

Sampling:

- sample No. 1- fragment of the valve with fibrin deposit

sample no. 2- fibrin deposits on the edge of the blood-red membrane near the chamber vent with a fragment of a blood-red canopy.



Deplanted chambers

PACTIENT NO 1

FISH analysis

Material 1 A few microorganisms were found on the basis of carried out staining of nucleic acids with the dye DAPI in the fibrin. FISH was not found to contain active bacteria, microorganisms or biofilms.

Material 2 Relative detection (uncertainty) of microorganisms with the application of nucleic acid staining with DAPI dye. FISH was not found to contain active bacteria, microcollies or biofilms.

16S rRNA GENE AMPLIFICATION TEST (PCR study)

The study was carried out using the bacterium *Sphingobium yanoikuyae*.

Material 1 No bacterial DNA was found with 16S rRNA amplification

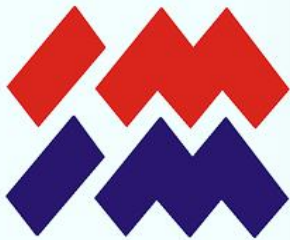
Material 2 No bacterial DNA was found with 16S rRNA amplification



Deplanted chambers

PATIENT No 1

No identification of active bacterial infection in the test samples. Due to the degradation of bacterial DNA and / or a small number of bacteria in the sample material, microorganisms detected microscopically were not effectively differentiated by PCR, amplification / sequencing.



Deplanted chambers

PATIENT No 2

Patient: a woman of 37 years. Diagnosed cardiomyopathy of an unknown cause. Two-chamber failure. There is no information about implantation. The chamber was replaced after 23 days after implantation.

Sampling:

test samples were taken from the right ventricle.

- sample 1 fragment of a blood-red membrane with fibrin deposit
- sample 2 fragment of a blood-red membrane with a large deposit of fibrin



Deplanted chambers

PATIENT No 2

BADANIE FISH

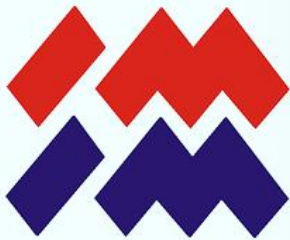
Materiał 1 Stwierdzono nieliczne mikroorganizmy na podstawie przeprowadzonych barwień kwasów nukleinowych barwnikiem DAPI, we włókniku. Nie stwierdzono metodą FISH aktywnych bakterii, mikroorganizmów ani biofilmów.

Materiał 2 Względna detekcja (brak pewności) mikroorganizmów przy zastosowanym barwieniu kwasów nukleinowych barwnikiem DAPI. Nie stwierdzono metodą FISH aktywnych bakterii, mikrokolonii ani biofilmów.

BADANIE AMPLIFIKACJI GENU 16S rRNA (badanie PCR)

Badanie przeprowadzono przy użyciu szczepu bakterii *Sphingobium yanoikuyae*. Jest to charakterystyczny gatunek bakterii rozwijający się w środowisku cieczy, wskazuje na skażoną kolonizację na powierzchni próbek. W niektórych przypadkach, może być związany z procesem infekcji u niektórych pacjentów o obniżonej odporności immunologicznej.

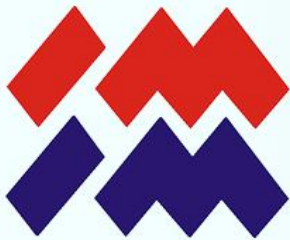
Materiał 1 99,3% 447 (par zasad)
Materiał 2 99,3% 456 (par zasad)



Deplanted chambers

PACJENT NR 2

Brak identyfikacji aktywnego zakażenia bakteryjnego w badanych próbkach. Leczona lub wcześniejsza infekcja nie może być wykluczona.



Deplanted chambers

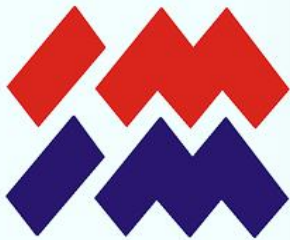
PACJENT NR 3

Pacjent: mężczyzna lat 28. Leczony od 14.07.2018 do 2.09.2018r. Zdiagnozowana kardiomiopatia o nieznanej etiologii. Przed wszczepieniem komór wspomagania POLVAD, stwierdzono frakcję wyrzutową na poziomie 10%, liczne skrzeliny w obu komorach serca. Dnia 2.09.2018 wykonano przeszczep serca z dobrym efektem.

Pobór próbek:

próbki do badań pobrano z prawej komory.

- próbka 1- fragment membrany krwistej ze złogiem włóknika
- próbka 2- fragment membrany krwistej z dużym złogiem włóknika



Deplanted chambers

PACJENT NR 3

BADANIE FISH

Materiał 1 Nie stwierdzono występowania mikroorganizmów przy zastosowaniu metody FISH ani barwień przy użyciu barwnika DAPI.

Materiał 2 Względna detekcja (brak pewności) mikroorganizmów przy zastosowanym barwieniu kwasów nukleinowych barwnikiem DAPI. Nie stwierdzono metodą FISH aktywnych bakterii, mikrokolonii ani biofilmów.

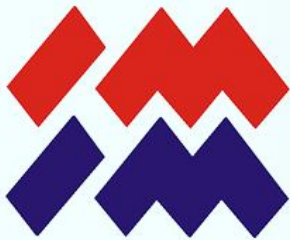
BADANIE AMPLIFIKACJI GENU 16S rRNA

(badanie PCR)

Badanie przeprowadzono przy użyciu szczepu bakterii *Sphingobium yanoikuyae*.

Materiał 1 Początkowo hamowanie PCR przez materiał pacjenta. Po rozcieńczeniu (1:2) nie wykryto bakteryjnego DNA za pomocą amplifikacji PCR 16S rRNA o obniżonej czułości.

Materiał 2 Amplifikacja genu 16S rRNA, a następnie sekwencjonowanie zaszło w krótkim fragmencie, dalsze różnicowanie było niemożliwe.



Deplanted chambers

PACJENT NR 3

Brak identyfikacji aktywnego zakażenia bakteryjnego w badanych próbkach. Leczona lub wcześniejsza infekcja nie może być wykluczona. Z powodu degradacji bakteryjnego DNA i/lub małej liczby bakterii w materiale próbki 2, mikroorganizmy wykryte mikroskopowo nie zostały skutecznie zróżnicowane za pomocą PCR, amplifikacji / sekwencjonowania.



Surface modification

NICHE-LIKE STRUCTURES

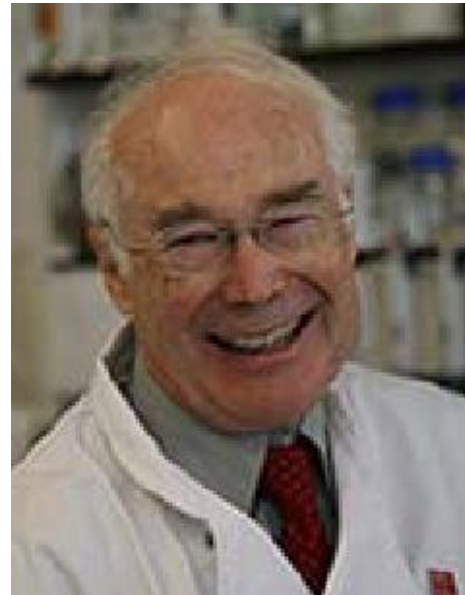


Surface modification

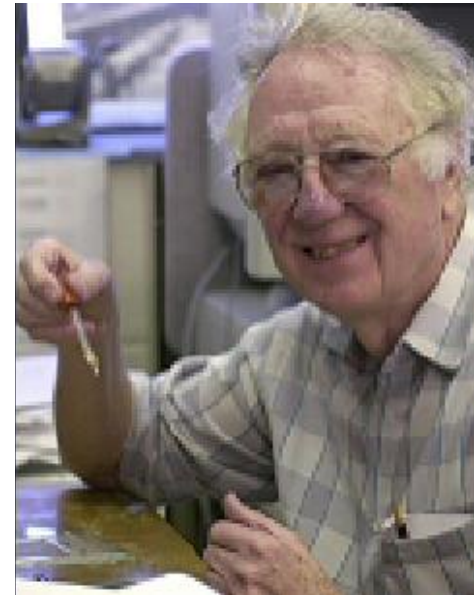
Mario Capecchi
University Utah



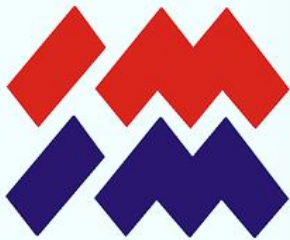
Martin J. Evans
University Cardiff



Olivier Smithies
University Chapel Hill

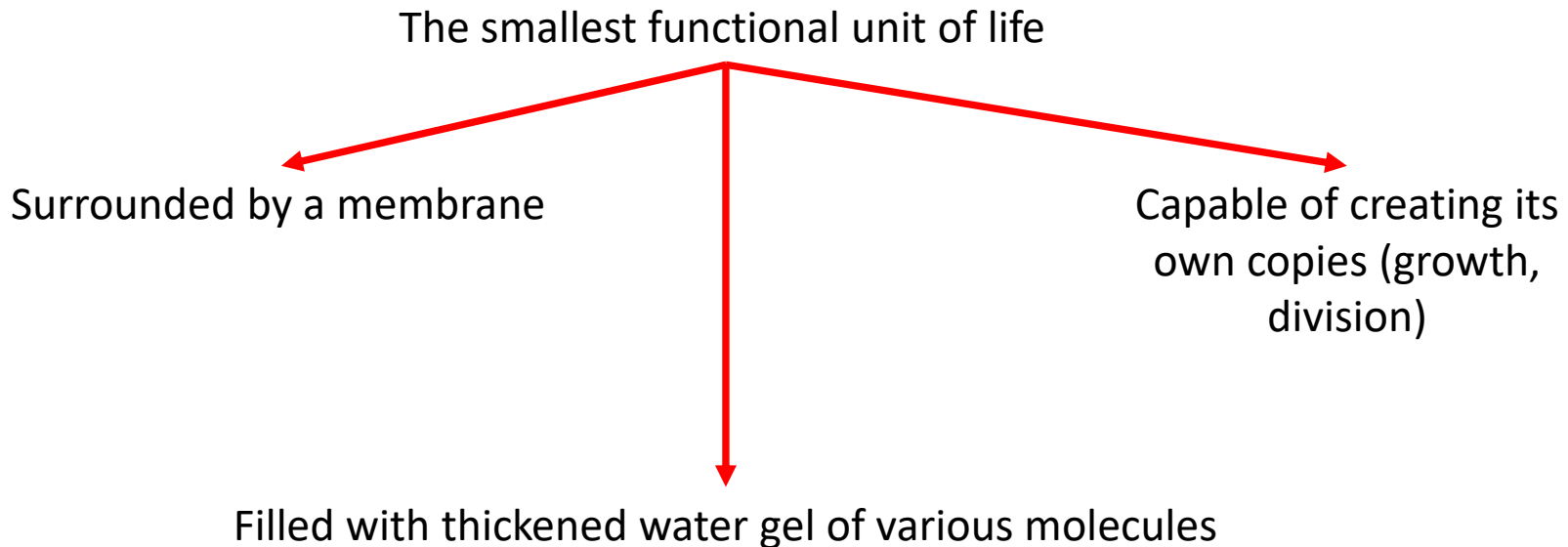


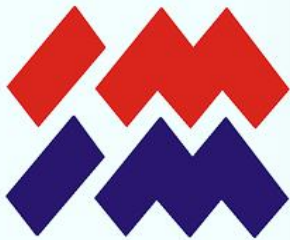
2007- Nobel Prize in Physiology and Medicine for discovery of the rules for use of embryonic stem cells for genetic modification of mice



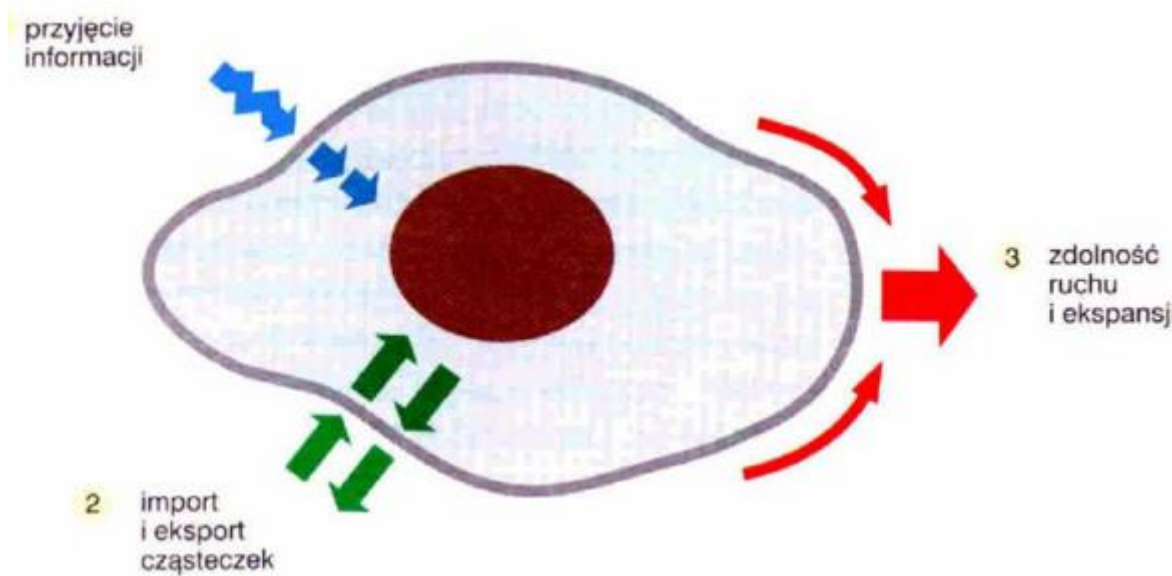
Biology of the cell

Cellula

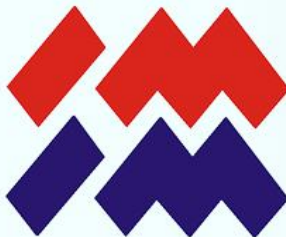




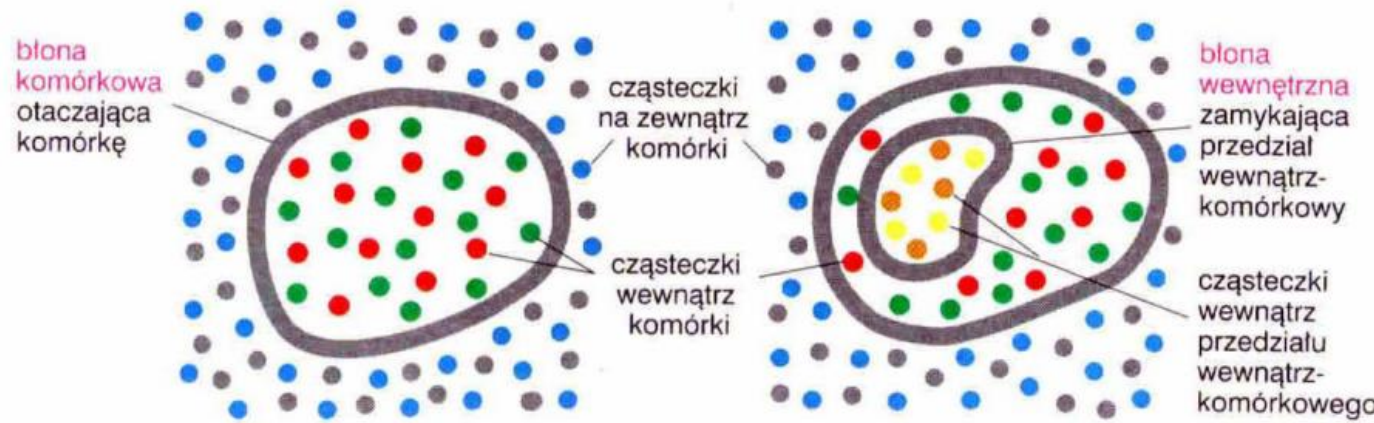
Cell membranes as barriers



- Transport inside of the interior (selective permeability)
- Receiving stimuli
- Ability of movement and expansion
- The possibility of transforming energy processes (ATP synthesis)



Cell membranes as barriers



Barriers between compartments (components)

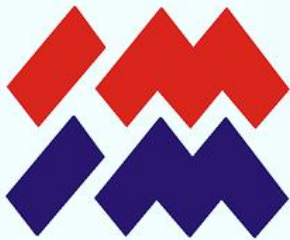
Prevent mixing of substances between compartments

Ensuring the maintenance of differences in the composition and function between organelles

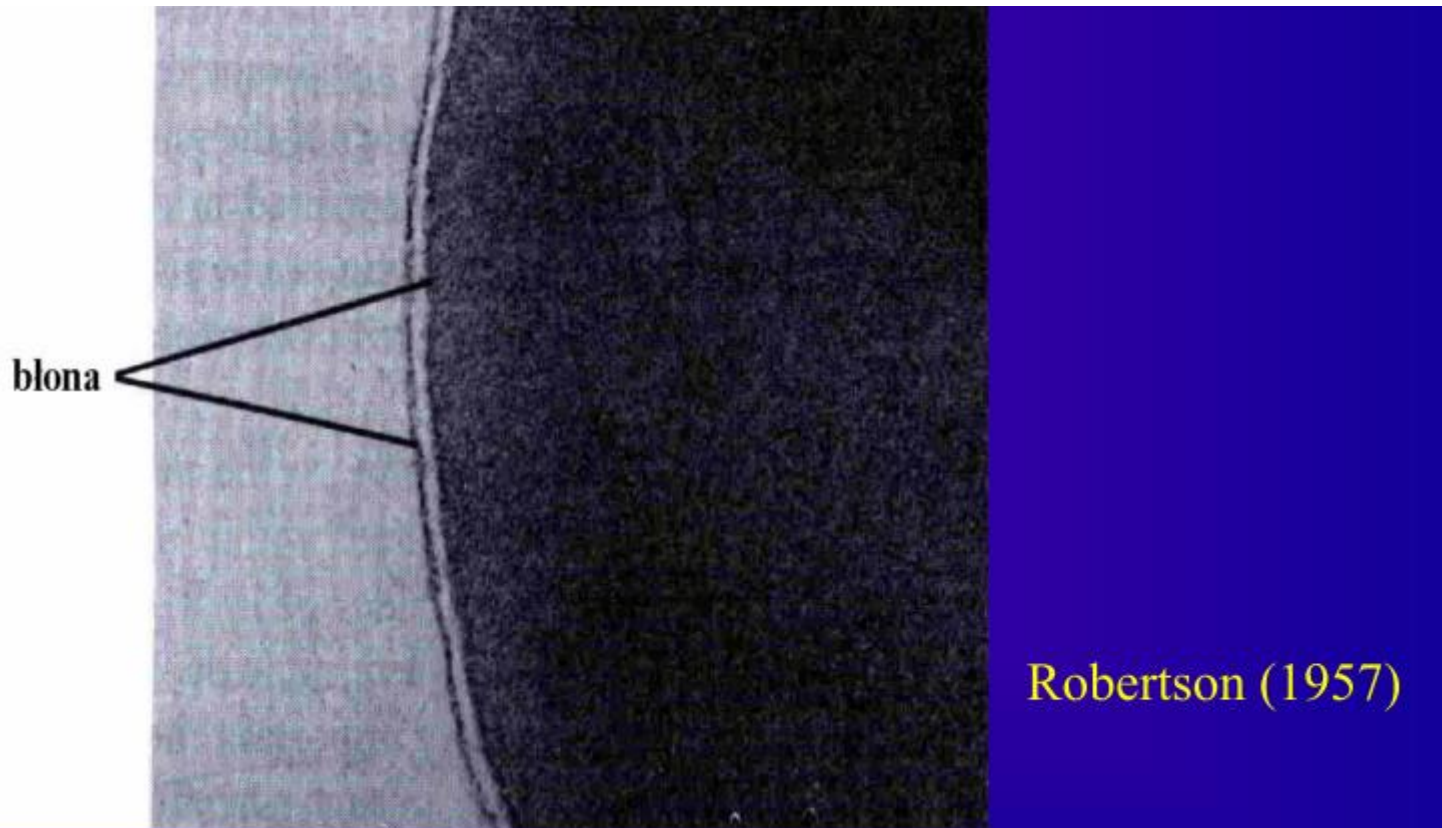
Composition control

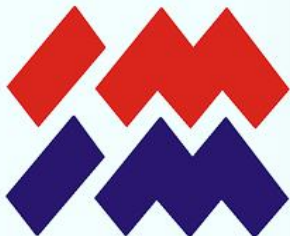
The membrane itself is a cellular compartment with unique functions

Dynamic structure (movement, synthesis and degradation of components)

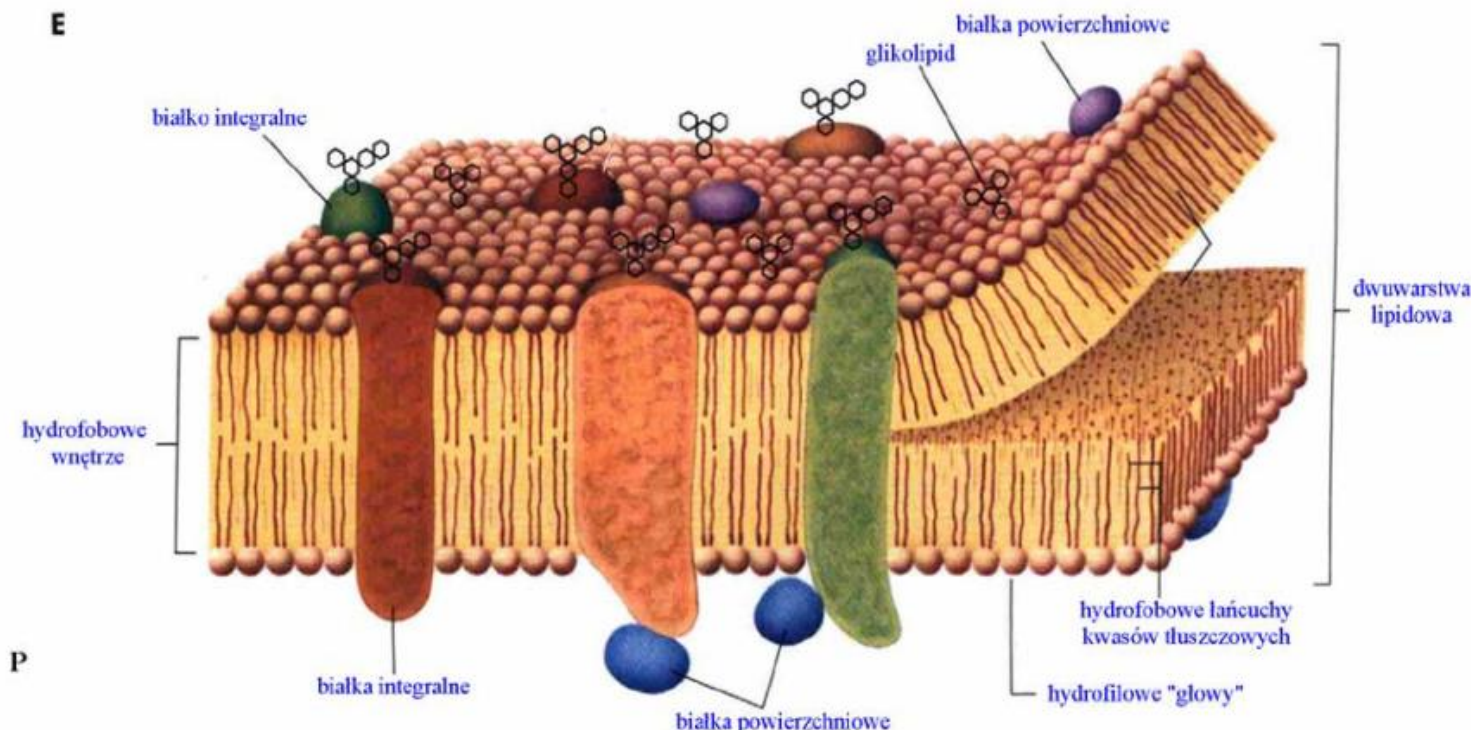


The structure of the cell membrane





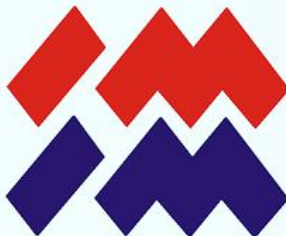
The structure of the cell membrane



- lipid bilayer
- membrane protein

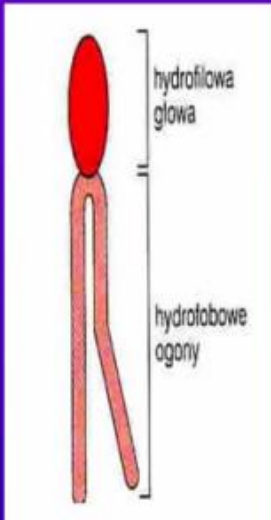


Membrane lipids



Membrane lipids

membrane molecules - amphipathic molecules

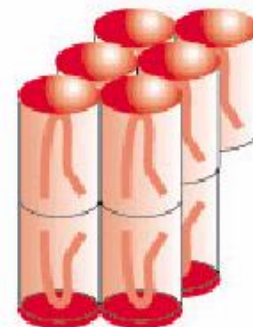
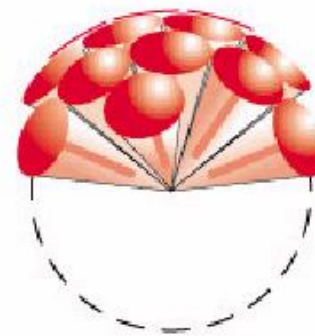


oddziaływanie
cząsteczki
hydrofilowej
hydrofobowej
z cząsteczkami wody

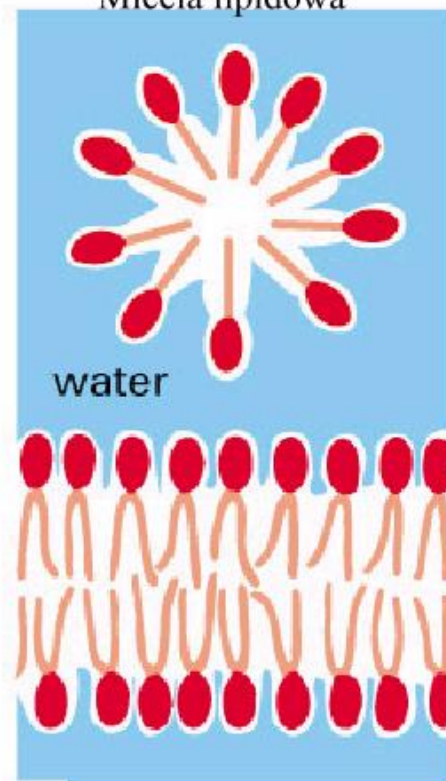
shape of lipid molecule



packing of lipid molecules



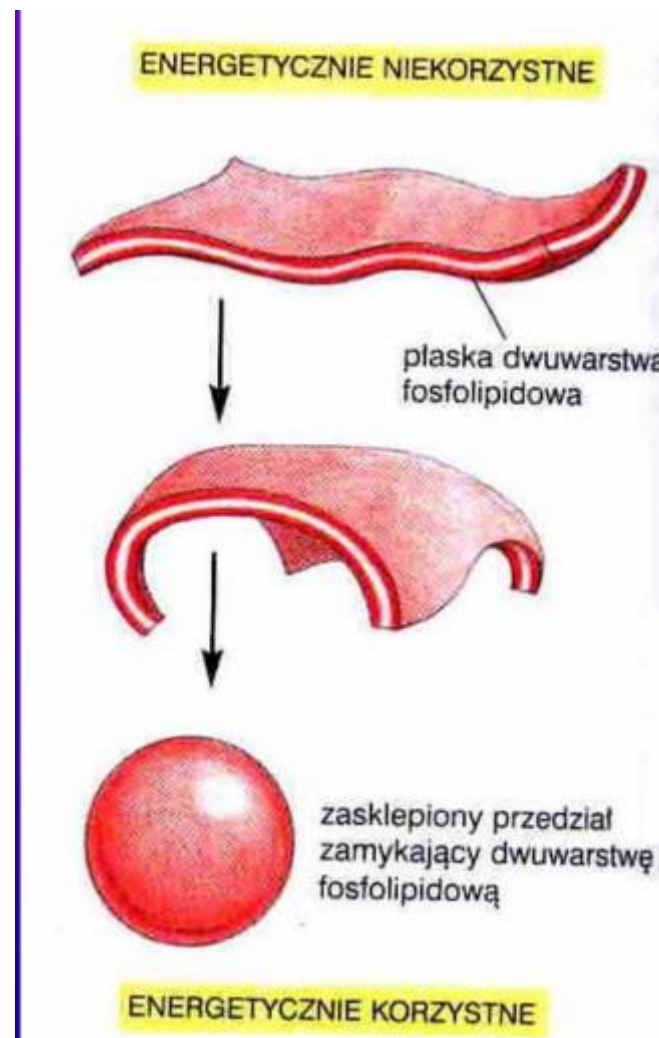
Micela lipidowa

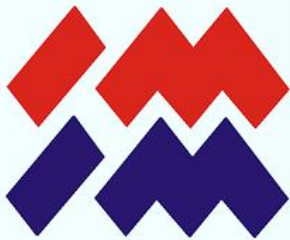


Dwuwarstwa lipidowa



Membrane lipids

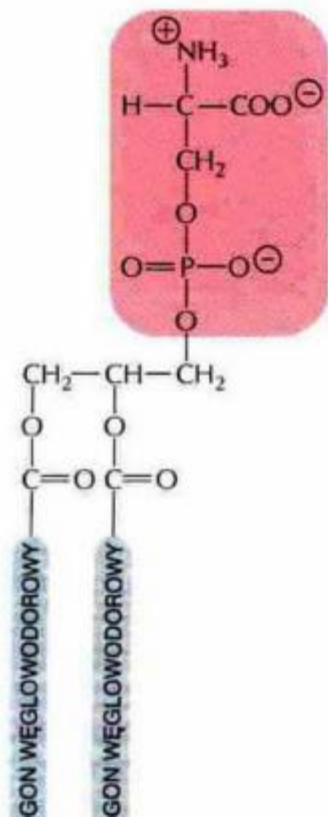




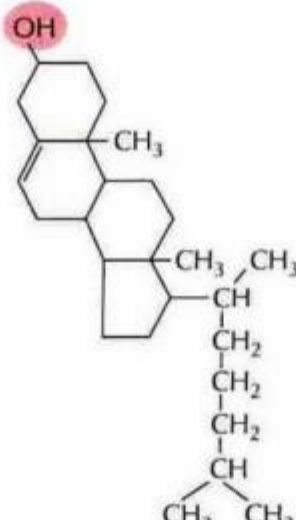
Membrane lipids

Membrane lipids

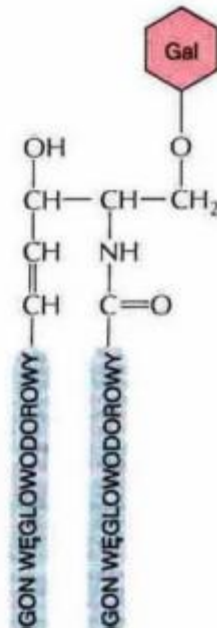
- phospholipids
- glycolipids
- steroids:
 - sulfolipids
 - lizolipids
 - other



fosfatydiloseryna
(fosfolipid)



cholesterol
(steroid)

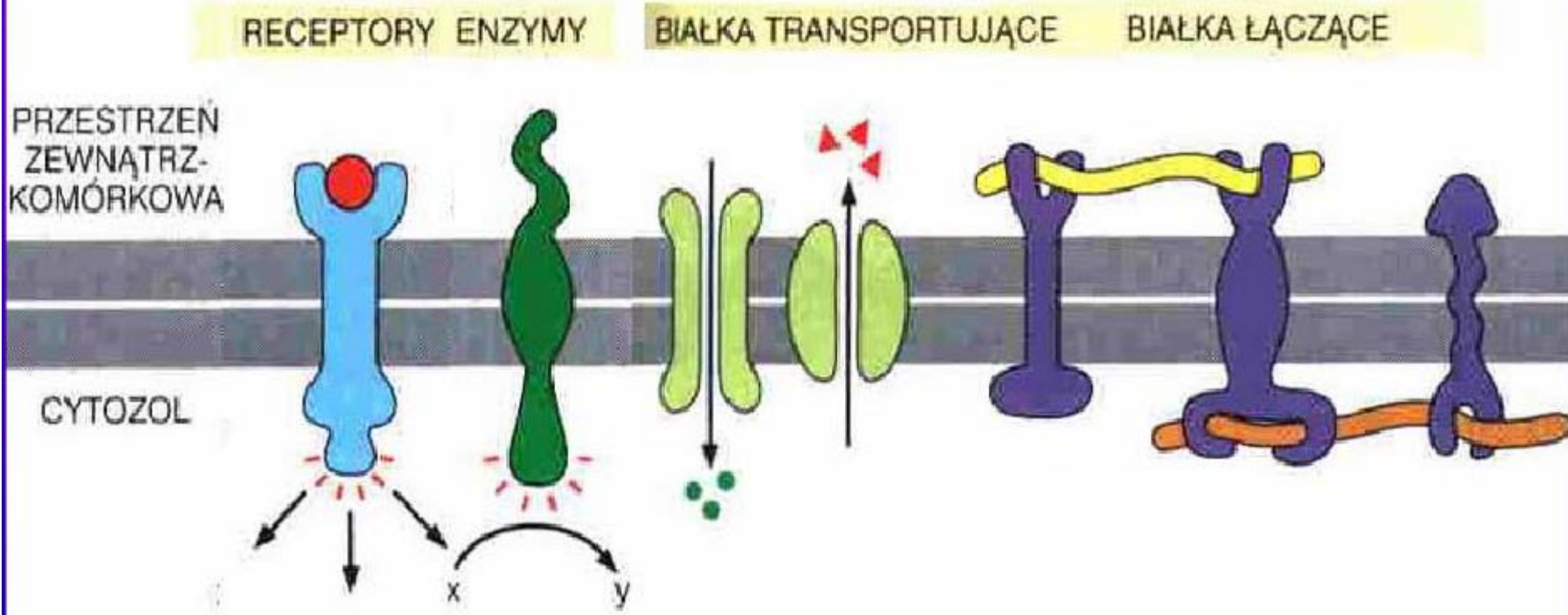


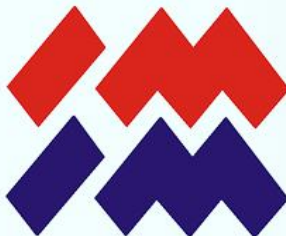
galaktocerebrozyd
(glykolipid)



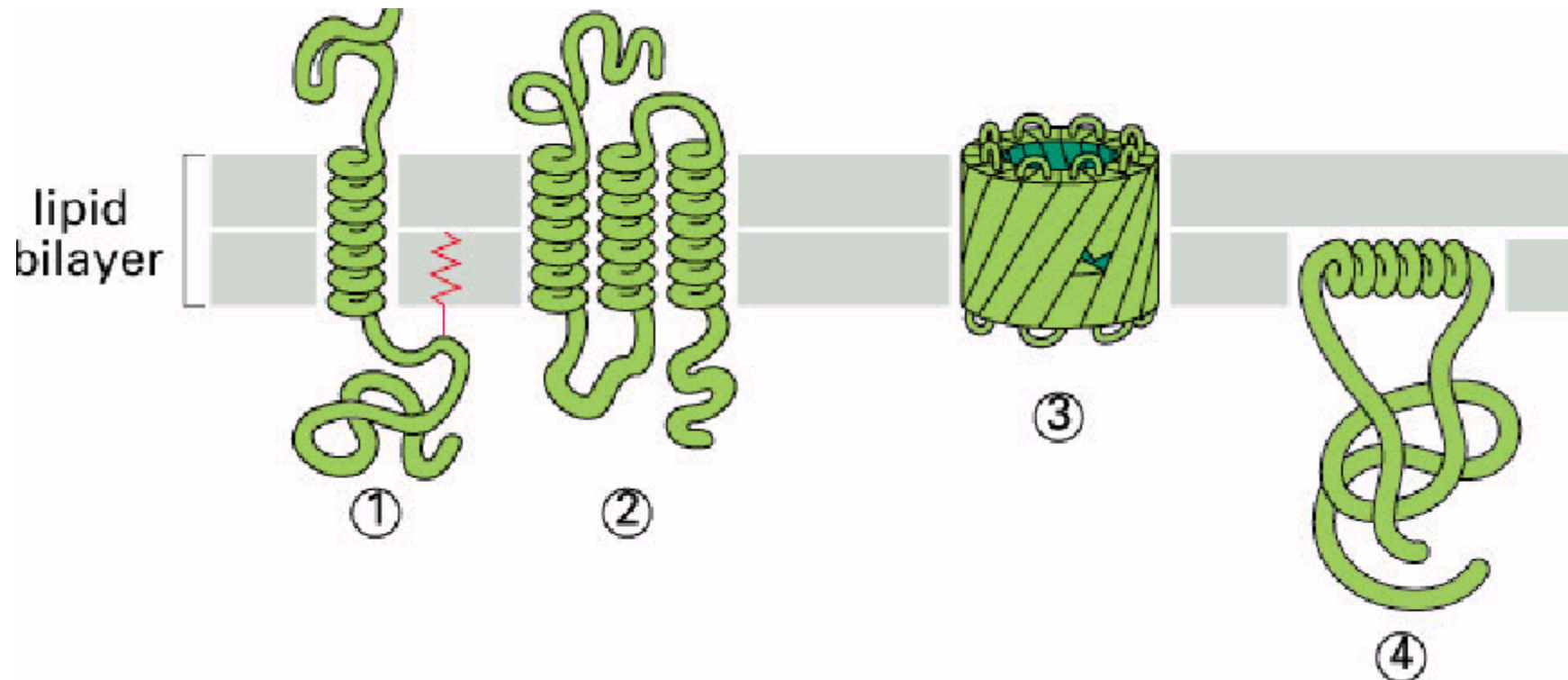
Membrane proteins

Functions of proteins





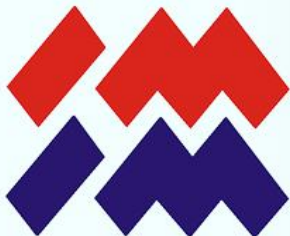
Functions of proteins



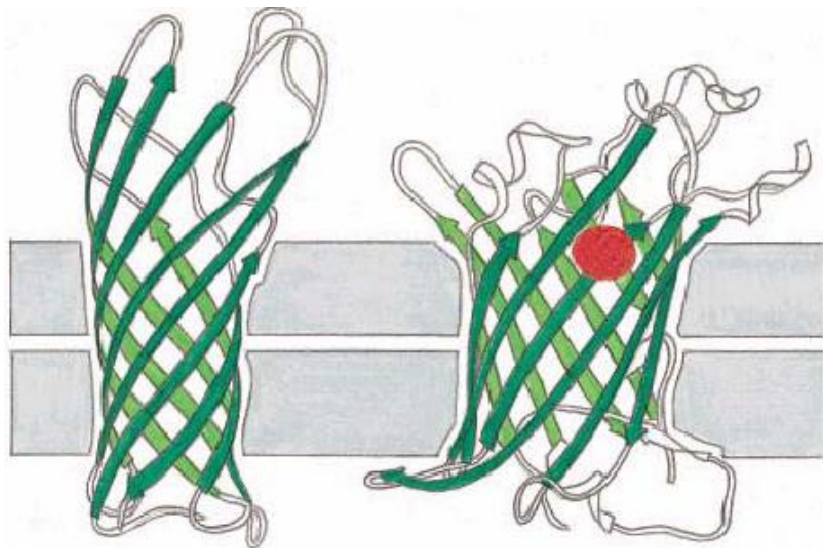
- Trans-membrane placement - transmembrane proteins
- Anchoring through covalent lipids

}

Integral proteins



Integral-transmembrane proteins

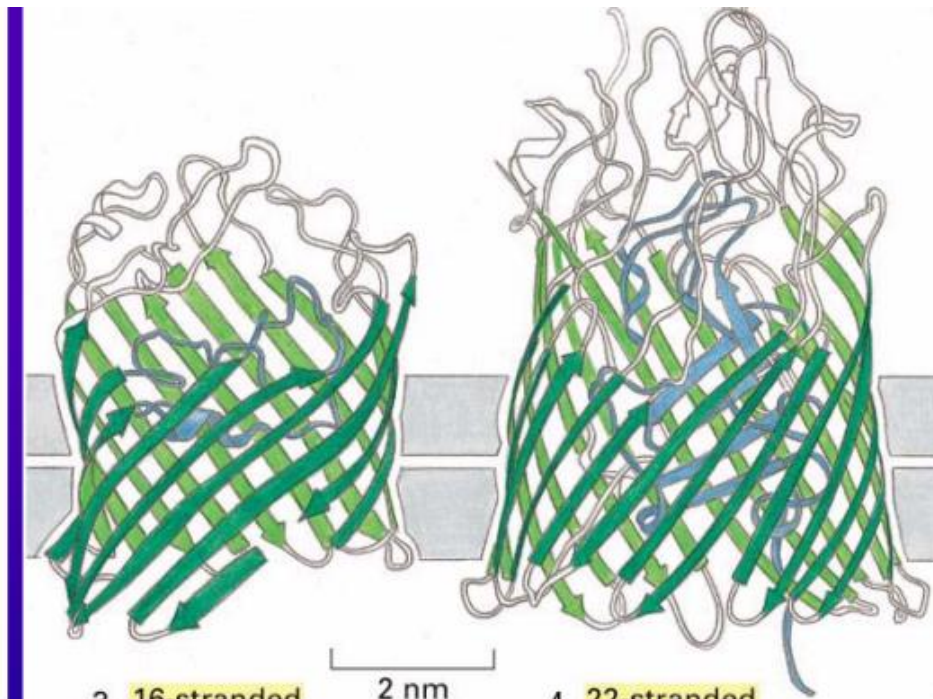


1. 8-stranded
OmpA

Receptor OmpA
E. coli

2. 12-stranded
OMPLA

LipazaOMPLA
E. coli

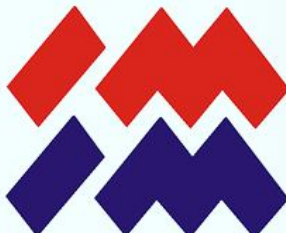


3. 16-stranded
porin

Poryna błony
Rhodobacter capsulatus

4. 22-stranded
FepA

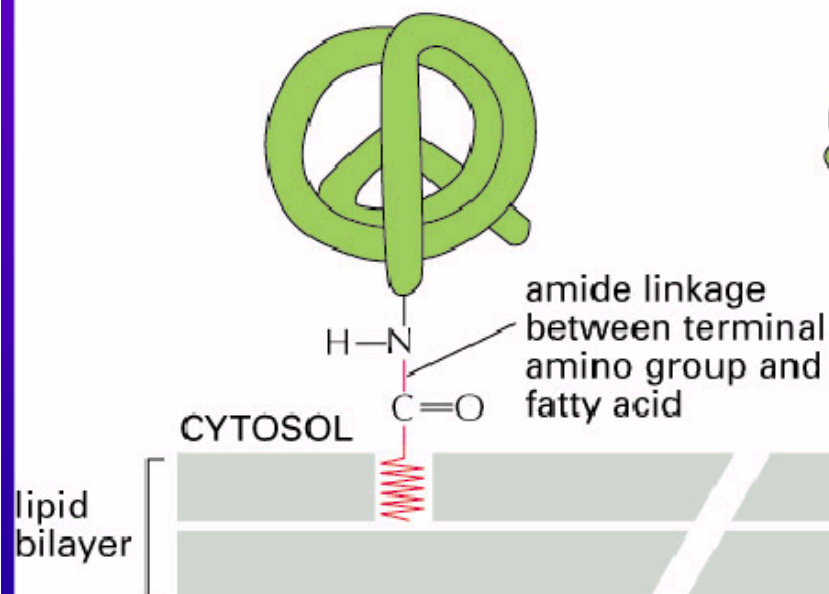
Transporter jonów Fe
E. coli



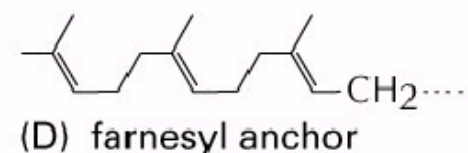
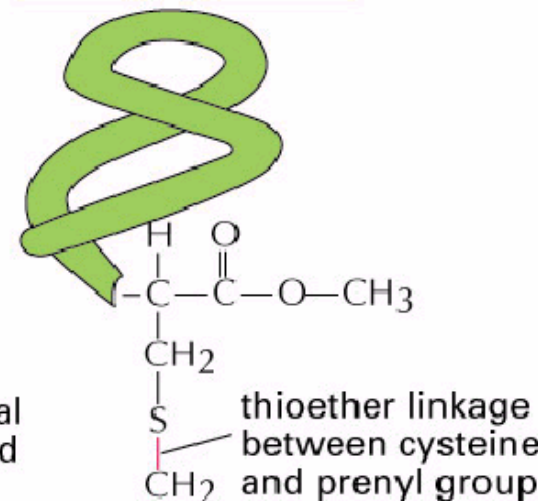
Integral proteins - anchored through lipids

Białka integralne, zakotwiczone przez lipidy

(A) protein anchored to membrane by a fatty acid chain



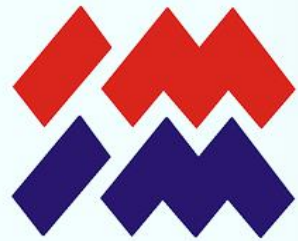
(B) protein anchored to membrane by a prenyl group





Membrane proteins - surface proteins

- Membrane bound by interacting with other proteins
- Different on both sides of the membrane
- Release (by extraction) without destroying the structure of the lipid bilayer



Membrane properties



Fluidity (mov)

Asymmetry

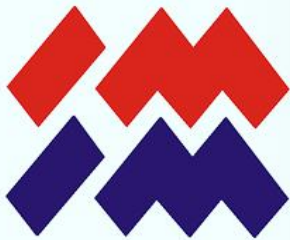
Selective permeability



Membrane properties

Fluidity (lipid bilayer)

- film cohesion (fusion)
- membrane flexibility
- displacement of proteins (cell signaling)



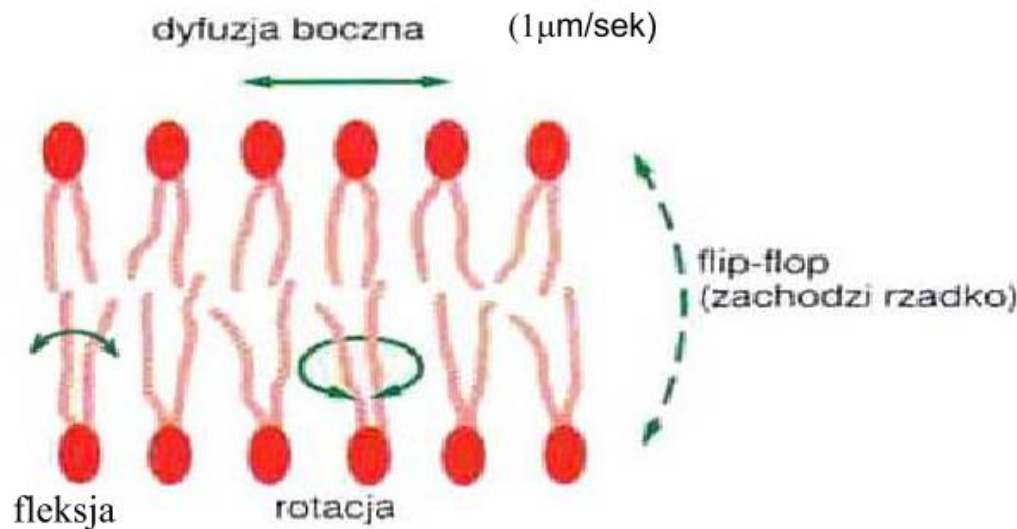
Membrane properties

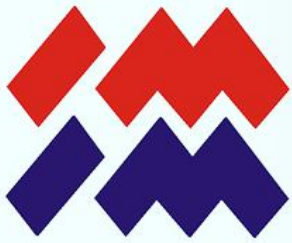
Rotational movements:

- Intramolecular
- rotating around its own axis

Translational movements

- lateral movement = lateral diffusion
- transversal movement = flip flop movements





Part 2.2

Executed projects

Cardiovascular system



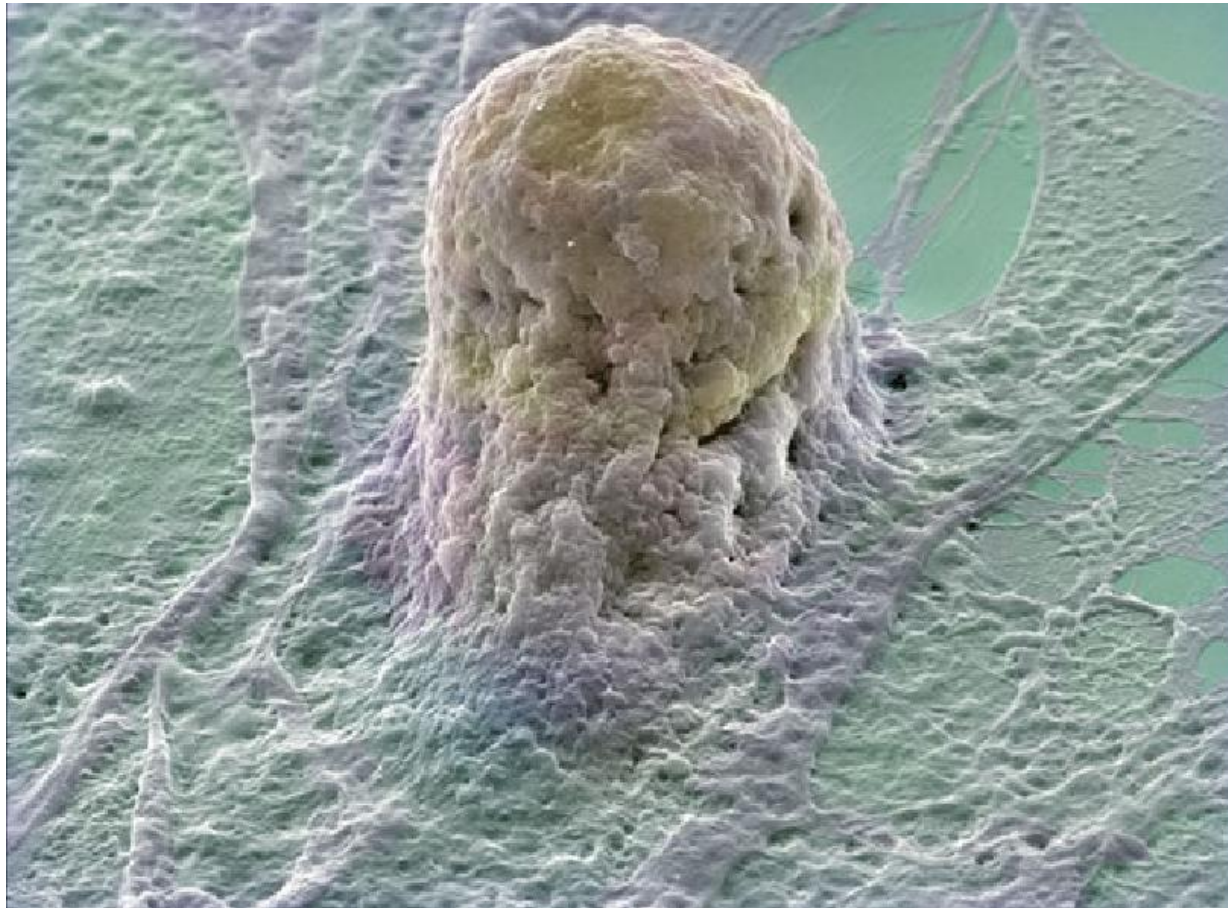
„Bio-inspired thin film materials with the controlled contribution of the residual stress in terms of the restoration of stem cells microenvironment”

2014/13/B/ST8/04287



Bio-inspired materials

Artificial materials modification





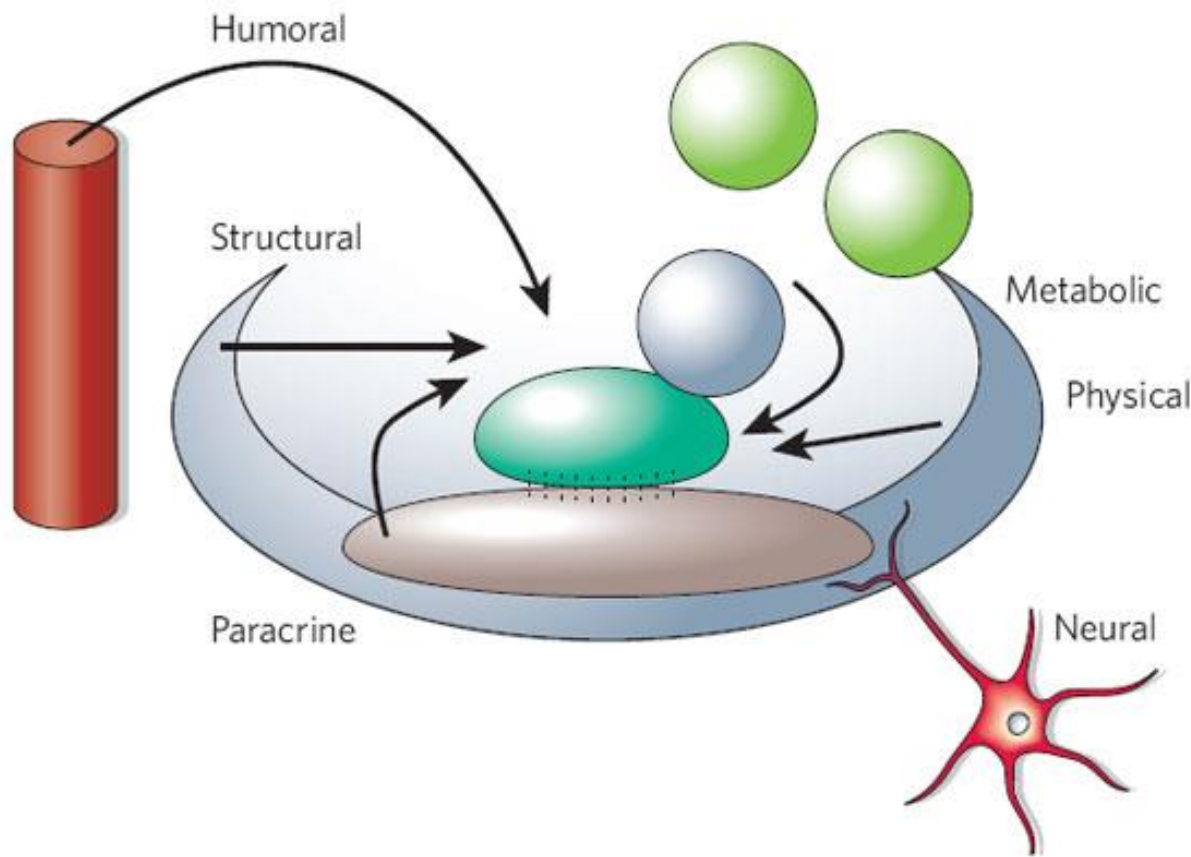
Bio-inspired materials

Coating material / process	Thickness
a-C:H	110nm
	60nm
a-C:H low gas flow sputtering	Magnetron sputtering 100nm
a-C:N	105nm
a-C:H (DLC) (Ti)	85nm
	43nm
	65nm
	86nm



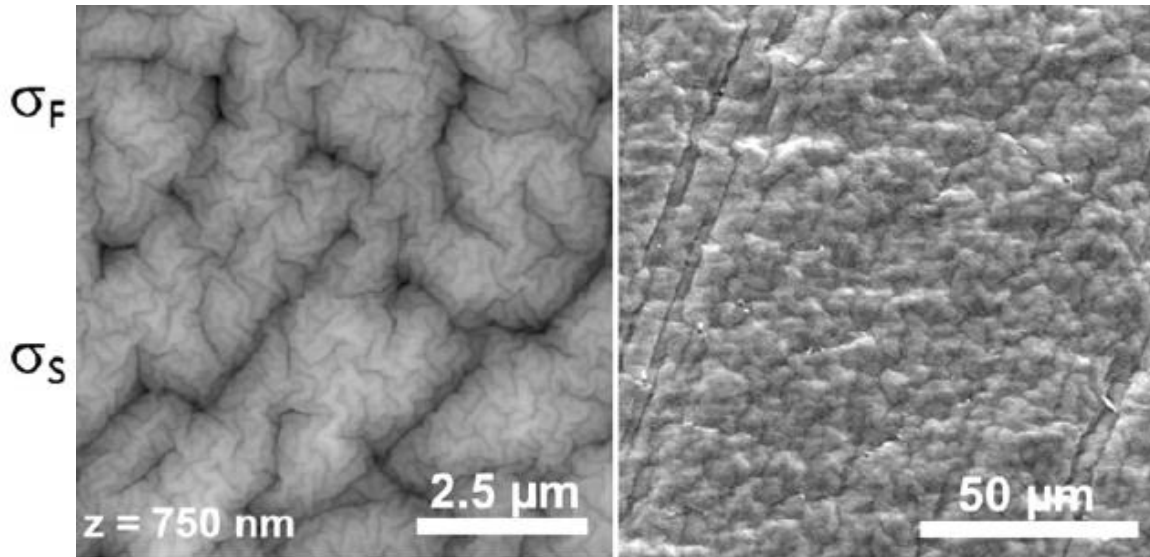
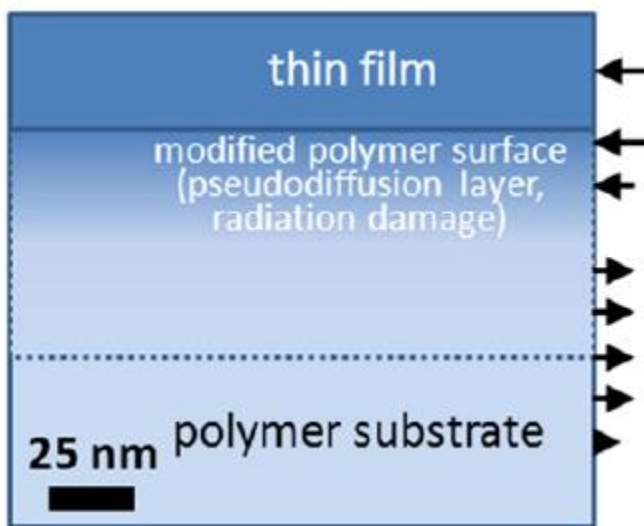
Bio-inspired materials

"The concept of a niche as a specialized microenvironment housing stem cells"
first proposed by Schofield.



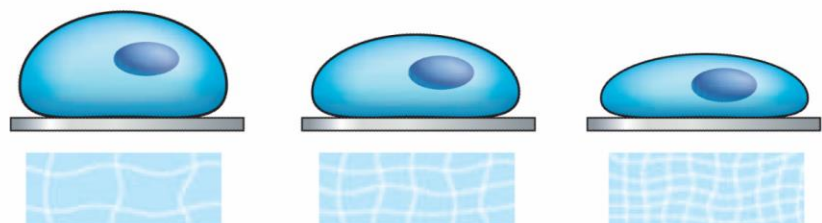


Bio-inspired materials



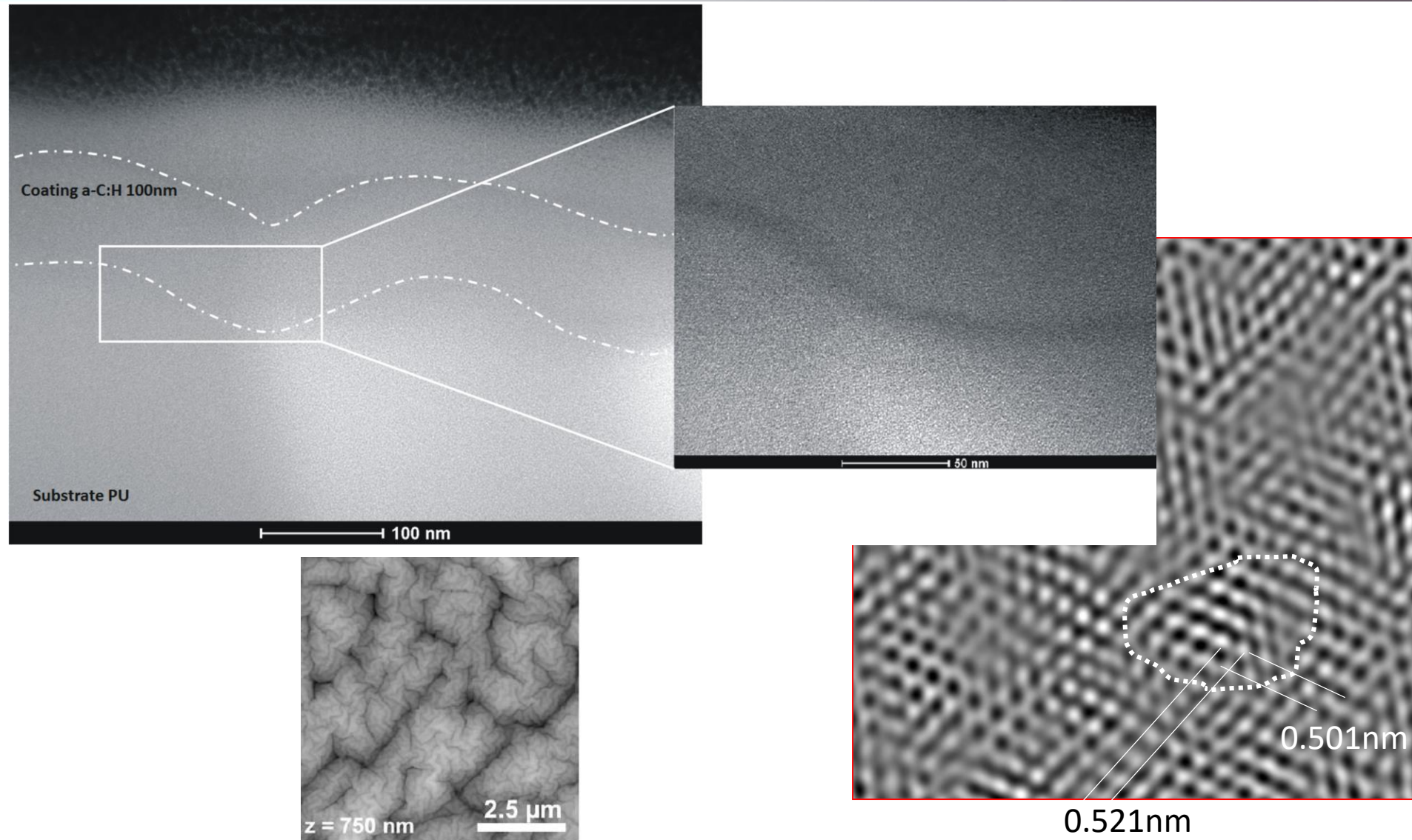
$$\lambda_c = 2\pi h \left[\frac{(1-v_f^2)E_s}{3(1-v_s^2)E_f} \right]^{1/3}$$

c Modular substrate stiffness





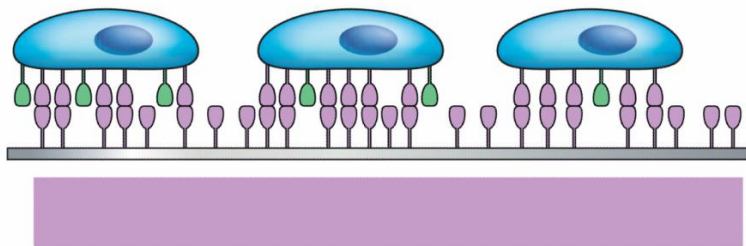
Bio-inspired materials



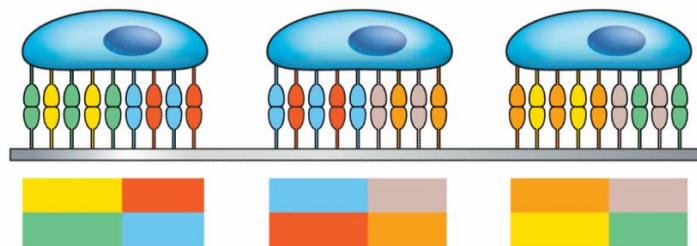


Bio-inspired materials

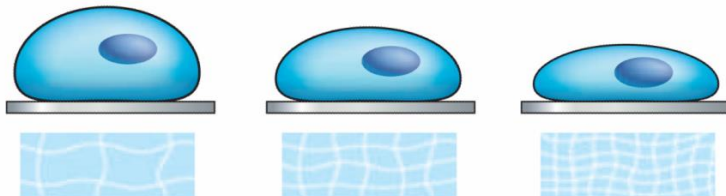
a Individual signals



b Combinatorial signal mixtures



c Modular substrate stiffness



M-ERA.NET

Nonthrombogenic metal-polymer composites
with adaptable micro and
macro flexibility for next generation heart
valves in artificial heart devices

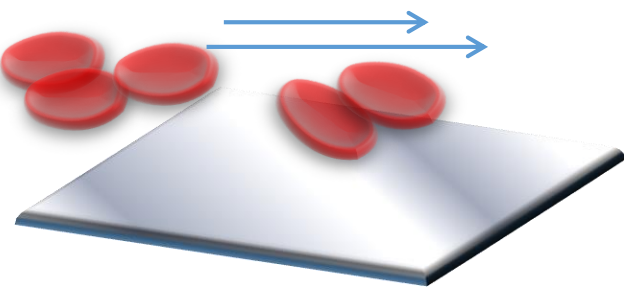


„Artificial Heart Laboratory“

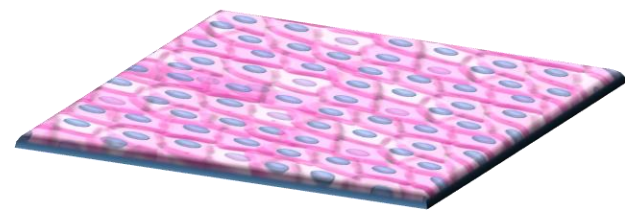


Bio-inspired materials

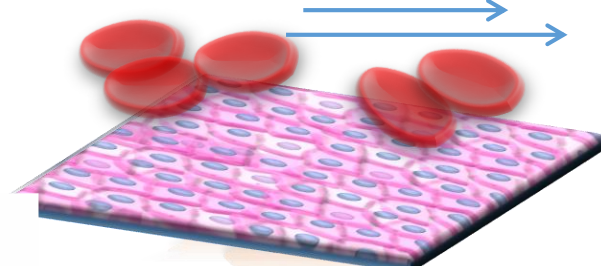
Hemocompatible



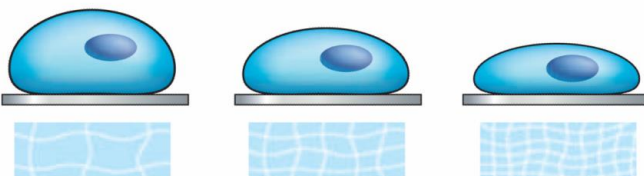
Pro-endothelial



- Surface topography
- Mechanical properties of the material
- The structure of the niche (2D or 3D)
- Residual stresses
- The chemical composition of the substrate

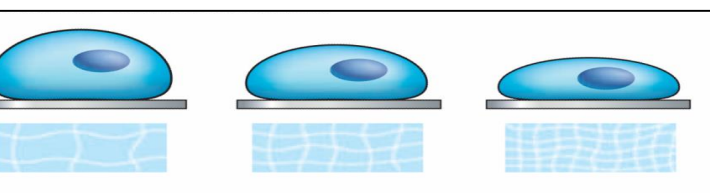
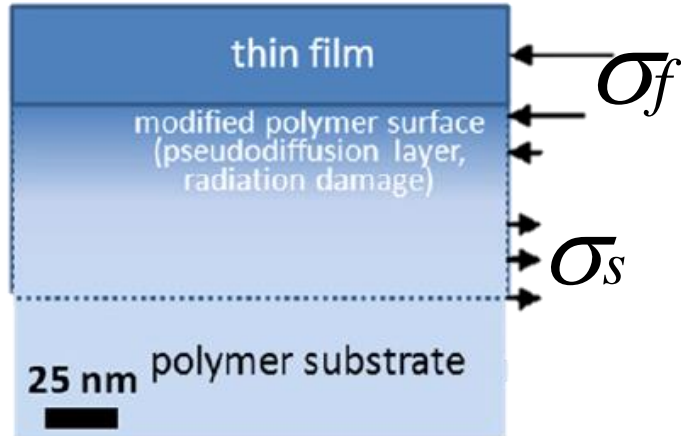


c Modular substrate stiffness





Bio-inspired materials

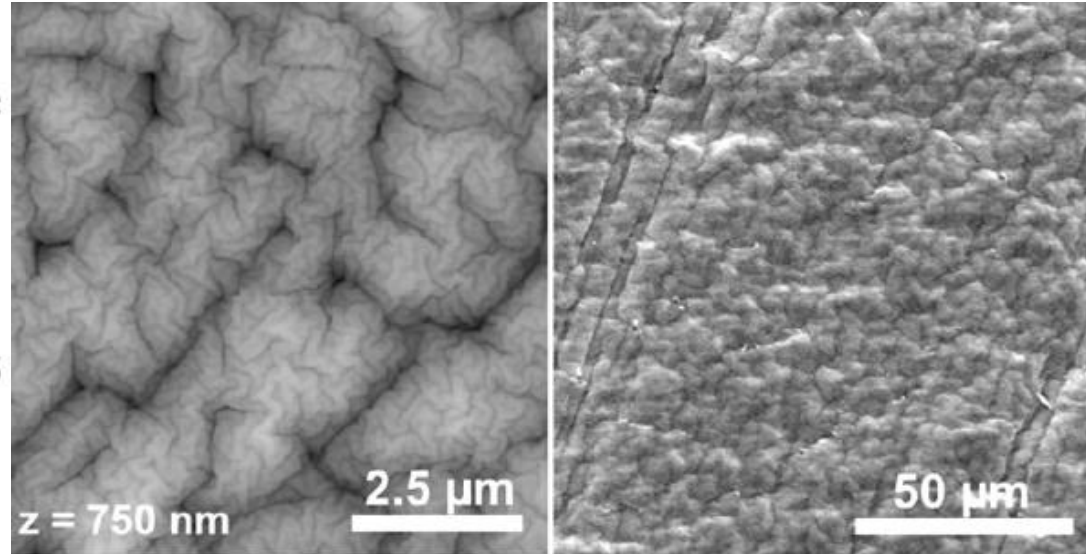
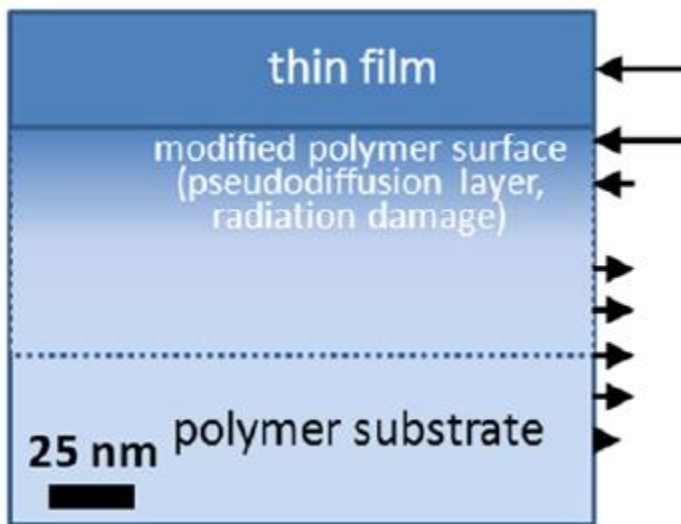


Layer	Thickness
a-C:H (sputtered)	110nm
a-C:H (sputtered)	60nm
a-C:H (lower gas flow; sputtered)	100nm
a-C:N (sputtered)	105nm
DLC (ALS)	85nm
DLC (ALS)	43nm
DLC (ALS)	65nm
DLC lower gas flow (ALS)	86nm

ALS- Anod Laser Sorce



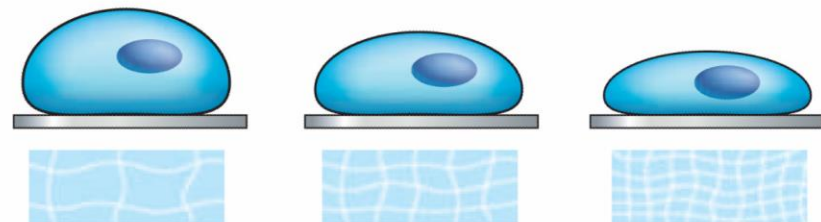
Bio-inspired materials



Surface reconstruction:

c Modular substrate stiffness

$$\lambda_c = 2\pi h \left[\frac{(1-v_f^2)E_s}{3(1-v_s^2)E_f} \right]^{1/3}$$

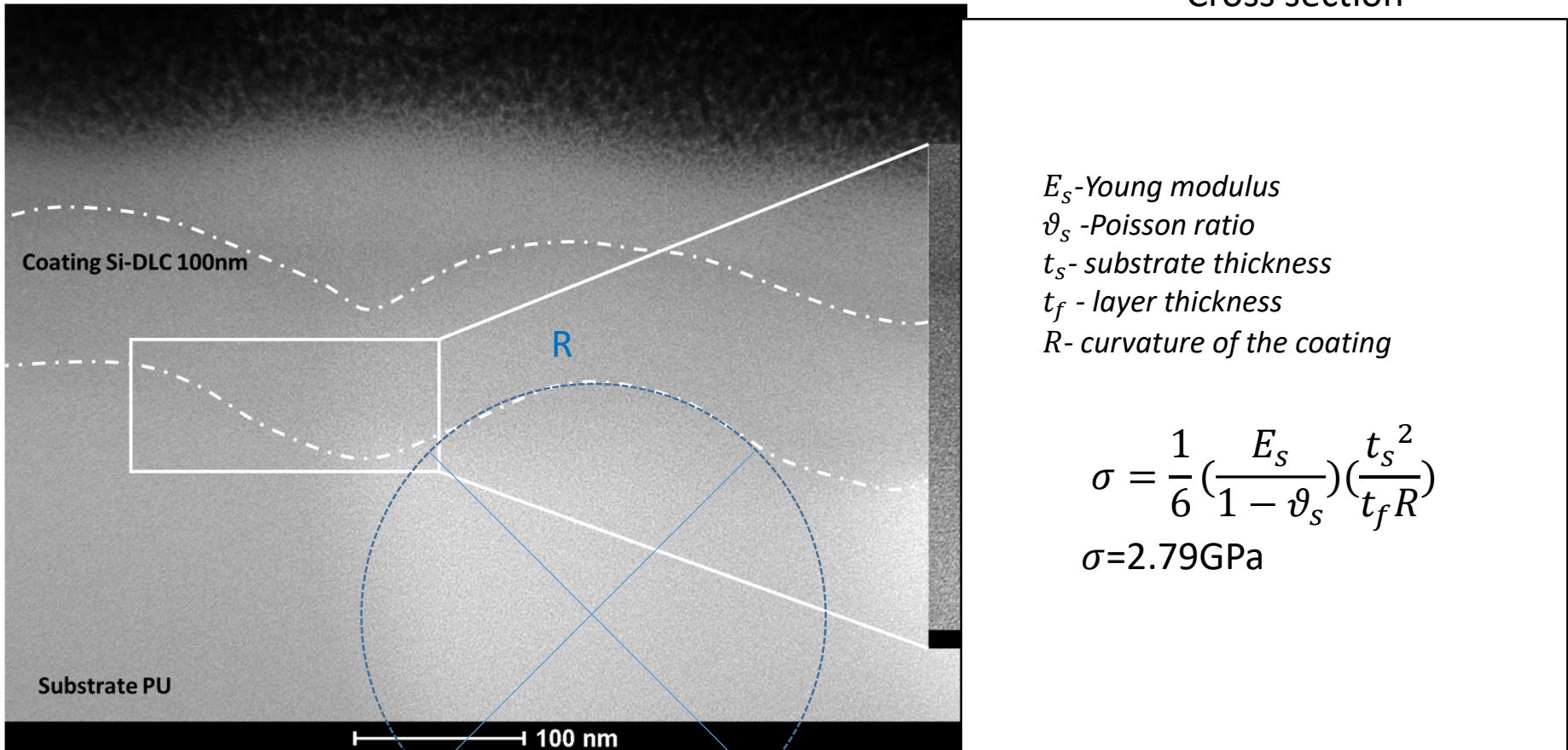




Bio-inspired materials

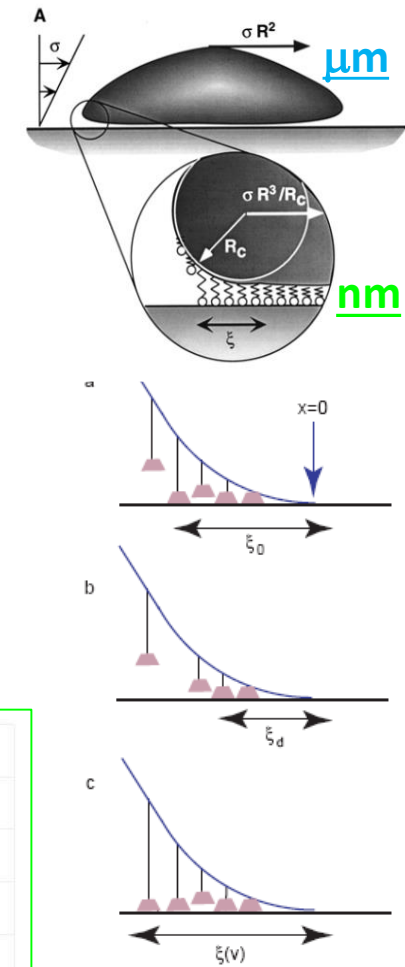
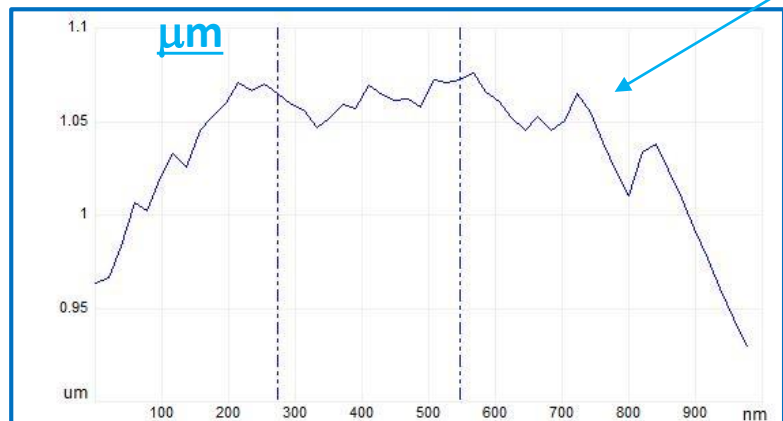
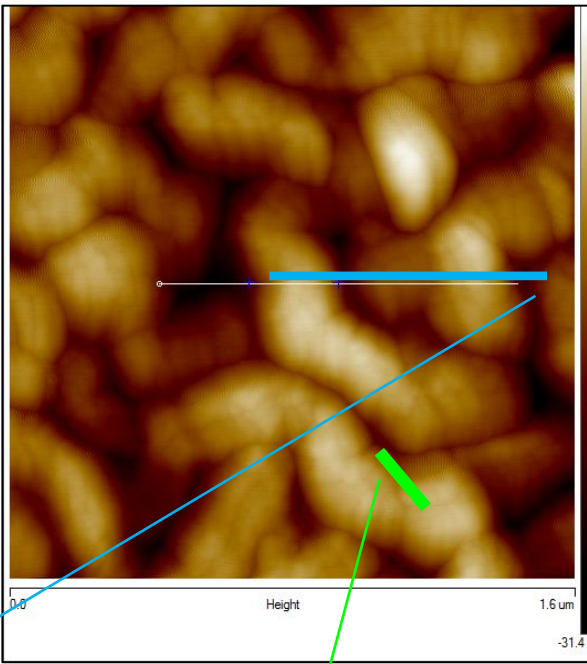
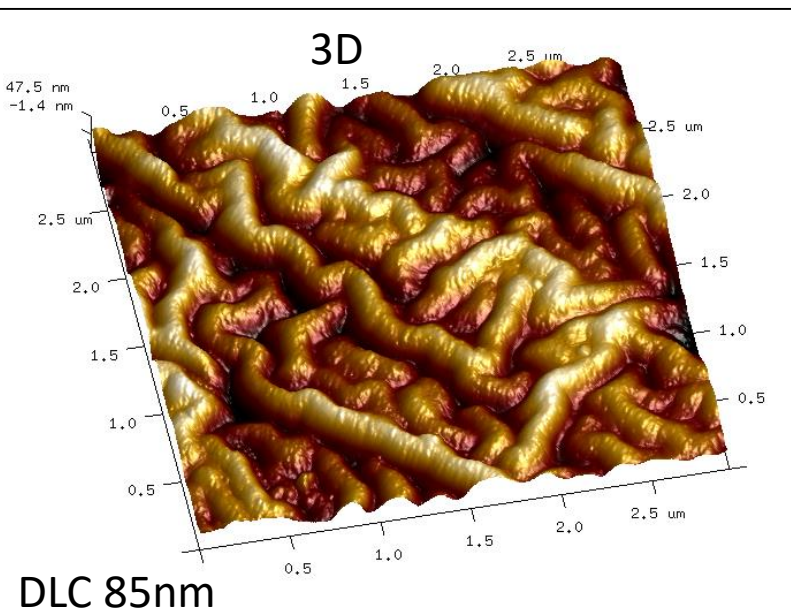
TEM BF

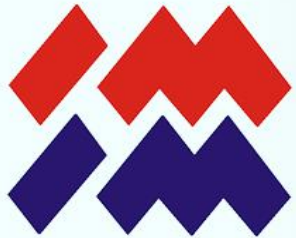
Transmission electron microscopy analysis:
Cross section





Bio-inspired materials





„Bio-inspired thin film materials with the controlled contribution of the residual stress in terms of the restoration of stem cells microenvironment”

2014/13/B/ST8/04287

CELL-MATERIAL INTERACTION

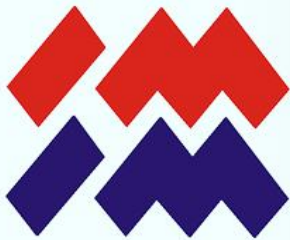


Confocal microscopy



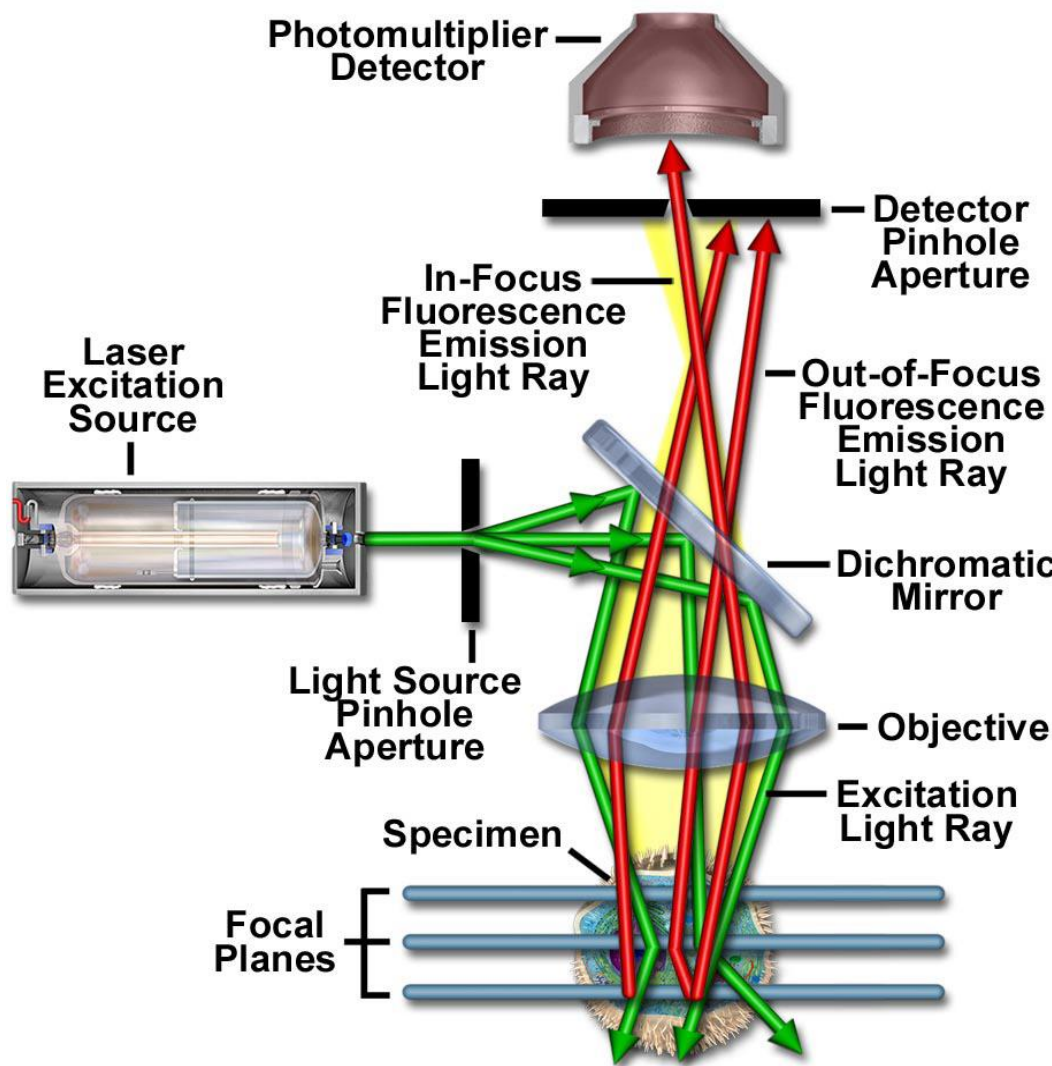
- Confokal Modul LSM 5 Exciter, two canals, RGB
- Laser HeNe 633nm 5mW
- Laser HeNe 543nm 1mW
- Laser argon 458/488/514nm, 25mW
- Laser diodowy V 405nm
- Main Beam Splitter turret PASCAL
- Software ZEN 2008 LSM 5 EXCITER
- Light division system (405, 458, 488, 514, 543 nm)
- Filtr BP 505-530
- Filtr BP 505-600
- Filtr BP 530-600
- Filtr BP 560-615
- Filtr LP 420
- Filtr BP 420-480
- System ECU LSM 5 EXCITER
- Moduł DIC I/0,9 z polaryzatorem
- Transmited light detector T-PMT LSM 710





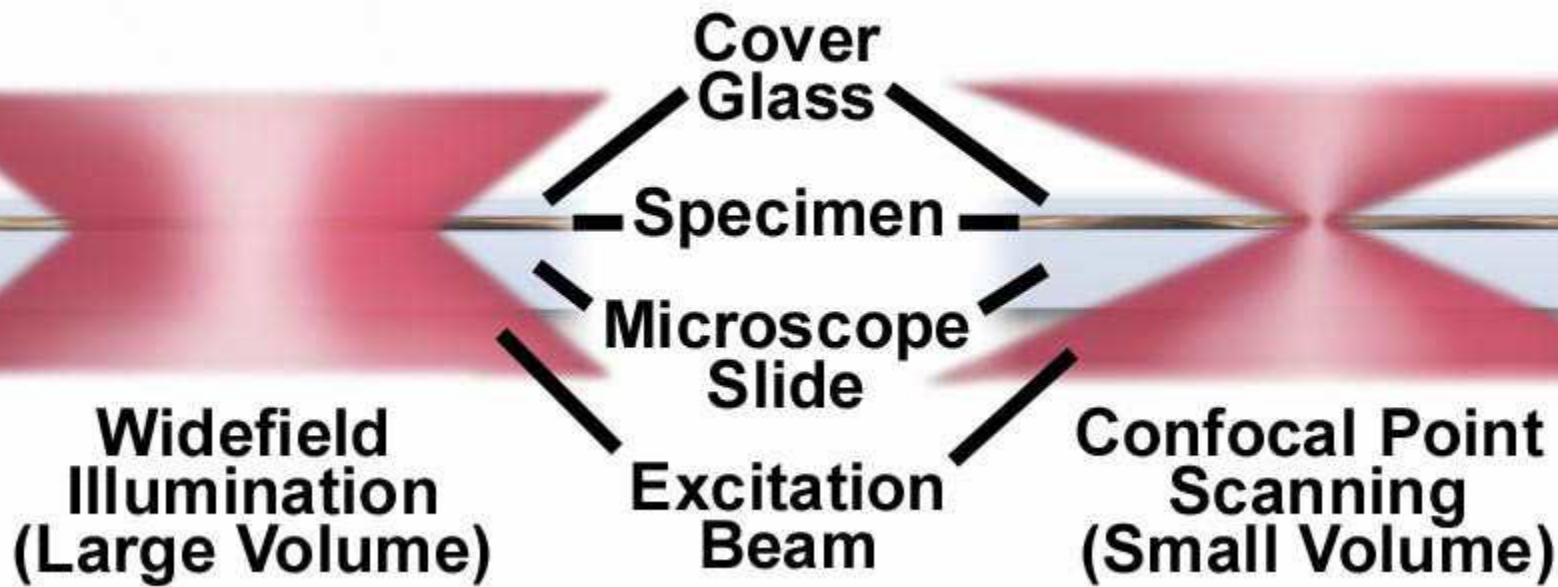
Confocal microscopy

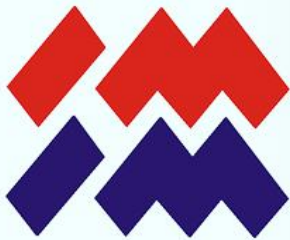
Layout



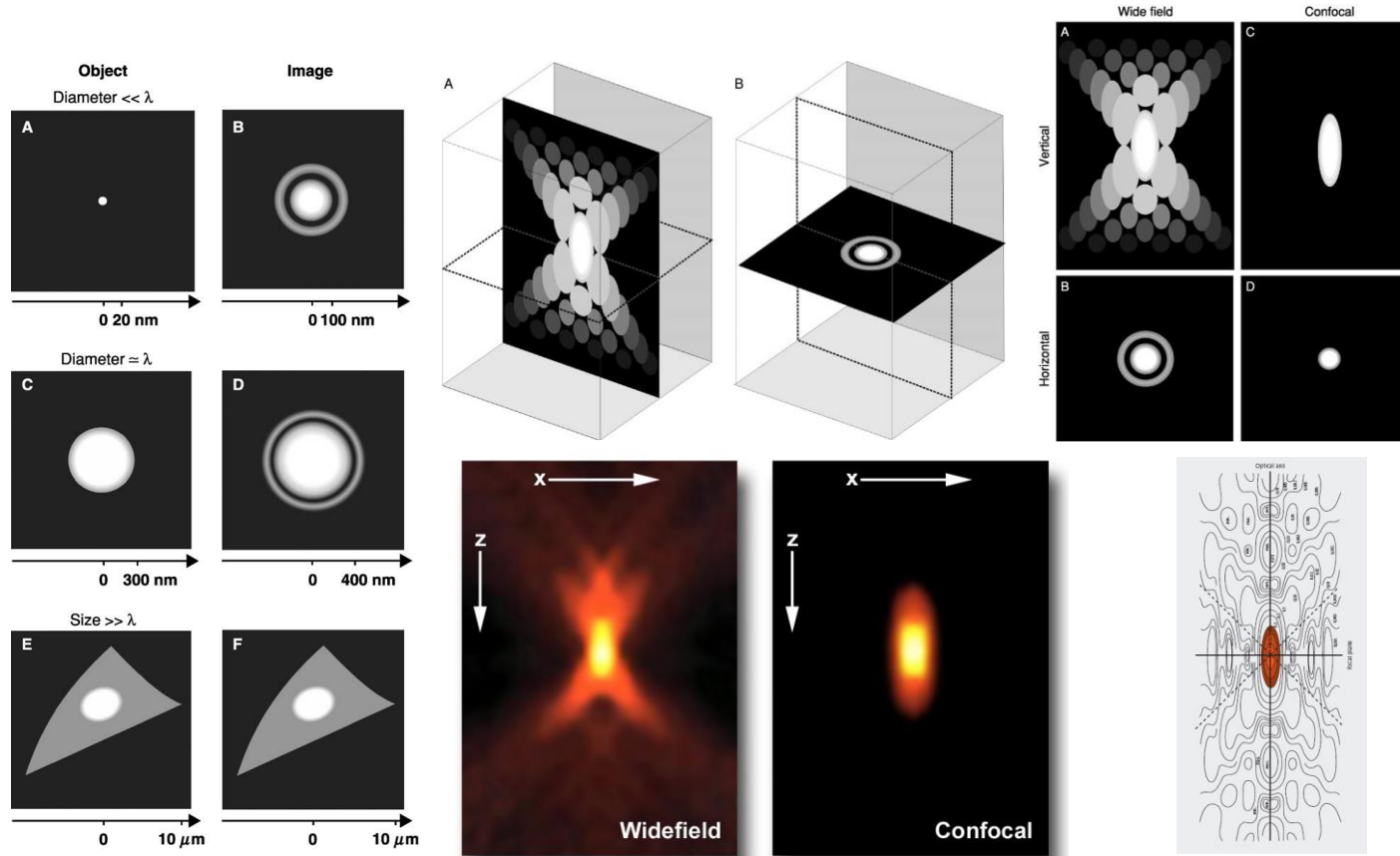


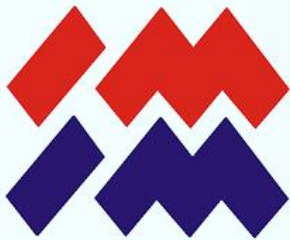
Confocal microscopy





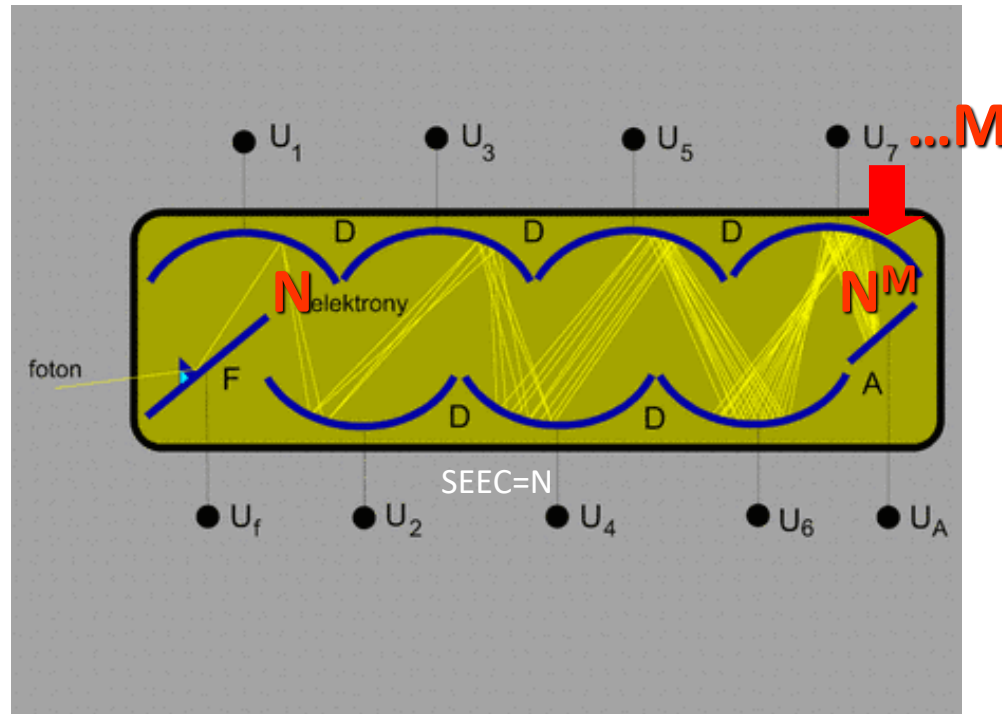
Confocal microscopy

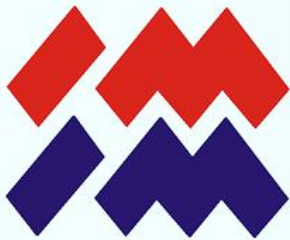




Confocal microscopy

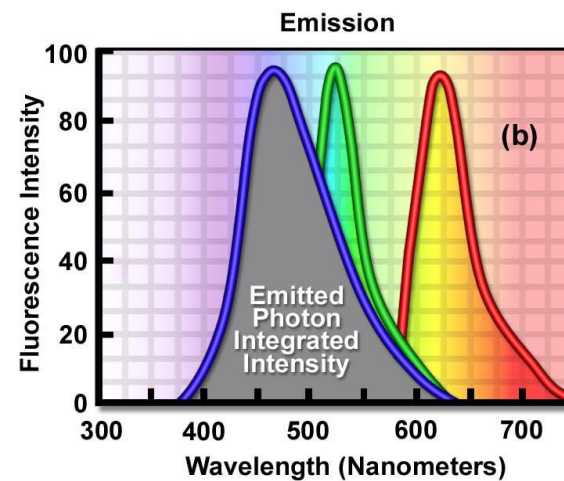
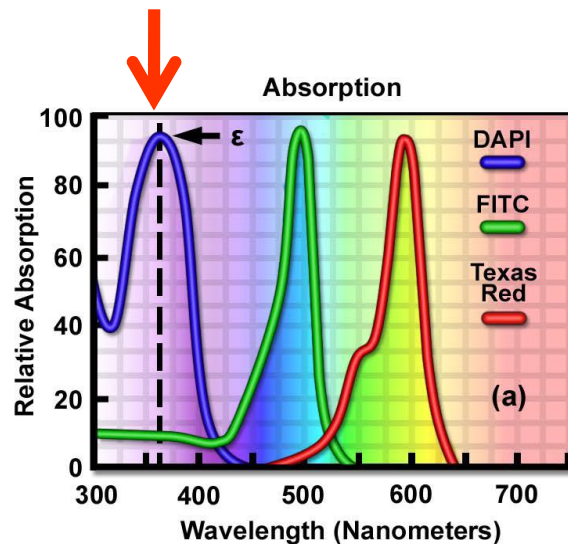
Photomultiplier





Confocal microscopy

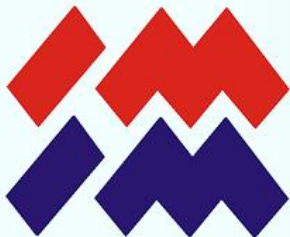
Fluorochromes



Absorptive and fluorescent properties

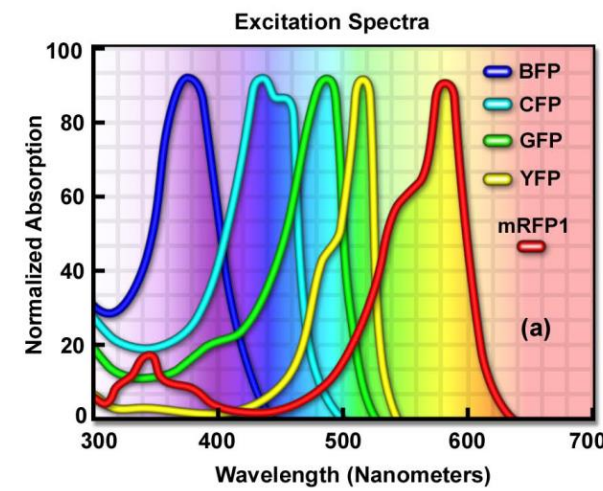
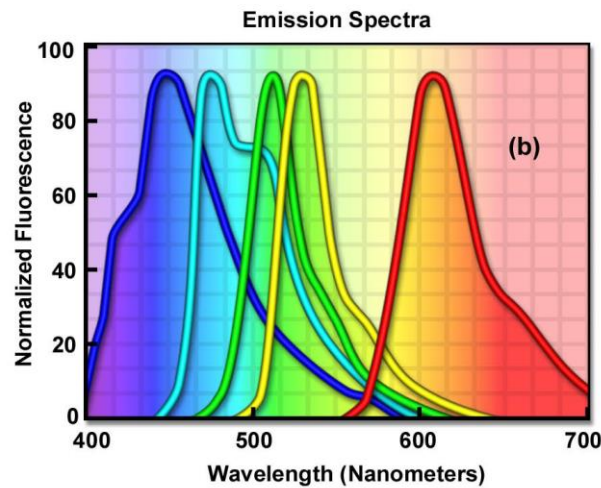
Wavelength of maximum absorption and emission

Intensity of fluorescence of emitted light

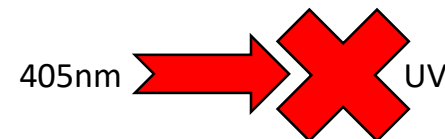


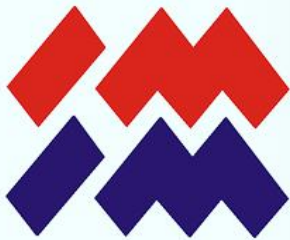
Confocal microscopy

Excitation and imaging



- 488 nm blue-green argon laser
- 543 nm helium-neon green laser
- 633 nm helium-neon red laser





Confocal microscopy

1. Cytotoxicity

2. Photobleaching

Differential Photobleaching in Multiply-Stained Tissues

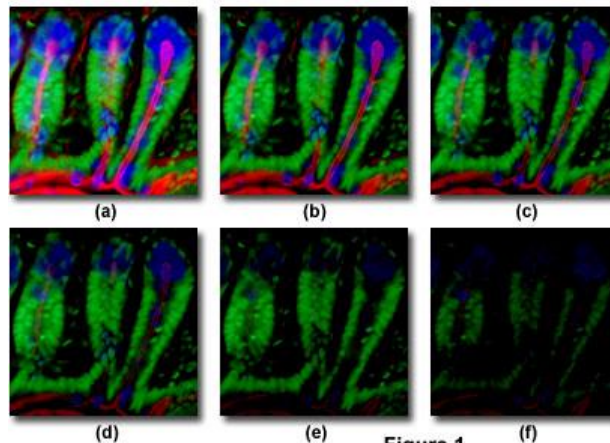


Figure 1

Photobleaching Rates in Multiply Stained Specimens

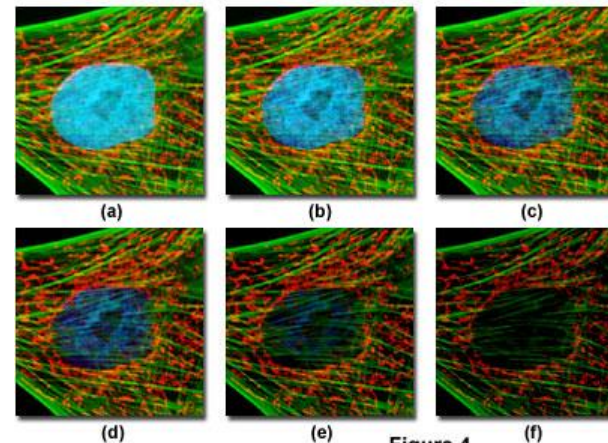


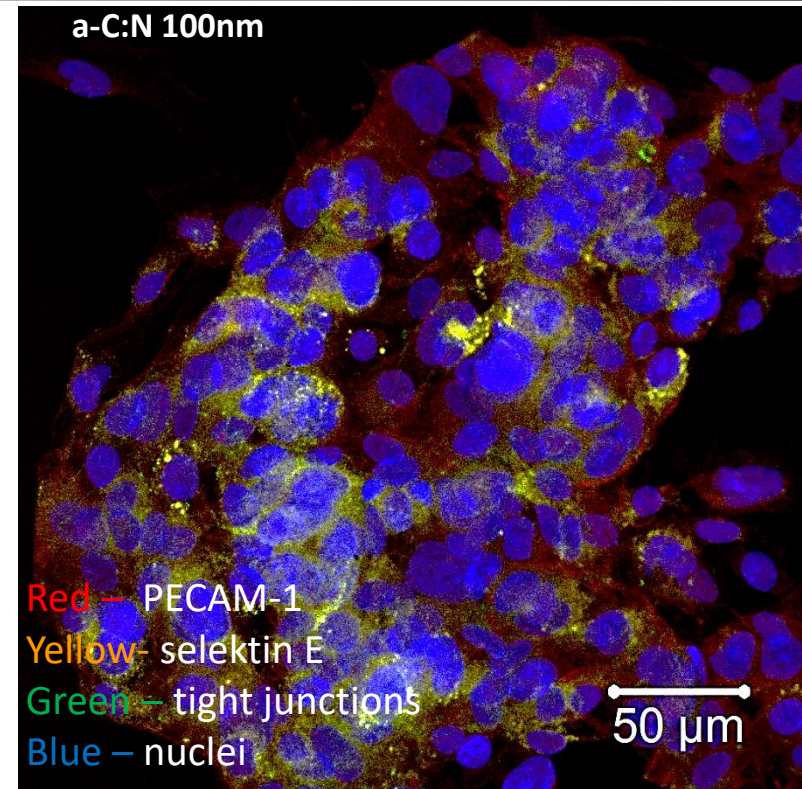
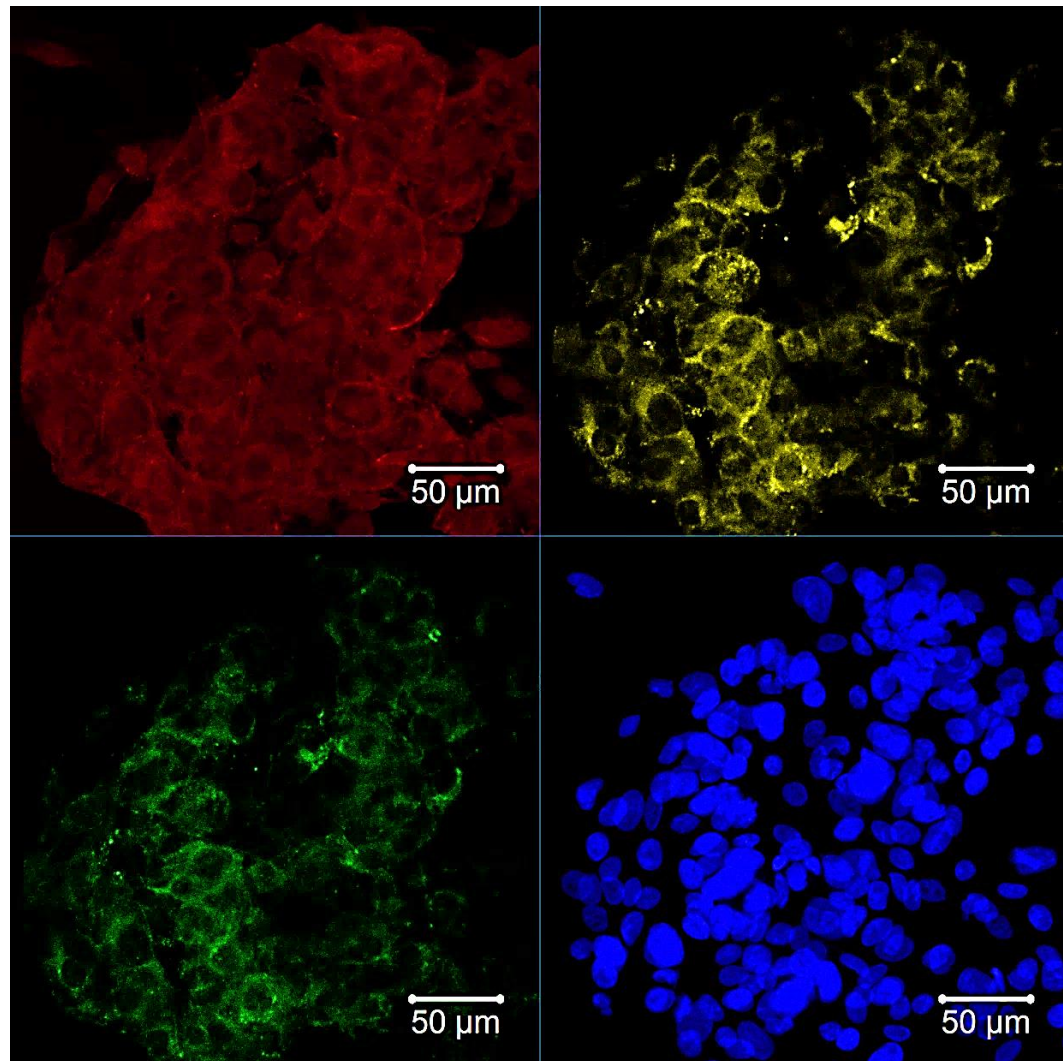
Figure 4

3. Phototoxicity

FRAP (mov) Laser twisers (mov)



Bio-inspired materials



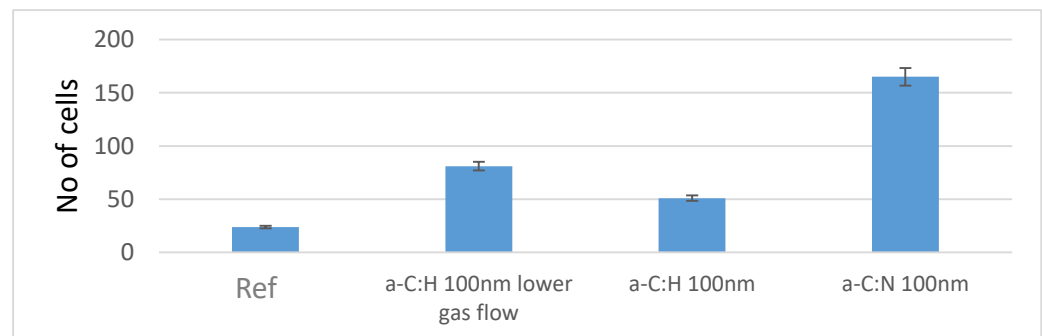
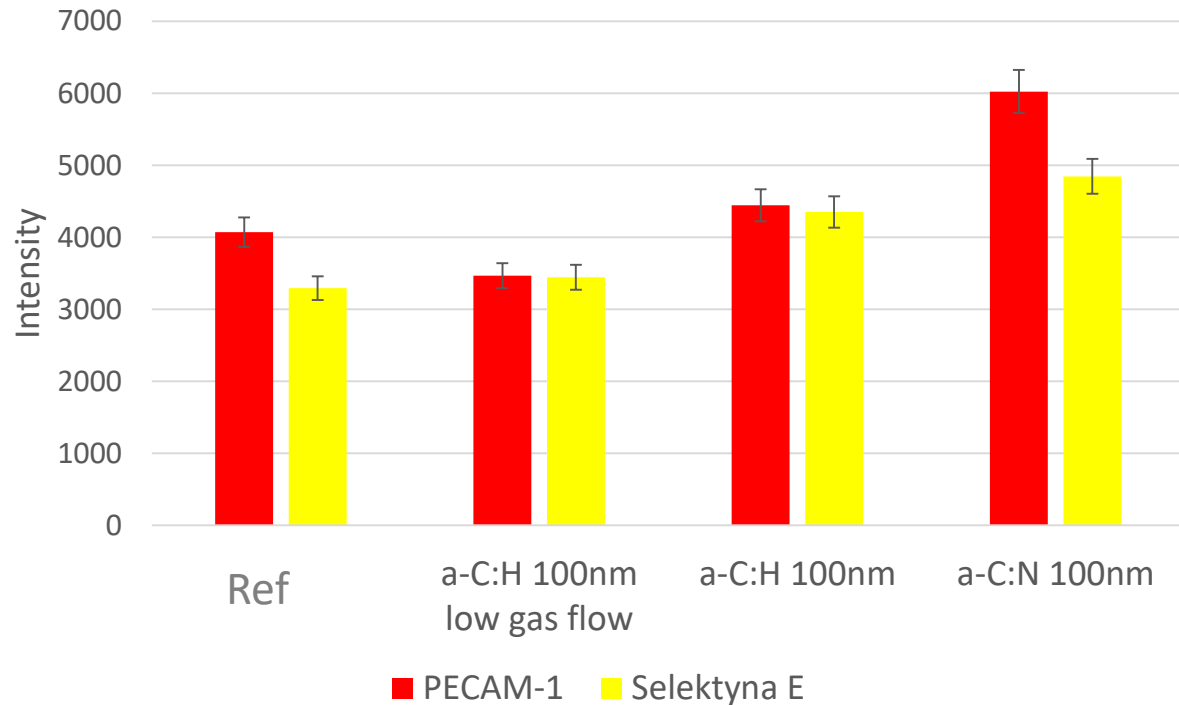
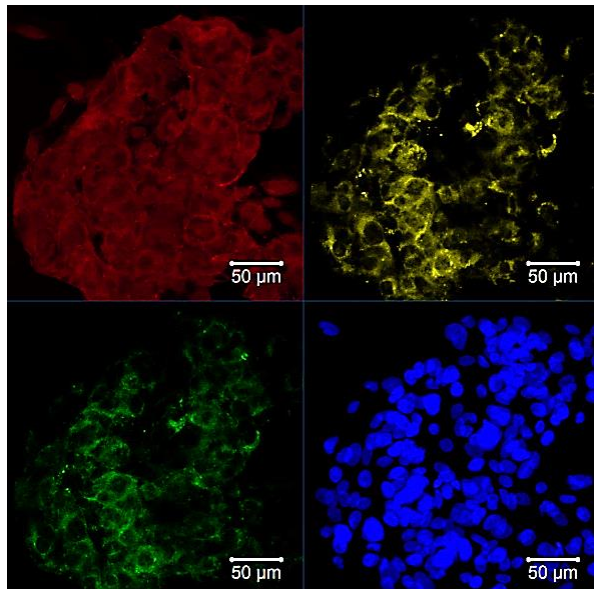


Bio-inspired materials

PLT-Endoth. Cell adhesive molecule

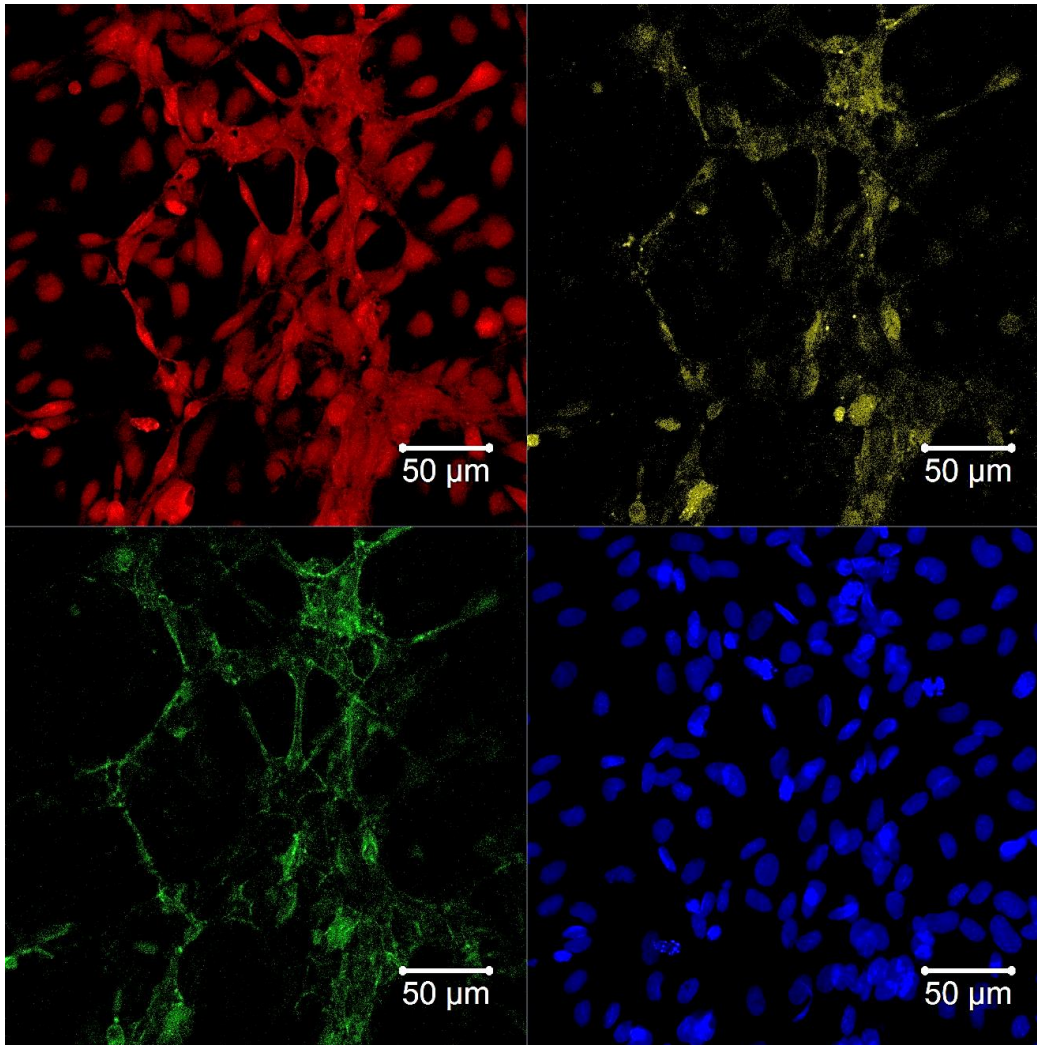
Klaster of differentiation 31

E-selektyna, antybody CD62 (CD62E),
Endoth.- leuc. Cell adhesive molecule





Bio-inspired materials



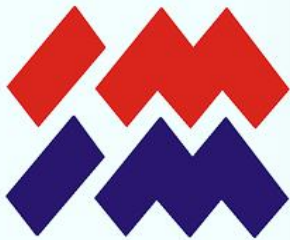
Optimal

Red – PECAM-1

Yellow- selektin E

Green – tight junctions

Blue – nuclei

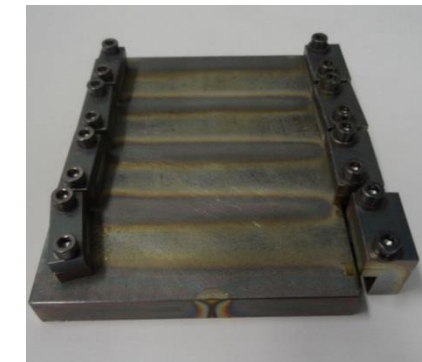
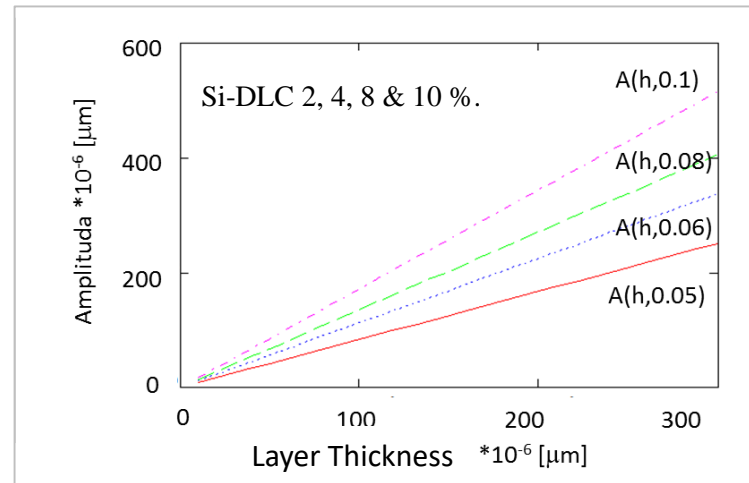
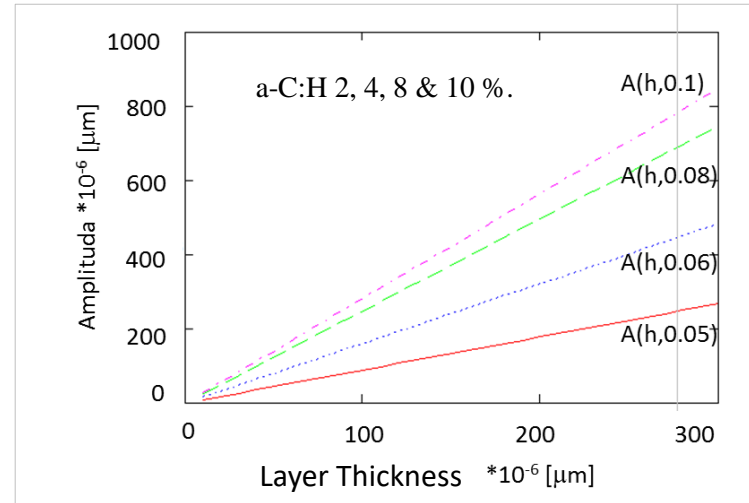


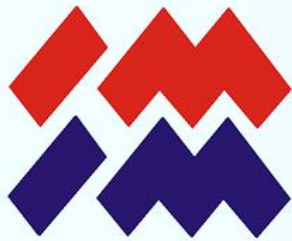
Bio-inspired materials

Wrinkles by strain

$$A(h, ed) = h \sqrt{\frac{ed}{ec} - 1}$$

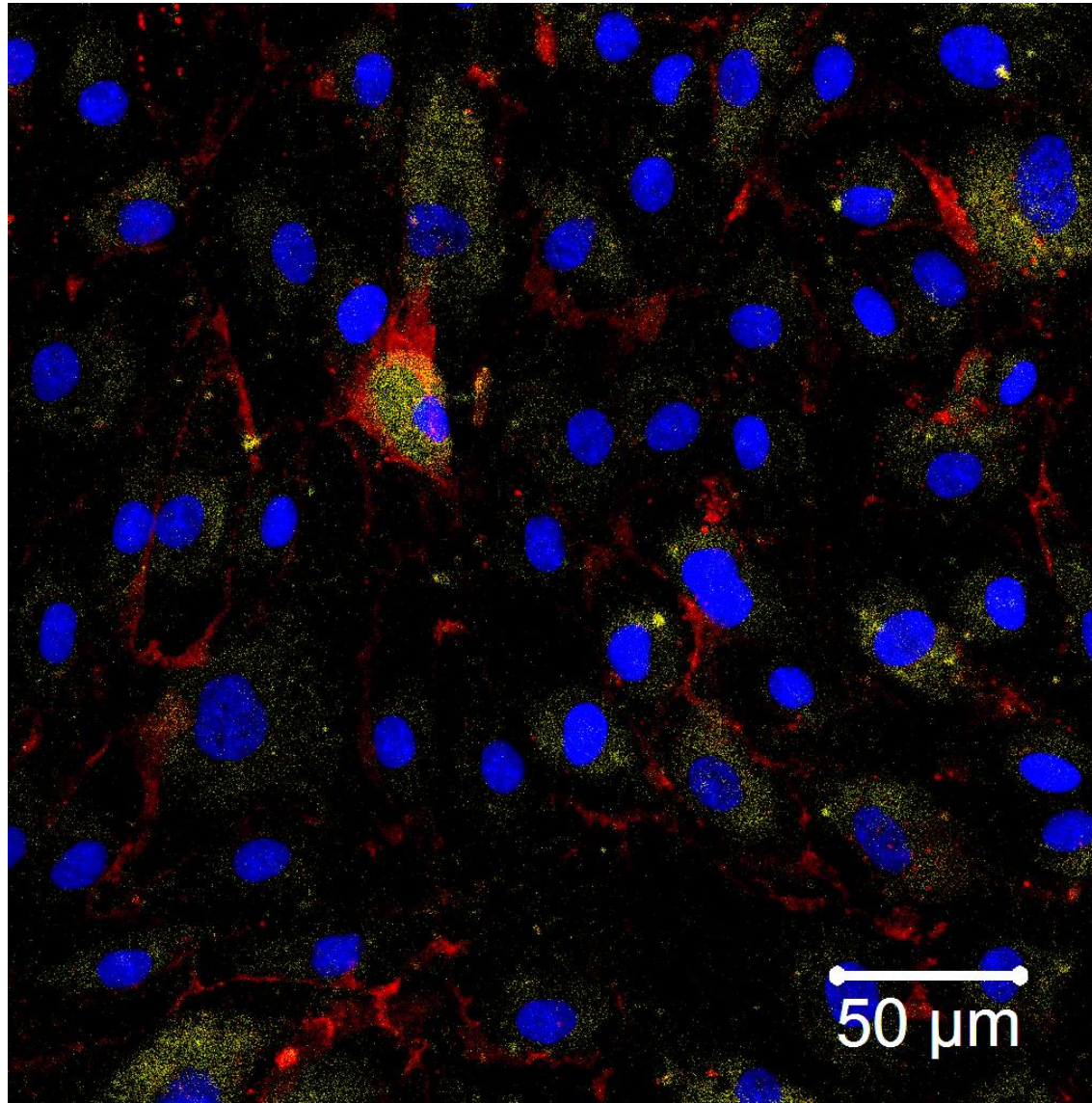
$$ec = 0,25 \left(\frac{3E_s}{E_f} \right)^2$$





Wrinkles by strain

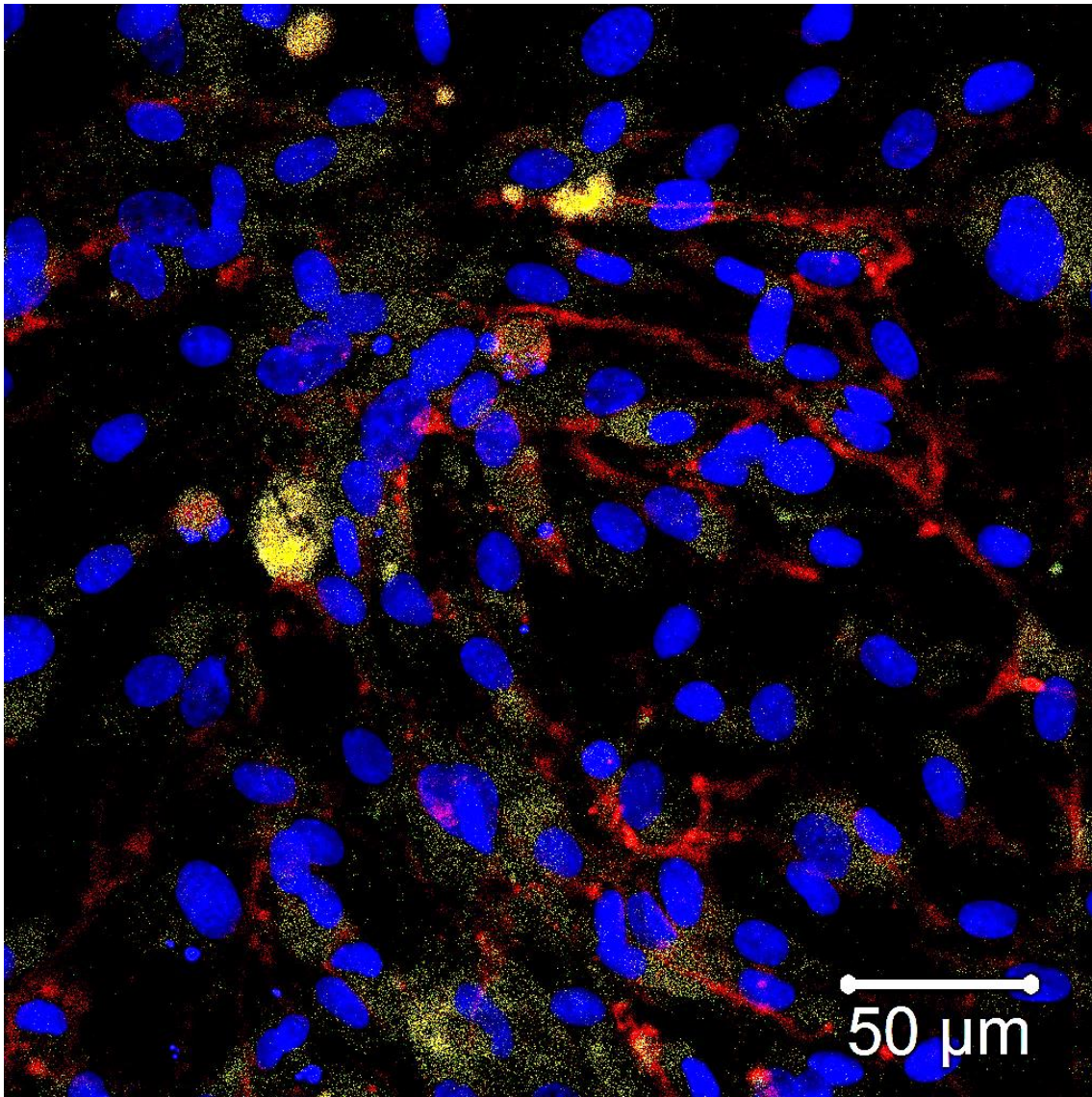
0%

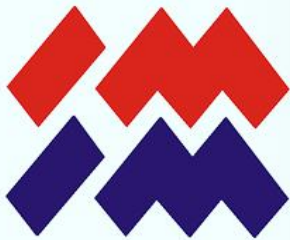




Wrinkles by strain

3%

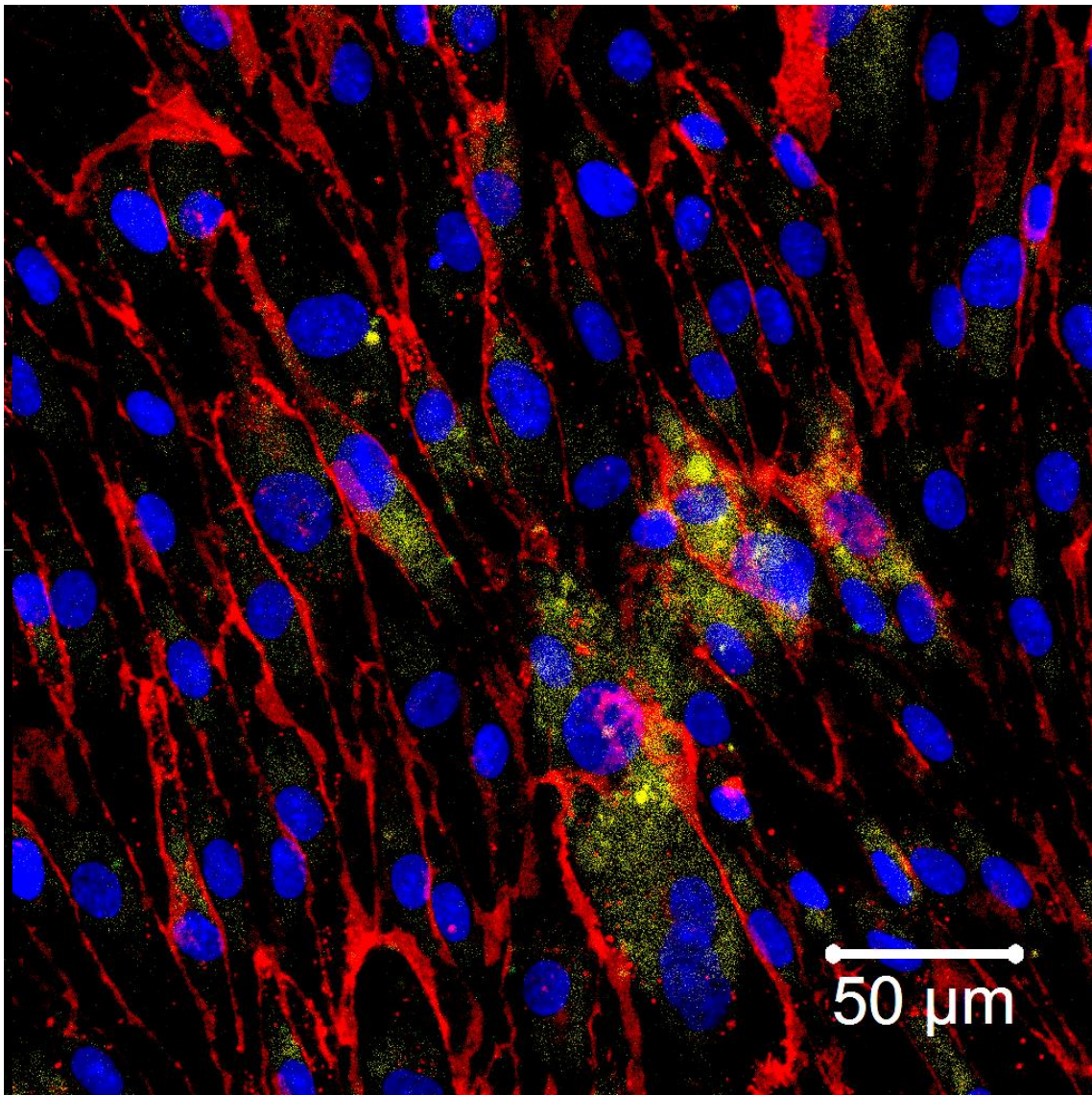


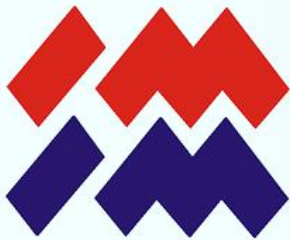


Bio-inspired materials

Wrinkles by strain

5%

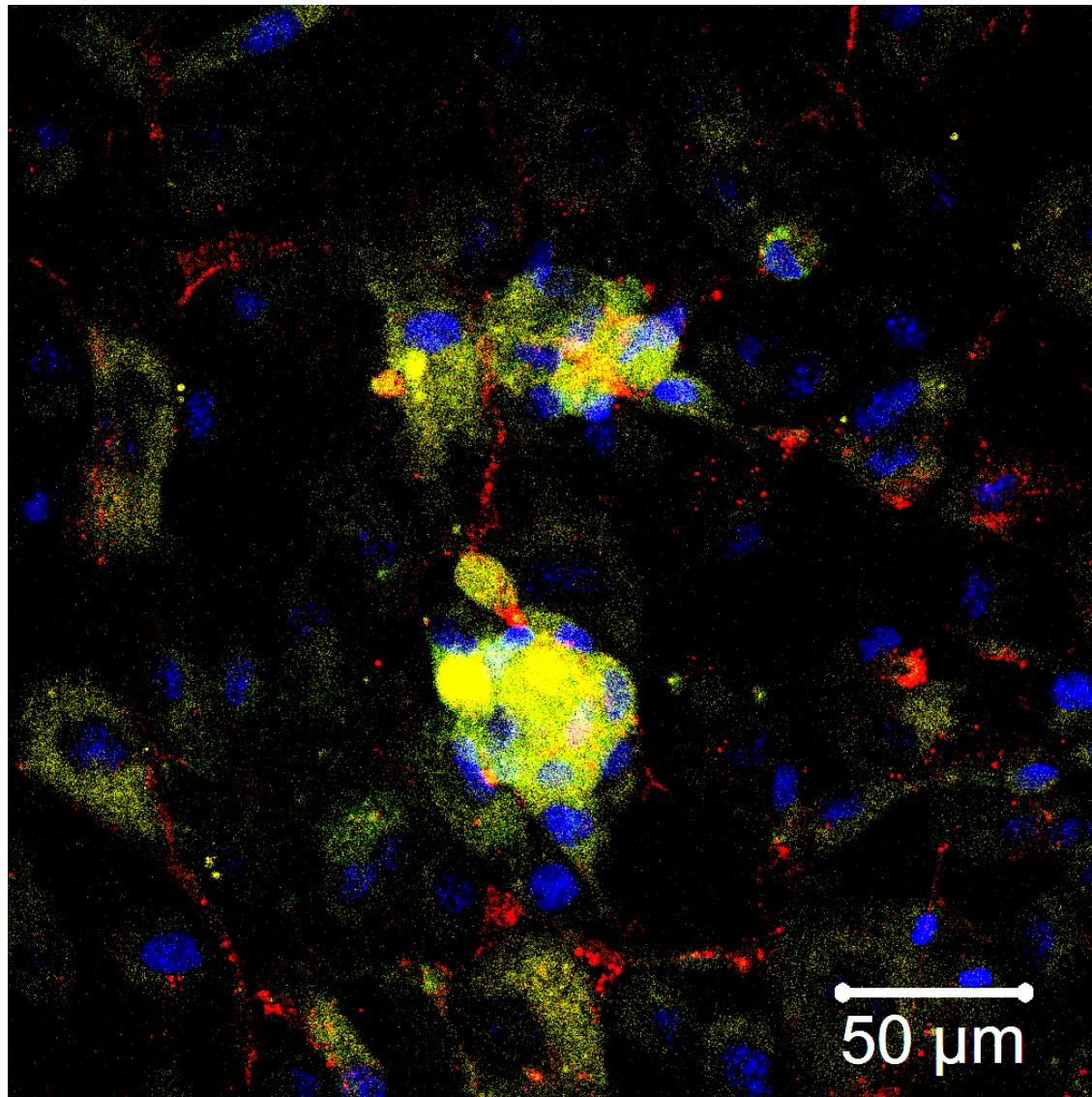


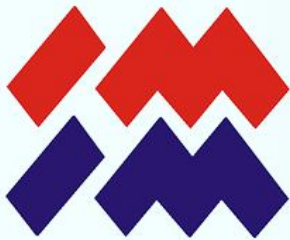


Bio-inspired materials

Wrinkles by strain

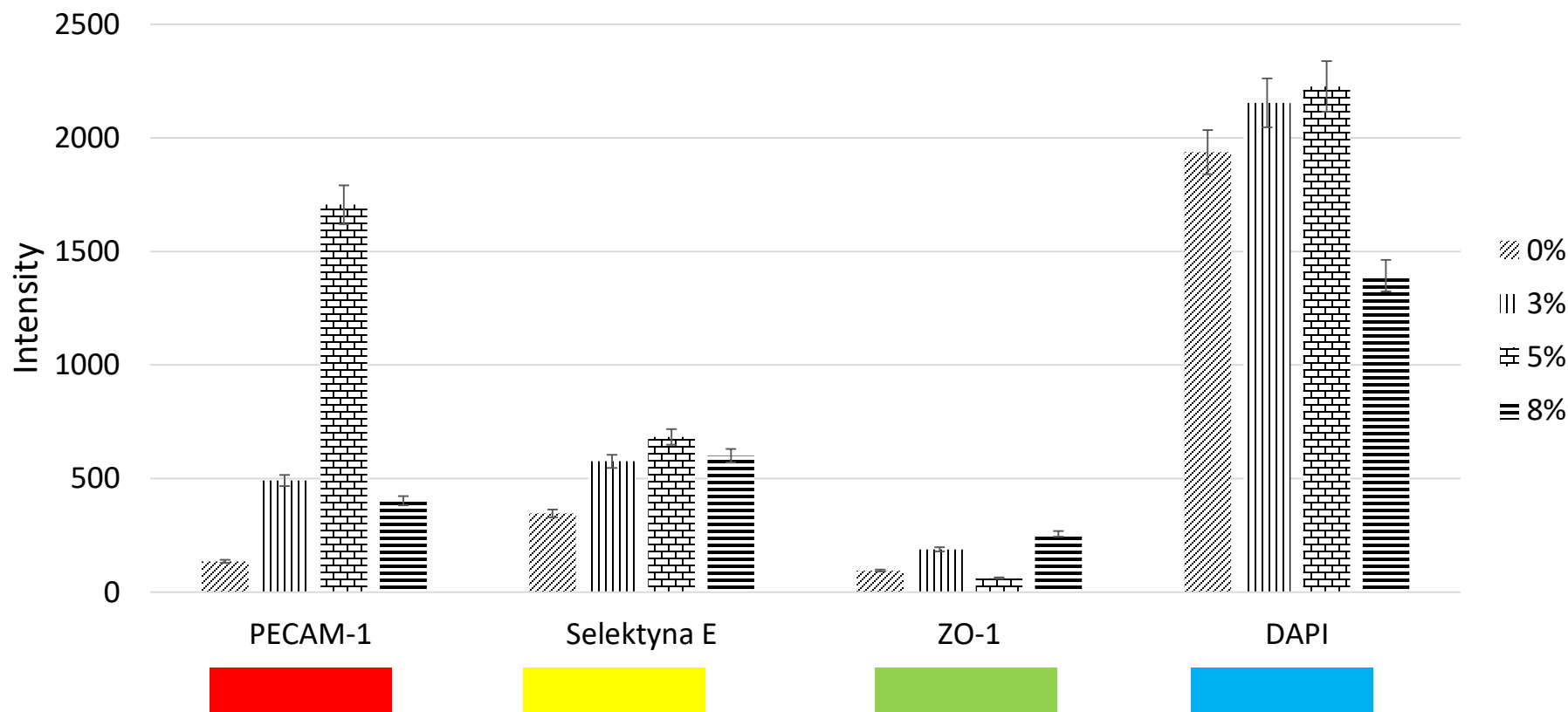
8%

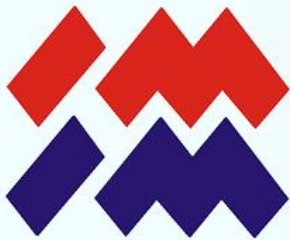




Bio-inspired materials

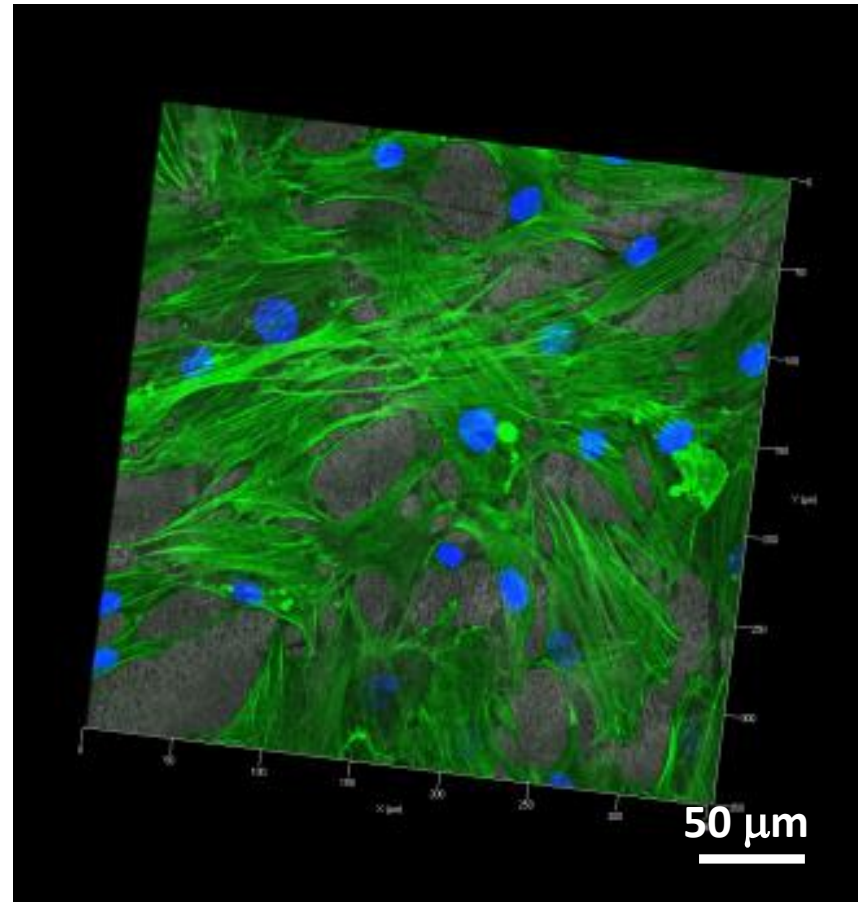
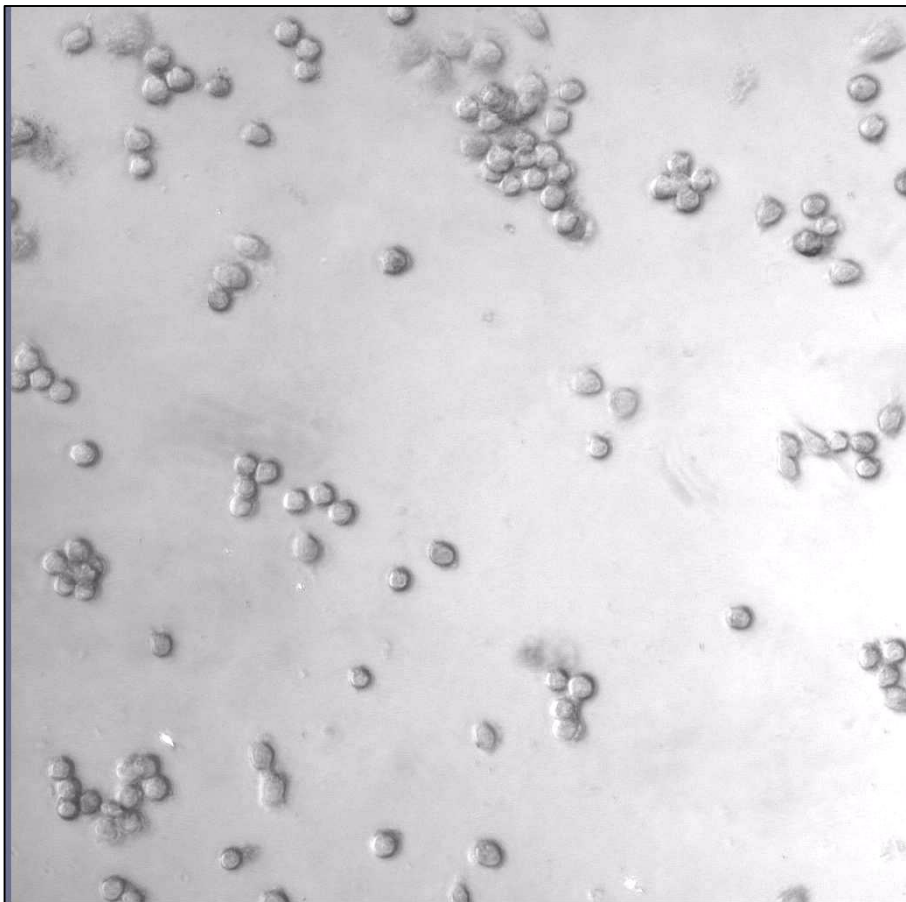
Wrinkles by strain

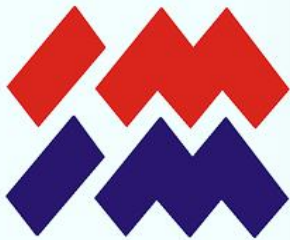




Bio-inspired materials

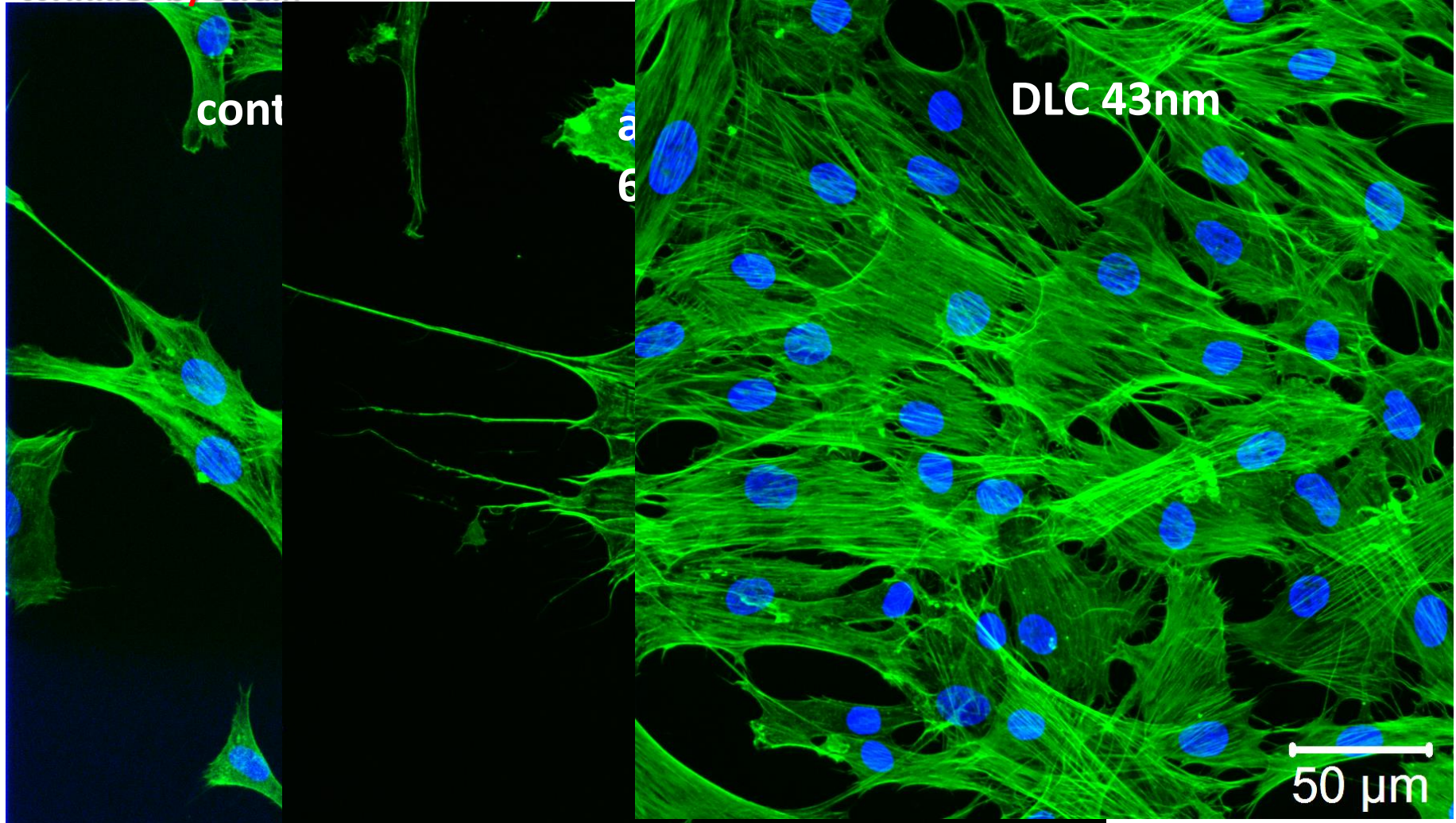
DLC 85nm

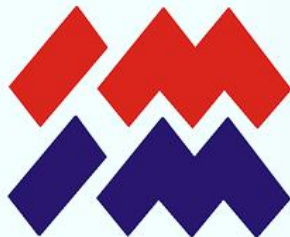




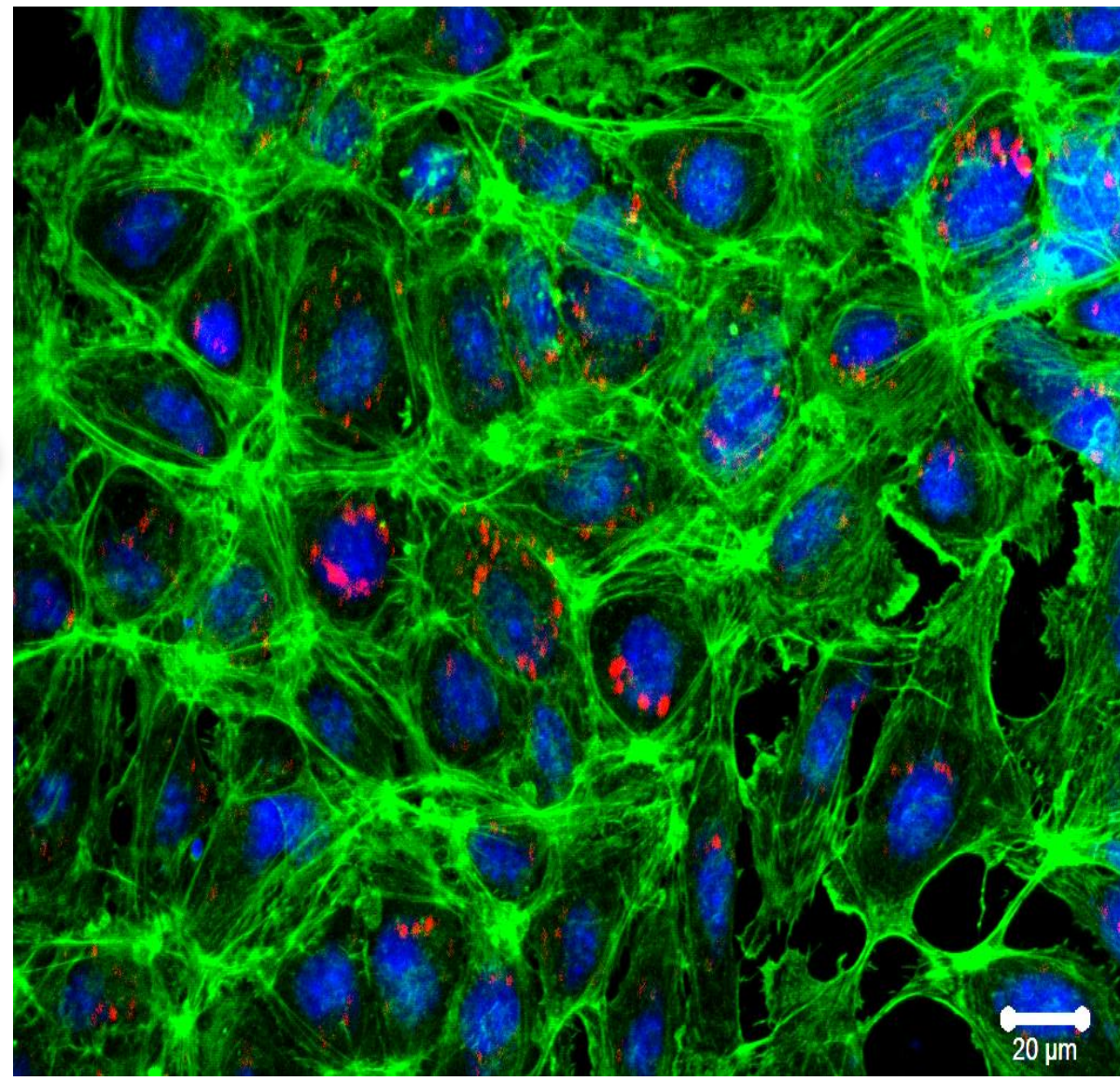
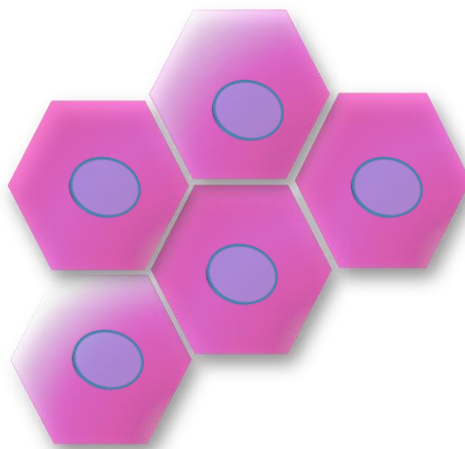
Bio-inspired materials

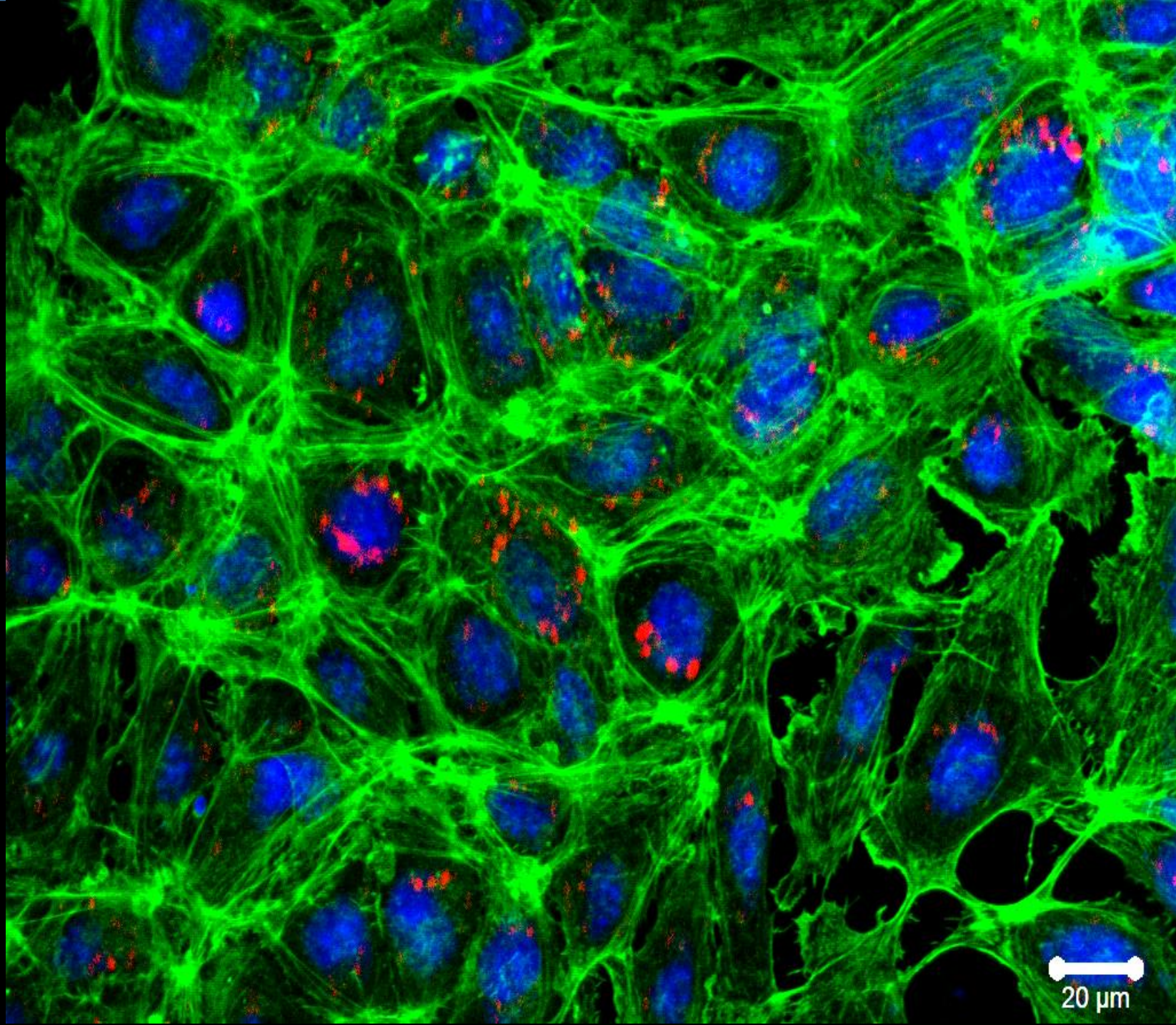
Wrinkles by strain





Bio-inspired materials







„Bio-inspired thin film materials with the controlled contribution of the residual stress in terms of the restoration of stem cells microenvironment”

2014/13/B/ST8/04287

BLOOD-MATERIAL INTERACTION



Bio-inspired materials

Whole human blood dynamic tests



ELSEVIER

Biomolecular Engineering 19 (2002) 91–96

**Biomolecular
Engineering**

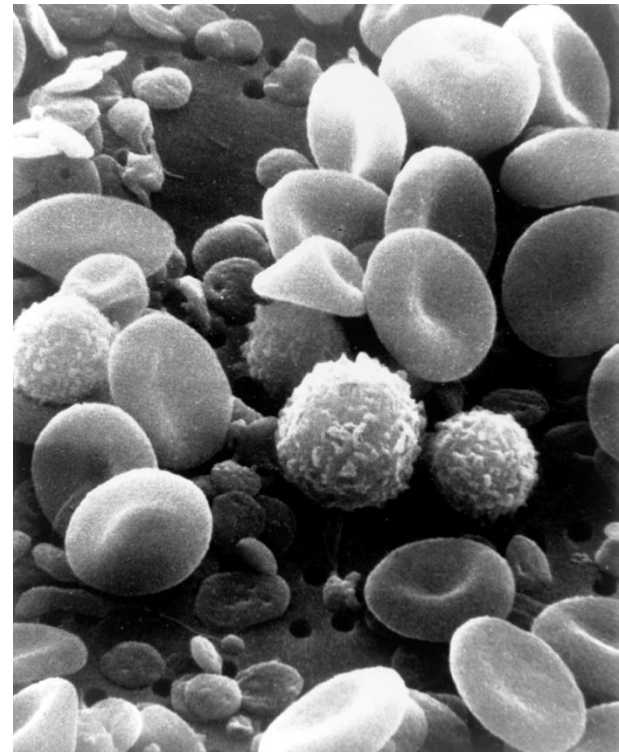
www.elsevier.com/locate/geneanbioeng

In vitro hemocompatibility testing of biomaterials according to the
ISO 10993-4

Ulrich Theo Seyfert ^{a,*}, Volker Biehl ^b, Joachim Schenk ^a

^a Abteilung Klinische Hämostaseologie und Transfusionsmedizin, Haus 75, Universitätskliniken, D-66421 Homburg, Germany

^b Universität des Saarlandes, Lehrstuhl für Metallische Werkstoffe, Im Stadtwald, D-66123 Saarbrücken, Germany

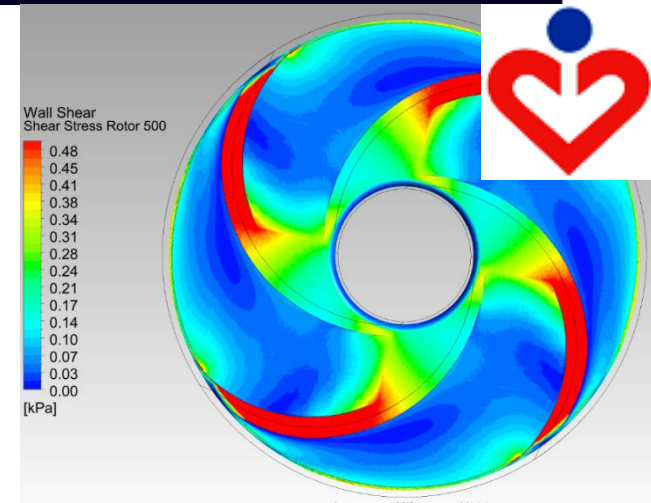
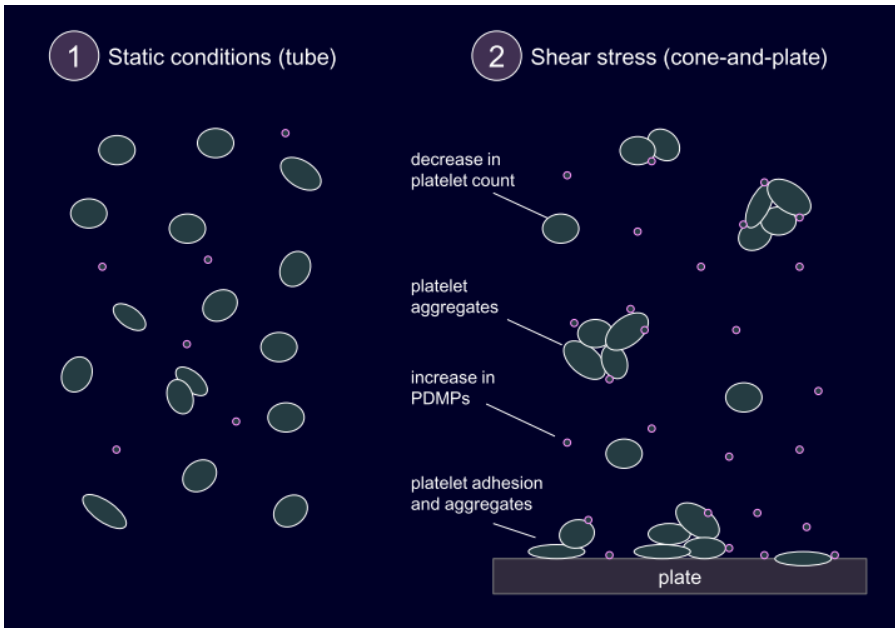
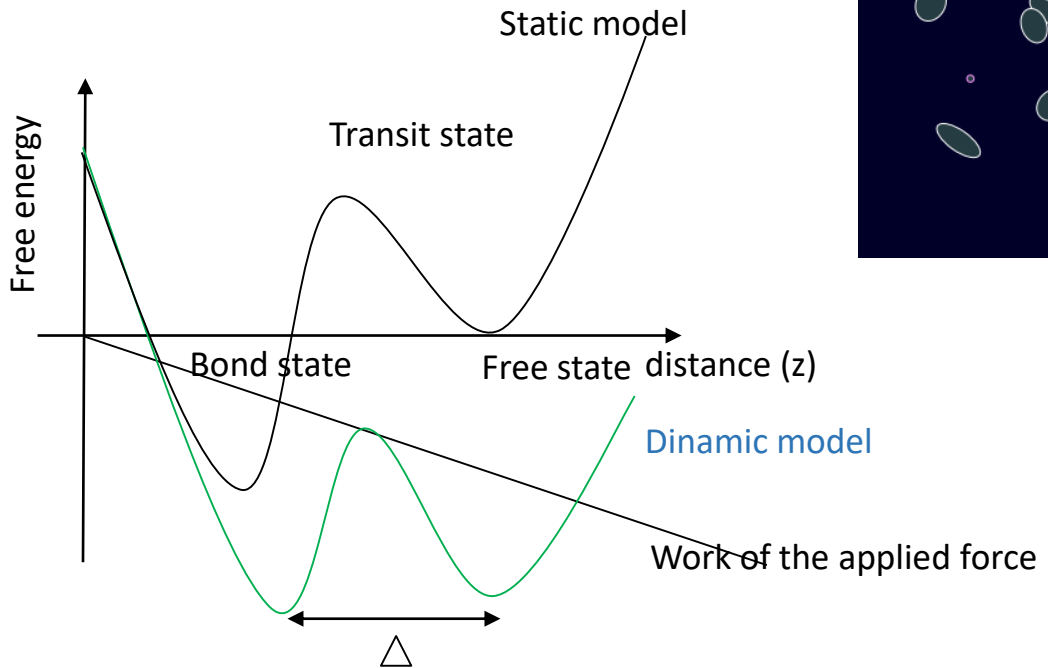


“A hemocompatible material must not adversely interact with any blood component”



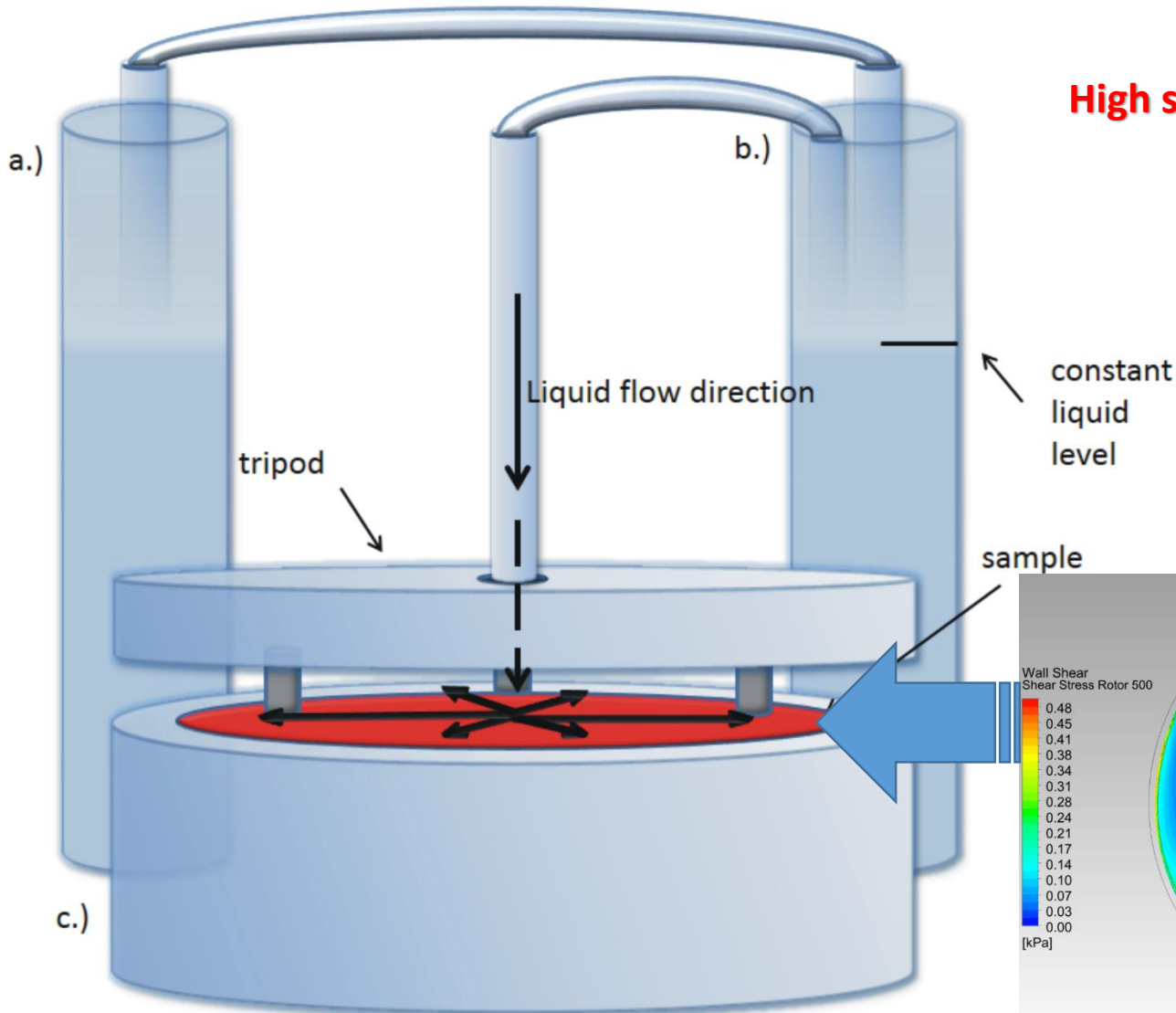
Bio-inspired materials

Material	Composition	Thickness
C170_2	a-C:H	100nm
C170_4	Si-DLC	500nm
C170_5	Si-DLC	300nm
C170_6	Si-DLC	200nm
C170_7	Si-DLC	125nm
C170_8	Si-DLC	15nm



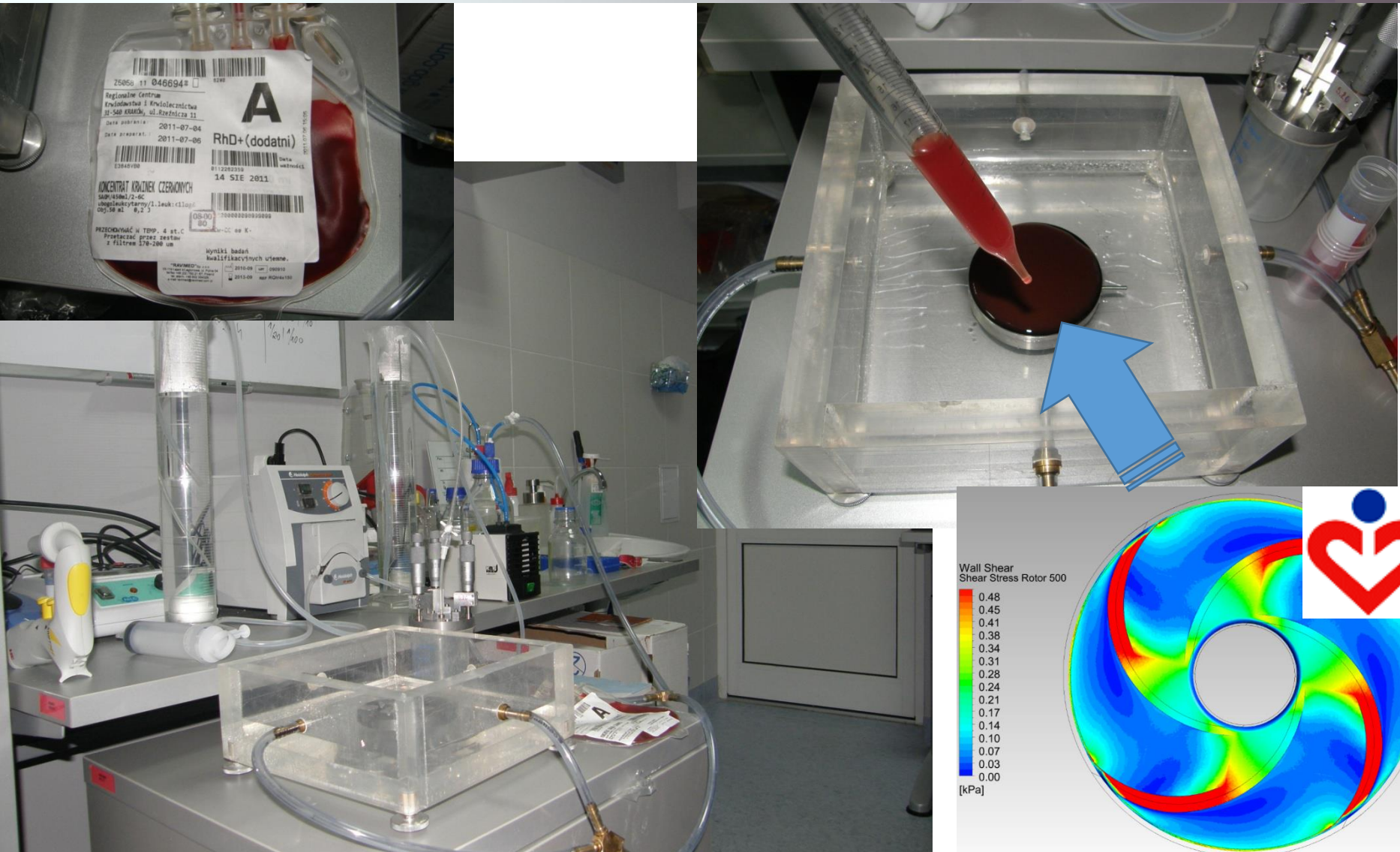


Bio-inspired materials





Bio-inspired materials



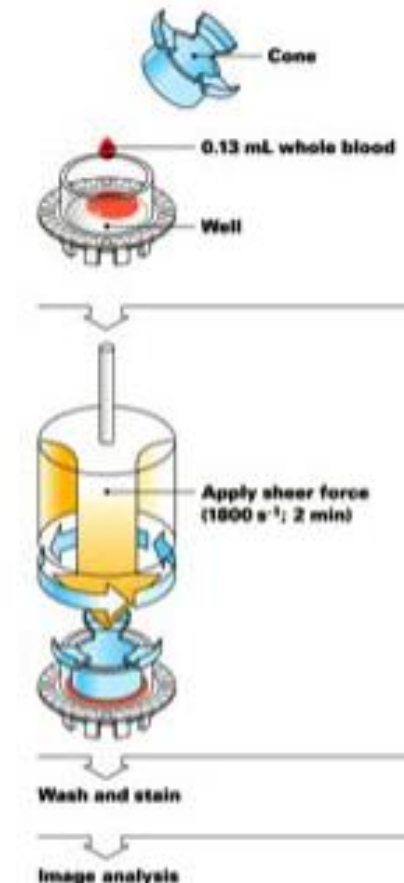
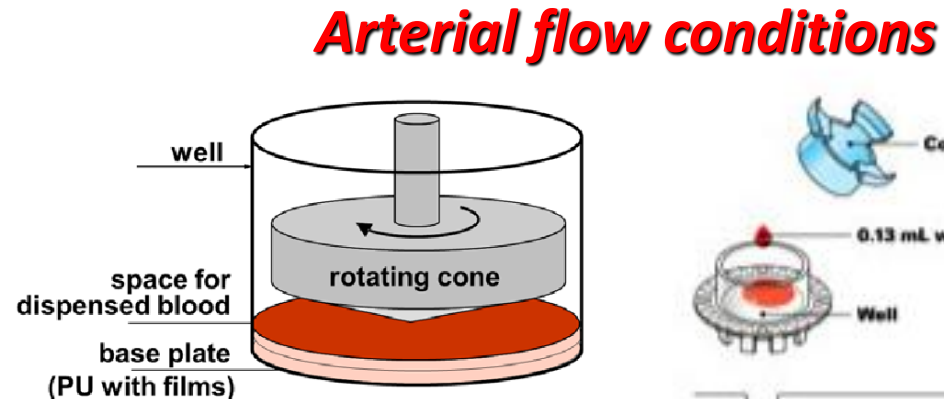
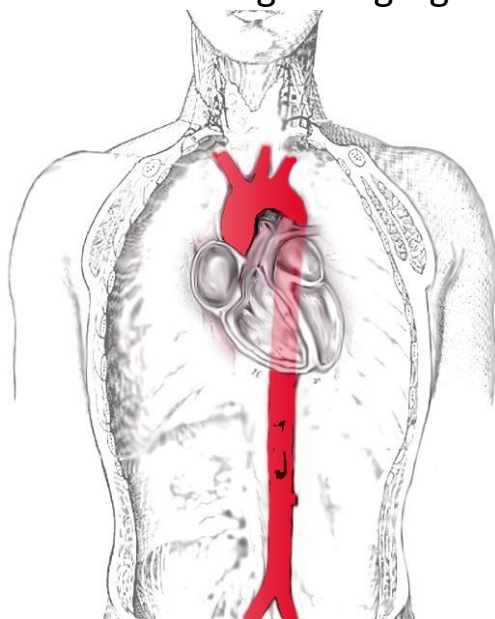


Bio-inspired materials

- Human blood (4 x 4.5 mL)
- ADP activation 5 min.
- Arterial flow condition simulation.
- 130 µL after the test.

Analysis:

- Platelet marker expression CD61
- PAC-1 glycoprotein IIb/IIIa
- CD62P for P-selectin
- Small and big PLT aggregates





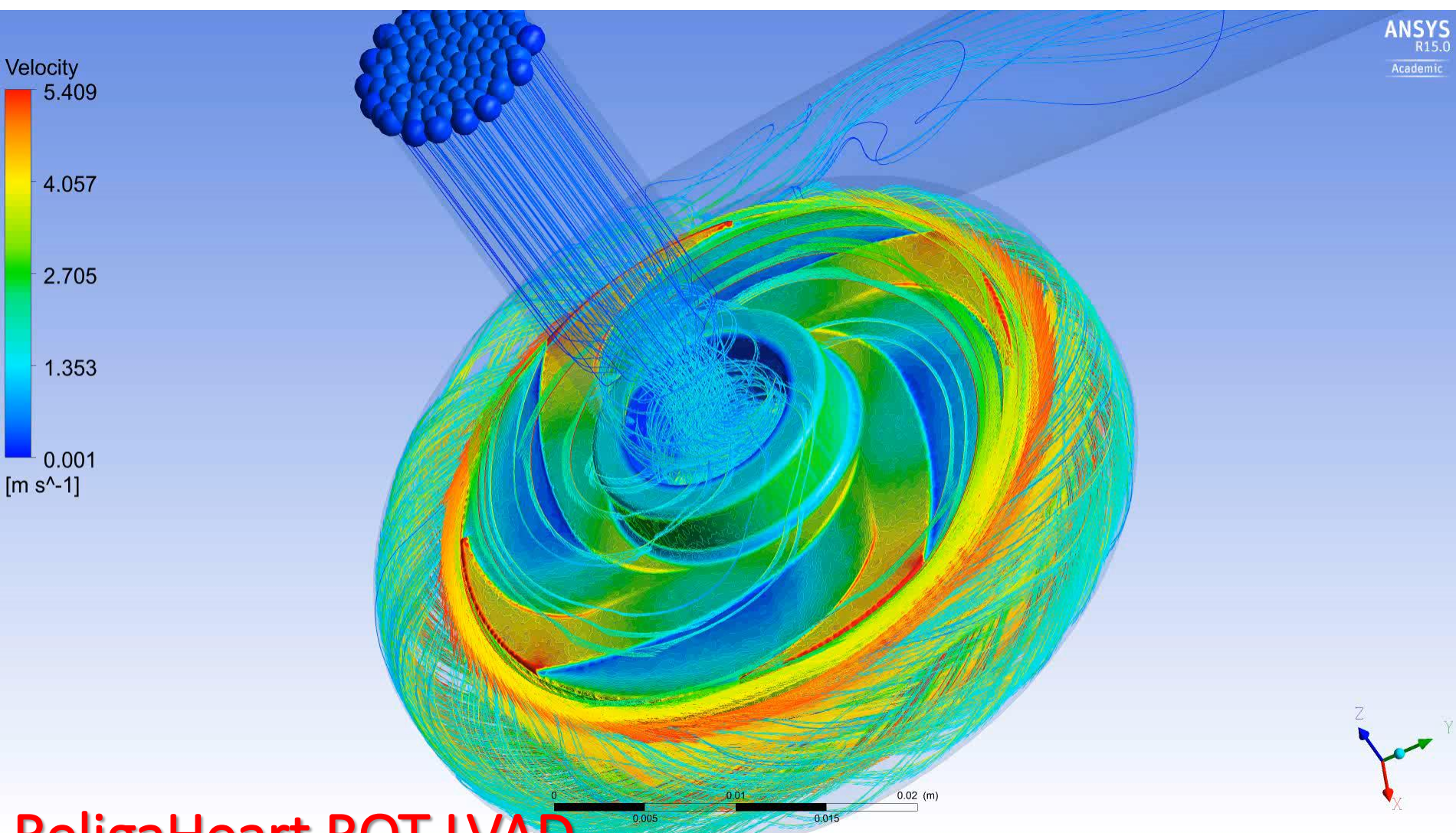
Bio-inspired materials

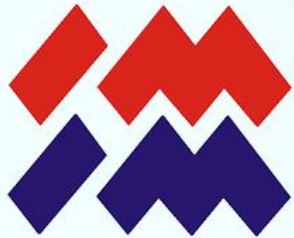


ReligaHeart ROT LVAD



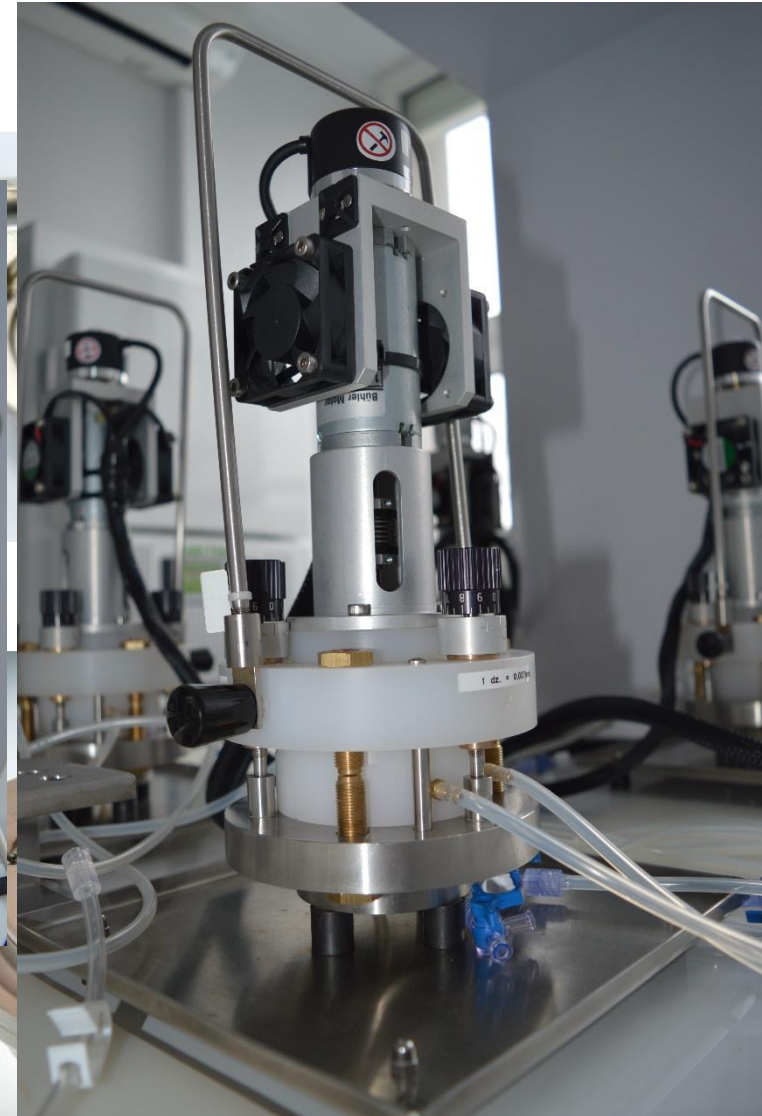
Bio-inspired materials

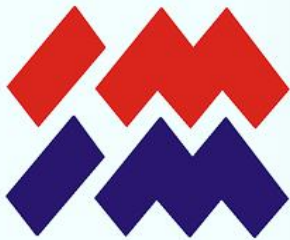




Bio-inspired materials

Tester IMIM PAN



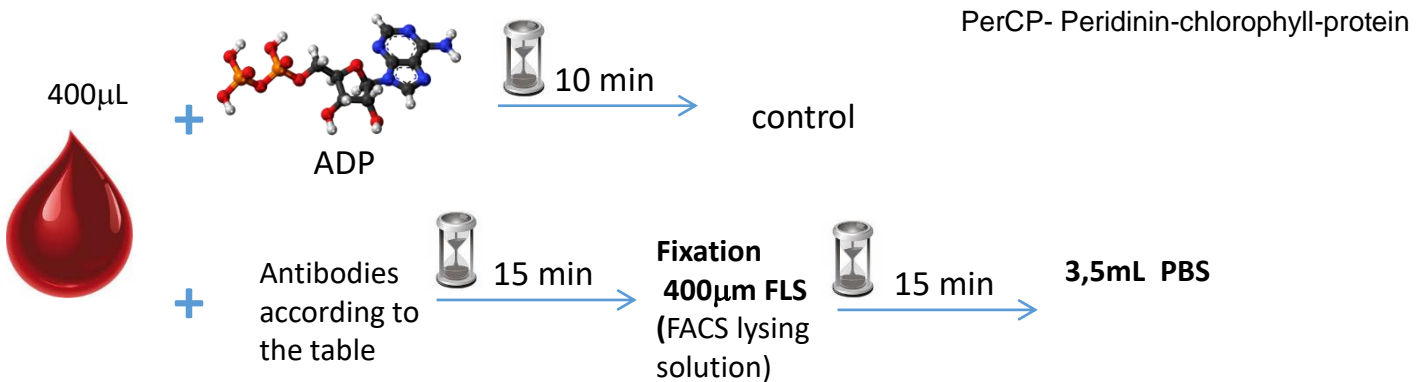


Bio-inspired materials

Blood-Material Interaction

Tester IMIM PAN

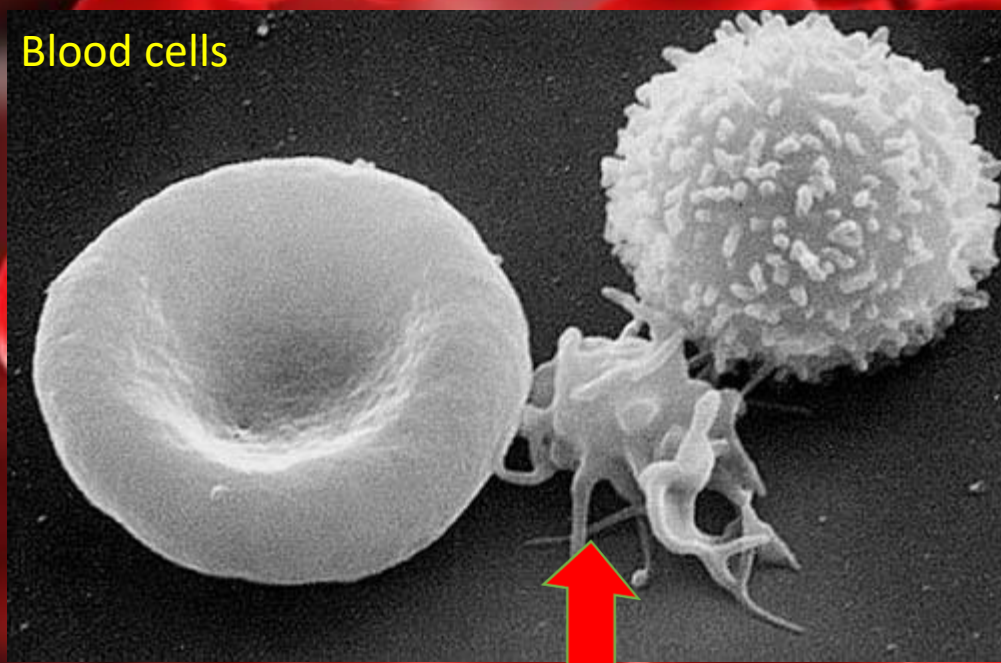
Name	Composition	Application
M	CD61-PerCP, CD62P, PAC-1	assessment of platelet activation under the influence of contact with the material (+ control)
A	CD61-PerCP, CD62P, PAC-1	assessment of platelet activation using ADP
ADP 1	ADP 0.4mM	Positive control
ADP	ADP 40mM	Kontrola pozytywna





Bio-inspired materials

CLSM-
CONFOCAL LASER SCANNING MICROSCOPY





Bio-inspired materials

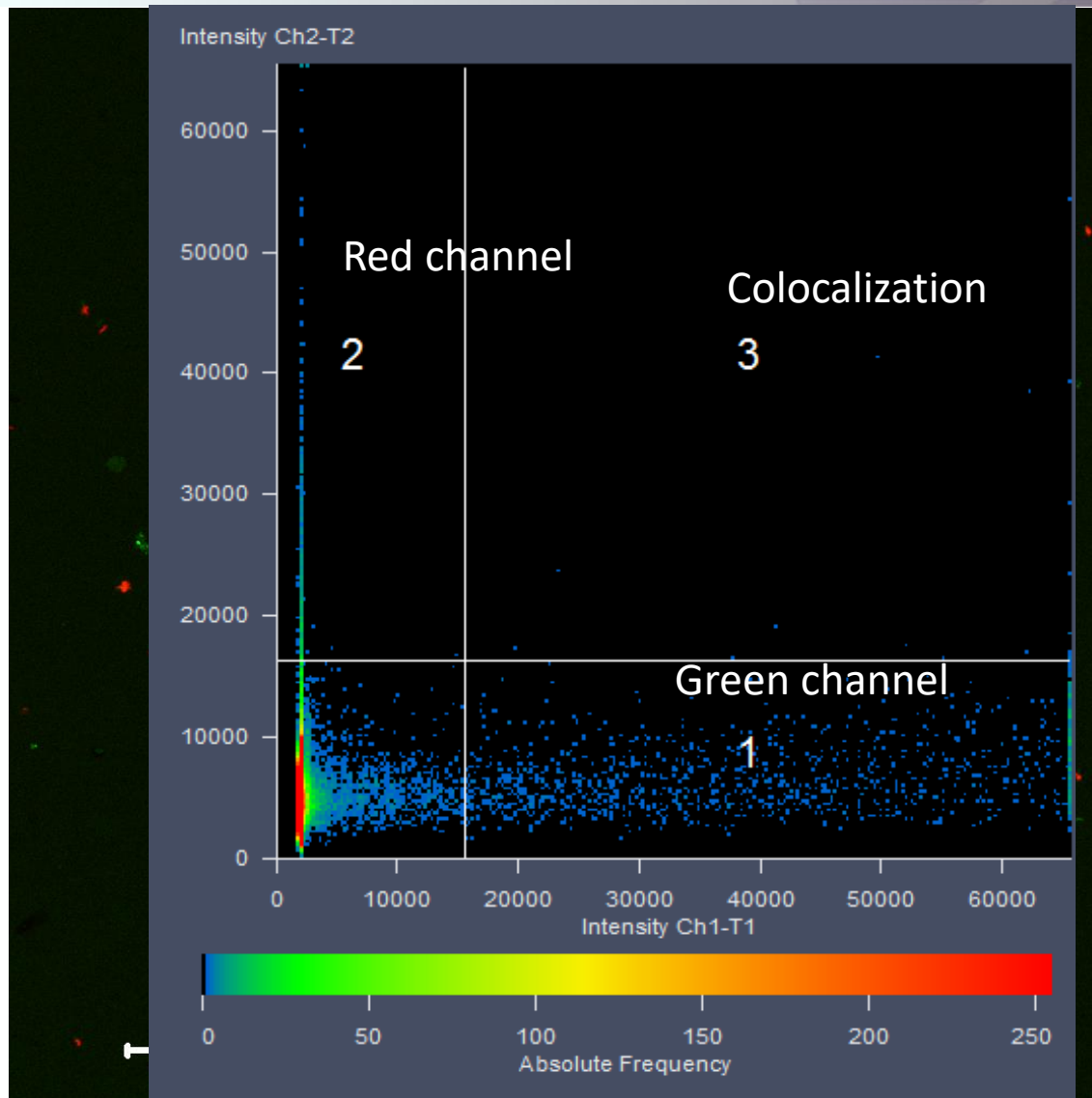


- Confokal Modul LSM 5 Exciter, two canals, RGB
- Laser HeNe 633nm 5mW
- Laser HeNe 543nm 1mW
- Laser argon 458/488/514nm, 25mW
- Laser diodowy V 405nm
- Main Beam Splitter turret PASCAL
- Software ZEN 2008 LSM 5 EXCITER
- Light division system (405, 458, 488, 514, 543 nm)
- Filtr BP 505-530
- Filtr BP 505-600
- Filtr BP 530-600
- Filtr BP 560-615
- Filtr LP 420
- Filtr BP 420-480
- System ECU LSM 5 EXCITER
- Moduł DIC I/0,9 z polaryzatorem
- Transmited light detector T-PMT LSM 710





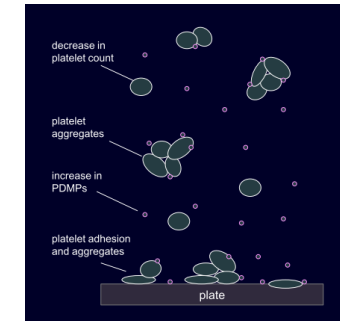
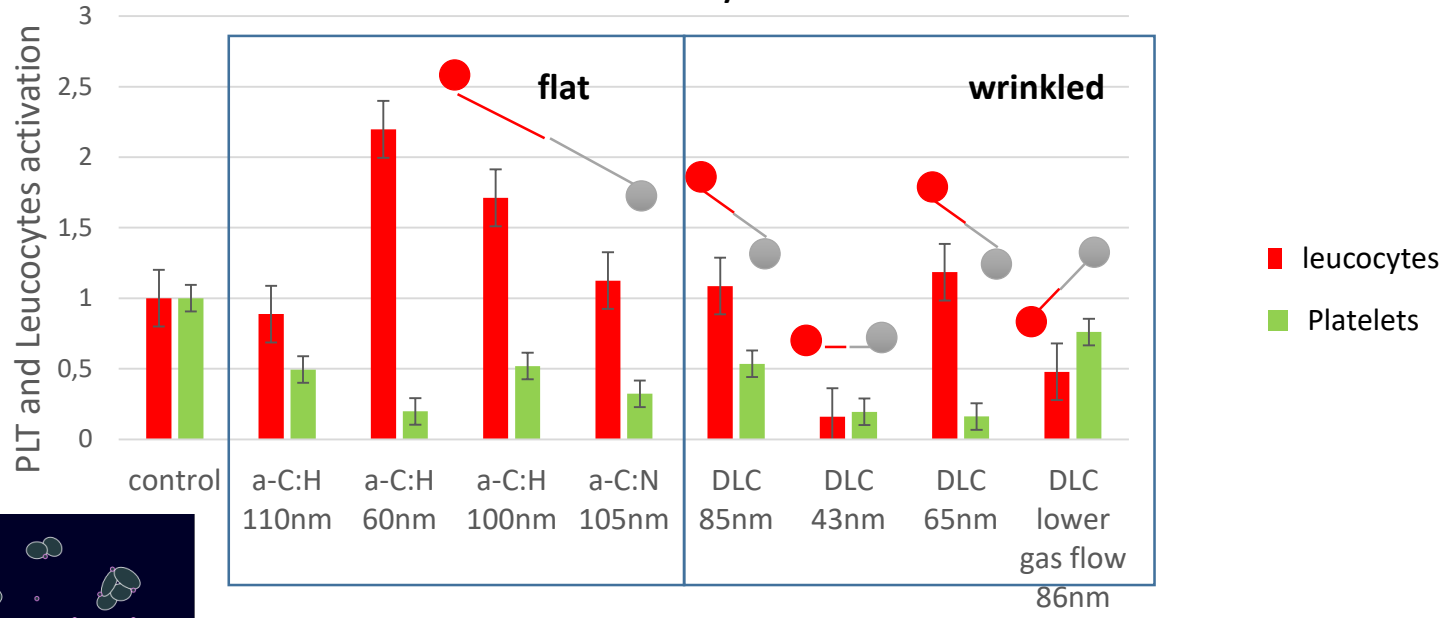
Bio-inspired materials





Bio-inspired materials

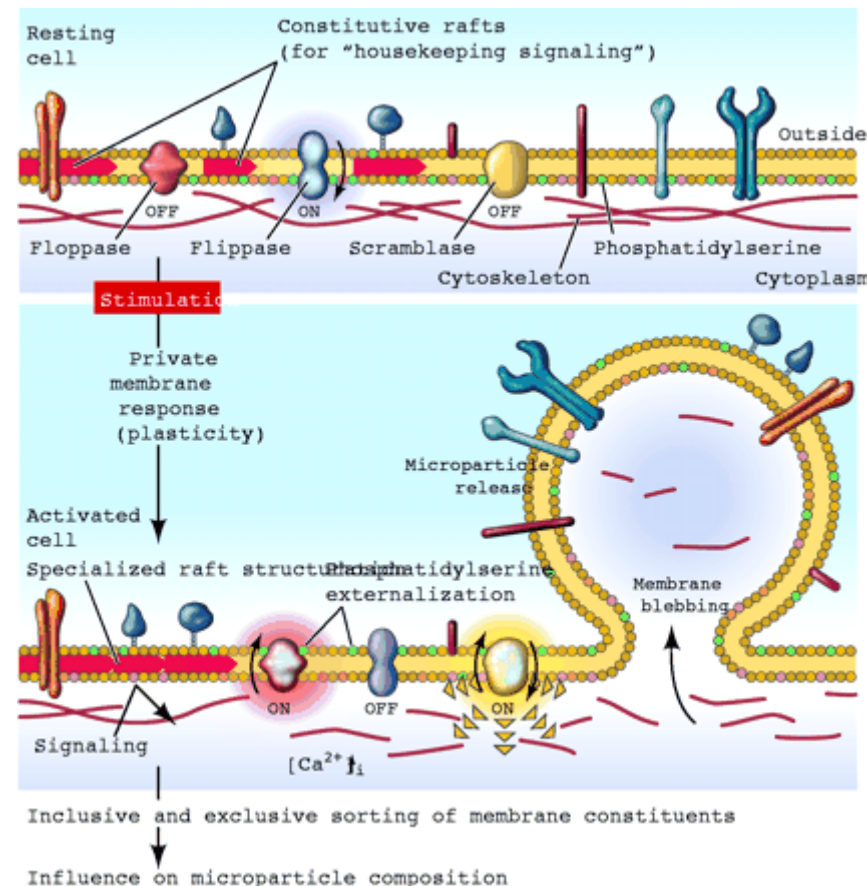
Blood activation analysis on the surface



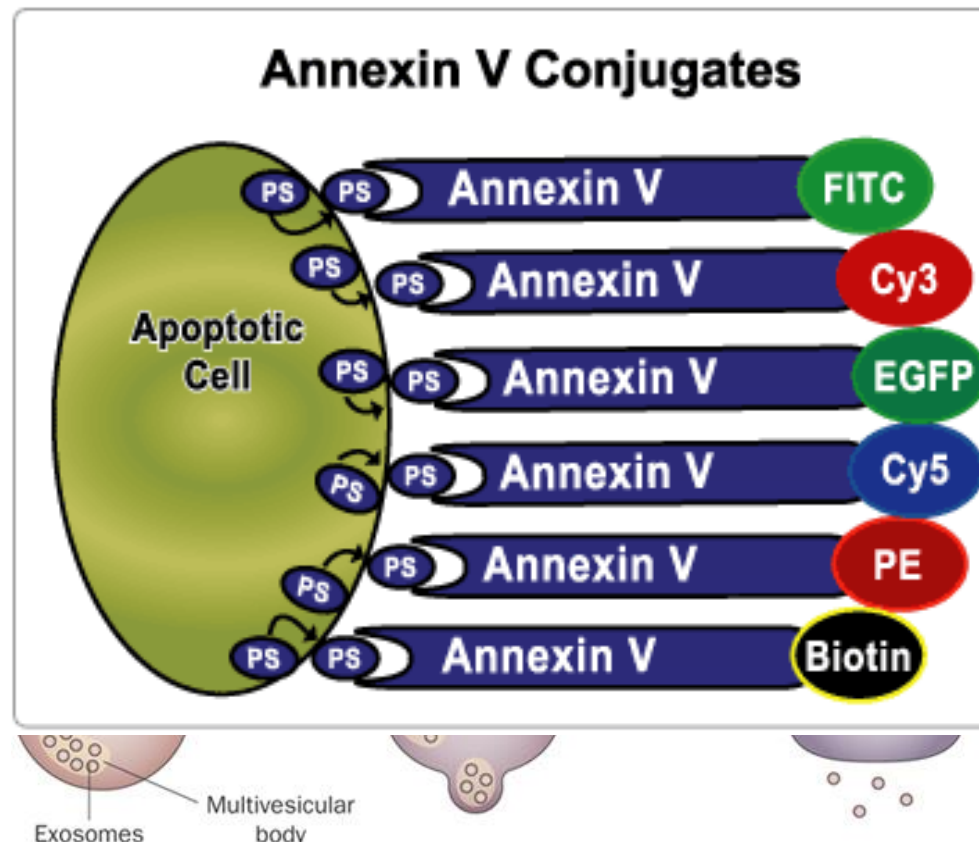
Confocal
microscopy

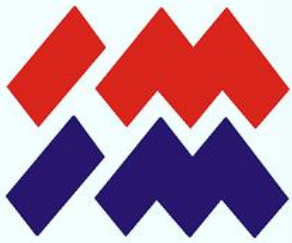


Bio-inspired materials



Microparticles





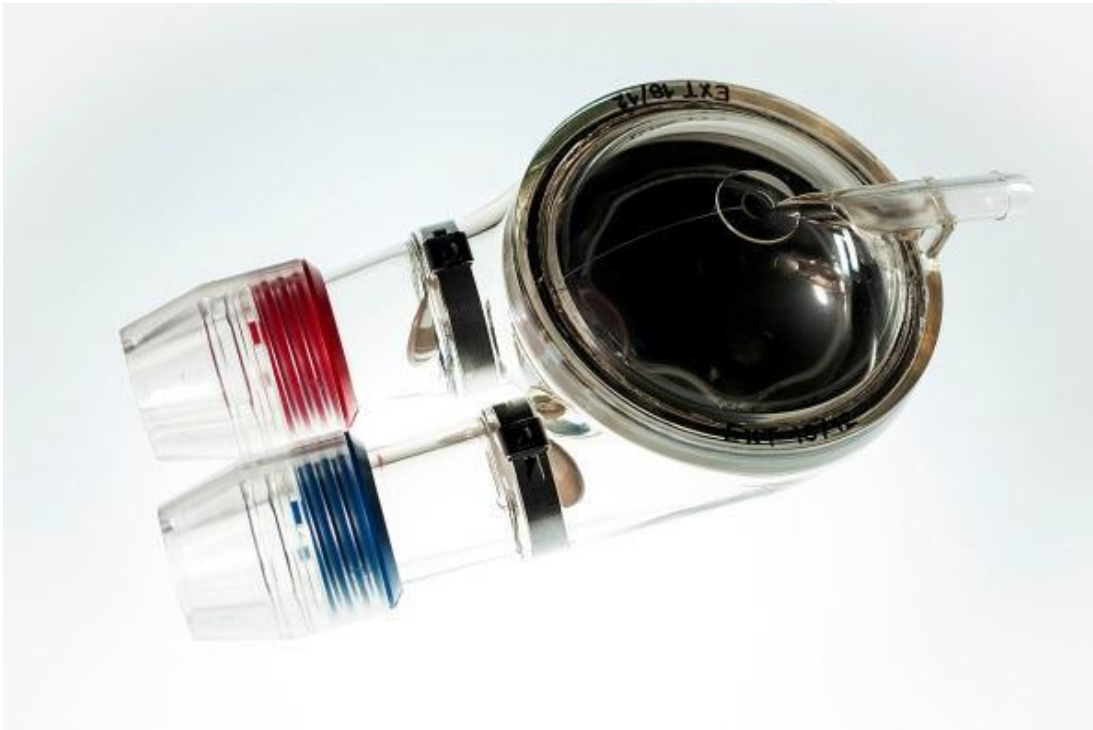
Part 2.3

Executed projects

Cardiovascular system



Artificial materials modification



ReligaHeart EXT VAD:

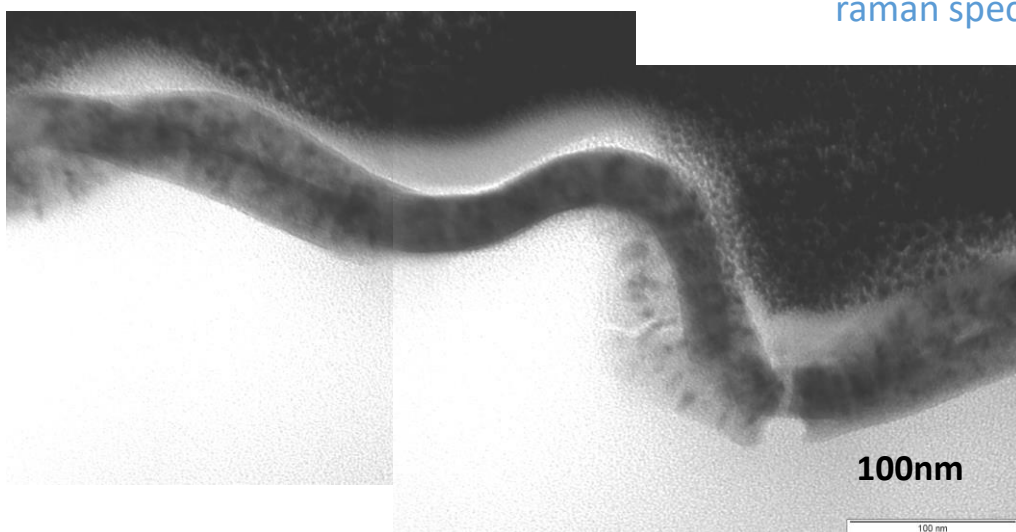
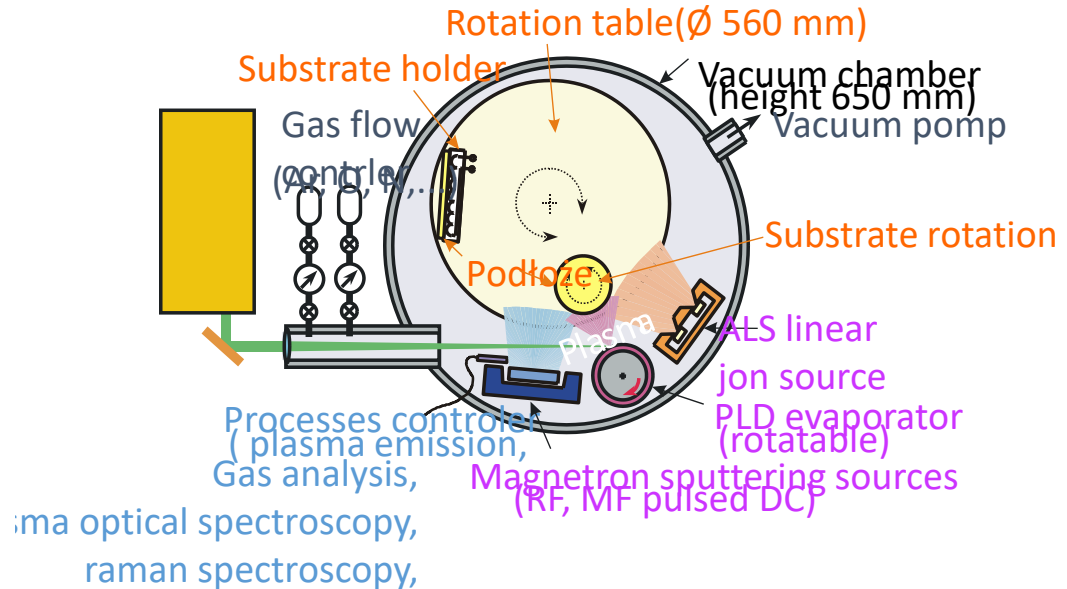
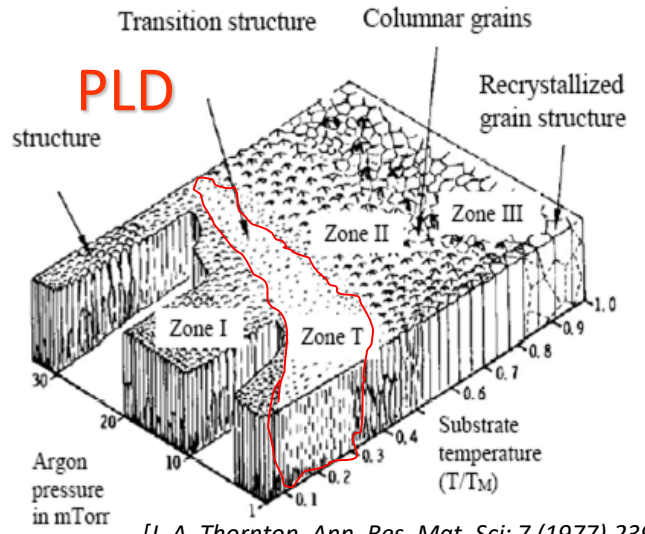
M-ERA.NET
Nonthrombogenic metal-polymer composites
with adaptable micro and
macro flexibility for next generation heart
valves in artificial heart devices



„Artificial Heart Laboratory”



Artificial materials modification



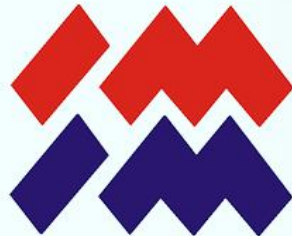
Main assumptions

Good adhesion

Biocompatibility

Lack of substrate degradation

TiN, TiO, Si-DLC, Ti(C,N), DLC

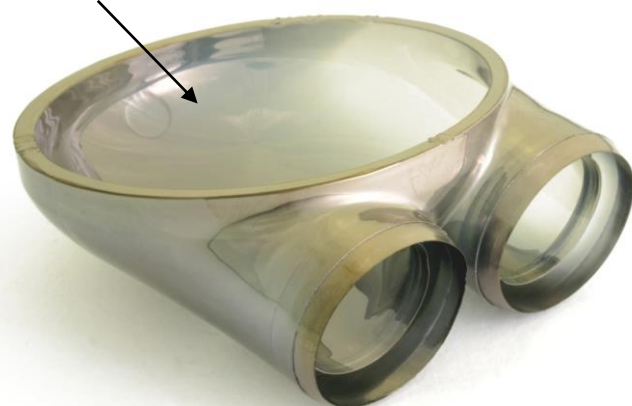


Artificial materials modification

Membrane



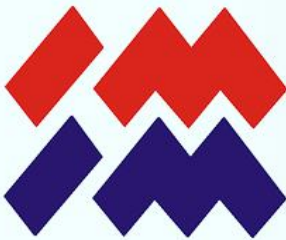
Chamber



The goal of the work is the reduction of life-threatening thrombo-emboli formation in heart assist systems by a new material design

Valve





Material development for miniaturized blood rotor

Bogusław MAJOR

Polish Academy of Sciences Institute of Metallurgy and Materials Science



Narodowe Centrum
Badań i Rozwoju

Projects:

M-ERA.NET Transnational Call 2014; Project Acronym: **bioVALVE**

Partners:

JOANNEUM RESEARCH Forschungsges.m.b.H., Institute for Surface Technologies and Photonics, Austria;

Polish Academy of Sciences Institute of Metallurgy and Materials Science in Cracow, Poland;

Collegium Medicum of Jagiellonian University Cracow, Poland;

Foundation for Heart Surgery Development, Poland;

Chirmed Sp. z o.o. Poland

M-ERA.NET Transnational Call 2017; Project Acronym: **4DbloodROT**

Partners:

JOANNEUM RESEARCH Forschungsges.m.b.H., Institute for Surface Technologies and Photonics, Austria;

Polish Academy of Sciences Institute of Metallurgy and Materials Science in Cracow, Poland

Foundation for Heart Surgery Development, Poland;

In-Vision Digital Imaging Optics GbH, Austria; Lithoz GmbH, Austria;

Polymer Competence Center Leoben GmbH, Austria;

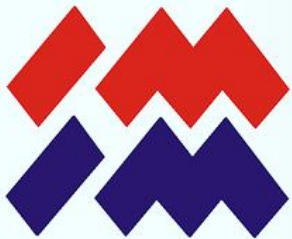
University of Leoben, Institute of Chemistry of Polymeric Materials, Austria,

MESco Sp.z o.o. Poland



The best choice for replacements for the human body or organs are biological materials or tissue analogs

Prof. Zbigniew Religa watches over the patient during heart transplant surgery
Photo: Jim Stanfield (1987 National Geographic)



Heart failure (HF)-
complex clinical syndrome resulting from any structural or functional impairment of heart ventricular filling or ejection of blood

HF is an epidemic of the 21th century, occurs in 33% of the population above 55 and 22% above 40 years; in Europe 15 milions patients with HF; responsible for up to 45% of deaths (more than cancer)

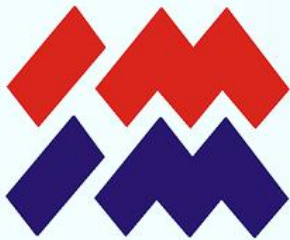
Heart transplantation is a gold standard for end-stage heart insufficiency;
small number of donor hearts (covering <0.5 % of the demand)

Alternative – application of mechanical heart assist systems LVADs

Implantable rotary blood pumps for continuous flow - technology leader (61% in 2016; 98.3% in 2015)

Rotary LVADs consist of a rotor equipped strong permanent magnet for rotor suspension and impulsion by coils in the stator.

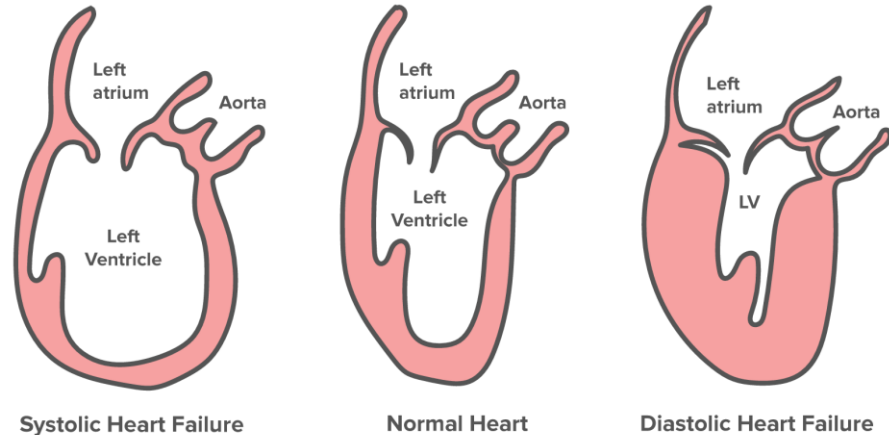
LVADs indicate 2 problems: **they are too expensive and far from being free from adverse events**; mainly strokes (trombus formation in the pump and blocking of vessels in distance), bleedings, infections and malfunctions



Heart insufficiency

A set of symptoms caused by damage to the myocardium to an extent that prevents its normal operation.

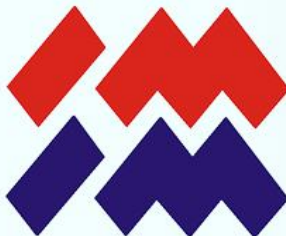
Failure is defined when the cardiac output and arterial pressure are sufficient to cover the body's current metabolic needs.



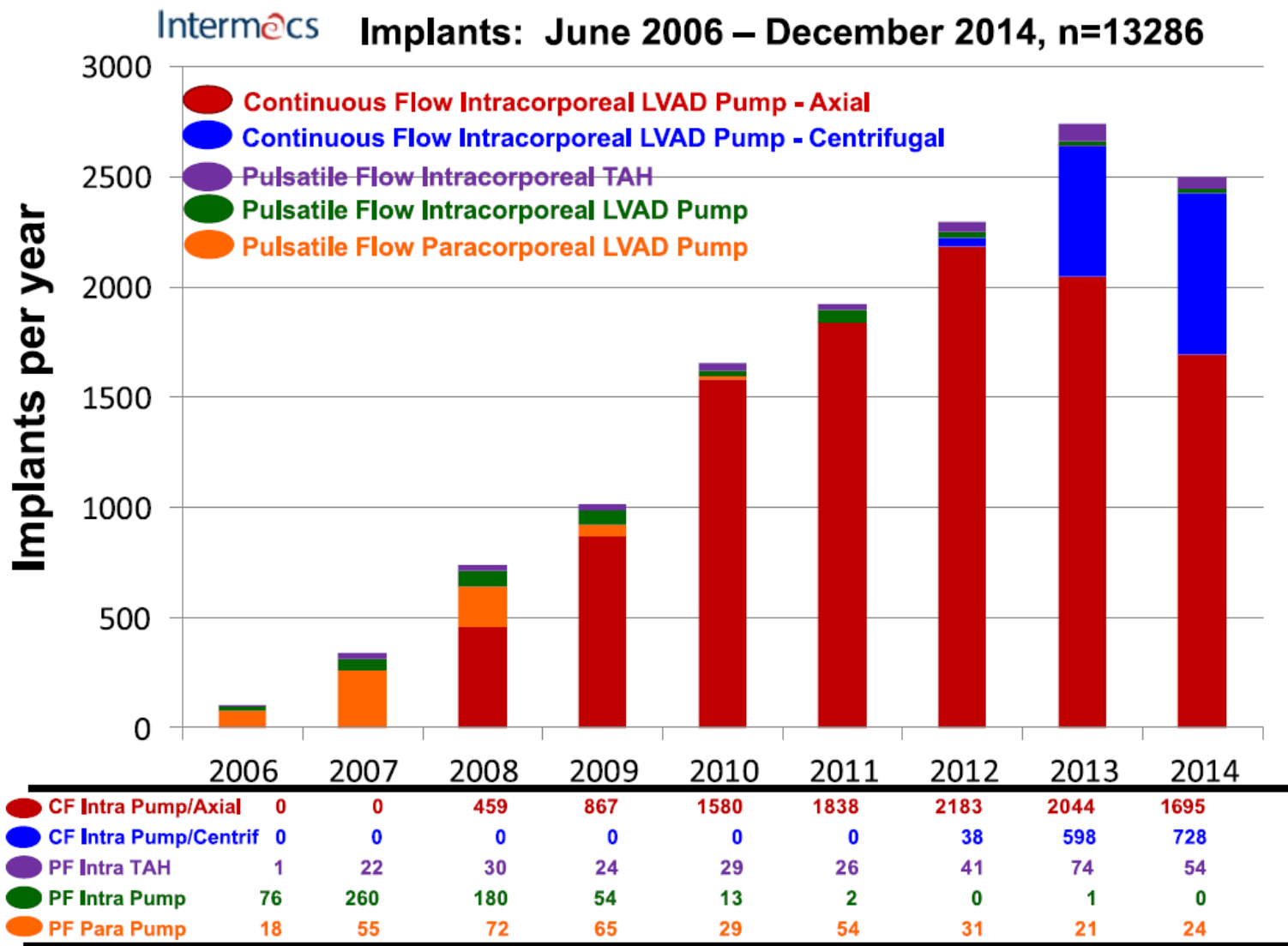
The problem usually affects the right or left ventricle, sometimes both chambers together.

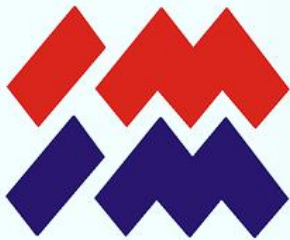
The most common causes of chronic heart failure include:

- ischemic heart disease,
- heart pressure resulting from increased blood pressure,
- **cardiomyopathy**,
- complications of myocardial infarction
- valve injury
- pericardial disease.



Statistics





Heart insufficiency

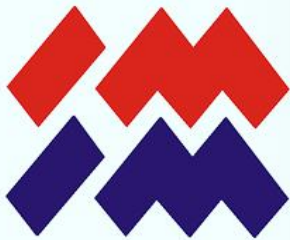
Heart valve states a regulatory part of the circulatory system, responsible for the proper blood flow in the heart.

The most natural solution in the case of valve pathology beyond standard drug therapy seems to be grafts from dead persons and animals; it is limited and it is not able to meet the needs of the patients.

Alternative solutions for transplantation are: artificial heart valves
Currently about 300 000 artificial heart valves are implanted annually

Mechanical valves can be divided into: ball, single-petal and double-sided

Currently Medtronic or Moll type artificial mechanical valves are in use



Narodowe Centrum
Badań i Rozwoju

M-ERA.NET Transnational Call 2014 Project Acronym: bioVALVE

Partners:

JOANNEUM RESEARCH Forschungsges.m.b.H., Institute for Surface Technologies and Photonics, Austria;

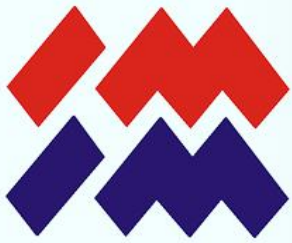
Polish Academy of Sciences Institute of Metallurgy and Materials Science in Cracow, Poland;
Collegium Medicum of Jagiellonian University Cracow, Poland;

Foundation for Heart Surgery Development, Poland;

Chirmed Sp. z o.o. Poland

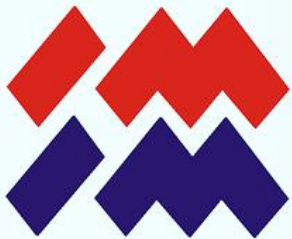
DZP/M-ERA.NET-2014/291/2015 “Nonthrombogenic metal-polymer composites with adaptable micro and macro flexibility for the next generation heart valves in artificial heart devices” of the Polish National Centre of Research and Development.

The aim of project bioVALVE was to life-treating thrombo-embolii formation in pulsatile assist devices by ***a new biomimetic heart valve design***



Task 1

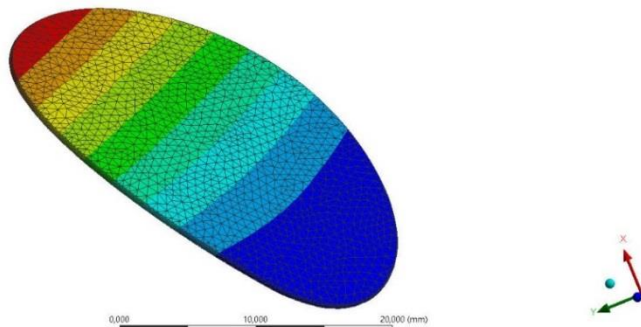
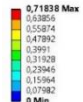
Optimization of mechanical properties and determination of fluid dynamics based on finite element methods for flexible heart valves



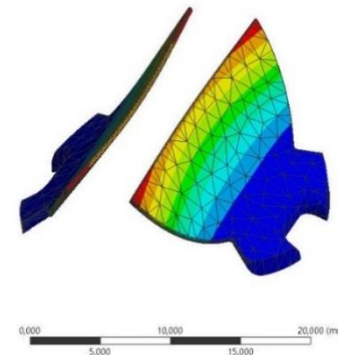
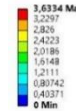
Optimisation

Optimization of mechanical properties and determination of fluid dynamics based on finite element methods for flexible heart valves

A: Transient Structural
Total Deformation
Type: Total Deformation
Unit: mm
Time: 00:00:00
2017-11-20 15:34



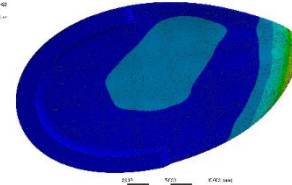
B: Transient Structural
Total Deformation
Type: Total Deformation
Unit: mm
Time: 00:00:00
2017-11-20 15:32



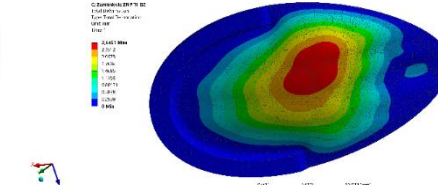
An example drawing of stress simulations in an inflow valve

An example drawing of stress simulations in an outflow valve

A: Deformable ZM7 2102
Type: Total Deformation
Unit: mm
Time: 00:00:00
2017-11-20 15:34

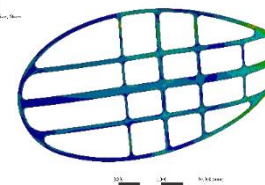


B: Deformable ZM7 2102
Type: Total Deformation
Unit: mm
Time: 00:00:00
2017-11-20 15:34

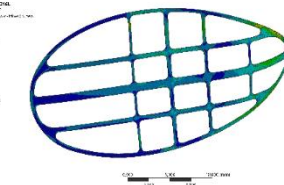


Strain of the inflow petal (Ti mesh) a- opened b- closed

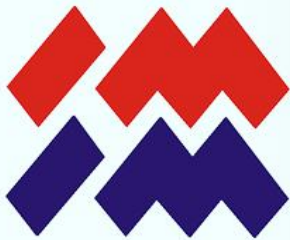
A: Deformable ZM7 2102
Type: Total Deformation
Unit: mm
Time: 00:00:00
2017-11-20 15:34



B: Deformable ZM7 2102
Type: Total Deformation
Unit: mm
Time: 00:00:00
2017-11-20 15:34

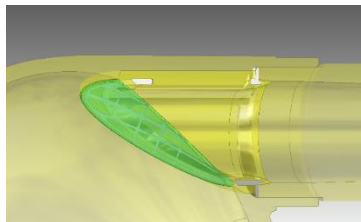
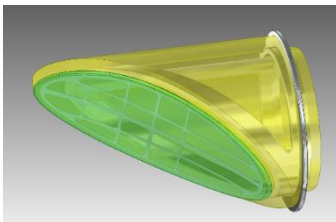


Stress in the inflow petal mesh a- Ti b- Steel

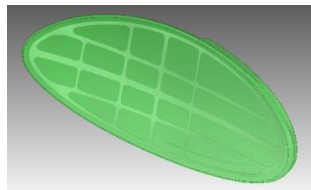


Optimisation

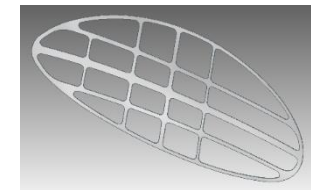
Optimization of mechanical properties and determination of fluid dynamics based on finite element methods for flexible heart valves



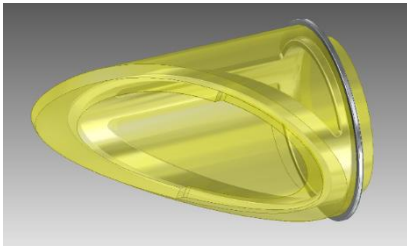
Inflow valve and cross-section through the area of the inflow channel.



a - Petal with embedded reinforcing mesh



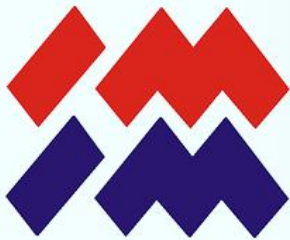
b – titanium reinforcing mesh



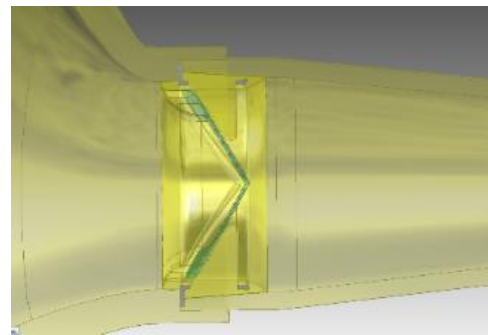
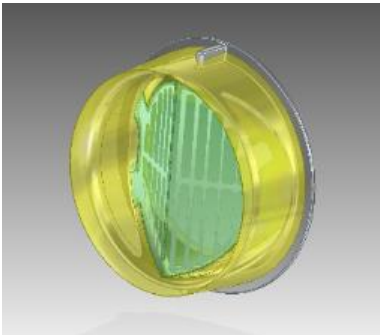
The carrier ring of the petal



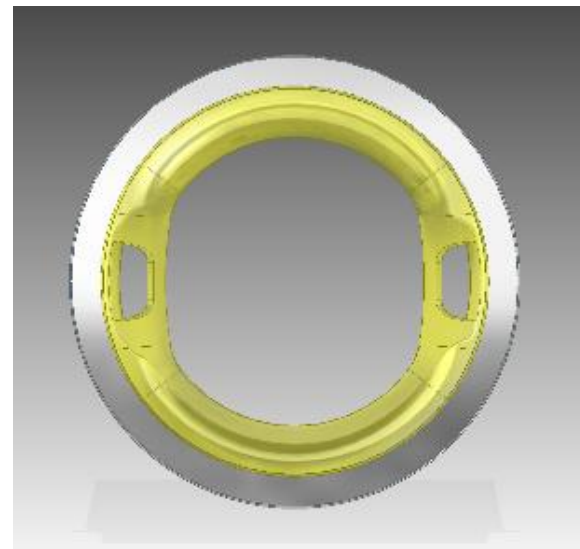
The frame of the ring



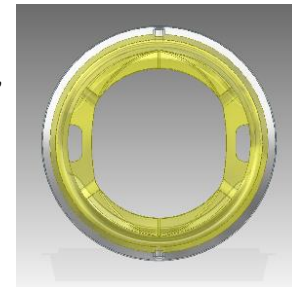
Optimisation



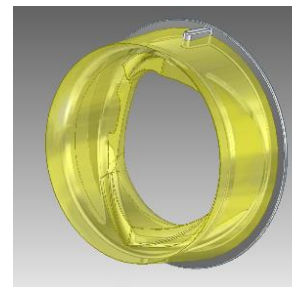
Polyurethane inflow valve and cross section through the outflow channel.



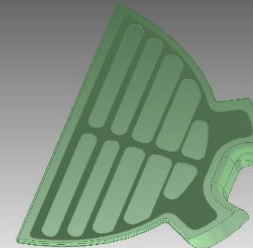
c - Valve ring; view from the inflow side



a - Valve ring: view from the outflow side



b - Valve ring: general view



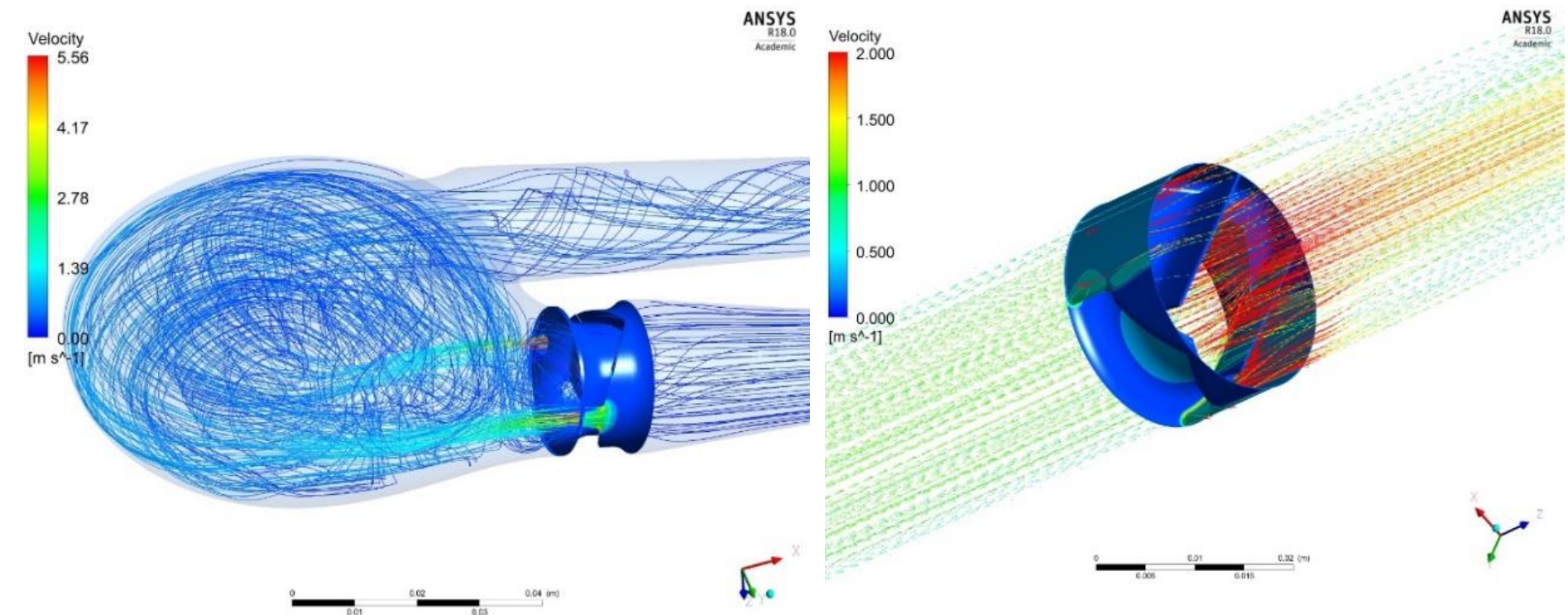
Polyurethane flake with covered frame



The frame of the ring



Optimisation



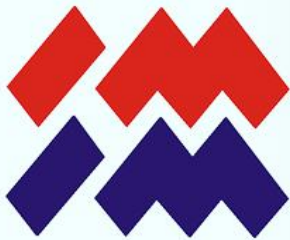
An example drawing of a flow velocity simulation (a) through a outflow valve in a ReligaHeart® heart assist pump equipped with new valve: (b) backflow flushing holes



Task 2

R&D on insert injection moulding

PU testing Bionate II 80A (DSM)



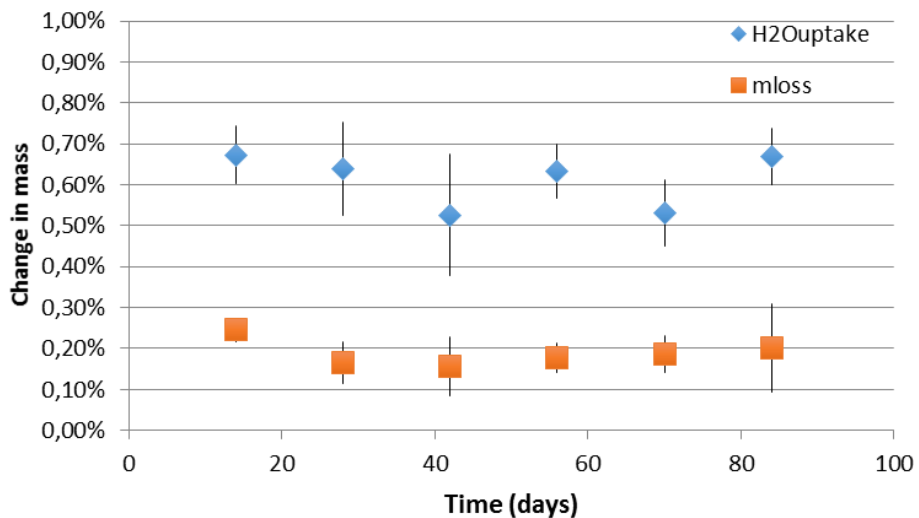
R&D injection moulding

Bionate II 80A (DSM)

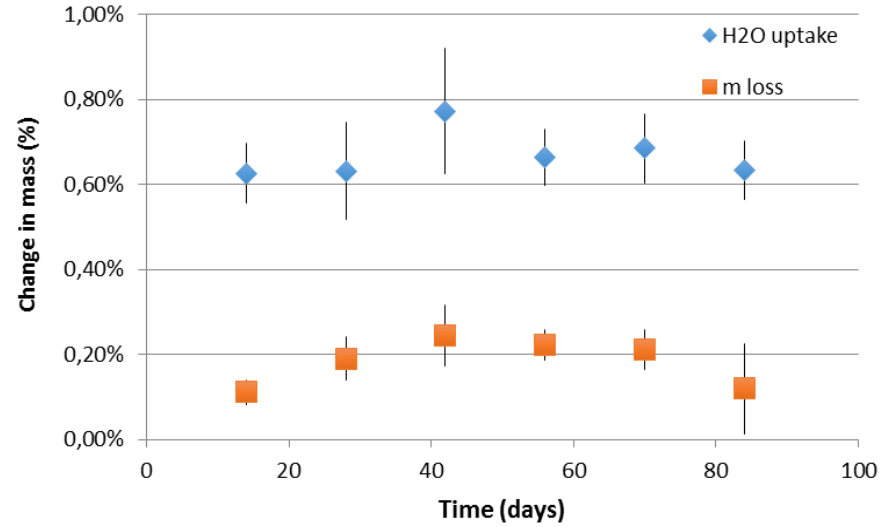
UPTAKE: Bionate II 80A, temperaturę 37 deg, 12 weeks

BIOEROSION: Bionate II 80A, temperaturę 37 deg, 72h

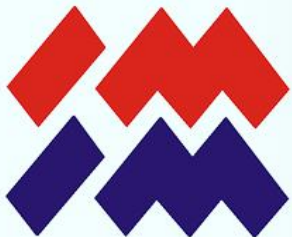
Change in mass after incubation in SBF



Change in mass after incubation in DPBS

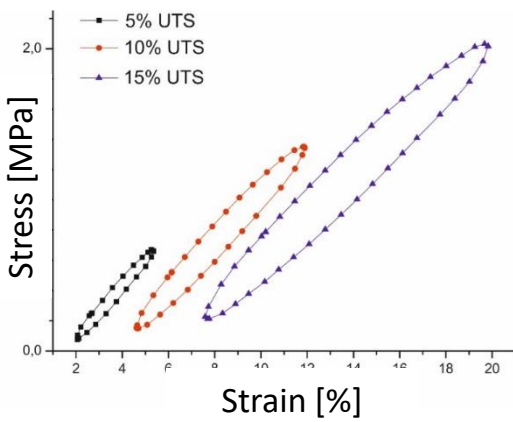


Changes in water absorption values and mass loss during degradation. a) degradation in SBF; b) degradation in PBS



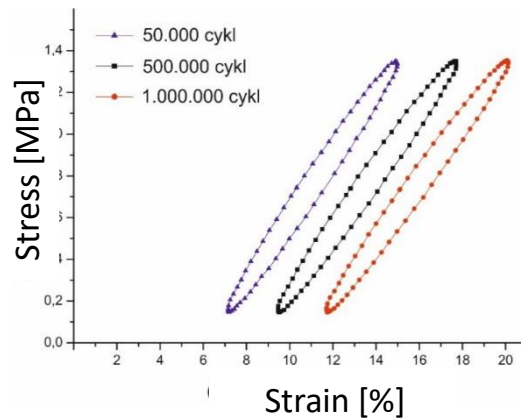
R&D injection moulding

Mechanical testing: Bionate II 80A (DSM)



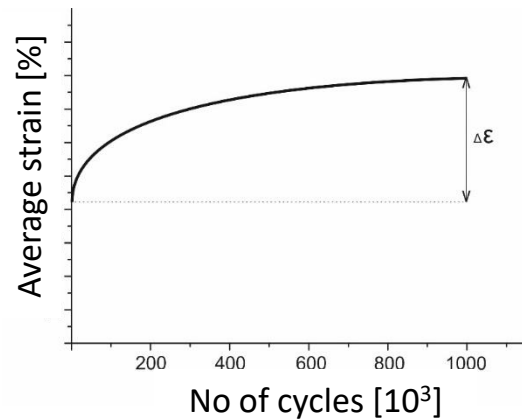
Hysteresis loops for individual load cycles

From the course of the hysteresis loop or individual load cycles it follows that as the stress on a particular step increases, the shape of the loop and their surface change significantly. The larger area of the loop indicates high damping.



Hysteresis loops of the tested material for cycles of 50,000; 500 thousand and 1 million

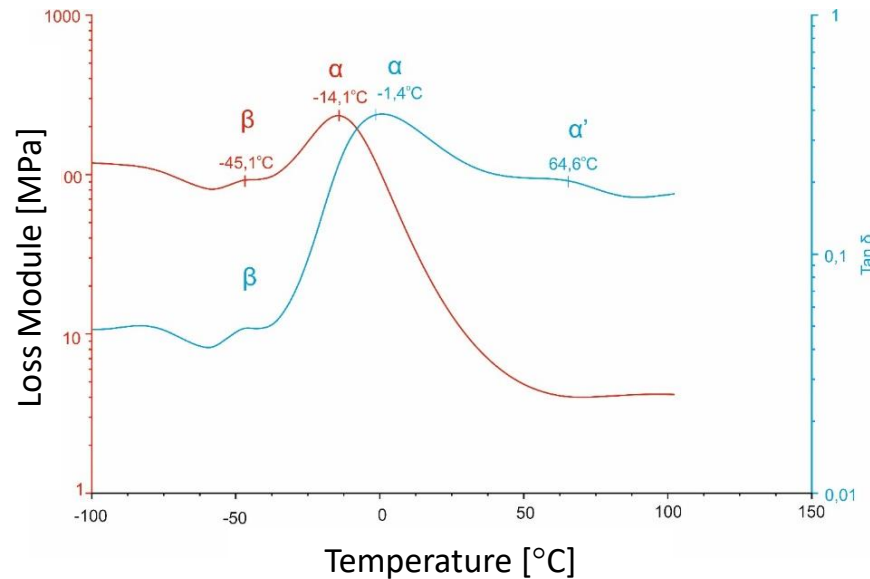
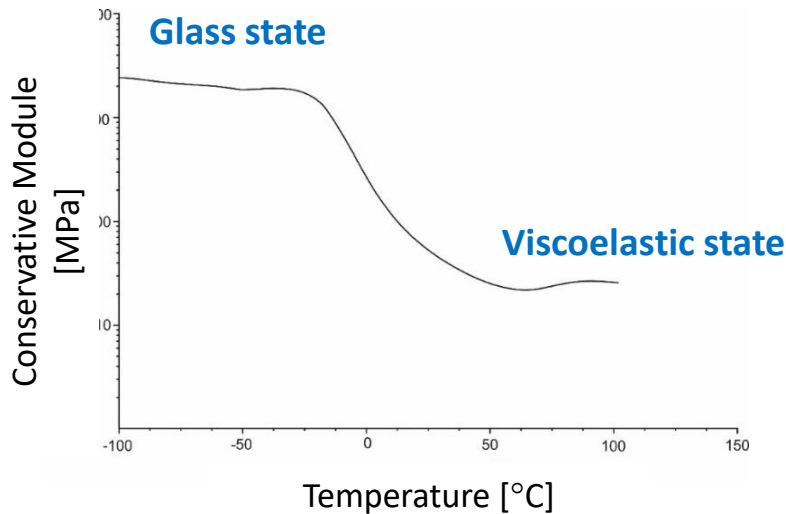
Despite the low creep resistance, the tested polyurethane Bionate 80A exhibits similar hysteresis loop characteristics, regardless of the number of load cycles. Hysteresis loops are characterized by a small surface area, which indicates low attenuation and thus low dissipation energy (energy dissipation).



Creep curve of dynamic Bionate 90A polyurethane

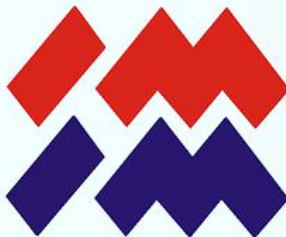
On the basis of the dynamic creep curve presented in it is stated that the total creep $\Delta\epsilon$, defined as the sum of delayed elastic strain ϵ_b and material flow ϵ_c , for the tested material was about 5.5 %. To the group of significant factors influencing the creep of the material should be not only the size of the load being applied and the duration of the test, but also the temperature and the environment in which the sample is located.

Thermodynamic testing: Bionate II 80A (DSM)



**Thermomechanical properties of the Bionate 90A elastomer on the example of:
a) a conserving module; b) loss modality and $\tan \delta$**

As the temperature rises, the characteristic plateau of the conserving module is observed, which includes a third temperature range of +50 °C to +100 °C. On the loss modulus curve and tangent of the loss angle, the maximum associated with the glass transition temperature (-14 °C and -1.4 °C respectively) is visible. In addition, small additional relaxation maxima (β) can be observed in the vitreous state at a temperature of about -45 °C, and in the viscoelastic state (α') at a temperature of about +65 °C, which corresponds to a slight decrease in the module.



R&D injection moulding

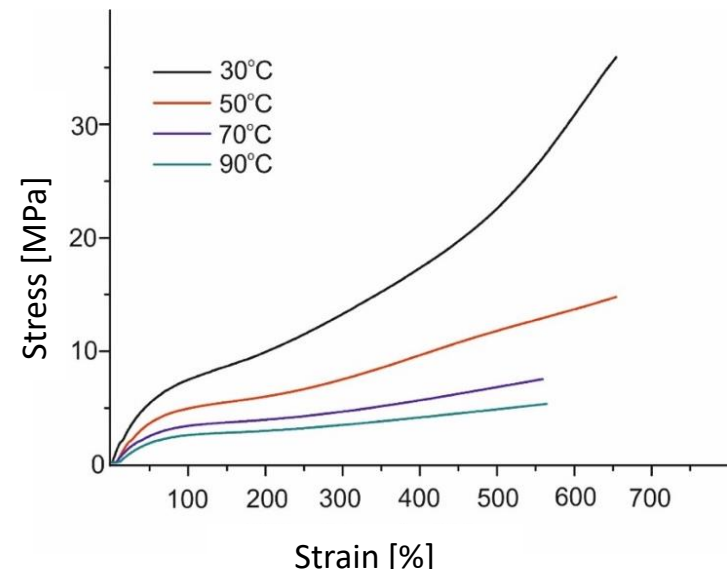
Thermomechanical testing: Bionate II 80A (DSM)

Mechanical properties of the investigated polymers

Temperature (°C)	Young's modulus (MPa)	Secant modulus at 50% strain (MPa)	Modulus at incisal at 100% strain (MPa)	Tensile stress (MPa)	Tensile strain (%)
30	16,6±2,1	10,6±1	7,2±0,5	36,2±1	>650
50	11,9±1,4	7,5±0,1	4,8±0,1	14,5±0,1	>650
70	7,2±0,3	5,1±0,2	3,3±0,2	7,3±0,1	>550
90	5,5±0,6	3,9±0,4	2,6±0,3	5,2±0,2	>550

Rheological research (MFI) of polymers:

The Bionate 90A polymer melt index was tested at two temperatures of +200 °C and +210 °C under a constant load of 2.16 kg. It was impossible to carry out the measurement at lower temperatures due to the very high melt viscosity of the tested elastomer. MFI (+200 °C, 2.16 kg) = 4.73 ± 0.35 [g/10min]; MFI (+210 °C, 2.16kg) = 6.22 ± 0.41 [g/10min]



Stress diagram as a function of deformation of Bionate 90A material for different measurement temperatures; (right) Universal testing machine Instron 3366

From the course of the hysteresis loop or individual load cycles it follows that as the stress on a particular step increases, the shape of the loop and their surface change significantly. **The larger area of the loop indicates high damping.**

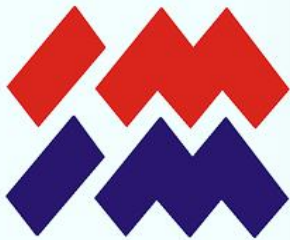
The need for reinforcement of the valve through a metal scaffold

On the basis of the dynamic creep curve presented in it is stated that the total creep $\Delta\epsilon$, defined as the sum of delayed elastic strain ϵ_b and material flow ϵ_c , for the tested material was about 5.5 %. To the group of significant factors influencing the creep of the material should be not only the size of the load being applied and the duration of the test, but also the **temperature and the environment in which the sample is located.**



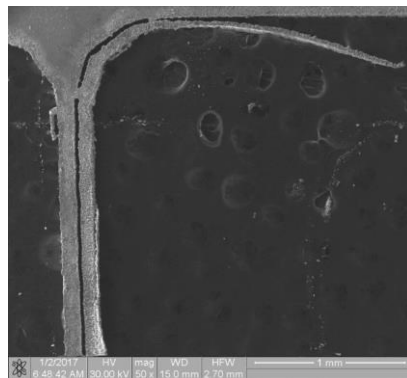
Task 3

R&D of mesh-like metal scaffold with smooth sealing surfaces



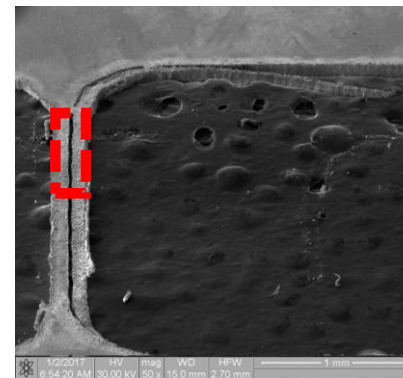
R&D mesh metal

Analysis of defects (SEM)

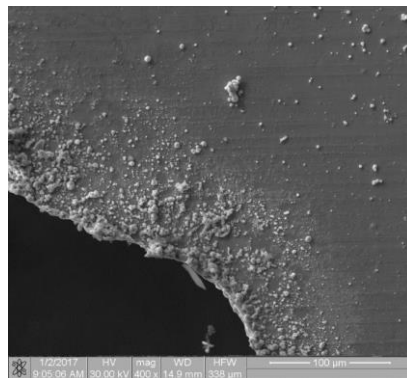


SE

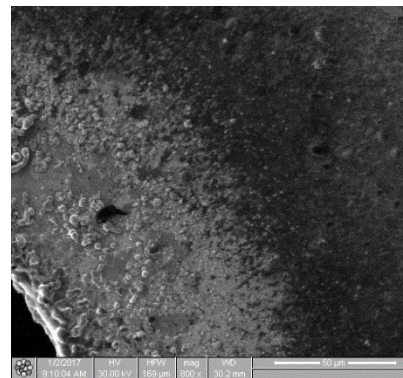
Secondary electrons



SE

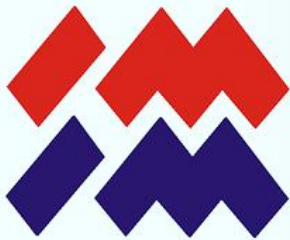


SE



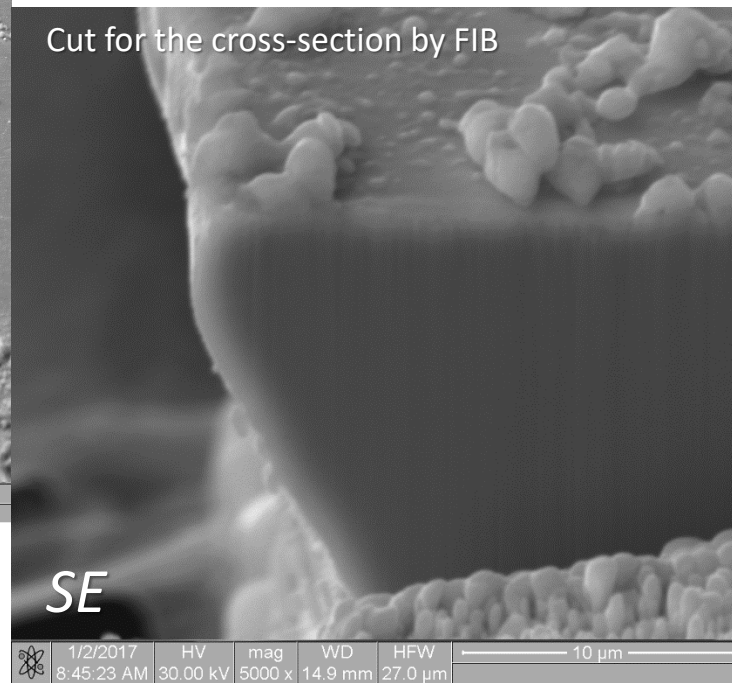
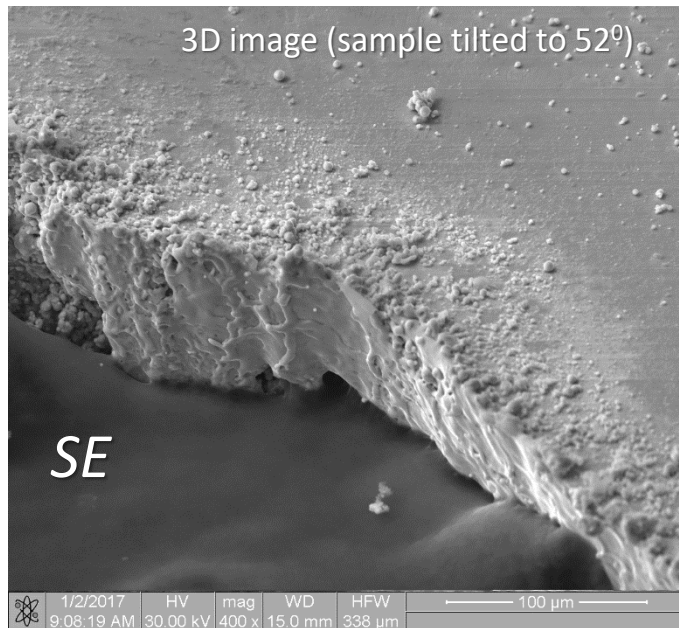
BSE

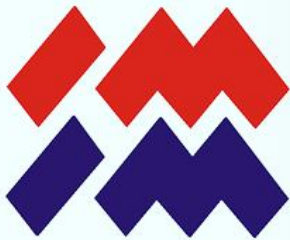
R&D of mesh-like metal scaffold with smooth sealing surfaces



R&D mesh metal

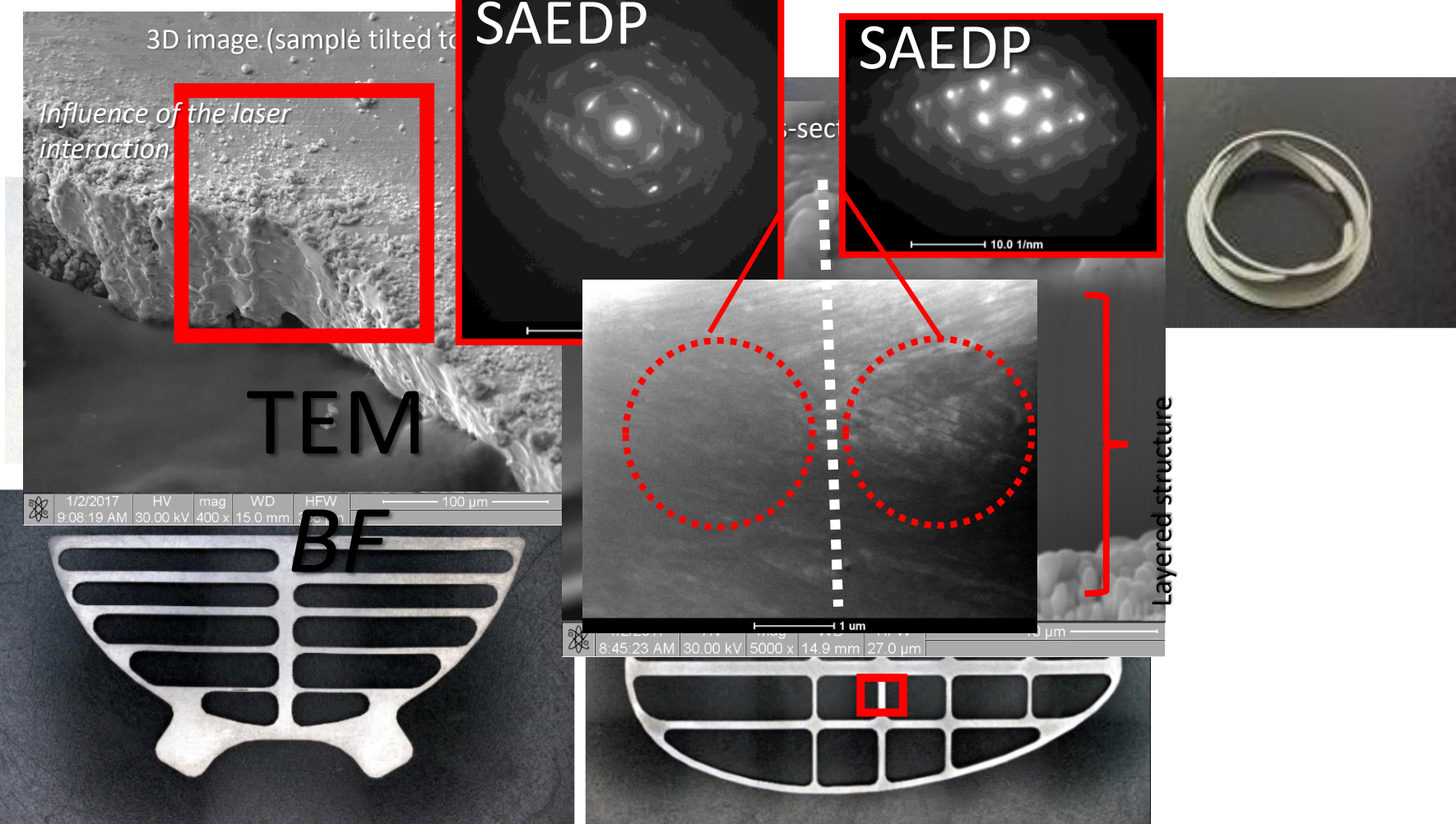
Analysis of defects (SEM)



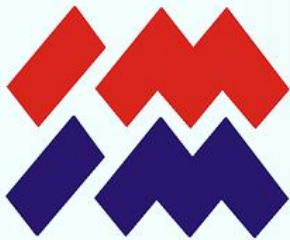


bio-VALVE

Analysis of defects (TEM)

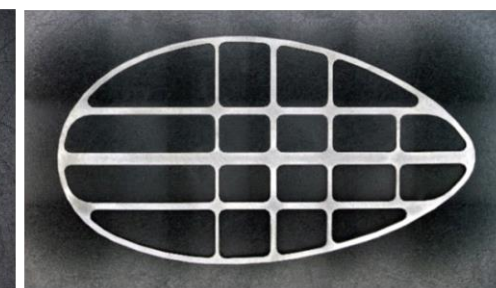


R&D of mesh-like metal scaffold with smooth sealing surfaces

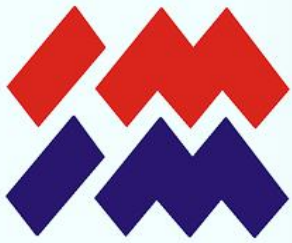


R&D mesh metal

Analysis of defects (adjudgement- MESH WITHOUT DEFECTS)

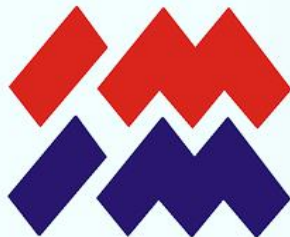


R&D of mesh-like metal scaffold with smooth sealing surfaces



Task 4

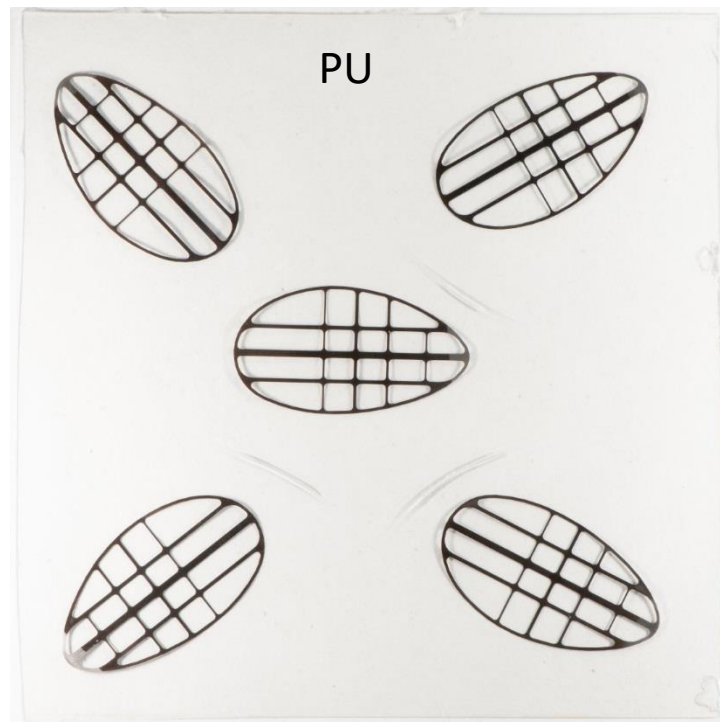
R&D of mesh-like metal scaffold covered by polymer



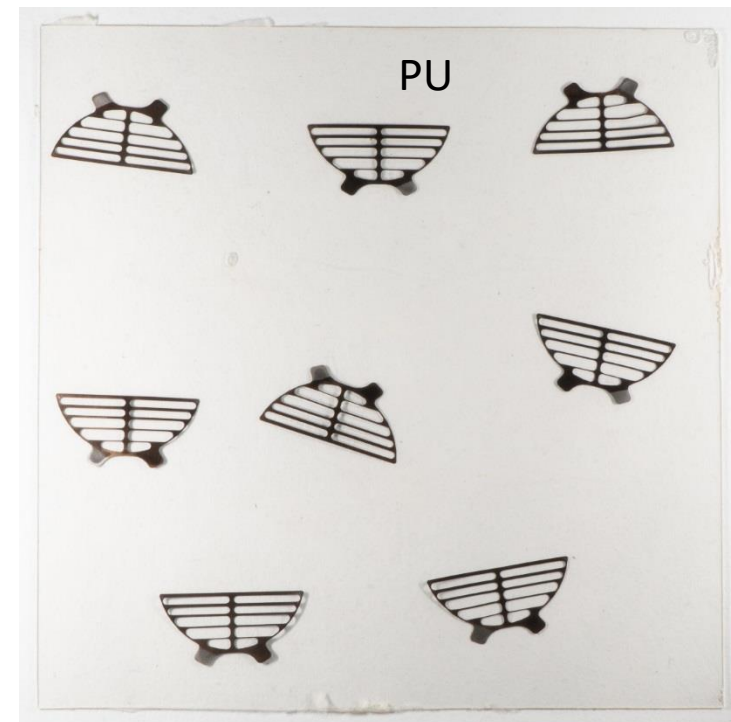
R&D mesh metal+PU

Metallic meshes pressed in PU

inflow valve



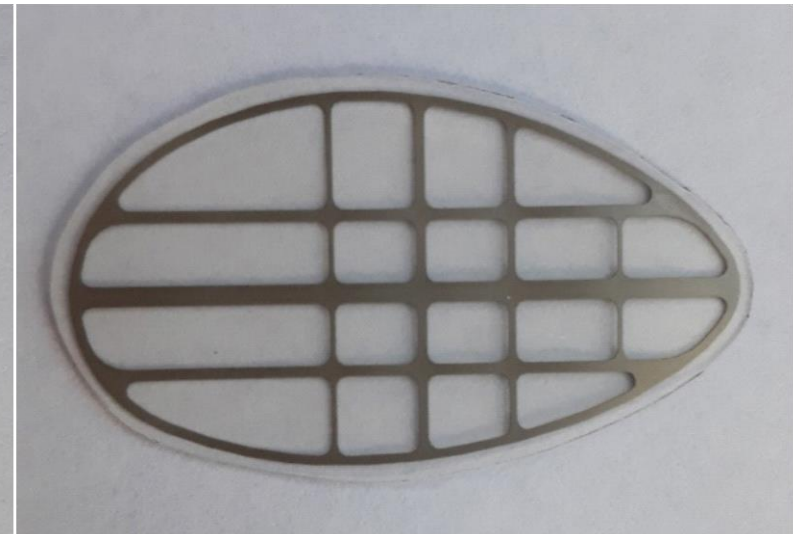
outflow valve

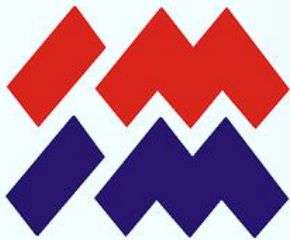


Heart valve testing



Valve flakes covered with polymer

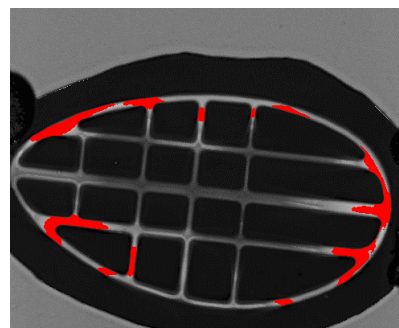




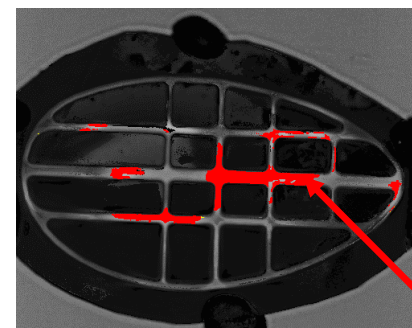
R&D mesh metal+PU

Polymer delamination analysis (SAM)

Tests of adhesion, i.e. the risk of delamination of the polymer sheath from the metallic frame, were carried out using a scanning acoustic microscope. The acoustic microscope works in pulse reflection mode. The most important element in scanning acoustic microscopy is a high frequency sound wave and a piezoelectric transducer.

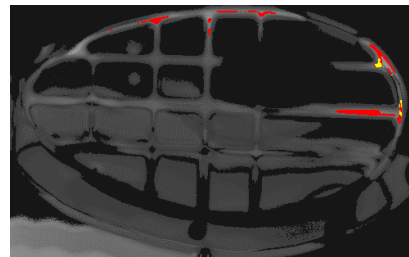


a.)



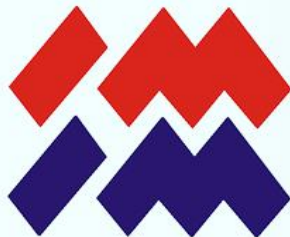
b.)

Delamination



c.)

**Scanning acoustic microscopy (SAM)
analysis after wear test**



R&D mesh metal+PU

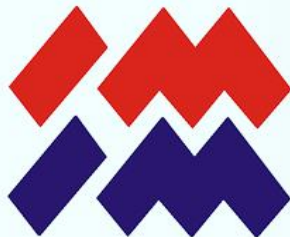
Rings dedicated for inflow and outflow valve- DRAWING

inflow valve



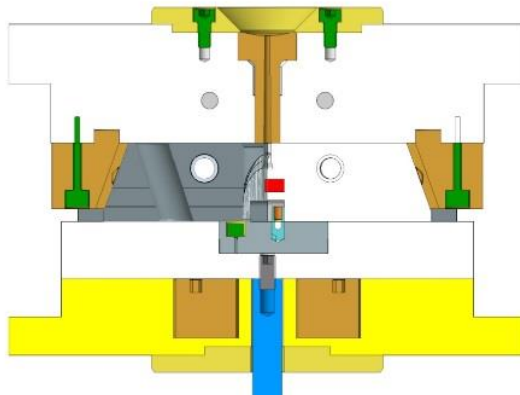
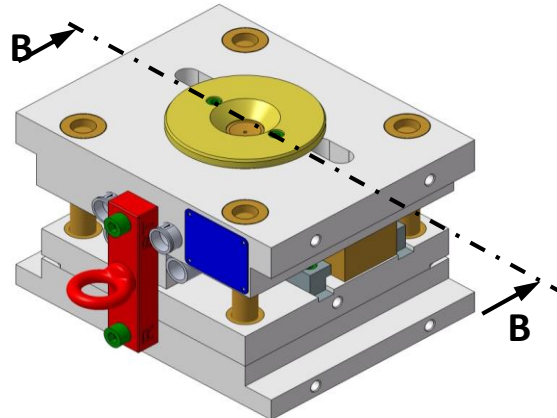
outflow valve





R&D injection moulding

Rings dedicated for inflow and outflow valve- IM PROCESS



Research Form INFLOW VALVE

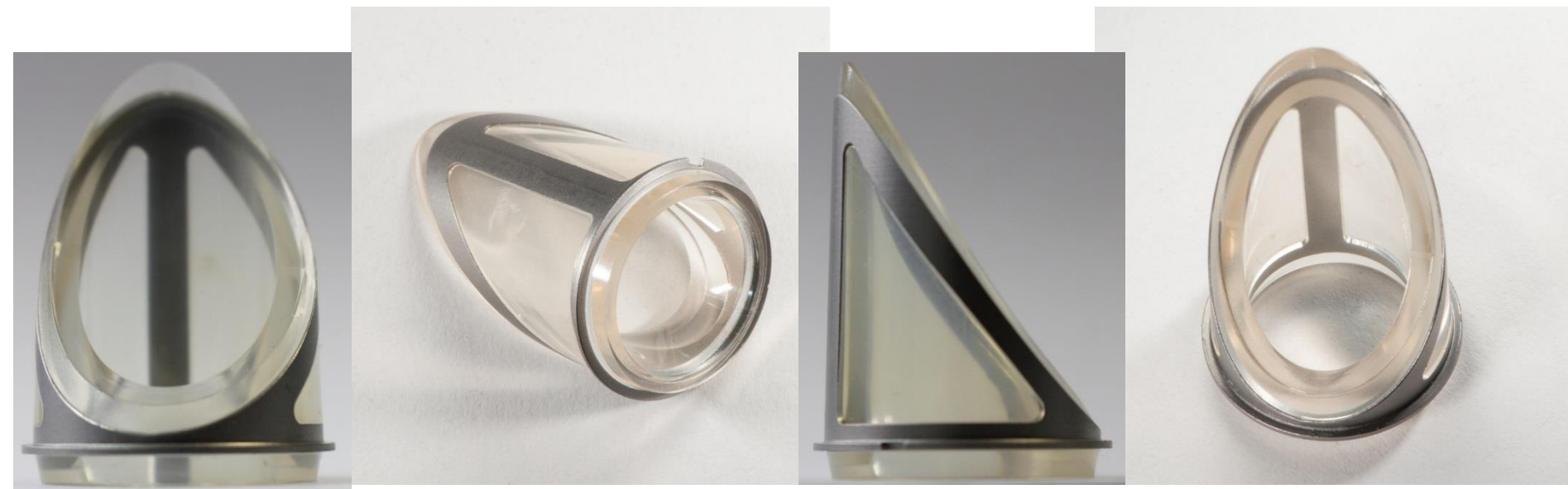
Shape concept of
component INFLOW VALVE



Research form OUTFLOW VALVE.



Inflow valve- PRODUCT

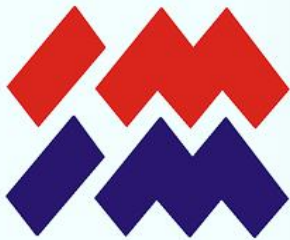


The need for improvement of the
metall scaffold surface with
hemocompatible, coatings
additionally improving METAL- PU
adhesion!



Task 5

R&D on surface coating



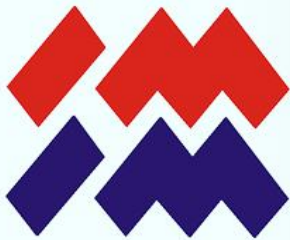
R&D on surface coating

R&D on surface coating deposition

Liferschein 2016096

Oznaczenie	Skład					Grubość [nm]	Przygotowanie	Atmosfera gazowa	Chropowatość Ra [nm]	Kąt zwilżania	Energia powierzchniowa		
	a-C:H	a-C:H:N	a-C:N	ta-C:H	ta-C:H:N	Si - a-C:H					polar	dispers	Summe
B334_7				x		92,2	Ionenquelle	20,0 C ₂ H ₂		79,9	3,5	40,0	43,4
B334_8				x		48,0	Ionenquelle	20,0 C ₂ H ₂		78,3	3,5	42,4	45,9
B334_10				x		67,4	Ionenquelle	20,0 C ₂ H ₂		79,7	3,3	41,4	44,6
B334_12				x		90,8	Ionenquelle	5,0 Ar + 15,0 C ₂ H ₂		84,0	2,1	40,8	43,0
B372_6	x					94,7	sputtern	24,0 Ar + 6,0 C ₂ H ₂	14,7	60,82	9,68	46,74	56,43
B372_7		x				103,8	sputtern	24,0 Ar + 4,5 C ₂ H ₂ + 1,5 N ₂	14,2	58,53	10,17	48,82	58,99
B372_8	x					103,1	sputtern	24,0 Ar + 3,0 C ₂ H ₂ + 3,0 N ₂	12,7	57,83	11,55	45,54	57,09
B372_9	x					95,2	sputtern	24,0 Ar + 1,5 C2H2 + 4,5 N2	24,0	53,03	13,70	46,55	60,25
B372_10			x			95,2	sputtern	24,0 Ar + 6,0 N ₂	19,0	45,90	17,14	47,45	64,59
B372_15			x			94,7	Ionenquelle	20,0 C ₂ H ₂	13,0	41,87	20,94	43,6	64,54
B372_16				x		110,2	Ionenquelle	17,5 C ₂ H ₂ + 2,5 N ₂	23,3	25,37	30,09	41,61	71,70
B372_17				x		100,3	Ionenquelle	15,0 C ₂ H ₂ + 5,0 N ₂	12,7	32,63	24,61	45,87	70,49
B372_18				x		82,7	Ionenquelle	12,5 C ₂ H ₂ + 7,5 N ₂	14,3	38,80	25,99	36,90	62,89
B372_23					x	124,3	sputtern	28,2 Ar + 1,8 C ₂ H ₂	16,3	27,80	27,07	45,35	72,42
B372_24					x	15,0	sputtern	28,2 Ar + 1,8 C ₂ H ₂	41,3	22,93	29,66	44,17	73,,83
B372_25					x	127,6	sputtern	27,0 Ar + 3,0 C ₂ H ₂	19,2	19,37	29,47	46,89	76,36
B372_26					x	15,0	sputtern	27,0 Ar + 3,0 C ₂ H ₂	38,3	25,97	29,98	41,36	71,33
B372_27					x	123,5	sputtern	24,0 Ar + 6,0 C ₂ H ₂	26,2	24,35	27,62	47,07	74,69
B372_28					x	15,0	sputtern	24,0 Ar + 6,0 C ₂ H ₂	27,7	23,33	30,11	43,05	73,16
B372_29					x	118,5	sputtern	18,0 Ar + 12,0 C ₂ H ₂	14,0	54,33	11,98	49,66	61,64
B372_30					x	15,0	sputtern	18,0 Ar + 12,0 C ₂ H ₂	52,7	51,17	14,28	47,68	61,96

Group	Symbol	Layer	Thickness [nm]
1	B372_6	a-C:H	94,7
	B372_7	a-C:H,N	103,8
	B372_8	a-C:H,N	103,1
	B372_9	a-C:H,N	95,2
	B372_10	a-C:N	95,1
	B372_15	a-C:H	94,7
2	B372_15+E059 (fluoridation)	a-C:H+SF6 (fluoridation)	94,7
	B372_16	a-C:H,N	110,3
	B372_17	a-C:H,N	100,3
3a	B372_17+E059 (fluoridation)	a-C:H,N+SF6 (fluoridation)	100,3
	B372_18	a-C:H,N	82,7
	B372_23	Si/a-C:H	124,3
	B372_25	Si/a-C:H	127,6
3b	B372_27	Si/a-C:H	123,5
	B372_29	Si/a-C:H	118,5
	B372_24	Si/a-C:H	15
	B372_26	Si/a-C:H	15
	B372_28	Si/a-C:H	15
	B372_30	Si/a-C:H	15



R&D on surface coating

R&D on surface coating deposition

Blood-Material Interaction



Biomolecular Engineering 19 (2002) 91–96

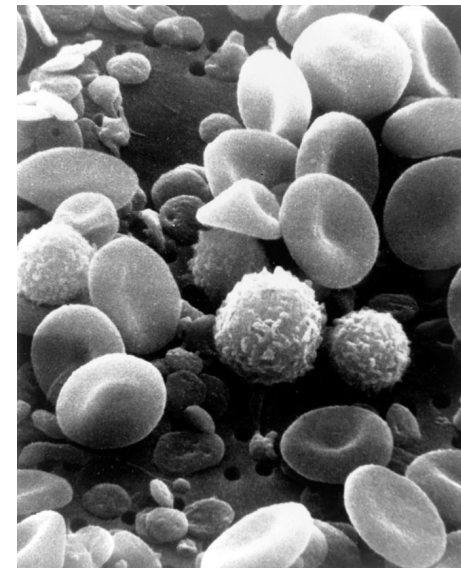
**Biomolecular
Engineering**

www.elsevier.com/locate/geneanbioeng

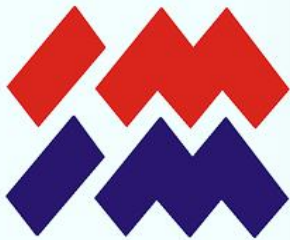
In vitro hemocompatibility testing of biomaterials according to the
ISO 10993-4

Ulrich Theo Seyfert ^{a,*}, Volker Biehl ^b, Joachim Schenk ^a

^a Abteilung Klinische Hämostaseologie und Transfusionsmedizin, Haus 75, Universitätskliniken, D-66421 Homburg, Germany
^b Universität des Saarlandes, Lehrstuhl für Metallische Werkstoffe, Im Stadtwald, D-66123 Saarbrücken, Germany



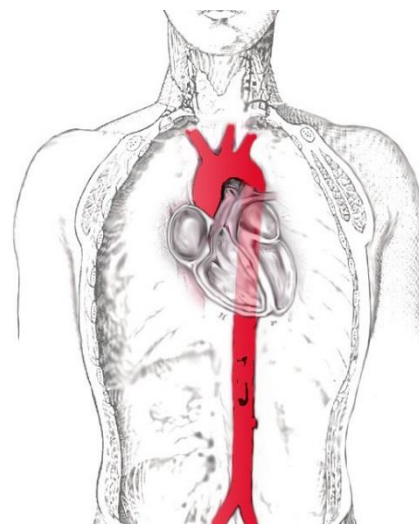
"A hemocompatible material must not adversely interact with any blood component"



R&D on surface coating

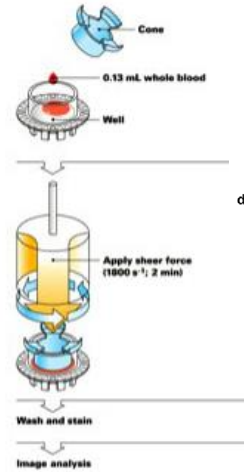
R&D on surface coating deposition

Blood-Material Interaction

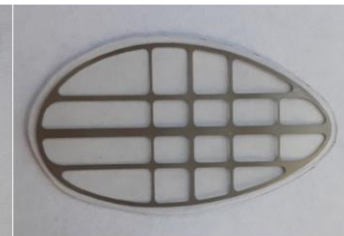
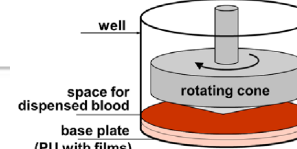


- Human blood (4 x 4.5 mL)
- ADP activation 5 min.
- Arterial flow condition simulation.
- 130 µL after the test.

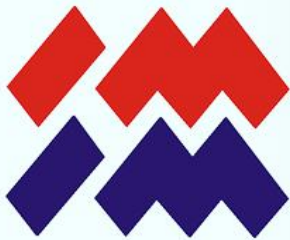
Arterial flow conditions on the flat surfaces



Impact R test



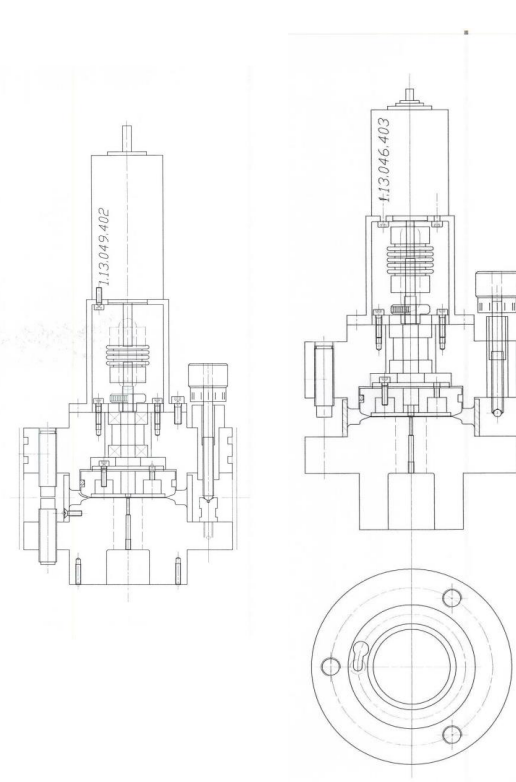
The blood-material interaction performed under the high shear stress conditions



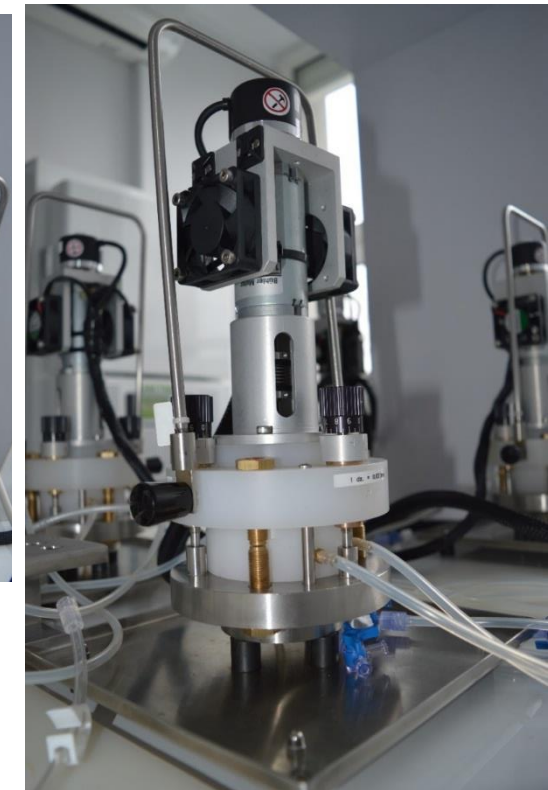
R&D on surface coating

R&D on surface coating deposition

Haemocompatibility in dynamic conditions



High speed rotor 3000-5000 rpm





R&D on surface coating

Hemocompatibility in dynamic conditions

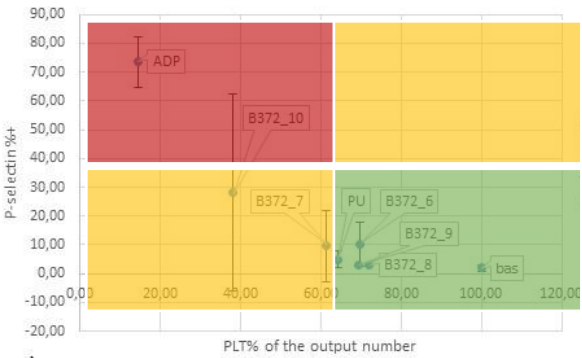
Blood-Material Interaction

P-selectin is protein that in humans is encoded by the SELP gene. P-selectin functions as a cel adhesive molecule
P-selectin- anti-selectin-P antibody

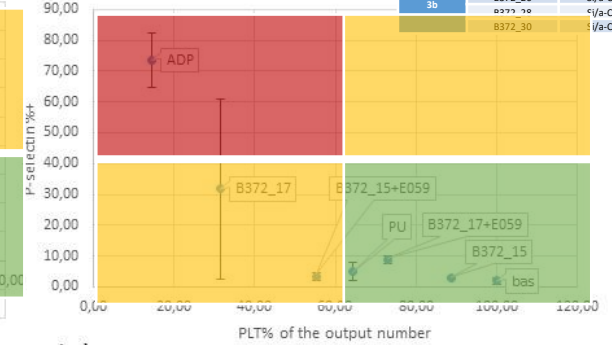
Integrin beta-3 (β_3)
 encoded by the ITGB3 gene. CD61 is a cluster of differentiation found on thrombocytes.



Group	Symbol	Layer	Thickness [nm]
1	B372_6	a-C:H	94,7
	B372_7	a-C:H,N	103,8
	B372_8	a-C:H,N	103,1
	B372_9	a-C:H,N	95,2
	B372_10	a-C:N	95,1
2	B372_15	a-C:H	94,7
	B372_15+E059	a-C:H,Sf6 (fluoridation)	94,7
	B372_16	a-C:H,N	110,3
	B372_17	a-C:H,N	100,3
3a	B372_17+E059	a-C:H,N+Sf6 (fluoridation)	100,3
	B372_18	a-C:H,N	82,7
	B372_23	Si/a-C:H	124,3
	B372_25	Si/a-C:H	127,6
	B372_27	Si/a-C:H	123,5
3b	B372_29	Si/a-C:H	118,5
	B372_24	Si/a-C:H	15
	B372_26	Si/a-C:H	15
	B372_30	Si/a-C:H	15
	B372_30	Si/a-C:H	15



a.)



b.)



c.)



d.)



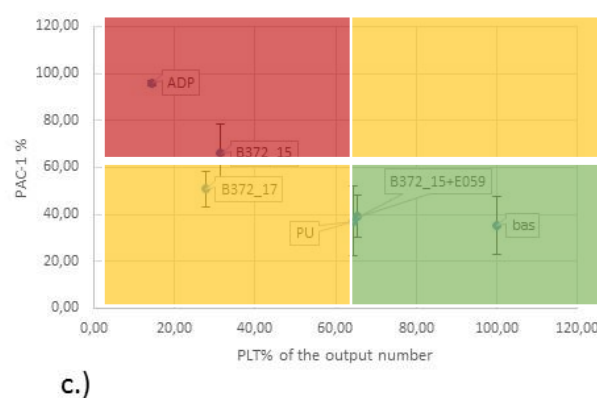
R&D on surface coating

R&D on surface coating deposition : IIb/IIIa activation

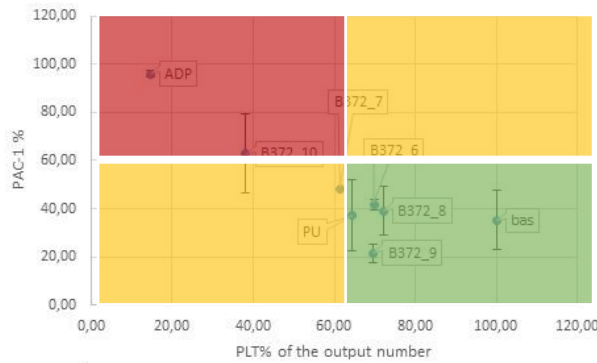
Haemocompatibility in dynamic conditions

Blood-Material Interaction

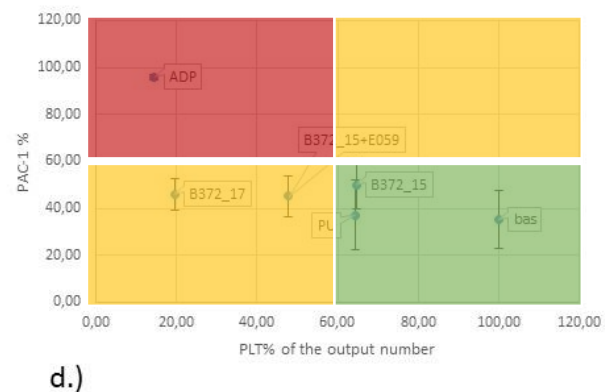
GP IIb/IIIa is an integrin complex found on platelets. It is a receptor for fibrinogen and von Willebrand factor and aids platelet activation



a.)



b.)



d.)

Integrin beta-3 (B3) encoded by the ITGB3 gene. CD61 is a cluster of differentiation found on thrombocytes.



Group	Symbol	Layer	Thickness [nm]
1	B372_6	a-C:H	94,7
	B372_7	a-C:H,N	103,8
	B372_8	a-C:H,N	103,1
	B372_9	a-C:H,N	95,2
	B372_10	a-C:N	95,1
	B372_15	a-C:H	94,7
2	B372_15+E059	a-C:H+SiF6 (fluoridation)	94,7
	B372_16	a-C:H,N	110,3
	B372_17	a-C:H,N	100,3
3a	B372_17+E059	a-C:H+SiF6 (fluoridation)	100,3
	B372_18	a-C:H,N	82,7
	B372_23	Si/a-C:H	124,3
	B372_25	Si/a-C:H	127,6
	B372_27	Si/a-C:H	123,5
	B372_29	Si/a-C:H	118,5
3b	B372_24	c1/a-C:H	15
	B372_26	Si/a-C:H	15
	B372_28	Si/a-C:H	15
	B372_30	Si/a-C:H	15

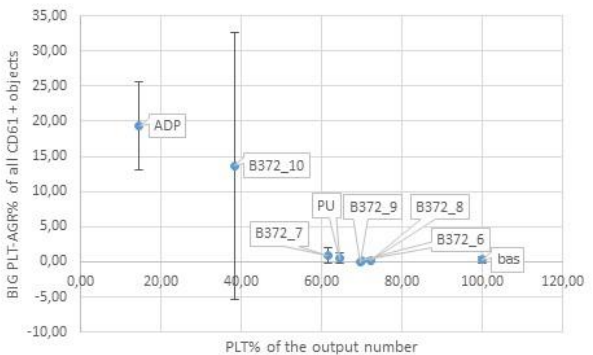


R&D on surface coating

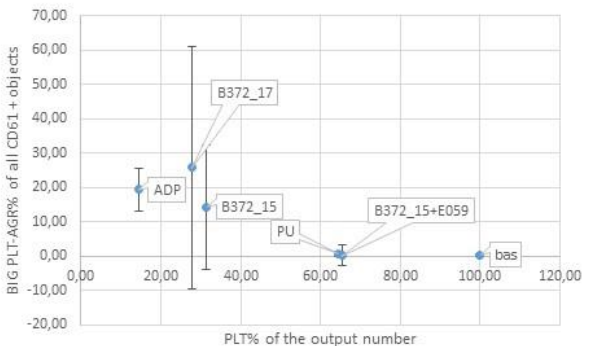
Haemocompatibility in dynamic conditions

AGGRESSION PLT
[%]

Blood-Material
Interaction



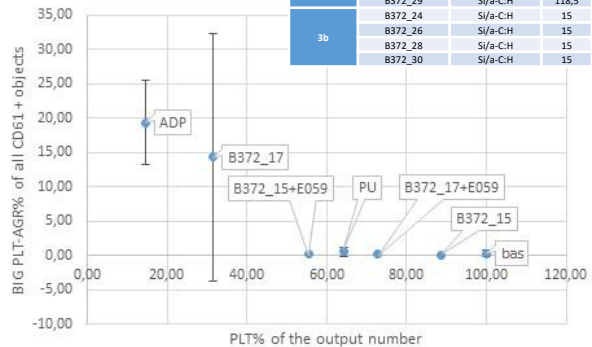
a.)



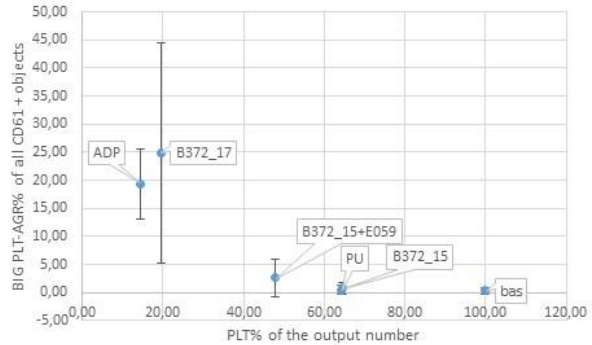
c.)



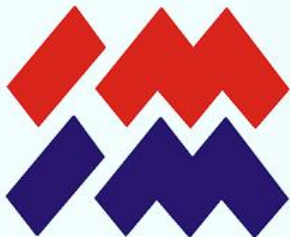
Group	Symbol	Layer	Thickness [nm]
1	B372_6	a-C:H	94,7
	B372_7	a-C:H,N	103,8
	B372_8	a-C:H,N	103,2
	B372_9	a-C:H,N	95,2
	B372_10	a-C:N	95,1
2	B372_15	a-C:H	94,7
	B372_15+E059	a-C:H+N (fluoridation)	94,7
	B372_16	a-C:H,N	110,3
	B372_17	a-C:H,N	100,3
3a	B372_17+E059	a-C:H+N+Sf6 (fluoridation)	100,3
	B372_18	a-C:H,N	82,7
	B372_23	Si/a-C:H	124,3
	B372_25	Si/a-C:H	127,6
	B372_27	Si/a-C:H	123,5
3b	B372_29	Si/a-C:H	118,5
	B372_24	Si/a-C:H	15
	B372_26	Si/a-C:H	15
	B372_28	Si/a-C:H	15
	B372_30	Si/a-C:H	15



b.)



d.)

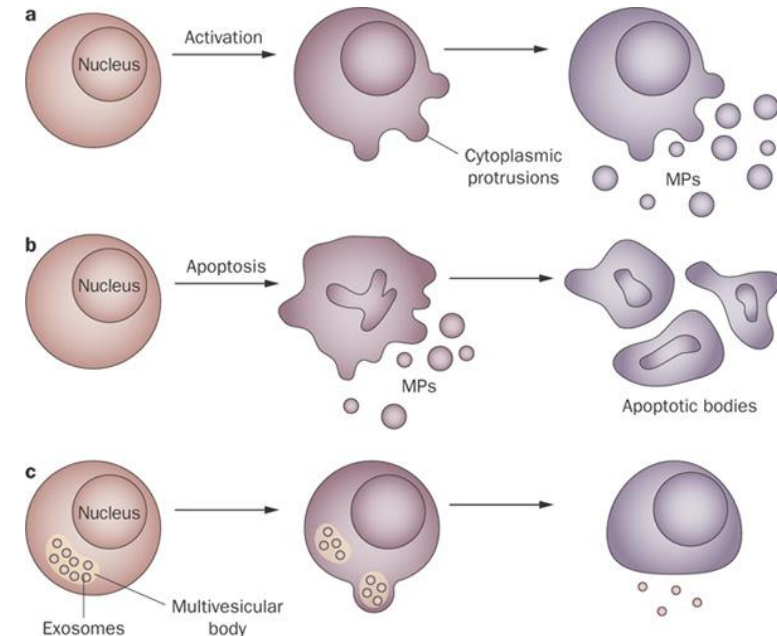
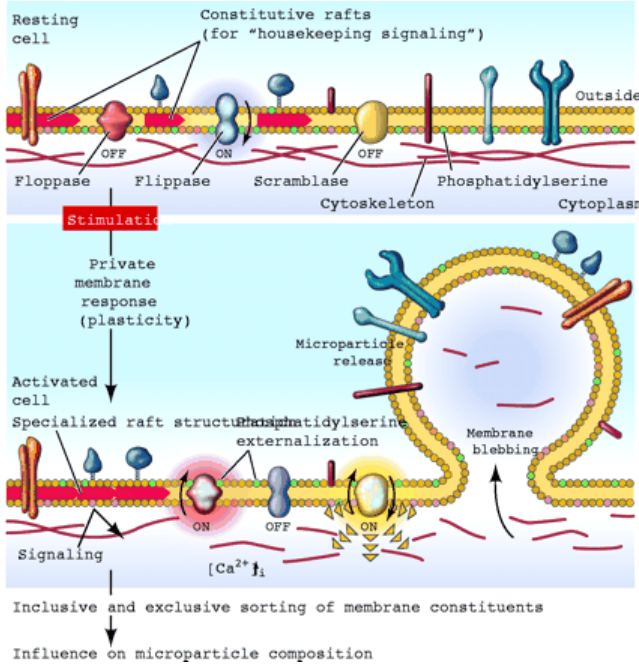


R&D on surface coating

Blood-Material Interaction

R&D on surface coating deposition

Microparticles (MPs) are small membrane vesicles that are released by activated or apoptotic cells.



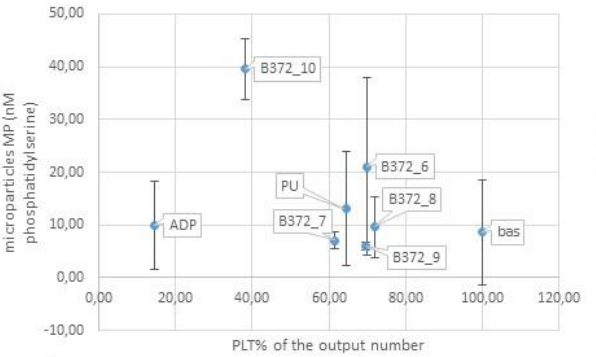


R&D on surface coating

Haemocompatibility in dynamic conditions

Blood-Material Interaction

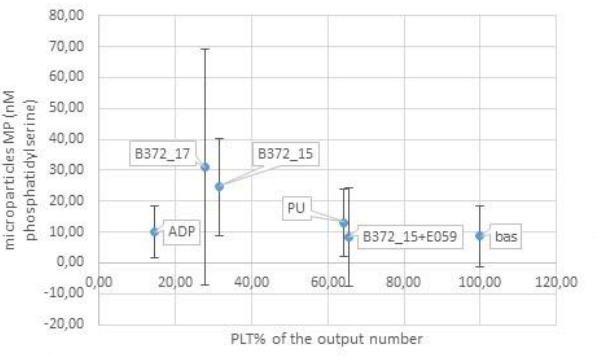
**Microparticles MP
[nm fosfatidylserine]**



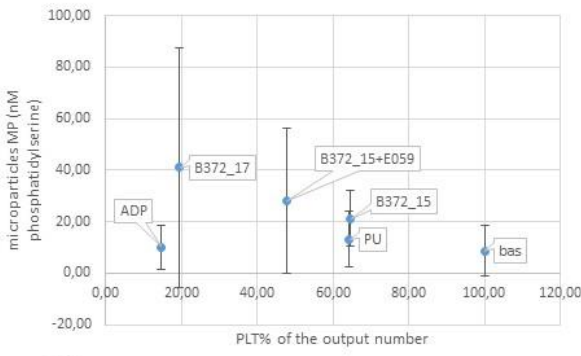
a.)



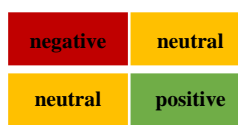
b.)



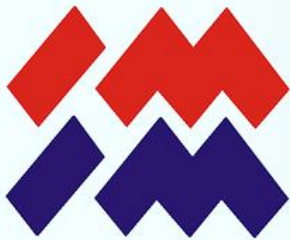
c.)



d.)



Group	Symbol	Layer	Thickness [nm]
1	B372_6	a-C:H	94,7
	B372_7	a-C:H,N	103,8
	B372_8	a-C:H,N	103,2
	B372_9	a-C:H,N	95,2
	B372_10	a-C:N	95,1
2	B372_15	a-C:H	94,7
	B372_15+E059	a-C:H,SF ₆ (fluoridation)	94,7
	B372_16	a-C:H,N	110,3
	B372_17	a-C:H,N	100,3
3a	B372_17+E059	a-C:H,N,SF ₆ (fluoridation)	100,3
	B372_18	a-C:H,N	82,7
	B372_23	Si/a-C:H	124,3
	B372_25	Si/a-C:H	127,6
	B372_27	Si/a-C:H	123,5
3b	B372_29	Si/a-C:H	118,5
	B372_24	Si/a-C:H	15
	B372_26	Si/a-C:H	15
	B372_28	Si/a-C:H	15
	B372_30	Si/a-C:H	15

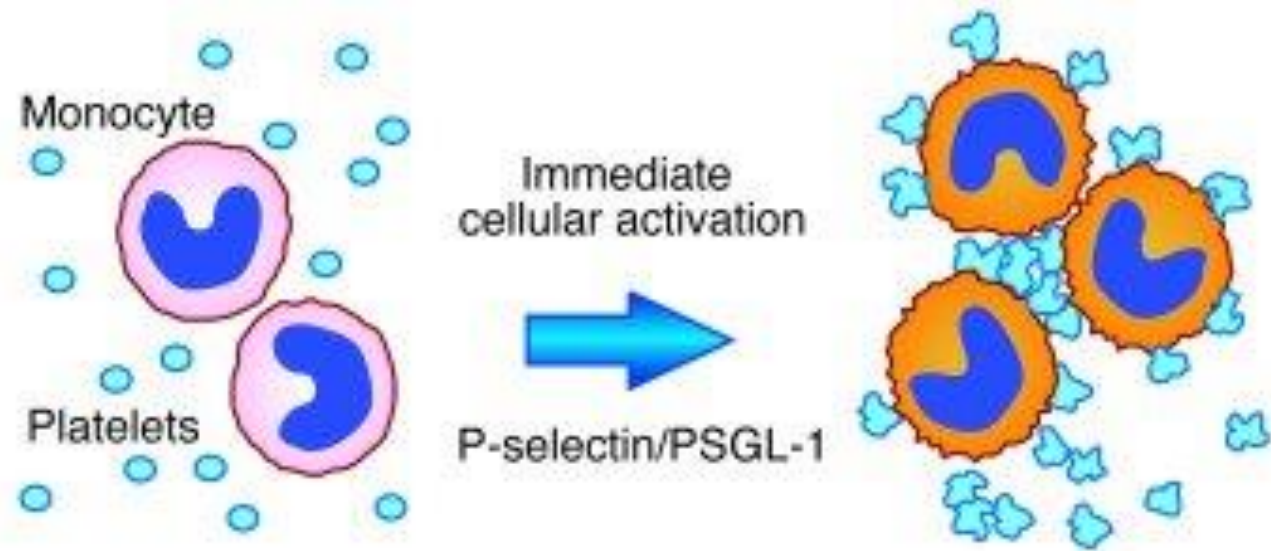


bio-VALVE

R&D on surface coating deposition

Haemocompatibility in dynamic conditions

Aggregation-
mon-PLT





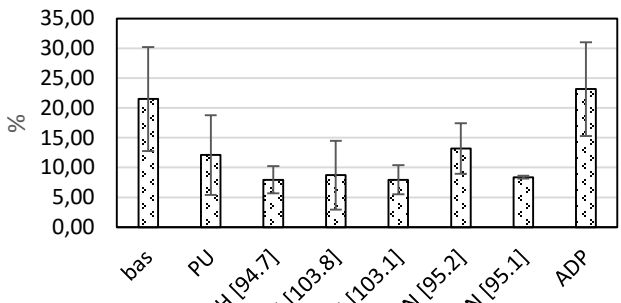
R&D on surface coating

Haemocompatibility in dynamic conditions

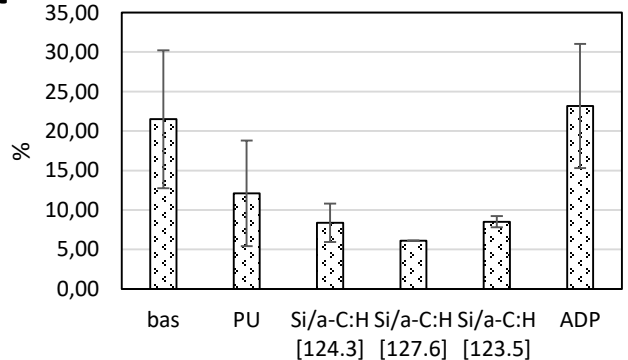
Blood-Material Interaction

Mon-PLT
P-SEL G1

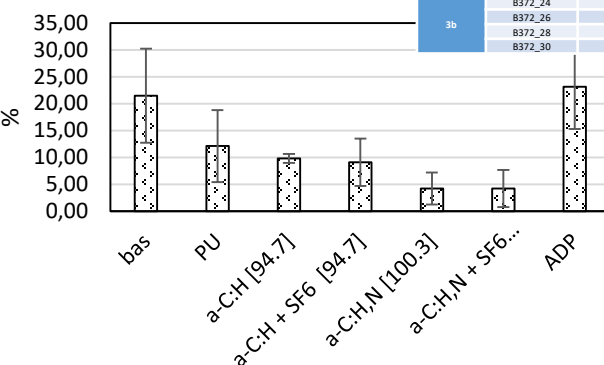
1



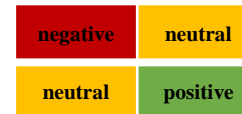
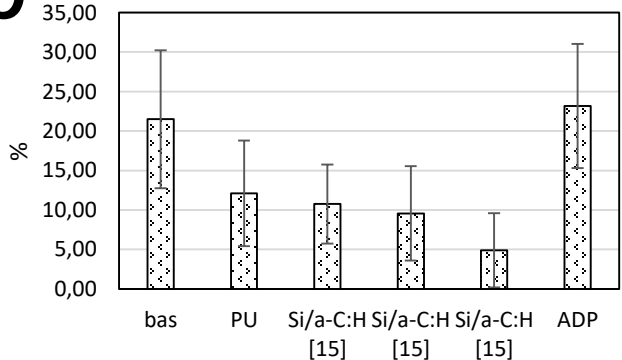
3a



2



3b



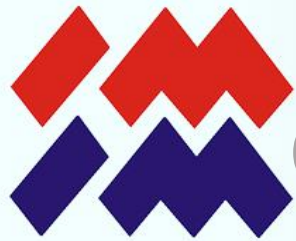
Group	Symbol	Layer	Thickness [nm]
1	B372_6	a-C:H	94,7
	B372_7	a-C:H,N	103,8
	B372_8	a-C:H,N	103,1
	B372_9	a-C:H,N	95,2
	B372_10	a-C:N	95,1
	B372_15	a-C:H	94,7
	B372_15+E059	a-C:H,SF6 (fluoridation)	94,7
	B372_16	a-C:H,N	110,3
	B372_17	a-C:H,N	100,3
	B372_17+E059	a-C:H,N,SF6 (fluoridation)	100,3
2	B372_18	a-C:H,N	82,7
	B372_23	Si/a-C:H	124,3
	B372_25	Si/a-C:H	127,6
	B372_27	Si/a-C:H	123,5
3a	B372_29	Si/a-C:H	118,5
	B372_24	Si/a-C:H	15
	B372_26	Si/a-C:H	15
	B372_28	Si/a-C:H	15
3b	B372_30	Si/a-C:H	15



Task 6

Complete valve testing

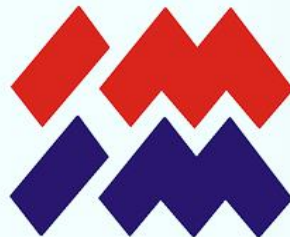
Studies of local reactions after implantation



Complete valve testing

In vivo tests of „simple” samples





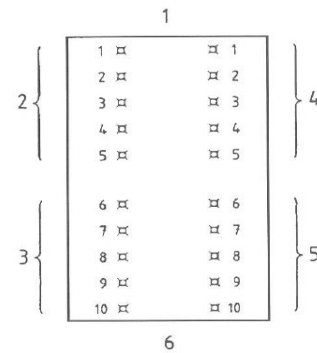
Complete valve testing

Reaction	Scoring irritation
Erythema formation	
No erythema	0
Very slight erythema	1
Well defined erythema	2
Moderate erythema	3
Severe erythema (dark red)	4
Edema formation	
Lack of edema	0
Very weak swelling (barely perceptible)	1
Well defined erythema (edges of the area well defined by elevation)	2
Moderate edema (elevation of about 1 mm)	3
Painful swelling (elevation above 1 mm goes beyond the area of exposure)	4
Maximum possible score	8



The scale of evaluation of responses in intradermal reactivity tests

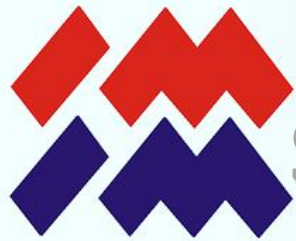
1- side of the animal's head, 2 injections of extract in polar solvent, 3 injections of pure polar solvent, 4 injections of the extract in a non-polar solvent, 5 injections of a pure non-polar solvent, 6 parts of the tail of the animal



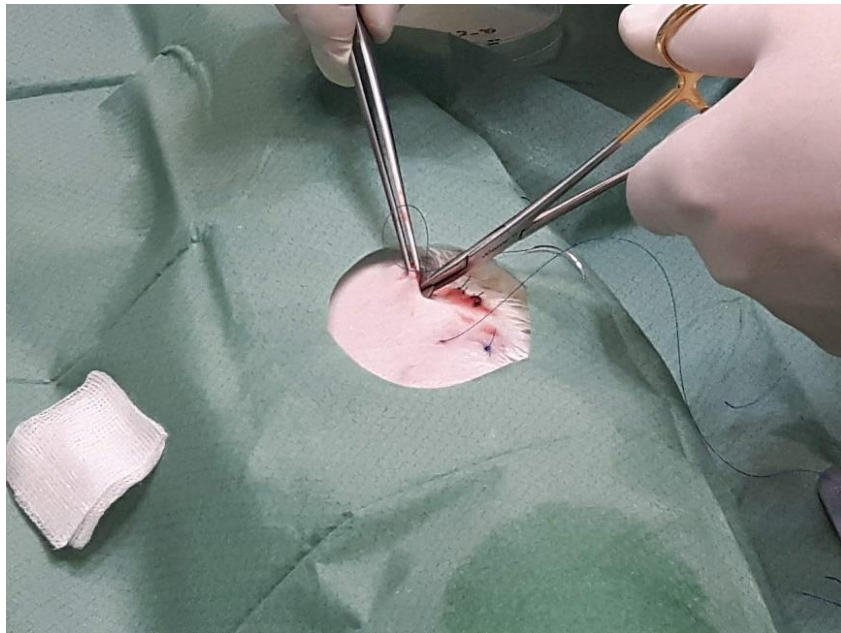
Exemplary image of the animal's skin 72h after injection.

Intradermal reactivity - location of injection points (according to ISO 10993-10)
Intradermal reactivity - location of injection points (according to ISO 10993-10)

The test results showed that the tested material extracted with apolar and polar extract did not irritate the skin of rabbits during the 72 h observation period. The tested material met the test requirements because the difference between the average test score and the average control score was less than 1.0 (= 0.13) and in accordance with the normative guidelines ISO 10993-10 was considered non-irritating. It can be concluded that the tested material does not induce intradermal reaction.



Studies of local reactions



Placing the disc of the tested material under the skin on the back of the animal.

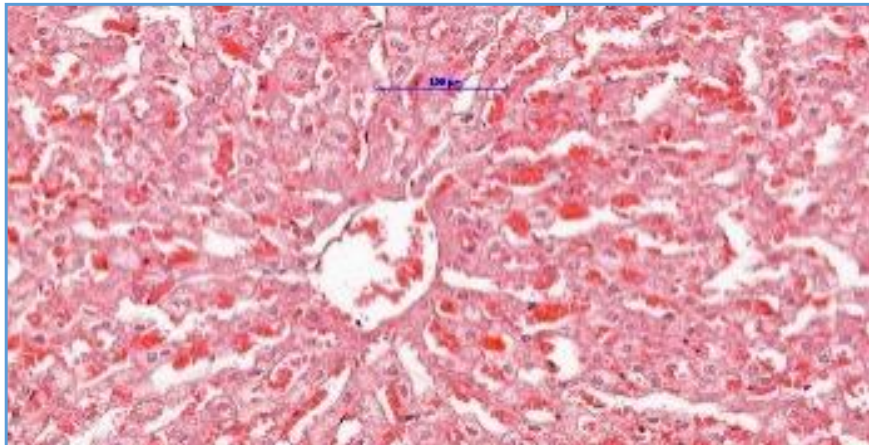


Study group, rabbit No. 2. Implanted site of implantation after 4 weeks, visible petechiae.

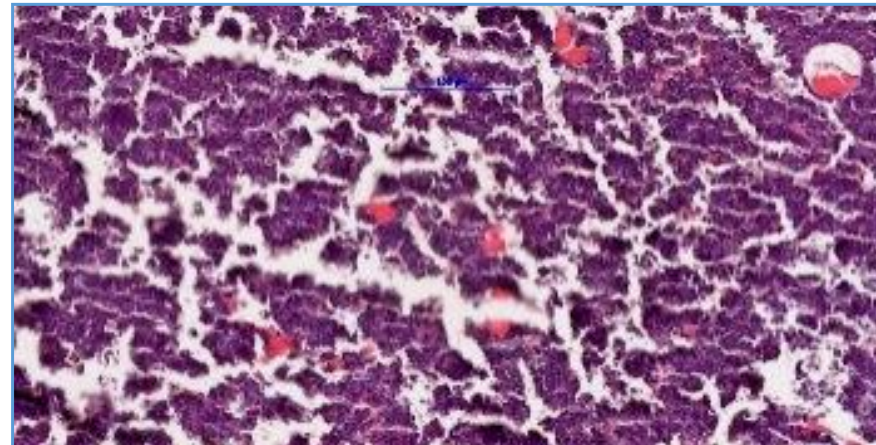


Studies of local reactions

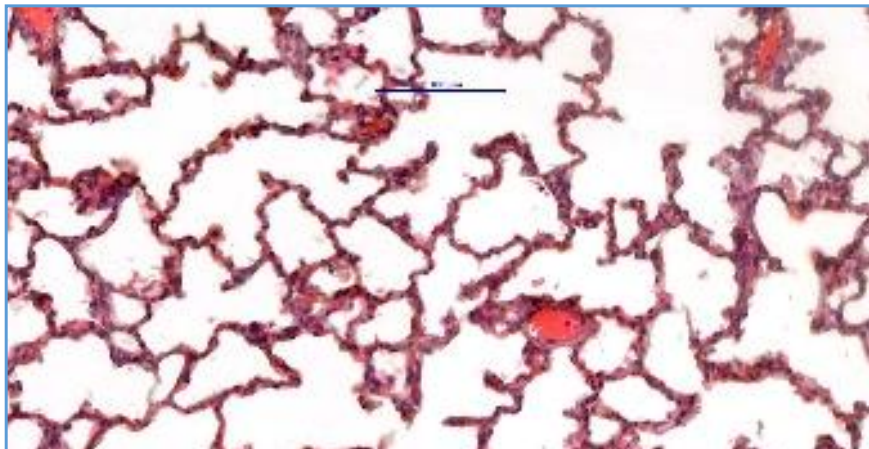
HISTOLOGY (liver, thymus, lung, myocardium)



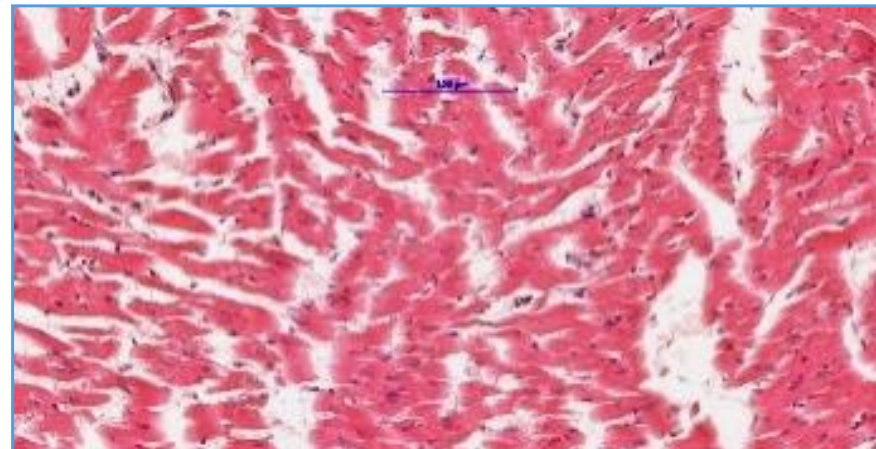
Correct liver lacunae. Mag. 200x



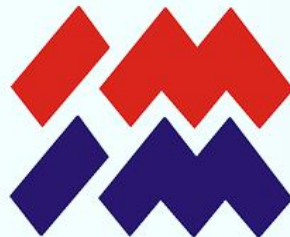
Proper thymic lacunae with Hassal's tiny pink bodies. Mag. 200x



Properly aerated lung parenchyma. Mag. 200x



Correct binding of the myocardium. Mag. 200x



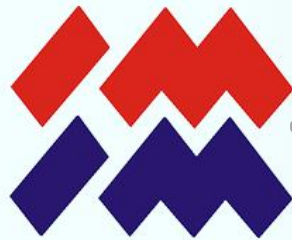
Technology readiness level



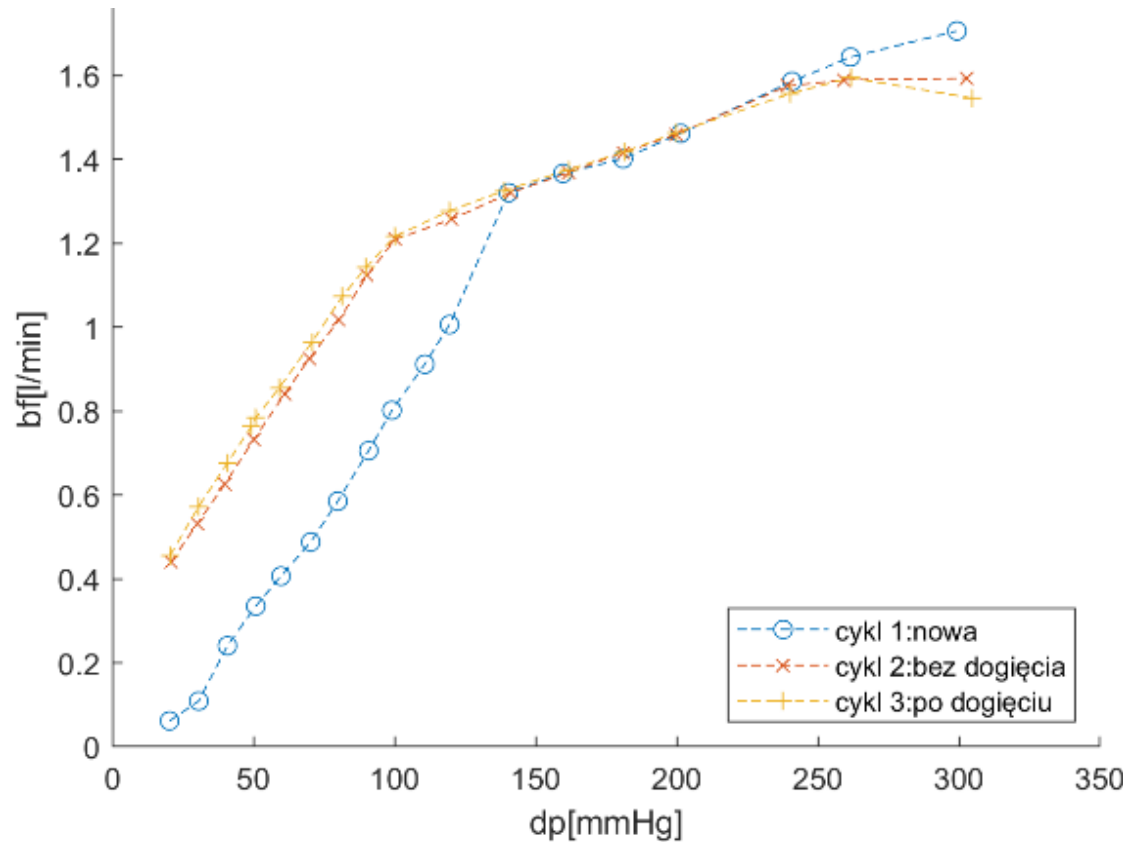


Technology readiness level

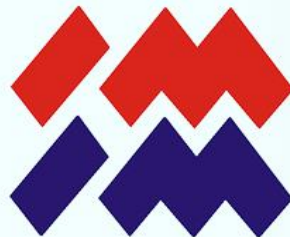




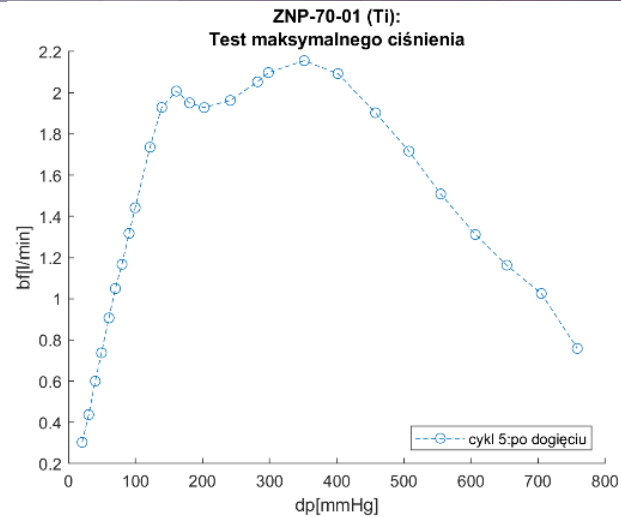
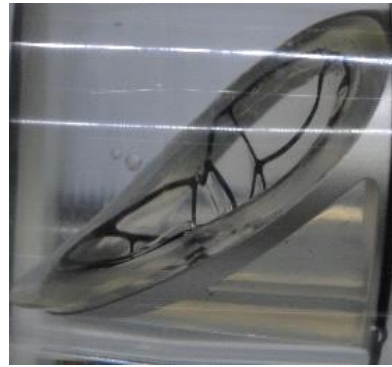
Technology readiness level



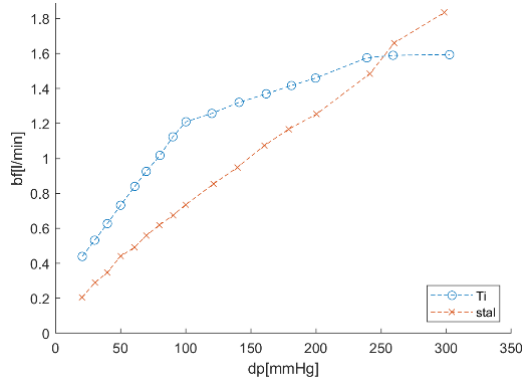
Hydrodynamic analysis in an artificial patient system
using a blood simulating medium (glycerin solution) and
determining the risk of turbulence and wear



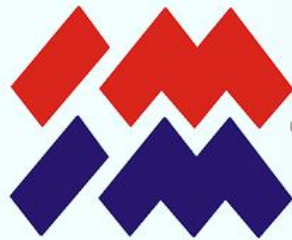
Technology readiness level



ZNP-Ti: flake deformation for: (1) $dp = 100\text{mmHg}$, (2) $dp = 760\text{mmHg}$, (3) after removal from the system. On the right: sealing of the valve under the deformation of the flap with pressure of $> 400\text{mmHg}$.



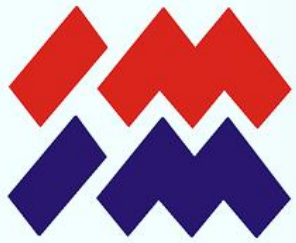
ZNP-S: (1) initial geometry, (2) deformation for $dp = 300\text{mmHg}$, (3) ditch is $dp = 0\text{mmHg}$. On the right: comparison of backflow of valves with a titanium and steel frame



Technology readiness level

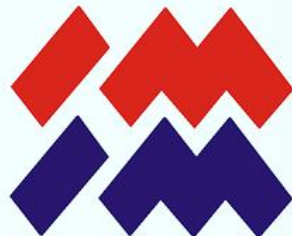


ZWP-Ti: breakthrough of the valve leaf at
a pressure of $dp = 45\text{mmHg}$.

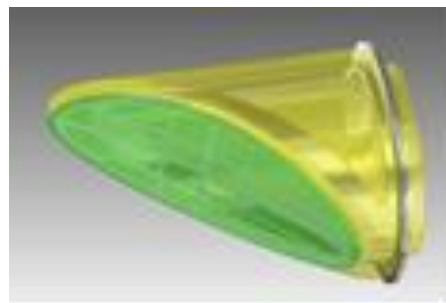


Improvement

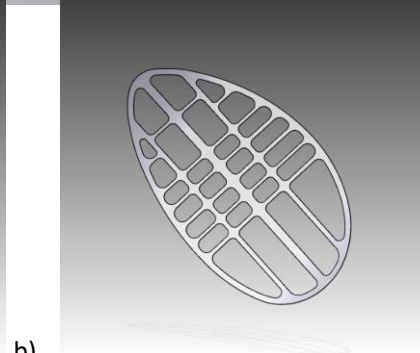
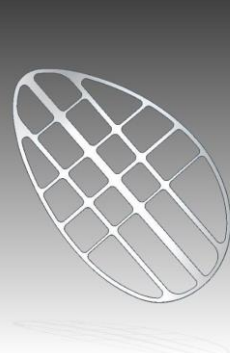
Design



Further steps

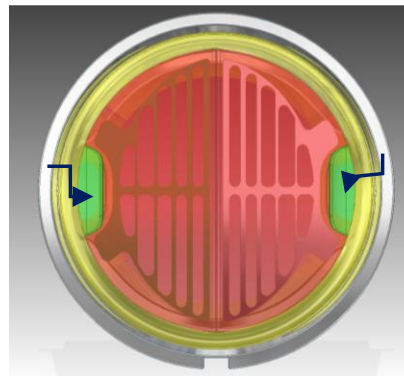
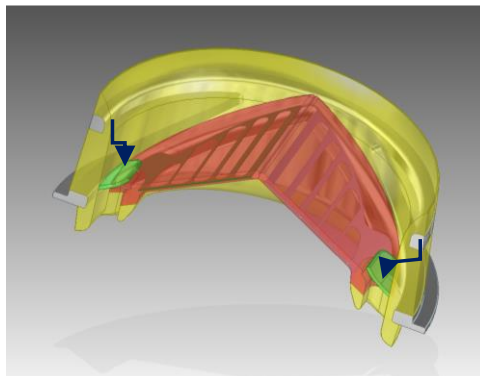
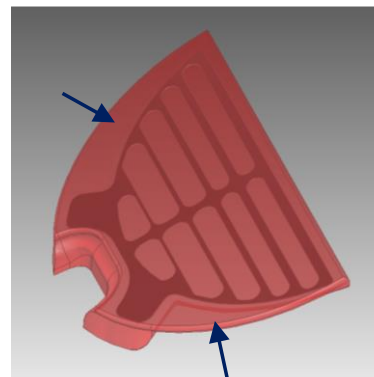
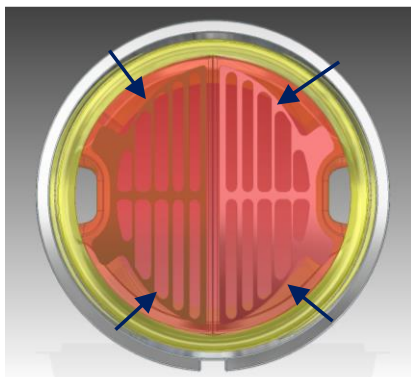


a)



b)

c)





Narodowe Centrum
Badań i Rozwoju

M-ERA.NET Transnational Call 2017

Project Acronym: 4DbloodROT

Partners:

JOANNEUM RESEARCH Forschungsges.m.b.H., Institute for Surface Technologies and Photonics, Austria;
Polish Academy of Sciences Institute of Metallurgy and Materiala Science in Cracow, Poland
Foundation for Heart Surgery Development, Poland;
In-Vision Digital Imaging Optics GhbH, Austria; Lithoz GmbH, Austria;
Polymer Competence Center Leoben GmbH, Austria;
University of Leoben, Institute of Chemistry of Polymeric Materials, Austria,
MESco Sp.z o.o. Poland

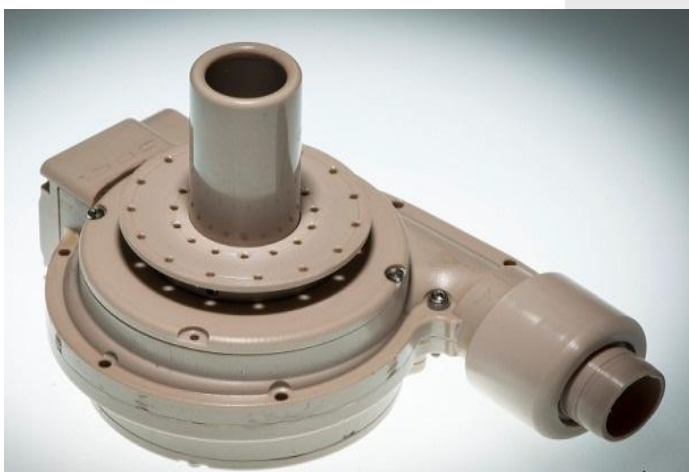
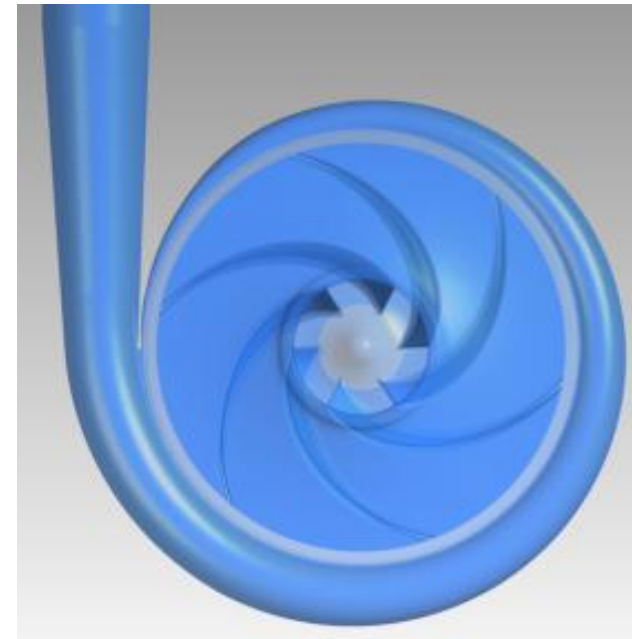
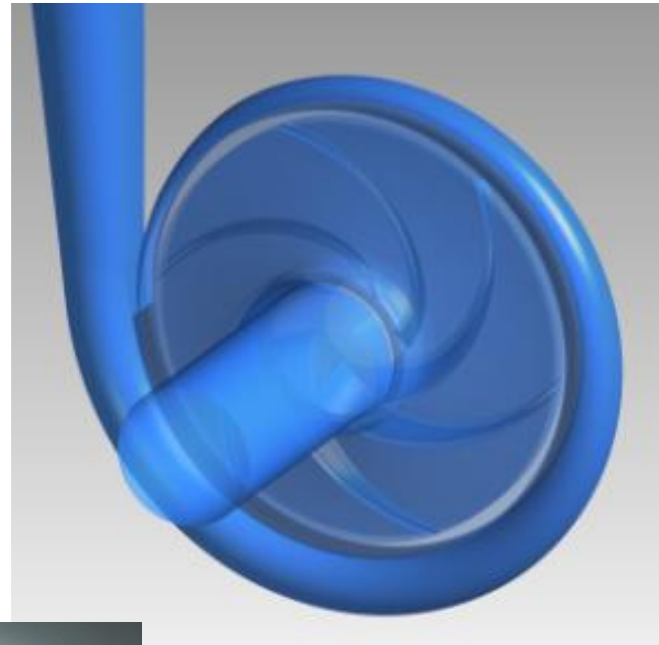
The research was financially supported by the Project no. DWM/M-ERA.NET-2017/16/2018
“4 Dimensional Single Piece Miniaturized Blood Rotor” of the Polish National Centre of
Research and Development.



1.) Modification of the rotor pump



ReligaHeart ROT

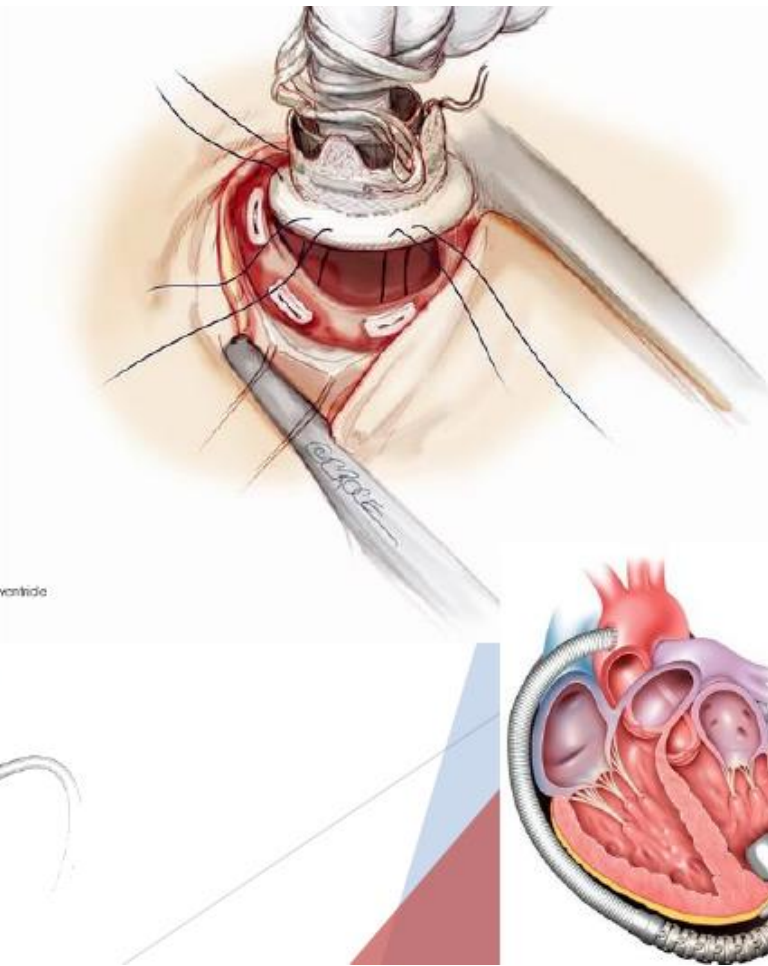
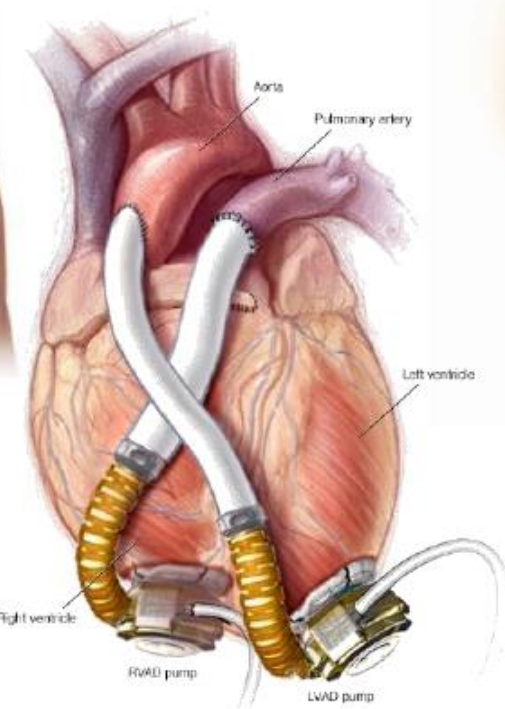
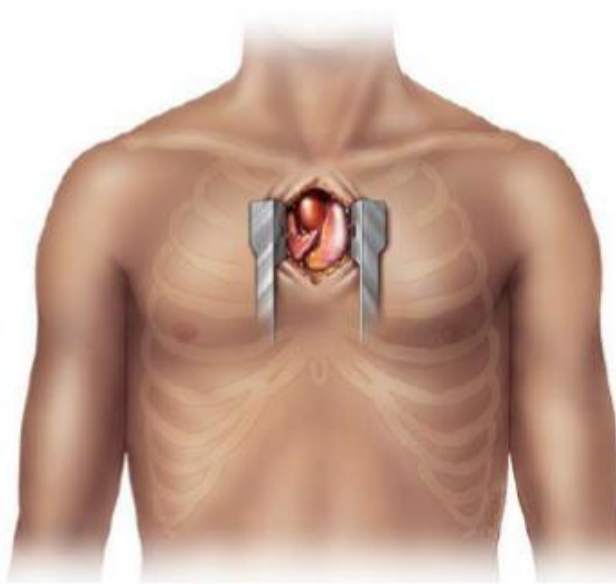


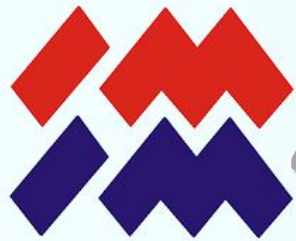


HeartWareInternational - Medtronic

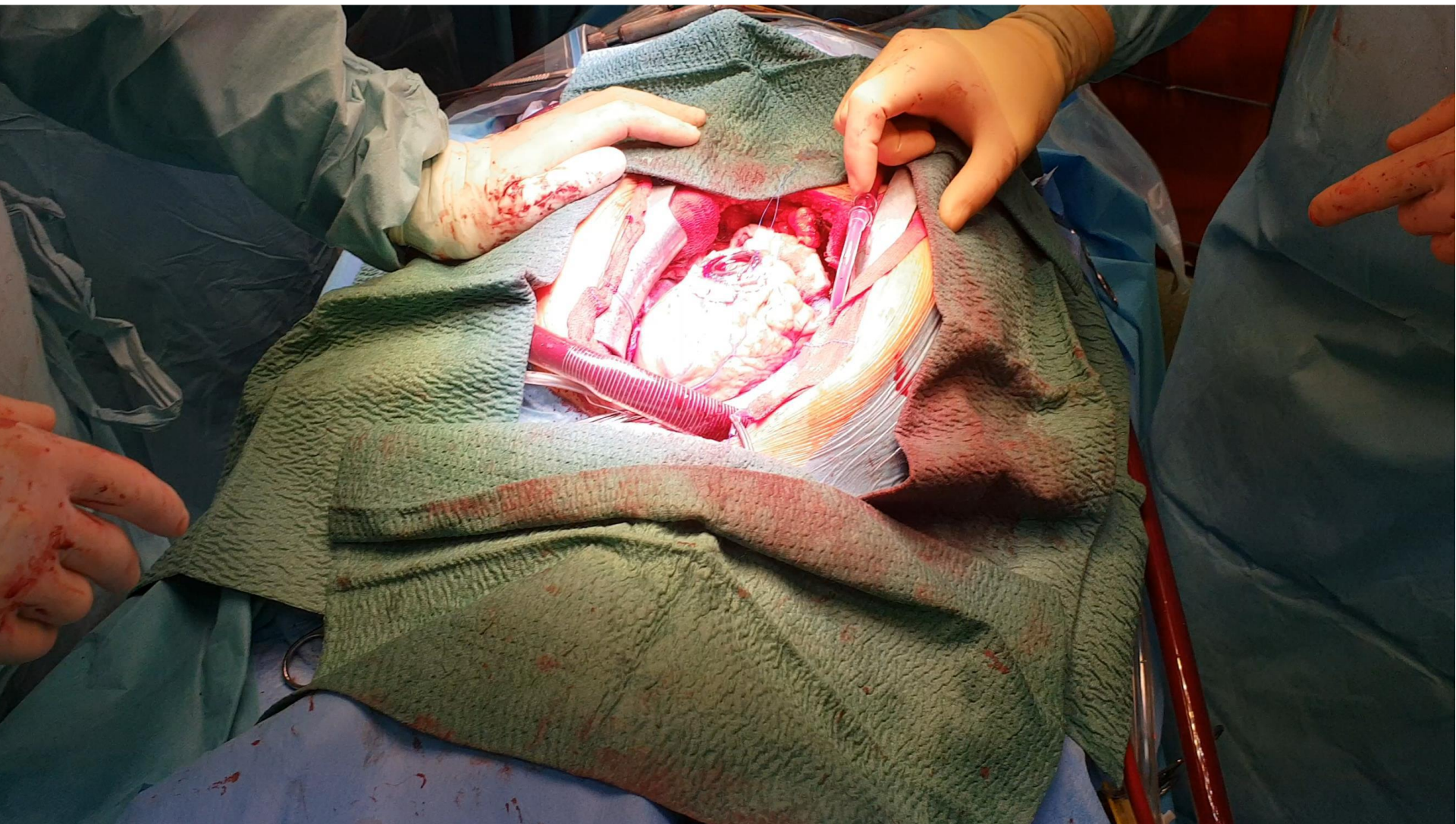


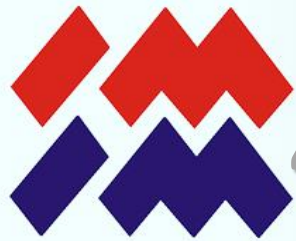
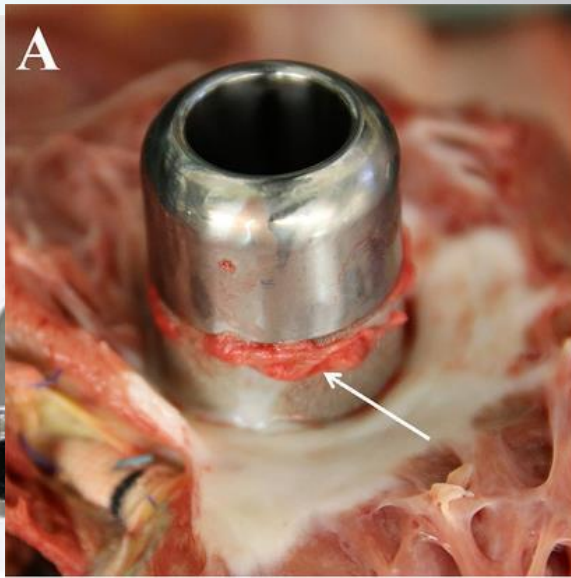
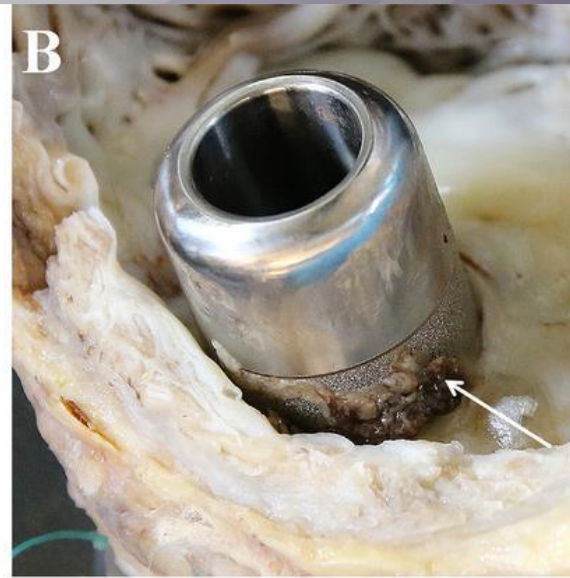
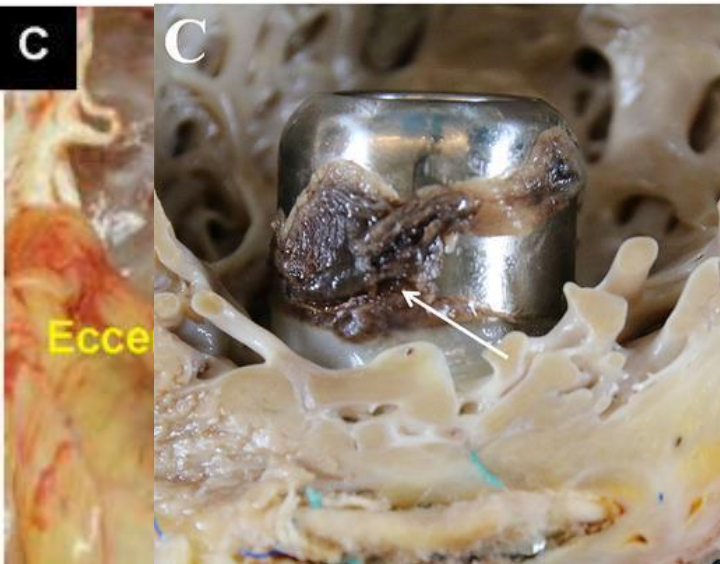
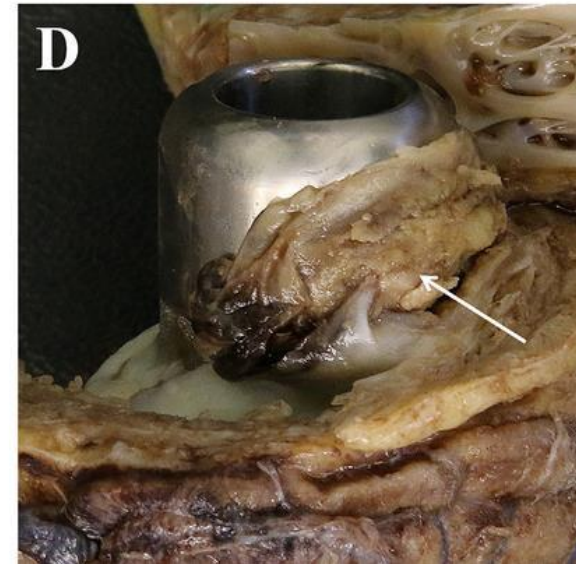
4DbloodROT

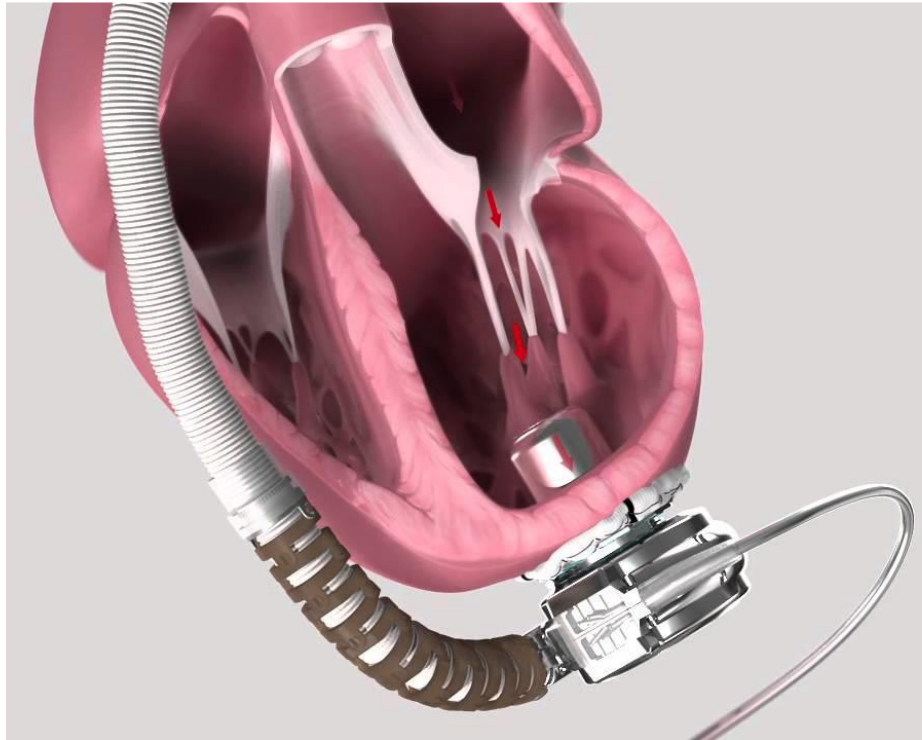




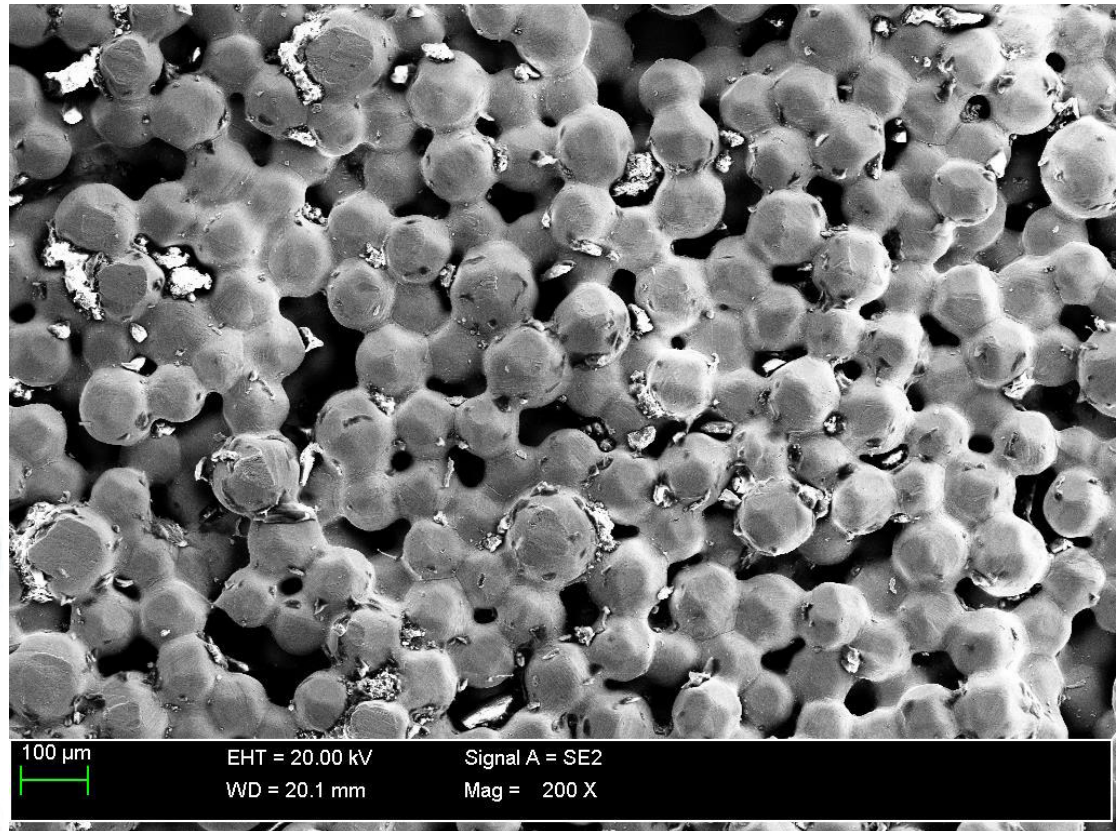
4DbloodROT



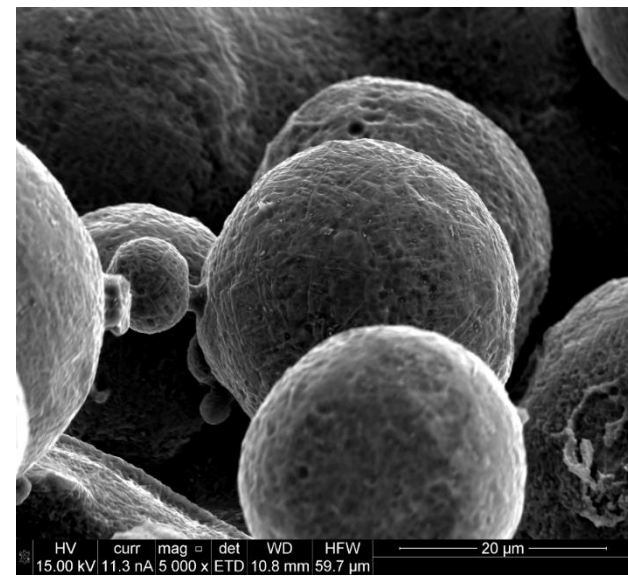
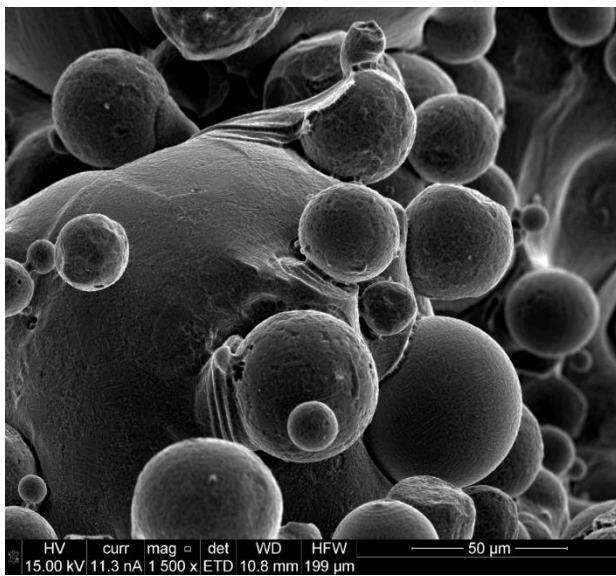
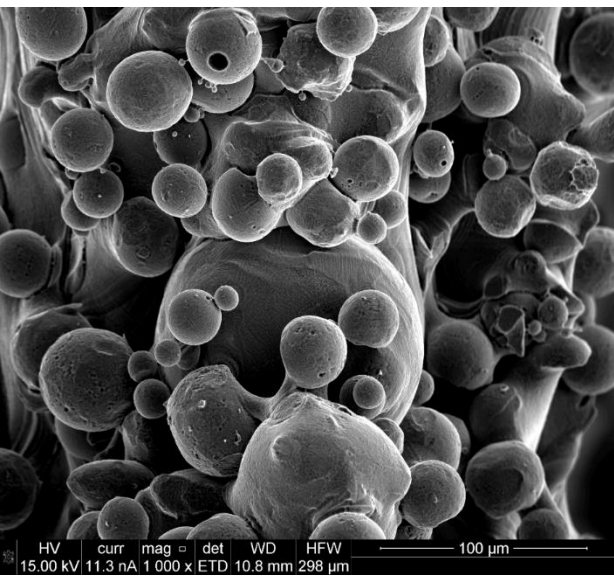
**A****A****B****C****C****D****D**



Thrombotic events are associated with:
the pump surface,
a drainage duct,
the bearing arrangement of the pump
the surface of the inflow cannula inserted into the apex of the left ventricle

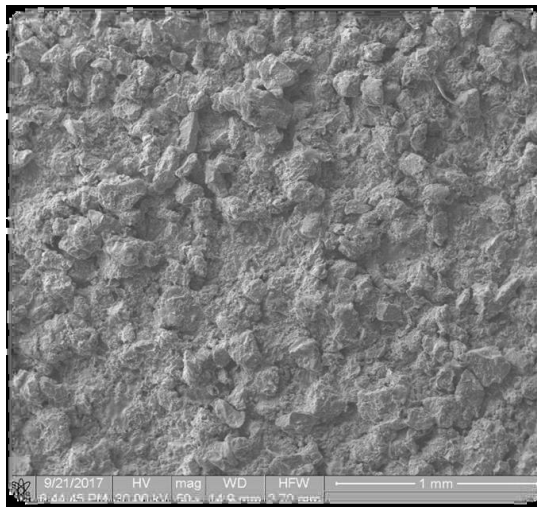
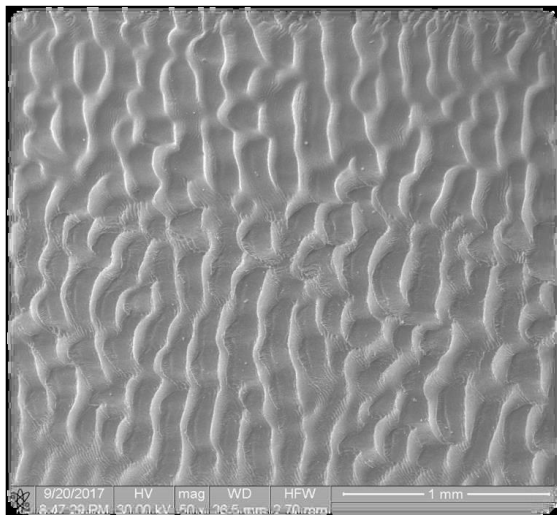
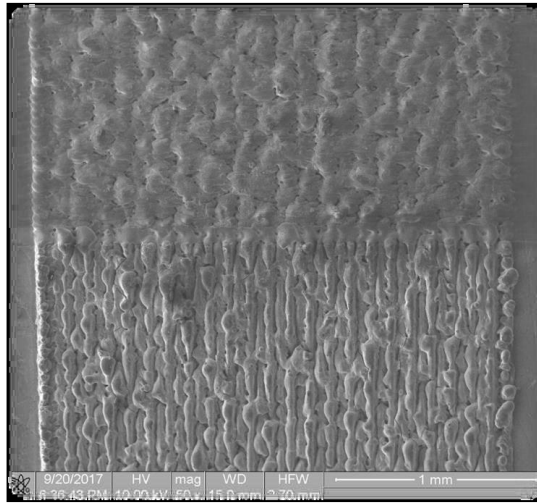
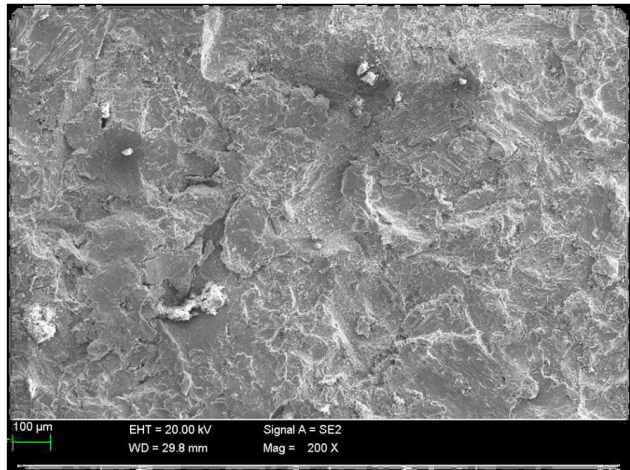


Scanning Electron Microscopy



Coating with TiAl6Nb4 alloy

Institute of Optoelectronics Military University of
Technology Warsaw, Poland





2.) New design of the miniaturized pump

HeartMate PHP

High flow, low profile

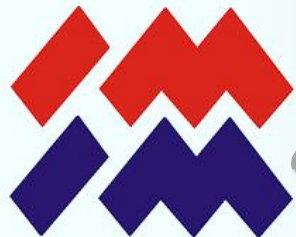
HeartMate PHP is an acute percutaneous heart pump that disrupts the traditional relationship between size and flow to provide care without compromise.

It is designed to deliver the blood flow needed to quickly stabilise haemodynamically compromised patients and provide optimal haemocompatibility.

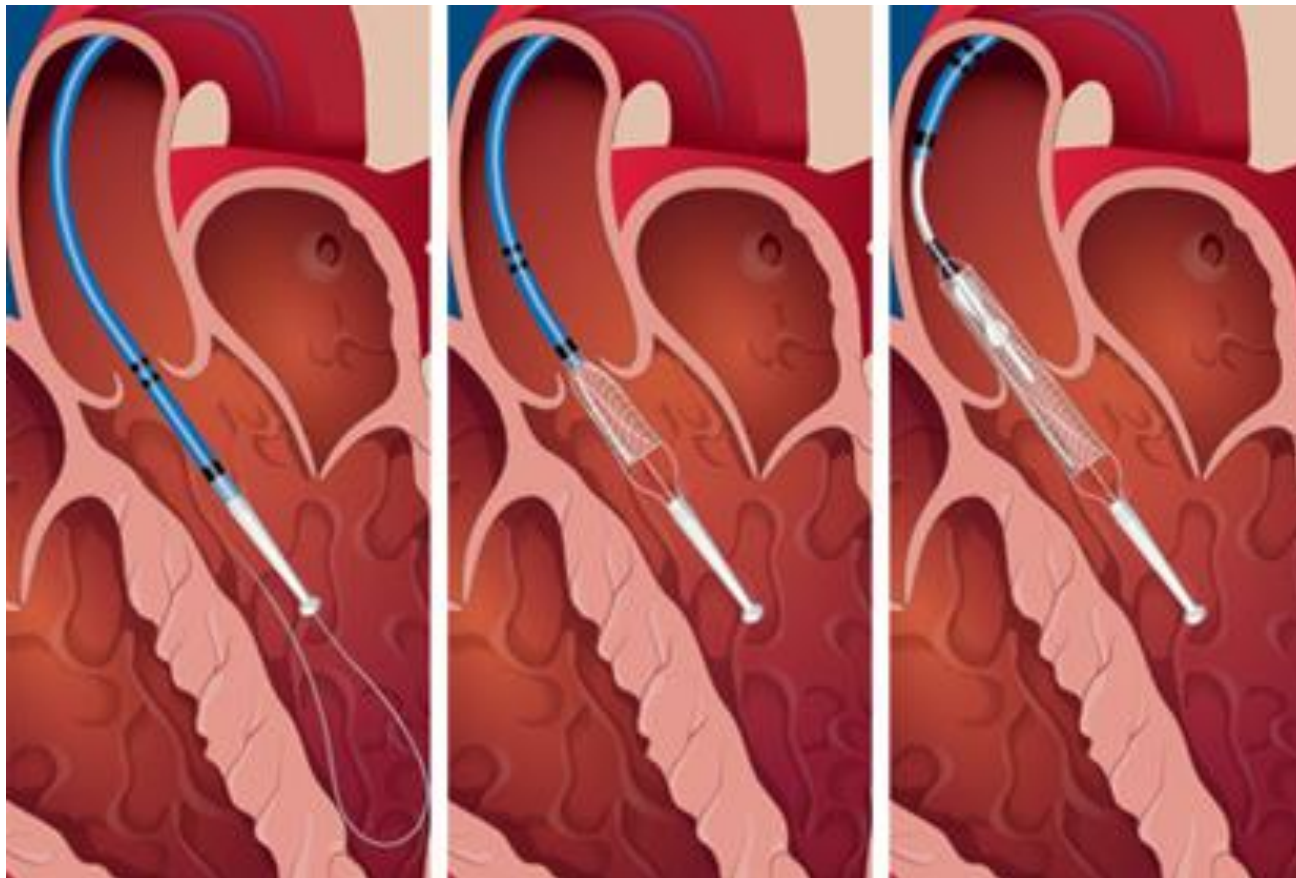
The catheter-based pump is designed for percutaneous entry through the femoral artery. Upon insertion via a low-profile introducer sheath, the catheter is advanced into the left ventricle where the cannula is unsheathed and fully expands to allowing for near-full physiological mean blood flow rates.

[View full HeartMate PHP System](#)

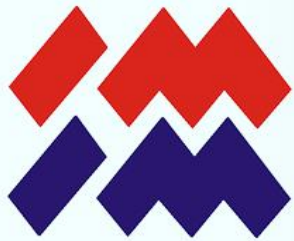




4DbloodROT



The covered nitinol cannula and integrated impeller expand from a low 13F insertion profile to 24F once unsheathed across the aortic valve for near-physiological mean blood flow of over 4 L/min



B3L



The interaction of ionizing radiation with tissue in the aspect of generating the process of acellularisation in the preparation of animal origin autologous tissue

Roman Major^{1,a}, Gabriela Imbir^{1,b}, Magdalena Kopernik^{2,c}, Piotr Wilczek^{3,d} and Roman Ostrowski^{4,e}

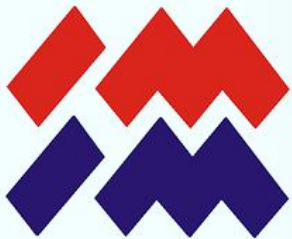
¹Institute of Metallurgy and Materials Science, PAS, 25 Reymonta St. 30-059 Cracow, Poland

²AGH University of Science and Technology al. Mickiewicza 30, 30 - 059 Cracow Poland

³Foundation of Cardiac Surgery Development, Wolności 345a, 41-800 Zabrze, Poland

⁵Institute of Optoelectronics, Military University of Technology, 2 Sylwestra Kaliskiego St.
00-908 Warsaw, Poland

^ar.major@imim.pl, ^bg.imbir@imim.pl, ^ckopernik@agh.edu.pl, ^dp.wilczek@frk.pl, ^eroman.ostrowski@wat.edu.pl



Purpose

The research was financially supported by the Project no. 2016/23/B/ST8/01481 Interdisciplinary methods of creating and functioning of biomimetic materials based on Animal origin extracellular matrix of the Polish National Center of Science. Part of the work was co-financed by the European Union from resources of the European Social Fund (Project No.WND-POWR.03.02.00-00-I043/16). The research was co-financed by the European Union from resources of the European Social Fund (Project No.WNDPOWR.03.02.00-00-I043/16).



Motivation

"My great desire to create a Polish artificial heart is finally being fully realized. Efforts to surround this undertaking to take care of the state, crowned with the adoption of the Multi-Year Program "Polish Artificial Heart", I consider a huge success. I am so happy and I wish you all the best for all those involved in the work".

prof. Zbigniew Religa

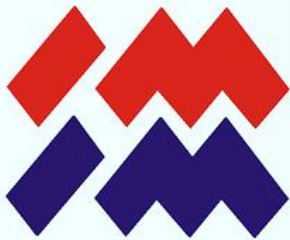


Motivation

Transcatheter Aortic Valve Implantation (TAVI)

From the beginning of the twenty-first century, the method of percutaneous aortic valve implantation has been developing.

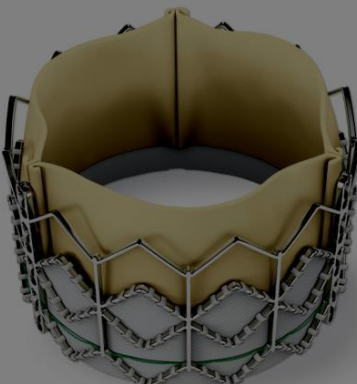
The valve for this procedure has a completely different structure from the classic one.



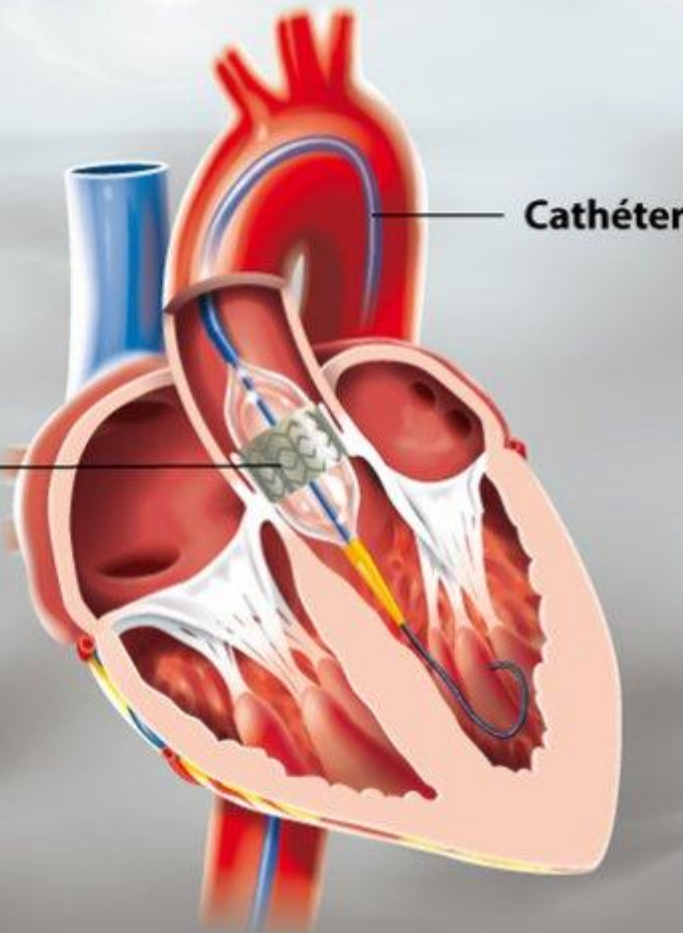
Motivation

TAVI

Prosthetic valve flakes are suspended on a special metal construction (self-expanding stent or expanded by means of a balloon). The valve is inserted through the transdermal system and expands in the damaged valve without removing it.



Valve
trans-artérielle
ou TAVI





Motivation

TAVI indications

This is a method for a group of patients who according to experts (heart team) are not eligible for the classic AVR cardiac surgery (aortic valve replacement) due to the severe general condition, the severity of the underlying disease and associated conditions.



Motivation

TAVI - clinical contraindications

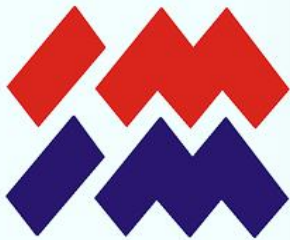
- Expected life expectancy <1 year
- A small chance to improve the quality of life due to the presence of comorbidities
- Severe primary related disease of another valve that causes symptoms and can only be treated surgically



Motivation

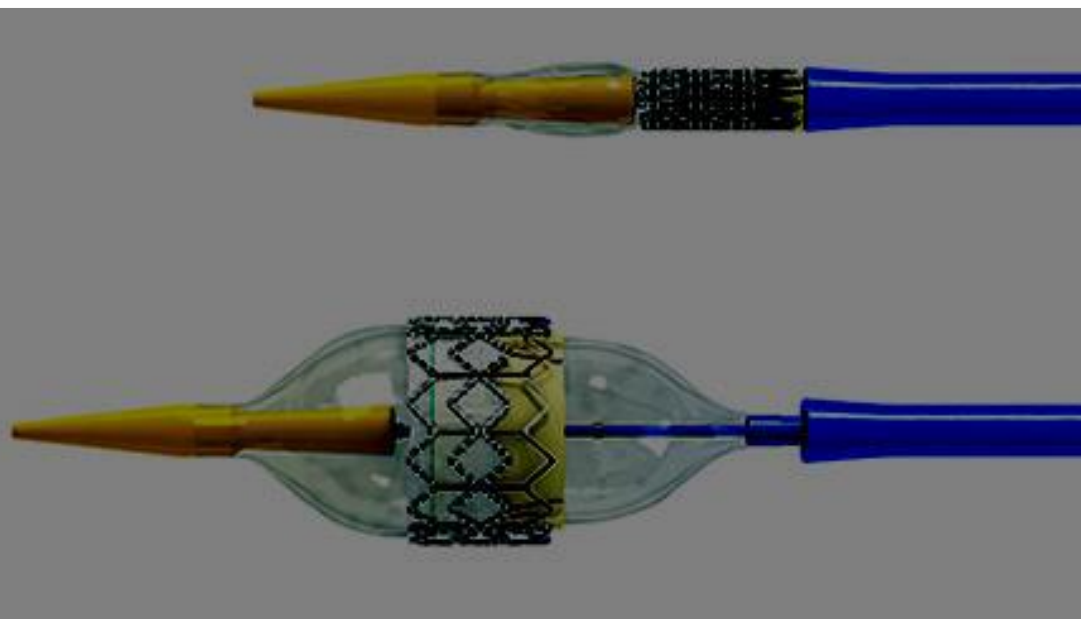
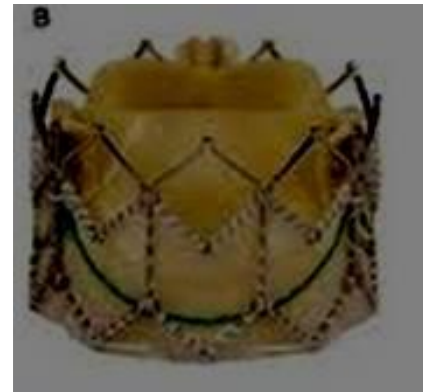
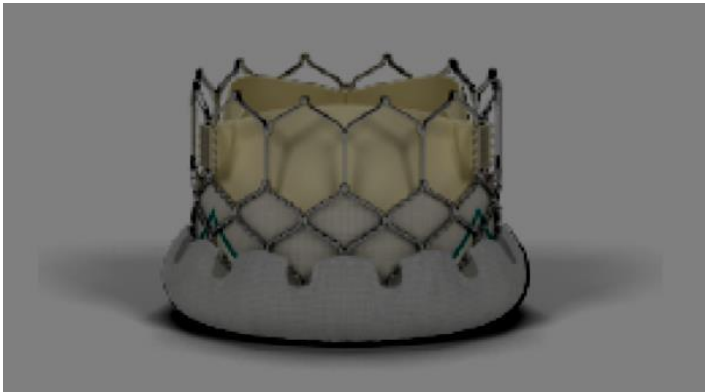
TAVI - anatomical contraindications

- Incorrect size of the aortic valve ring (<18 mm, > 29 mm)
 - Thrombus in the left ventricle
 - Active endocarditis
 - Increased risk of coronary artery blockage
(asymmetric calcification of the valve, short distance between the ring and the onset of coronary arteries, small aortic sinuses)
- Lamellae with moving blood clots in the ascending aorta or in the aortic arch
- For access via femoral and subclavian arteries: inappropriate vascular access
(vessel size, calcification, tortuosity)



Motivation

Extended by balloon

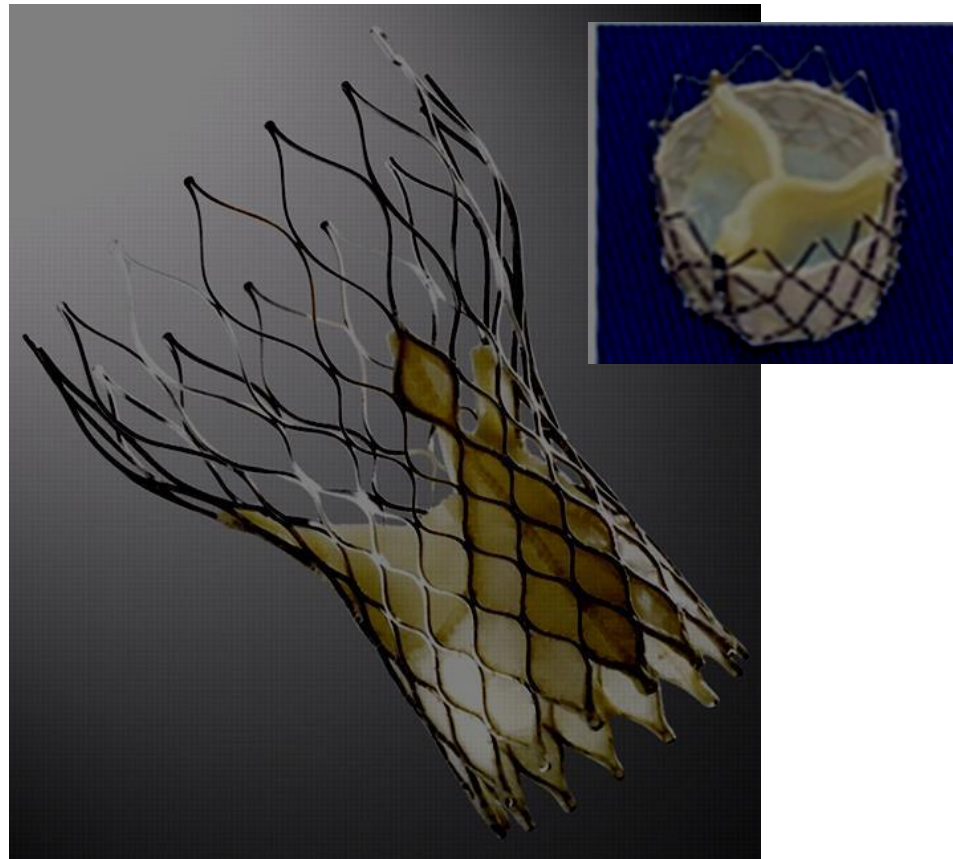


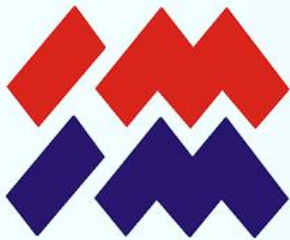
TAVI –types of valves



Motivation

TAVI –self extended

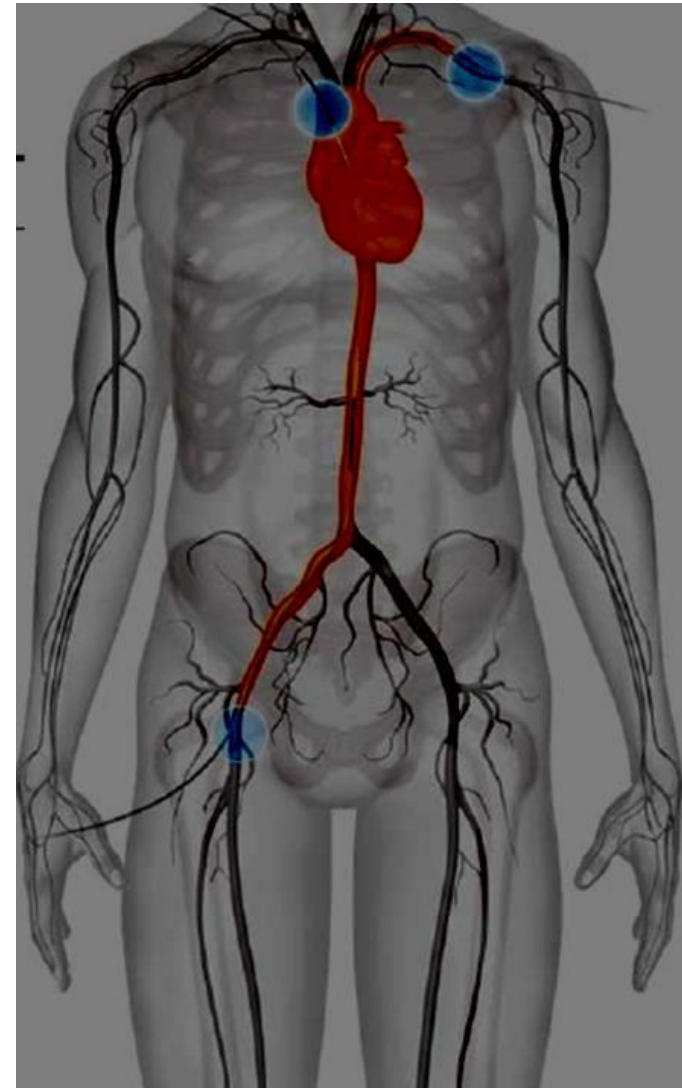


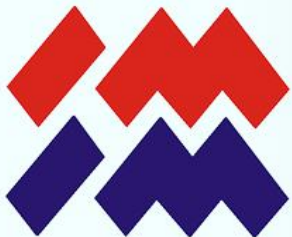


Motivation

TAVI –currently applied access

- Basic access:
 - Through the femoral artery
- Alternative access:
 - Through the apex of the heart
 - Through the ascending aorta
 - Arteria subclavia





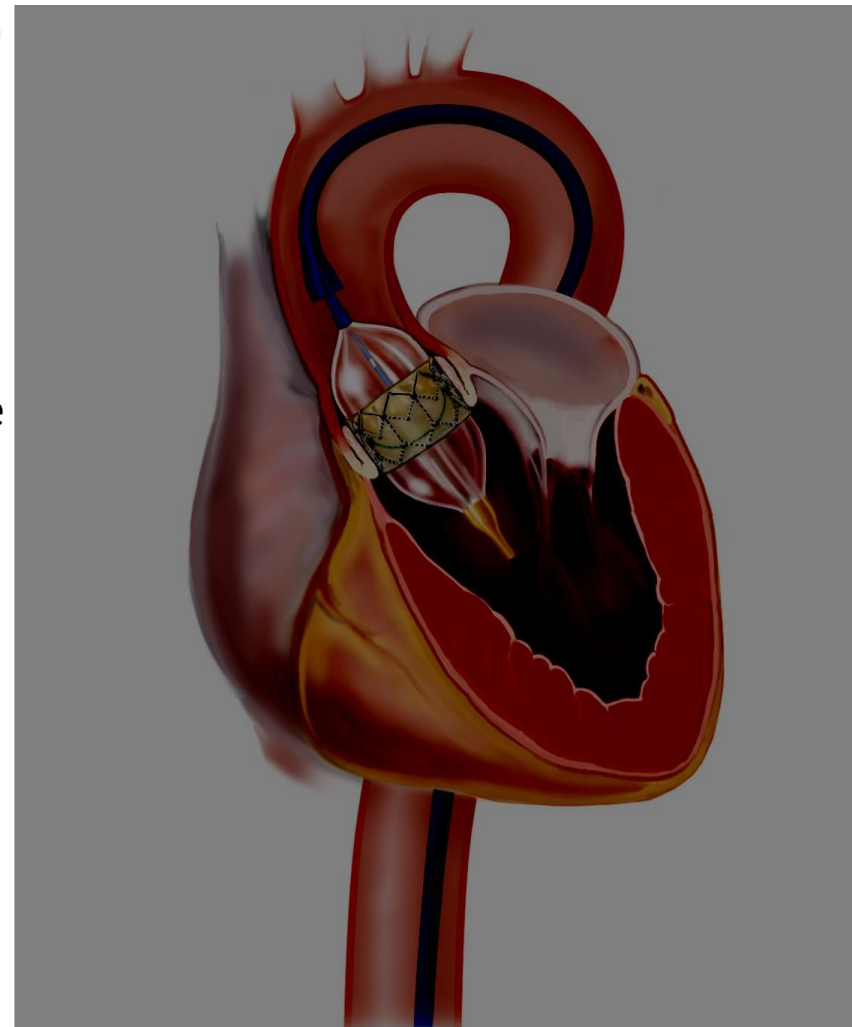
Motivation

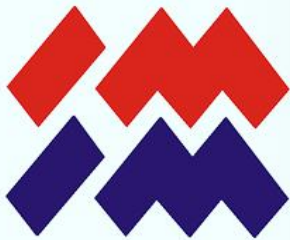
TAVI –currently applied access

Access through the femoral artery

Disadvantages:

- Risk of damage to the femoral and iliac arteries
- Difficult passage through the catheter through the aortic stenosis





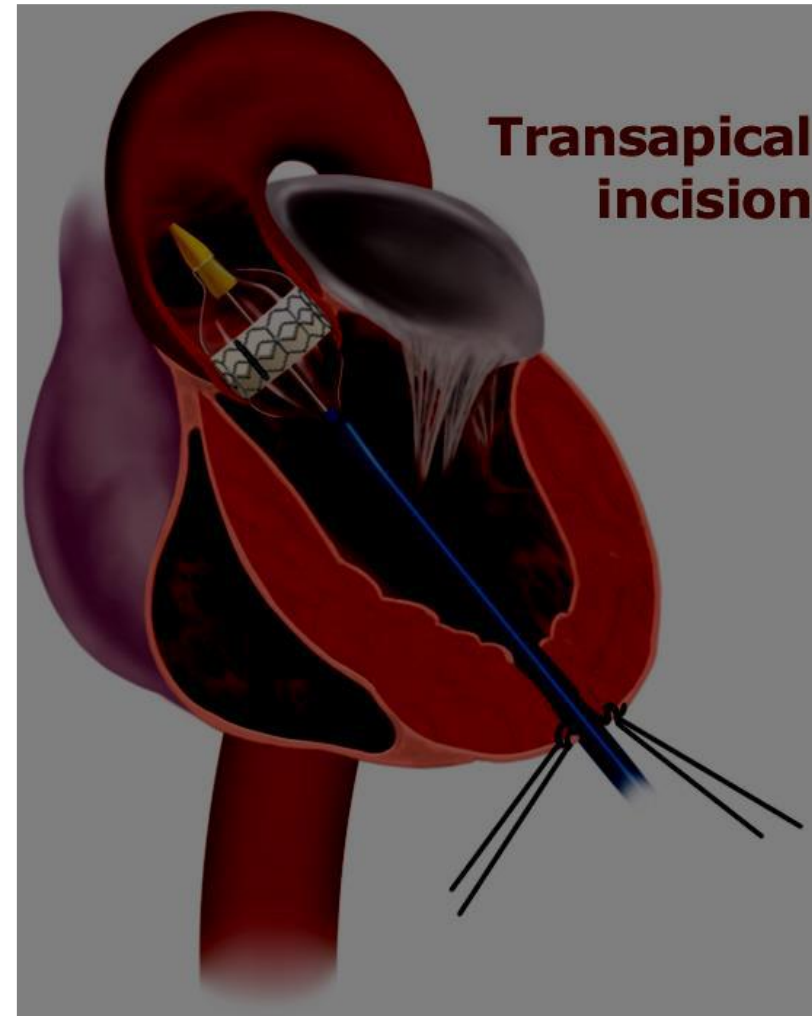
Motivation

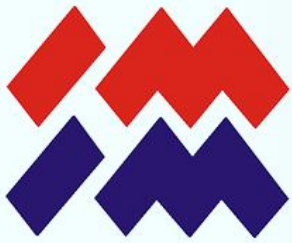
TAVI –currently applied access

Access through apex. The catheter is introduced by a small thoracotomy and then by a puncture of the apex.

Advantages: the most direct access to the valve. The risk of damaging the femoral and iliac artery as well as the passage through the atherosclerotic changed valve.

The disadvantage of this method is the potential complication of apex puncture, requires general anesthesia and pleural drainage.

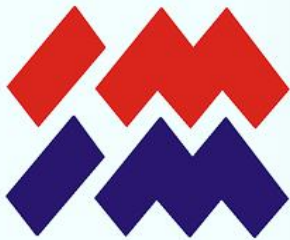




Substrate

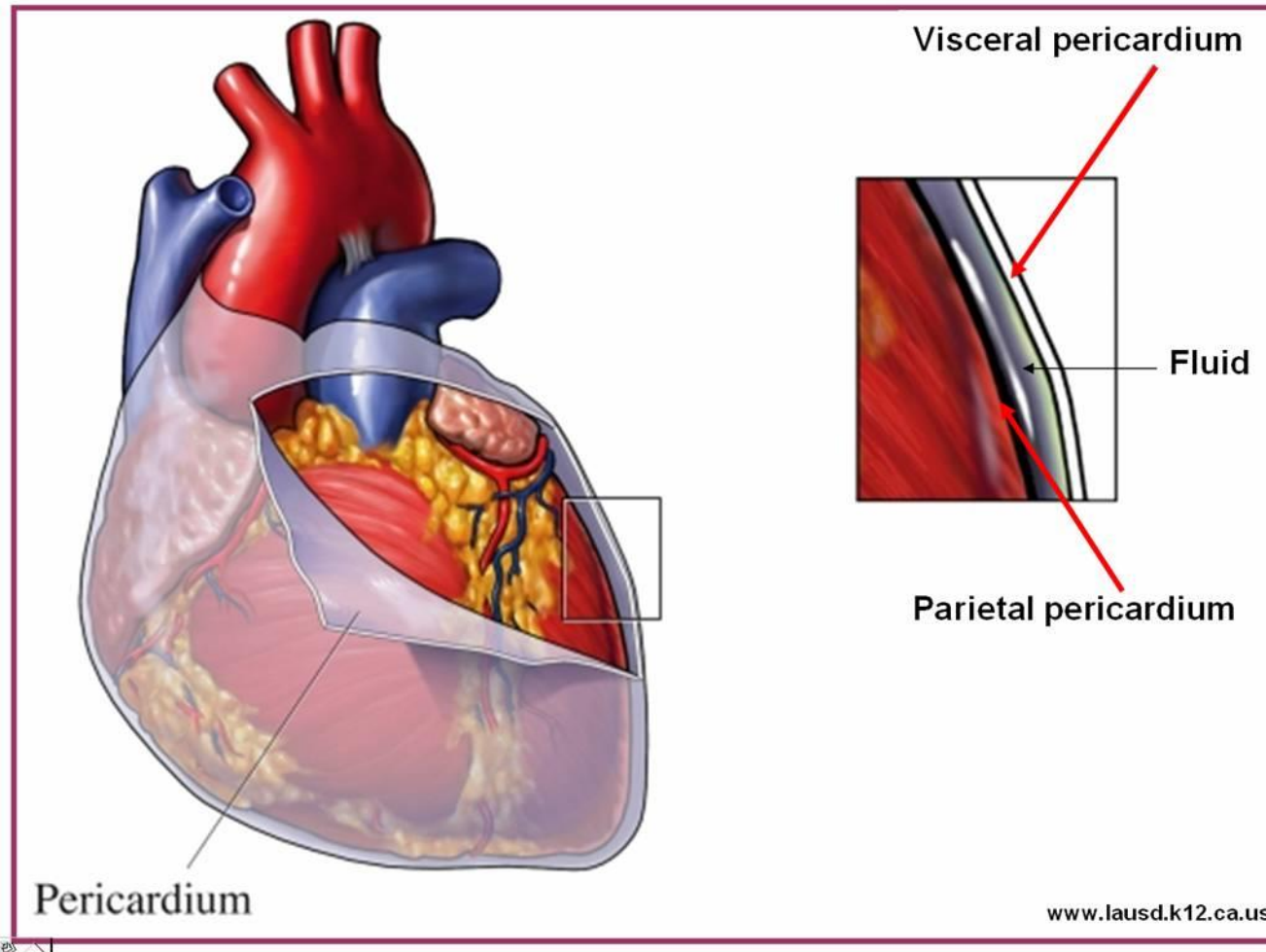
Acknowledgement

The research was financially supported by the **Project no. 2016/23/B/ST8/01481 "Interdisciplinary methods of creating and functioning of biomimetic materials based on Animal origin extracellular matrix" of the Polish National Center of Science.** Part of the work was co-financed by the European Union from resources of the European Social Fund (Project No.WND-POWR.03.02.00-00-I043/16).



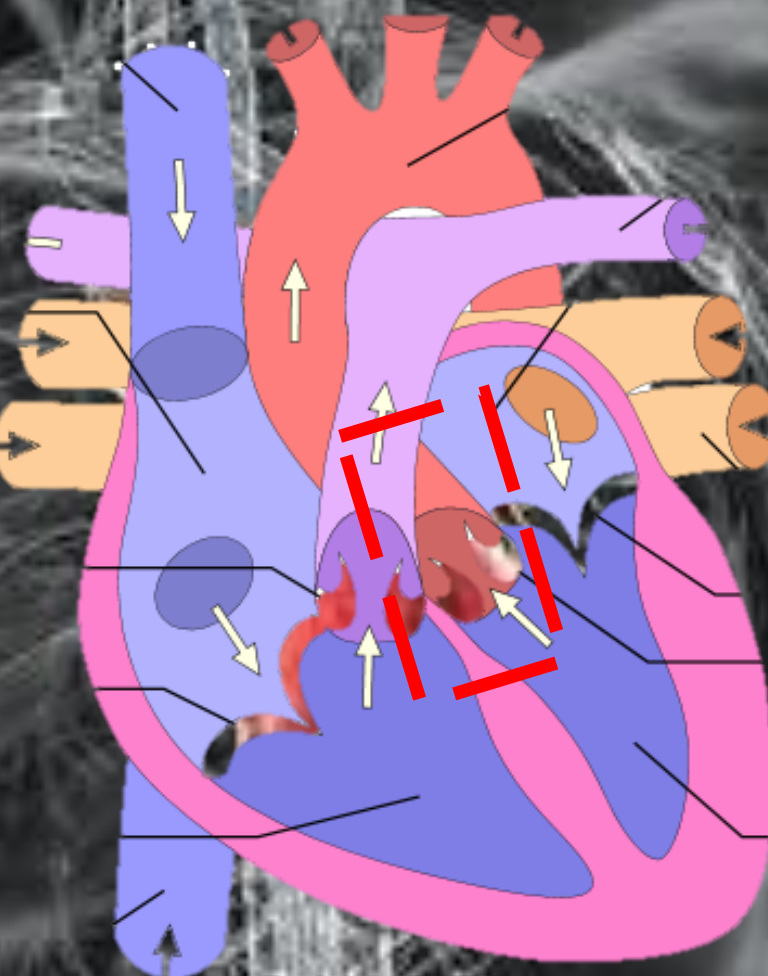
Substrate

Pericardium



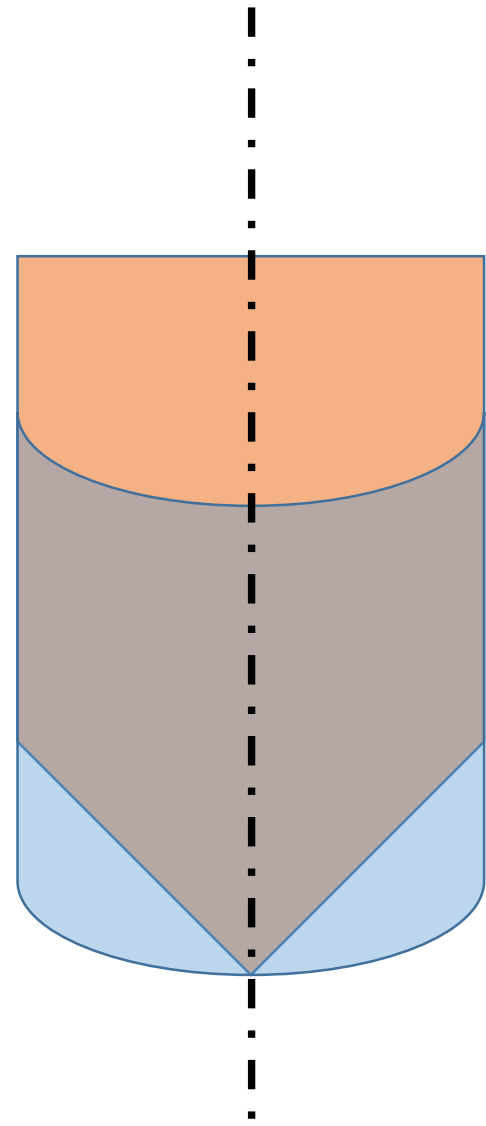
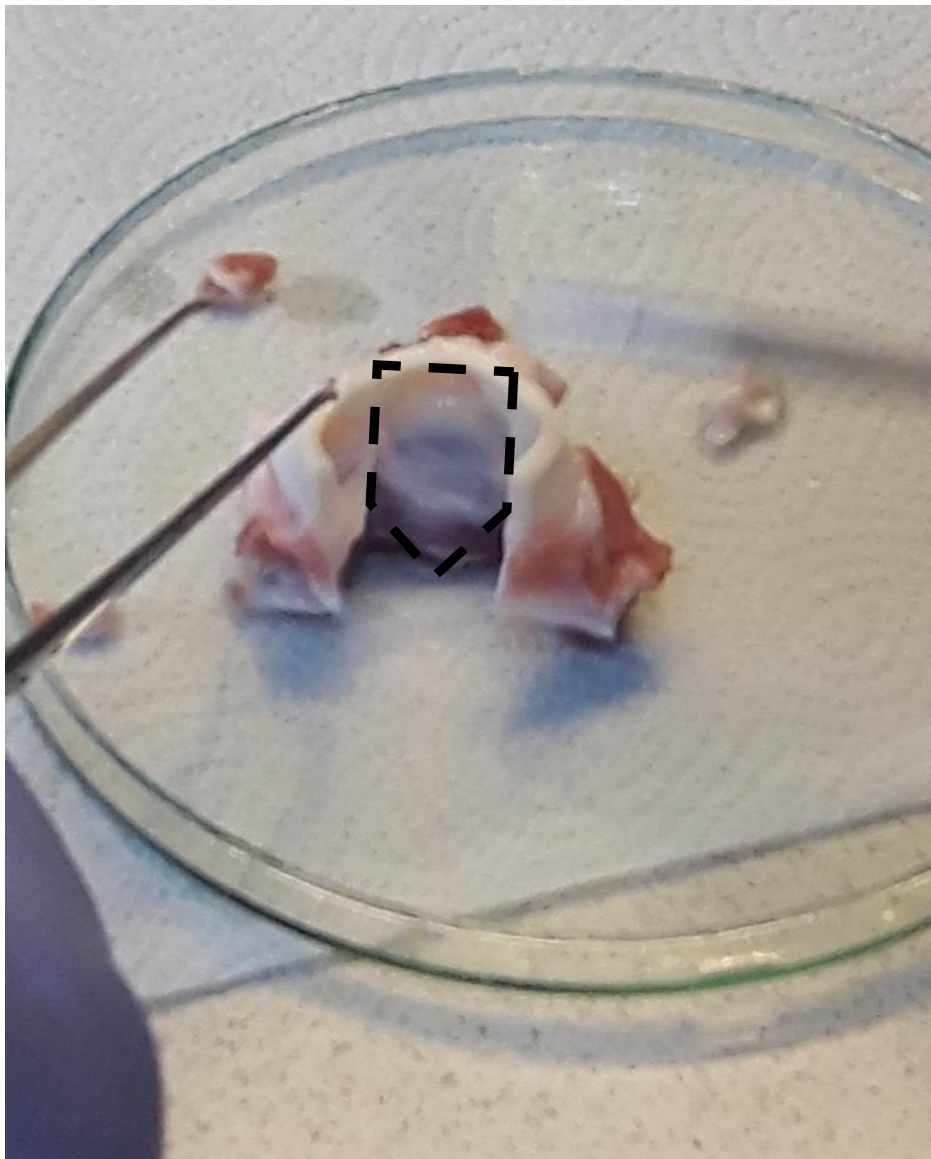


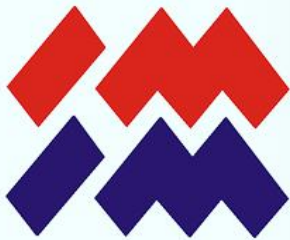
Aortic valve





Materials&Methods

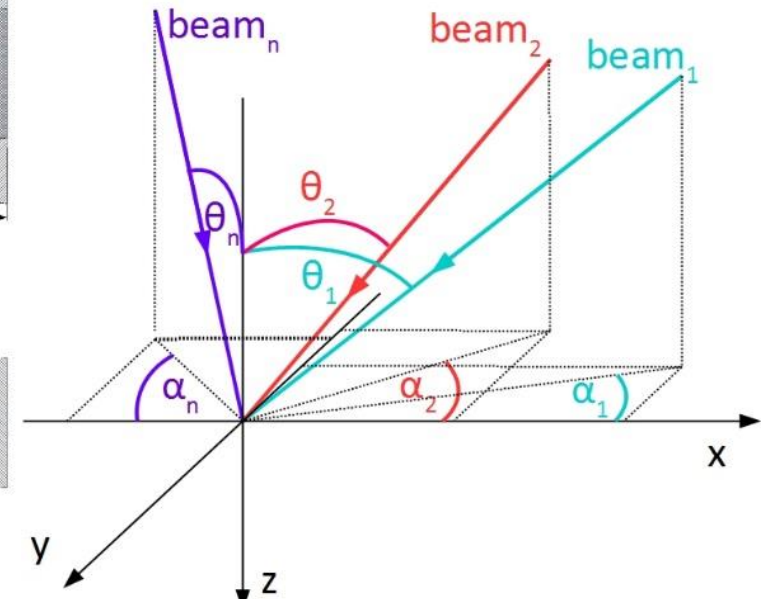
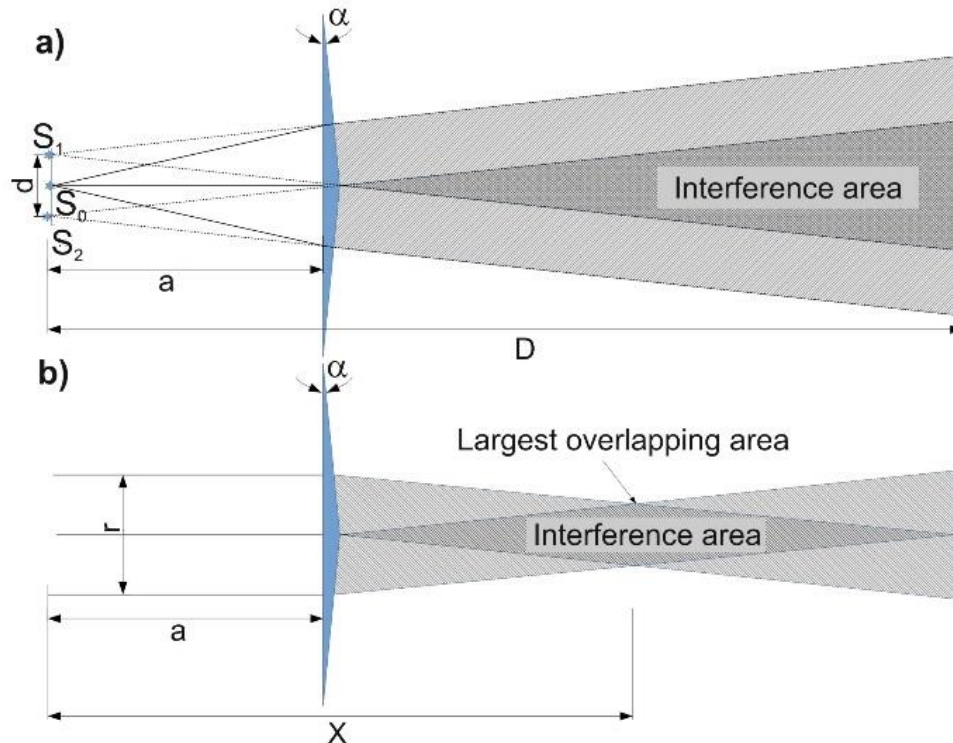




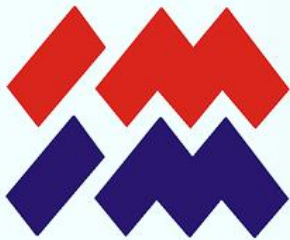
Materials&Methods

Radiation incidence on bi-prism

DLIL

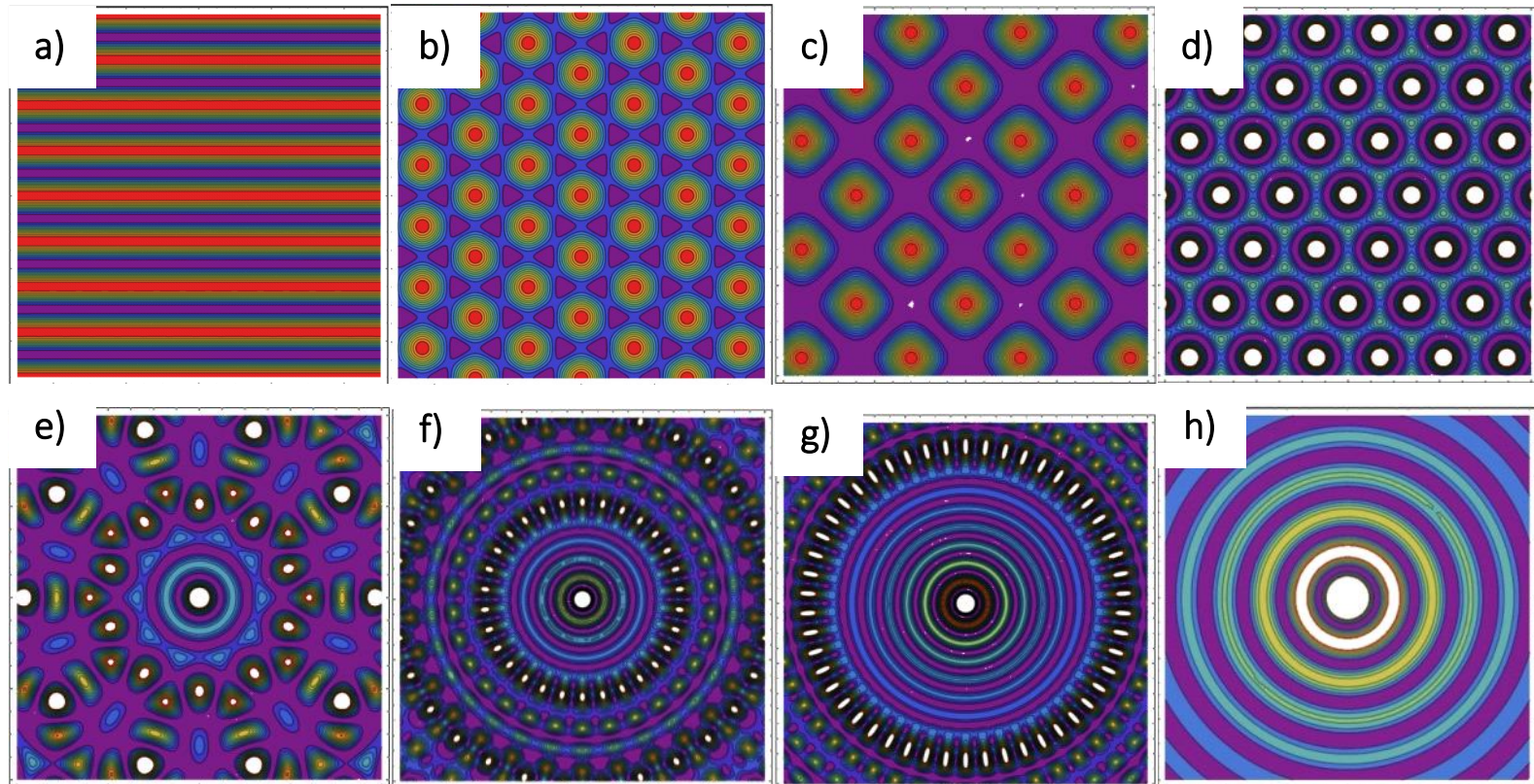


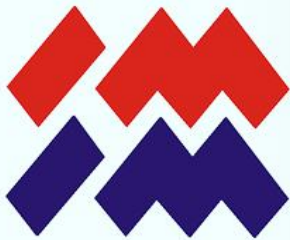
$$\Lambda = \frac{\lambda}{2\sin(\arcsin(nsina) - \alpha)}$$



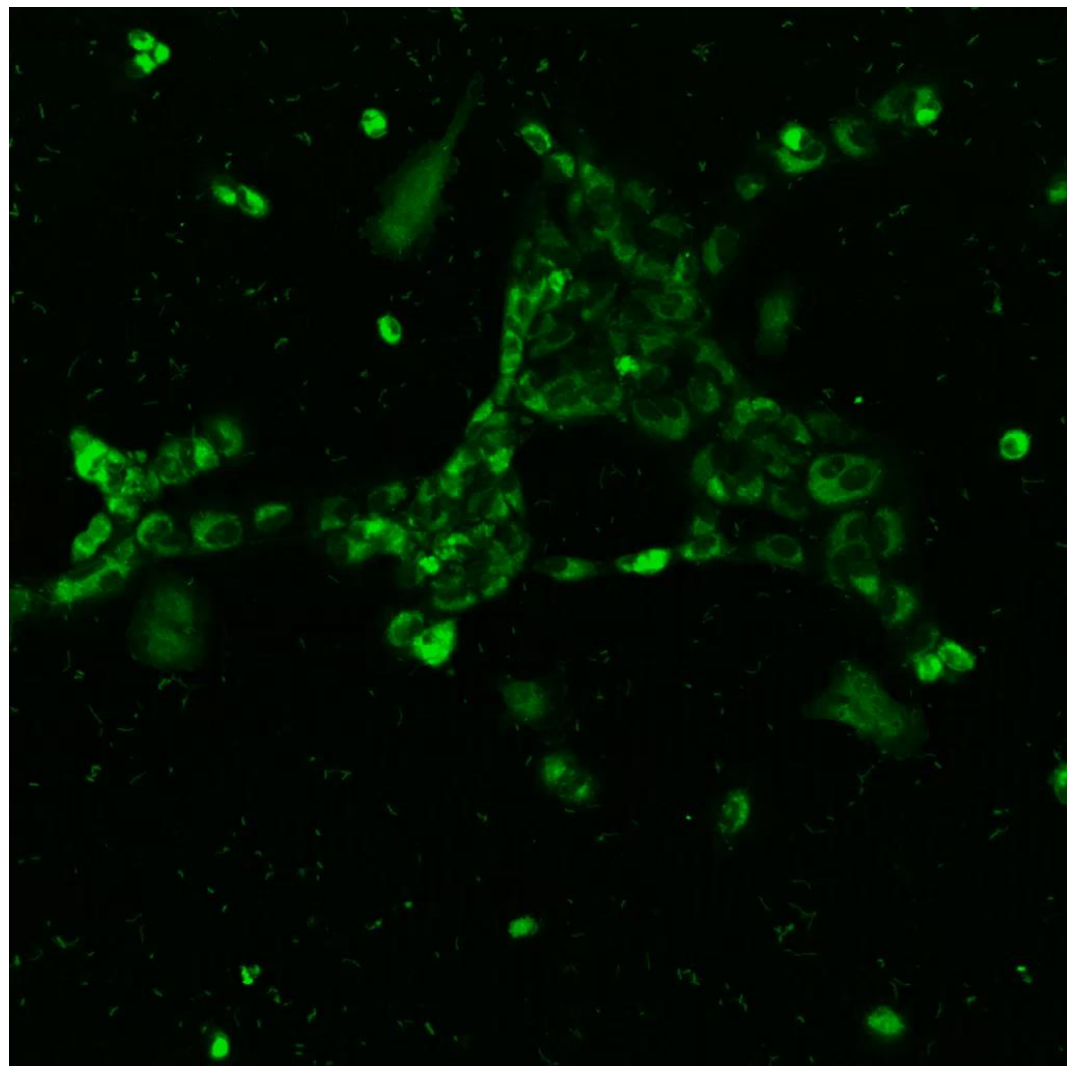
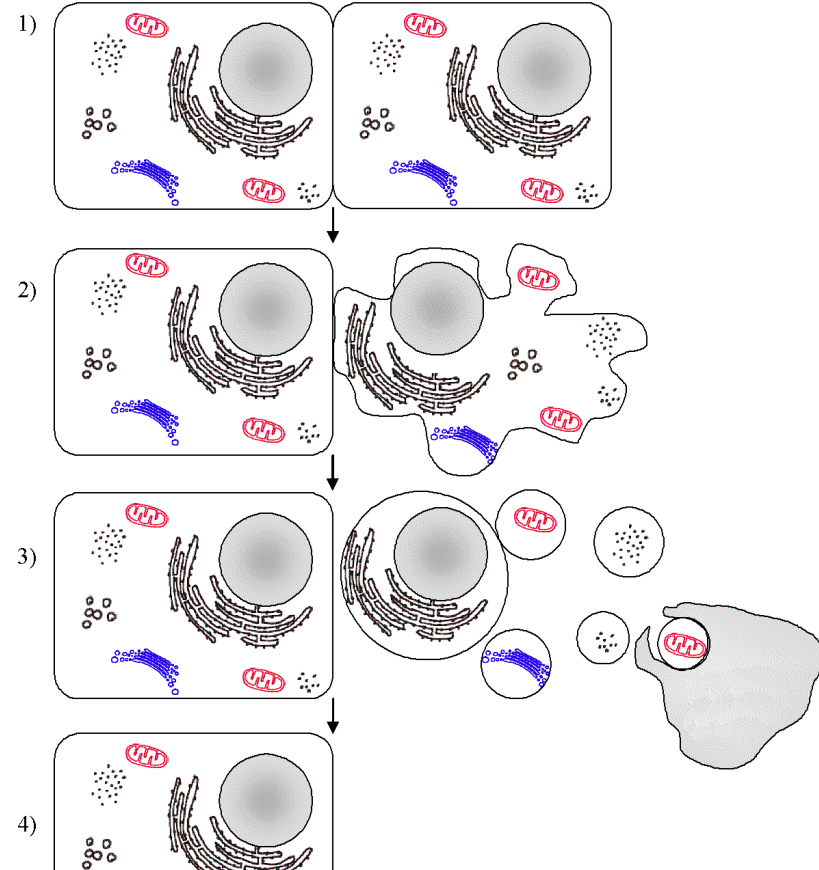
Materials&Methods

Radiation incidence on bi-prism

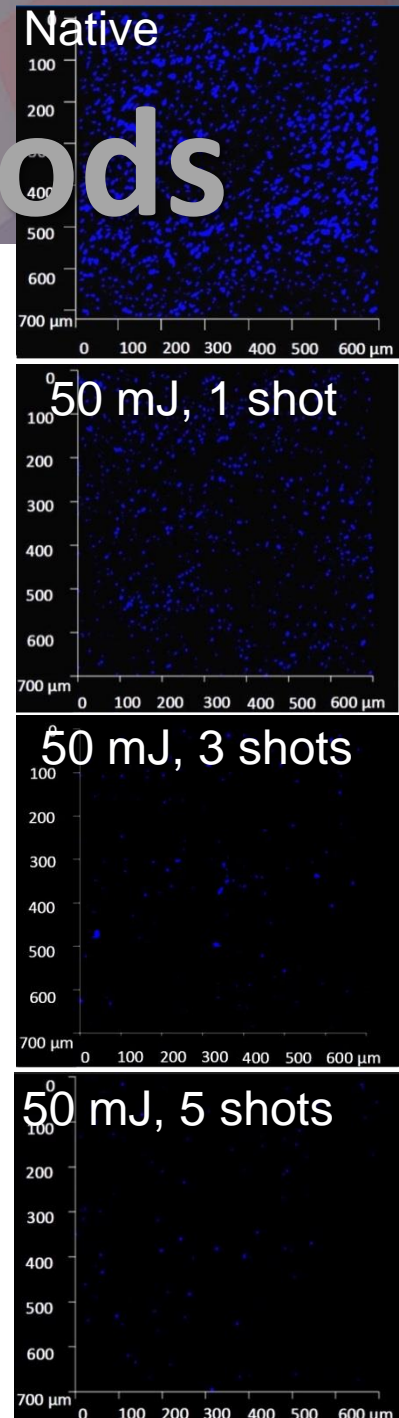
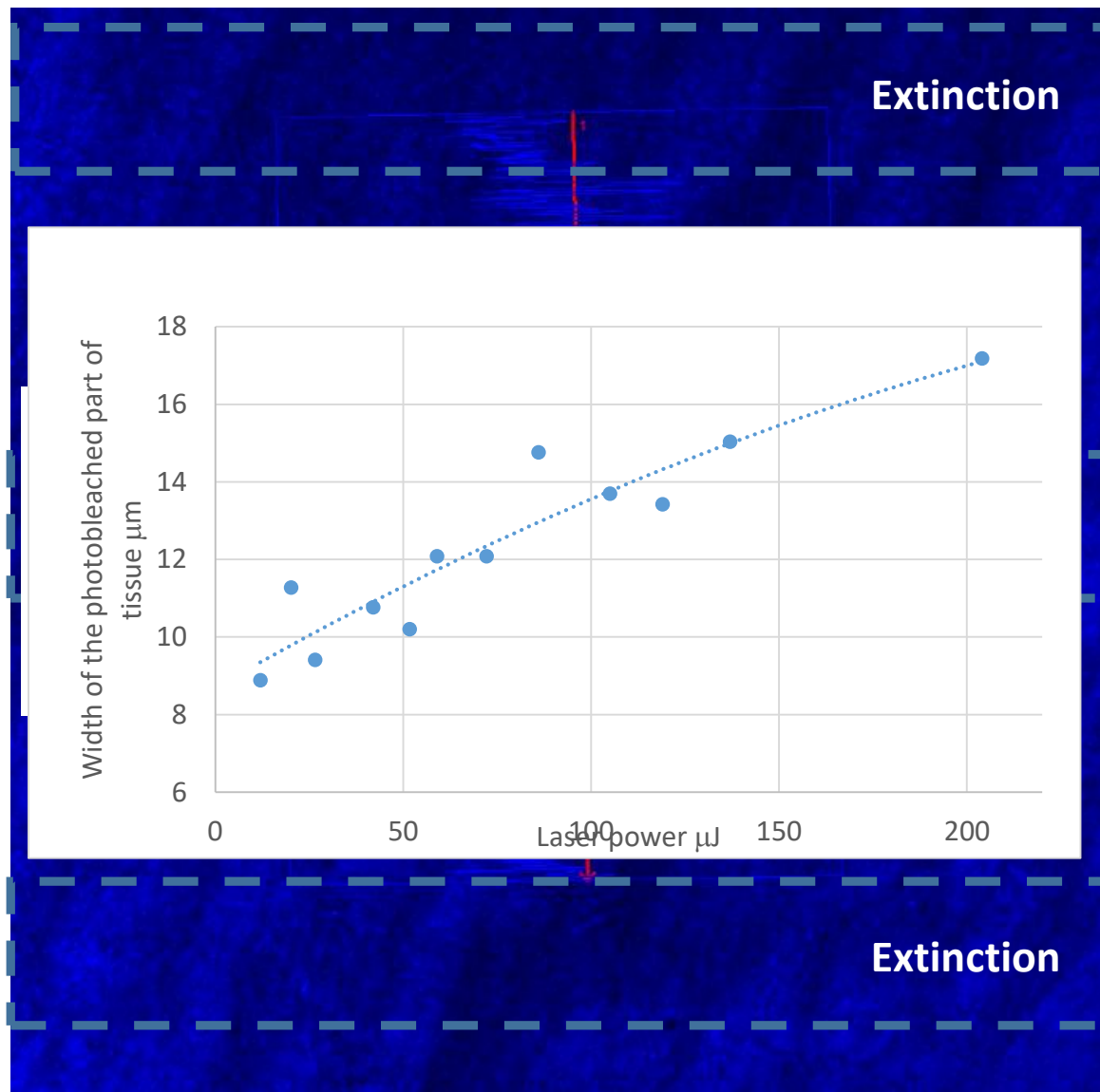


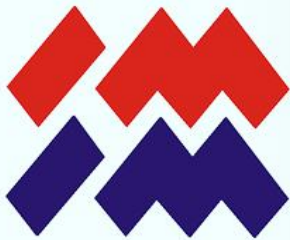


Materials&Methods



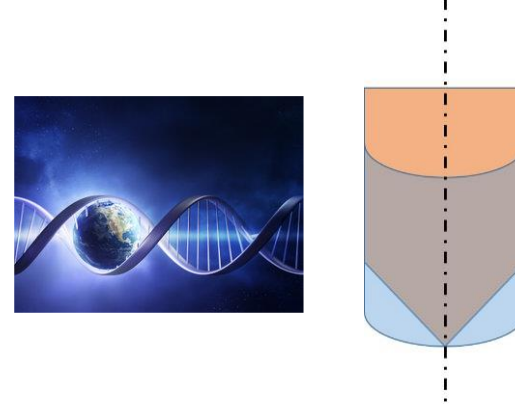
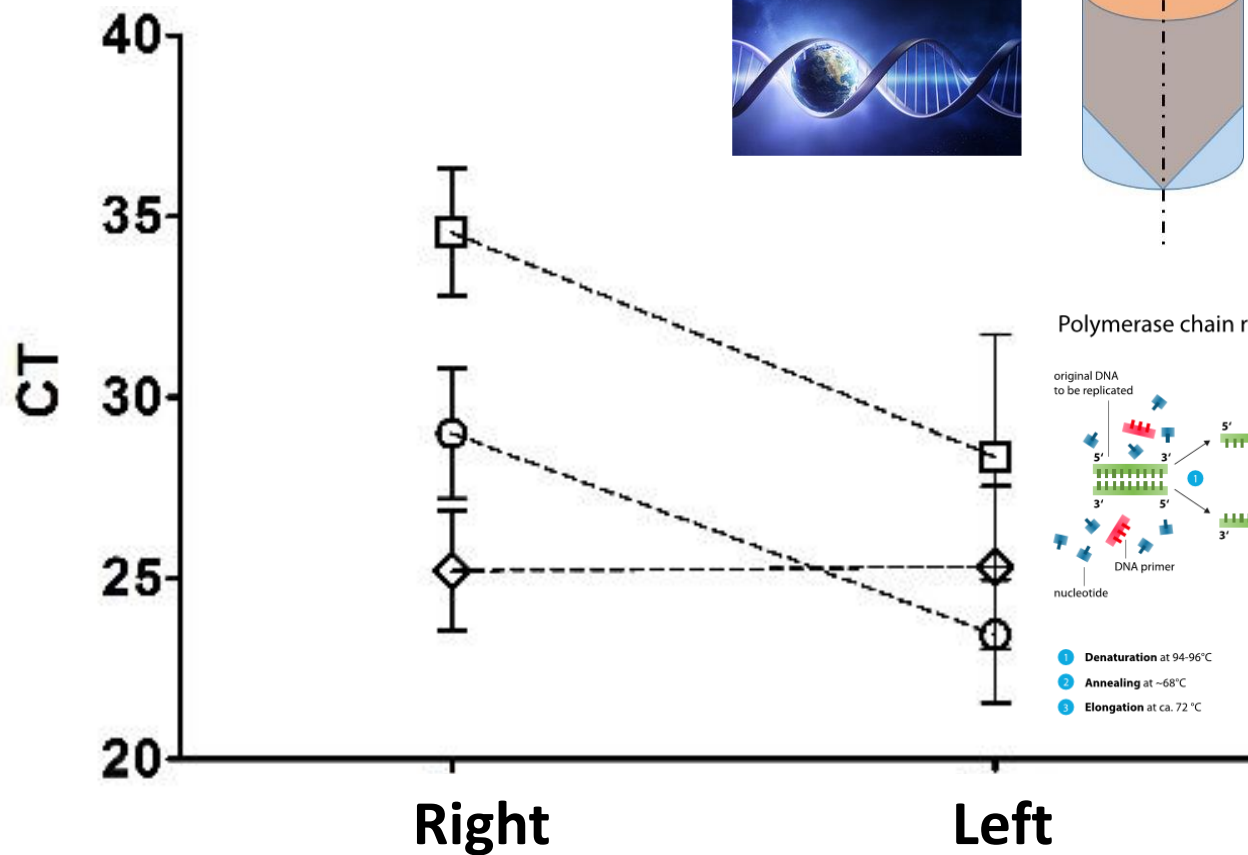
Materials&Methods



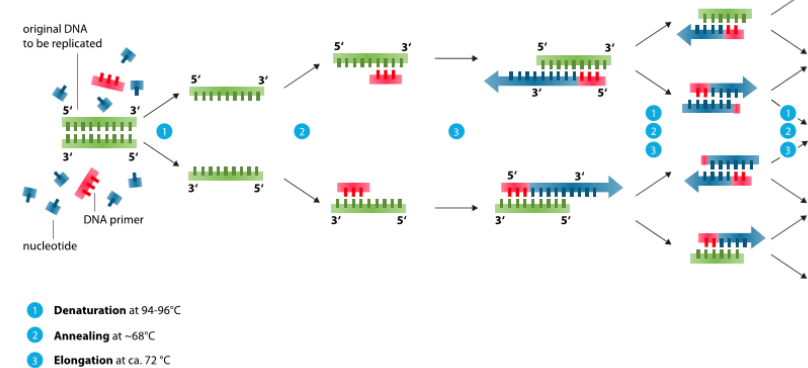


Real Time PCR

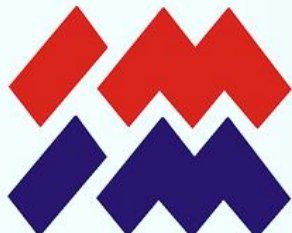
Real Time PCR



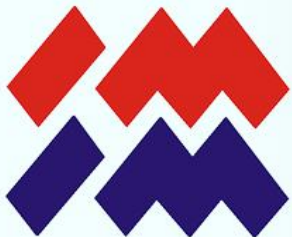
Polymerase chain reaction - PCR



[Kary Mullis](#)



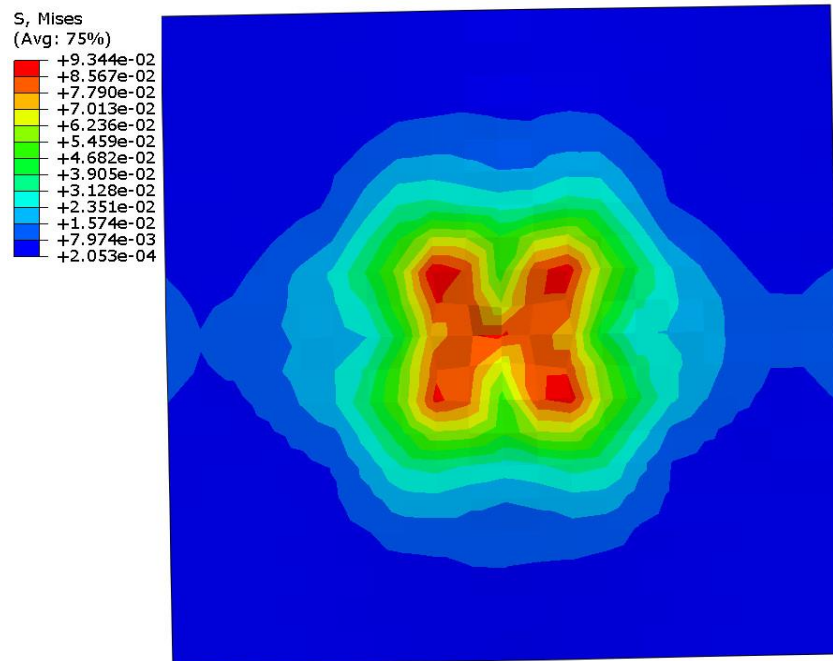
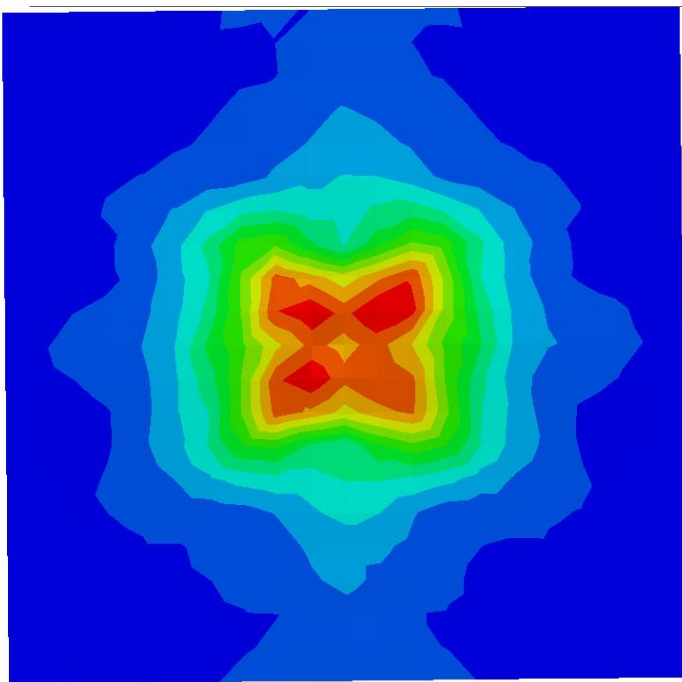
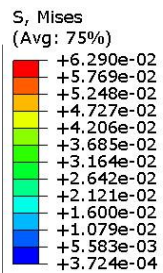
Sample	Energy	Energy density	Diameter of the beam	Repetition	No of impulses	Wavelength	
AA1	65mJ	0.169 J/cm ²	7 mm	5 Hz	100	1064 nm	
AA2				5 Hz	50		
AP3				5 Hz	10		
AP4				5 Hz	200		
AP5				5 Hz	500		
AP6				1 Hz	100		
XZ7	65mJ	0.169 J/cm ²		5 Hz	100		
XZ8	32 mJ	0.083 J/cm ²	7 mm	5 Hz	100	1064 nm	
AA9	32 mJ	0.083 J/cm ²		5 Hz	100		
AA10				1 Hz	100		
AA11				1 Hz	200		
AA12				5 Hz	200		
AA13				5 Hz	500		
AA14				5 Hz	50		
AA15				5 Hz	10		
AA16	62 mJ	0.109 J/cm ²	8.5 mm	5 Hz	500	532 nm	
AA17				5 Hz	200		
AA18				5 Hz	100		
AA19				1 Hz	100		
AA20				5 Hz	50		
AA21				5 Hz	10		
XZ22				5 Hz	100		
AP23	62 mJ	0.109 J/cm ²	8.5 mm	5 Hz	500	532 nm	
AP24				5 Hz	200		
AP25				5 Hz	100		
AP26				1 Hz	100		
AP27				5 Hz	50		
AP28				5 Hz	10		
AP29				5 Hz	500		
AP30	32 mJ	0.056 J/cm ²	8.5 mm	5 Hz	200	532 nm	
AP31				5 Hz	100		
AP32				1 Hz	100		
AP33				5 Hz	50		
AP34				5 Hz	10		
AA35	32 mJ	0.056 J/cm ²	8.5 mm	5 Hz	500	532 nm	
AA36				5 Hz	200		
AA37				5 Hz	100		
AA38				1 Hz	100		
AA39				5 Hz	50		
AA40				5 Hz	10		



FE- Simulation

Stress

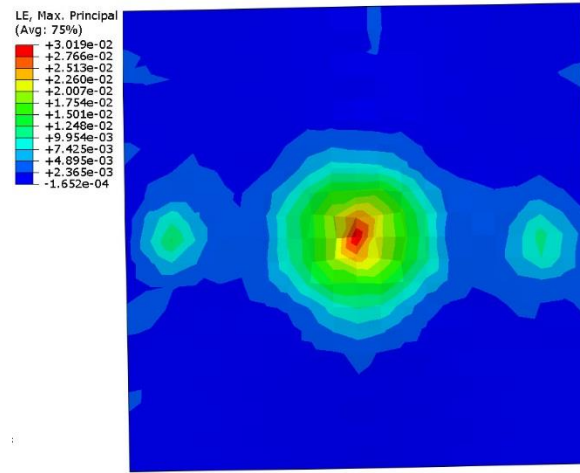
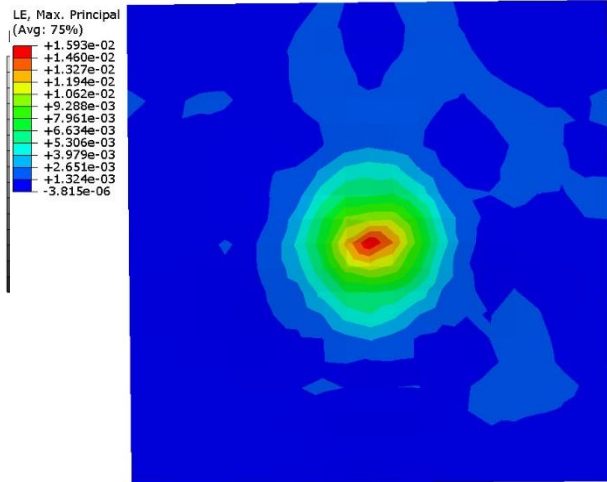
$$I(r) = \frac{2E}{\pi w^2} \exp[-2 r^2/w^2]$$



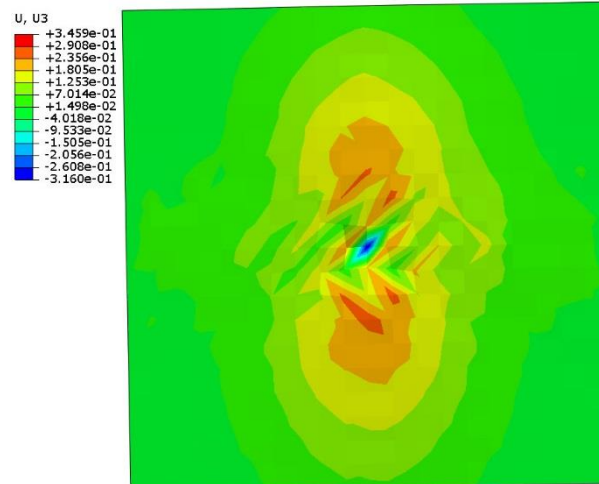
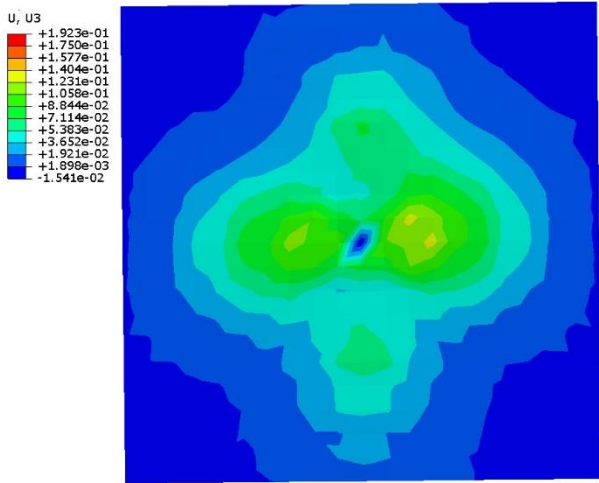
Distributions of von Mises stress, MPa for a) aortic and b) pulmonary valve sample models (top view).

FE- Simulation

Strain



Distributions of maximum principal strain for a) aortic and b) pulmonary valve sample models (top view).



Distributions of Z - displacement, mm for a) aortic and b) pulmonary valve sample models (top view).



Histology

Tissue Preparation

- Orcein for visualization of elastic fibers,
- Red syrium to visualize collagen fibers,
- Alcian blue for the visualization of the proteoglycans of the basic substance,
- Routine staining with hematoxylin / eosine and three- and multi-colored staining to visualize the overall morphology and evaluate the effectiveness of acellularisation,
- Hoechst 33342 / DAPI fluorescence staining reveal cell nuclei to assess the effectiveness of acellularisation.

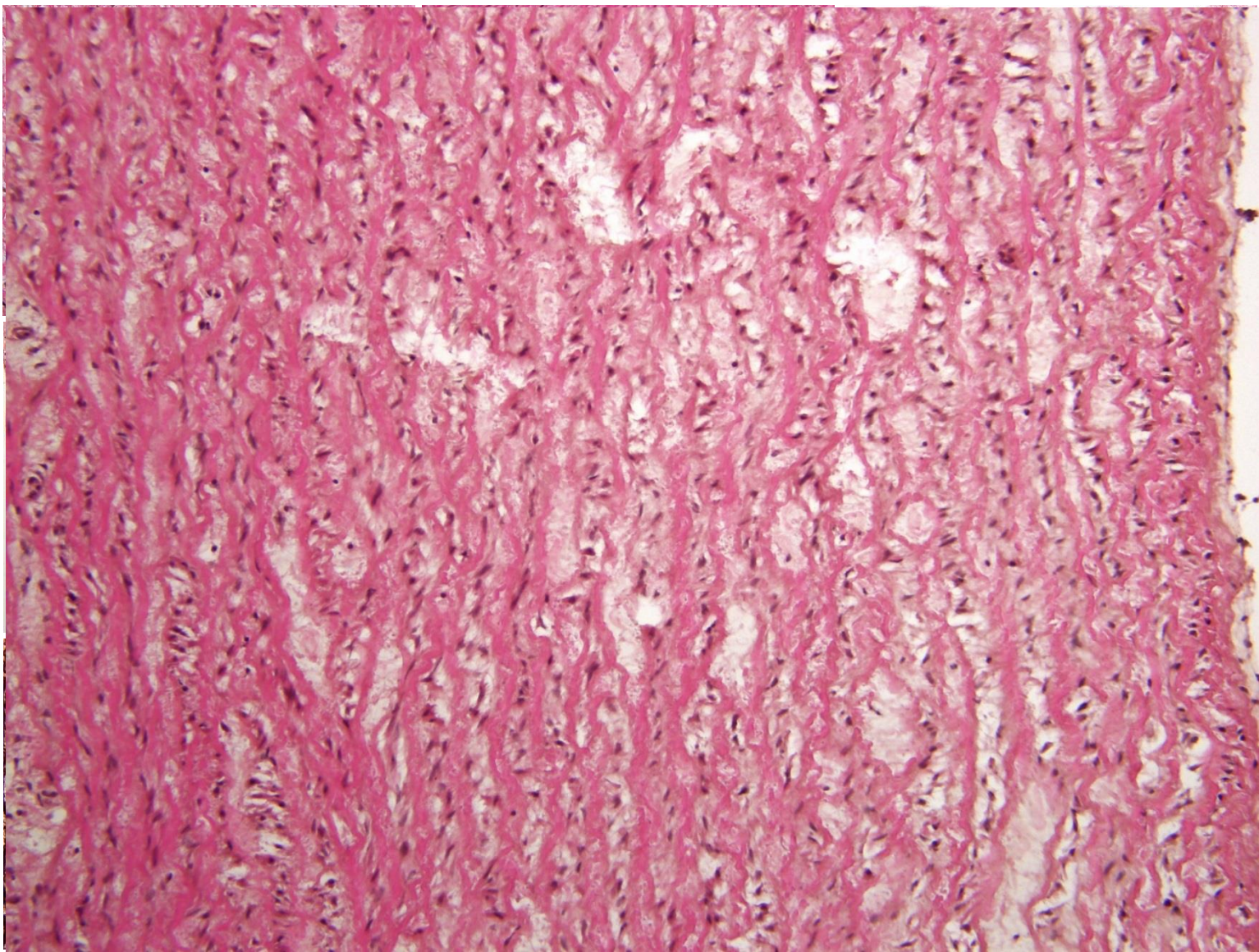


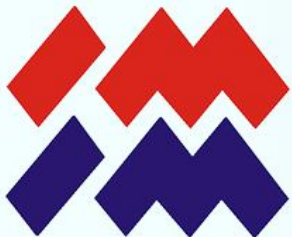
Histology



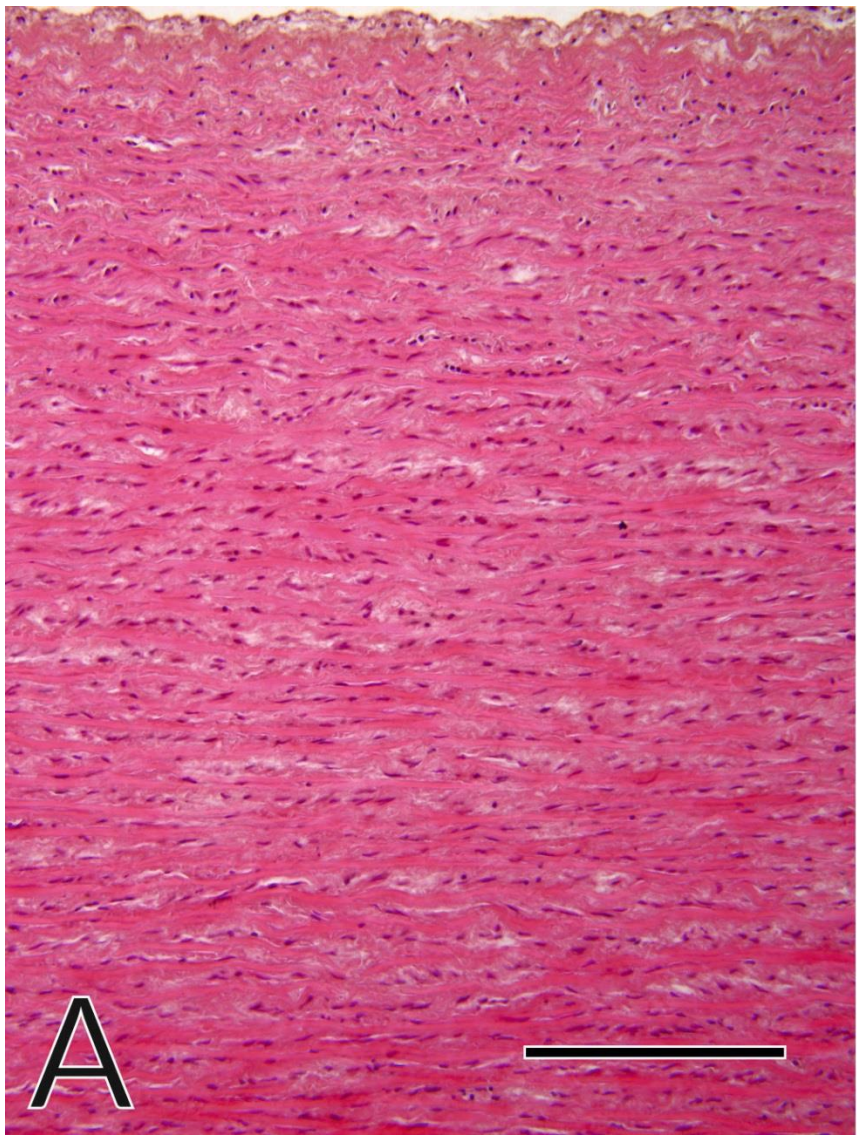


Histology

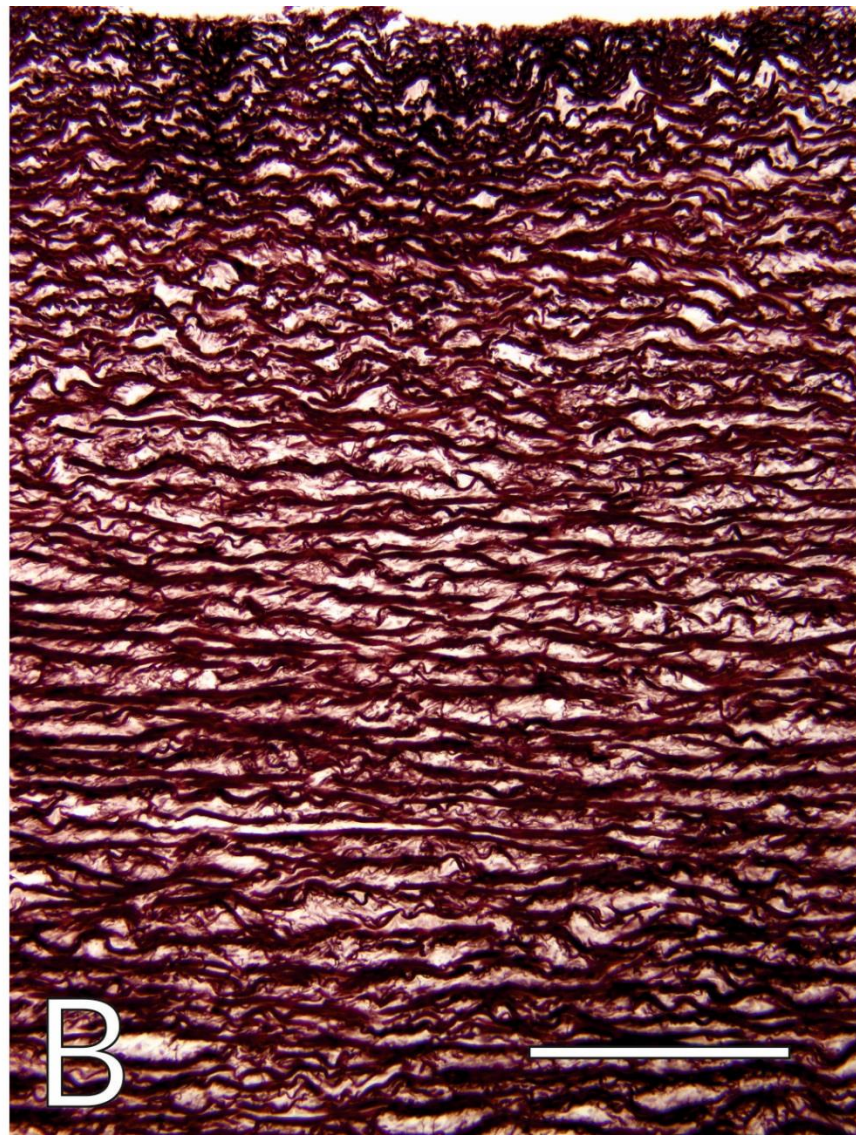




Histology



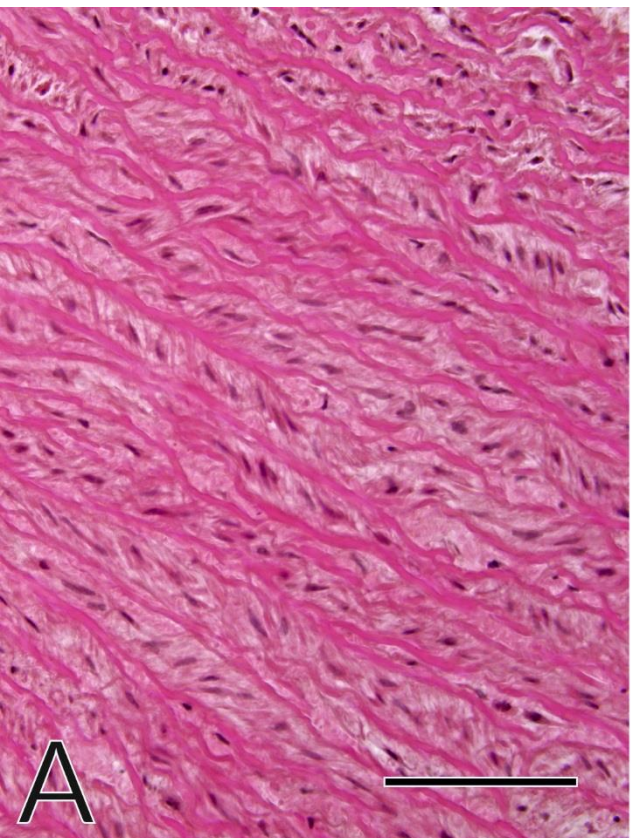
A



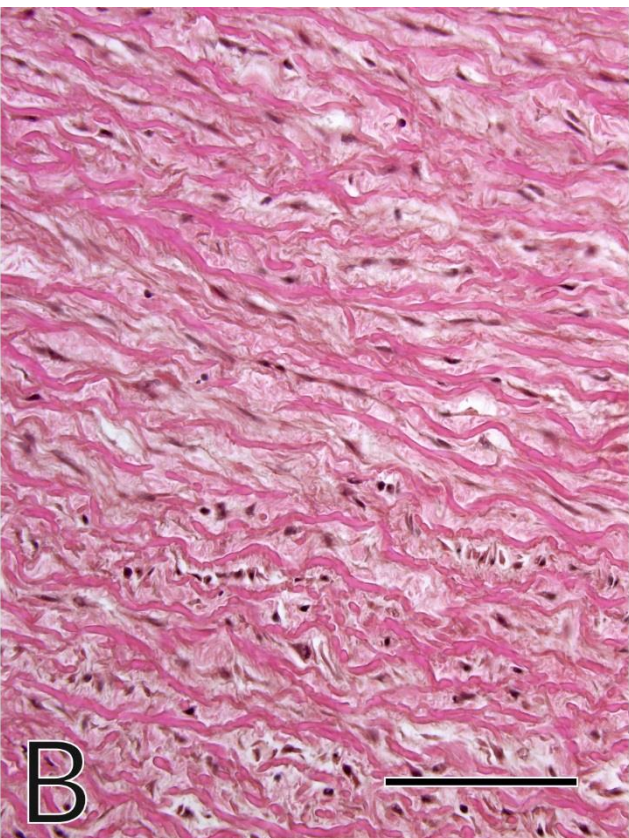
B



Histology



A



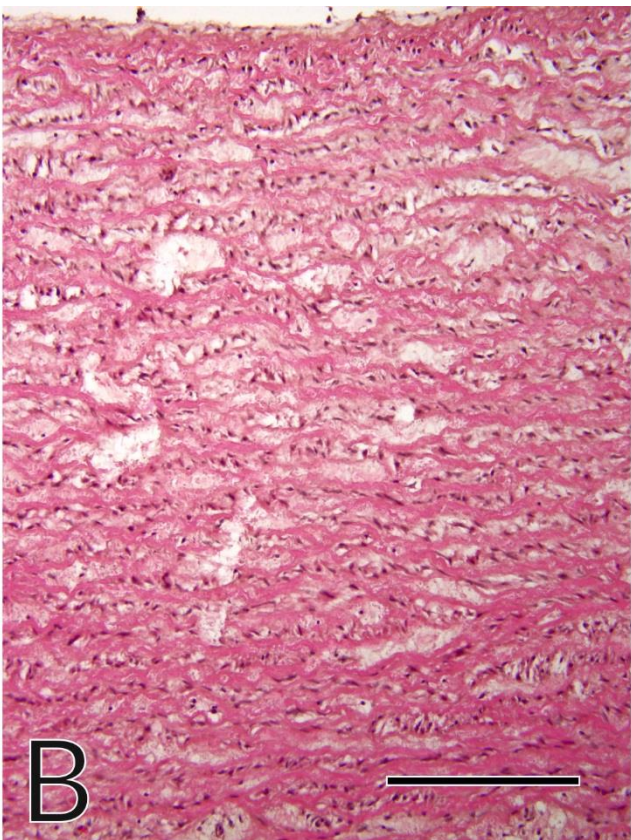
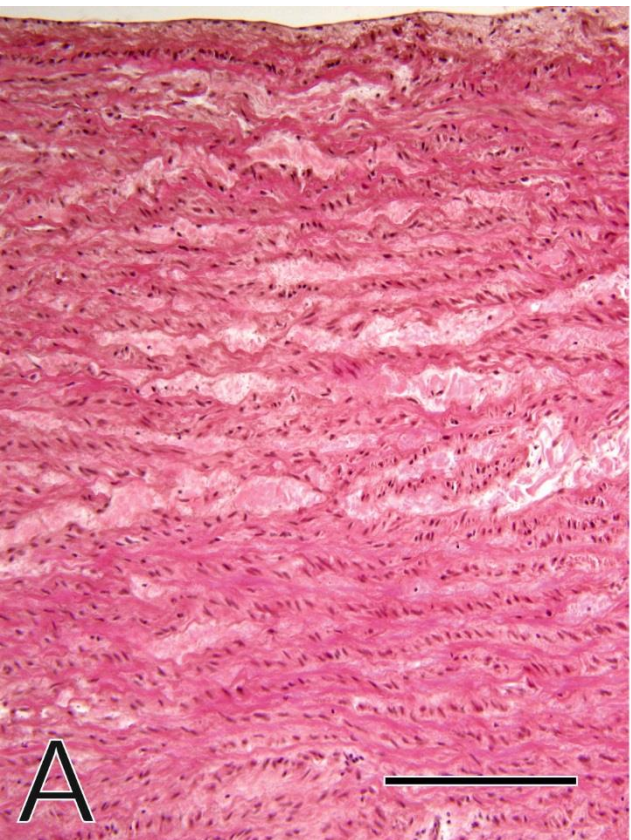
B



C

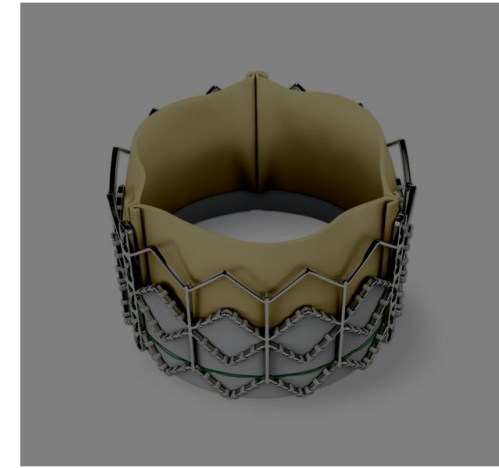


Histology





Coating

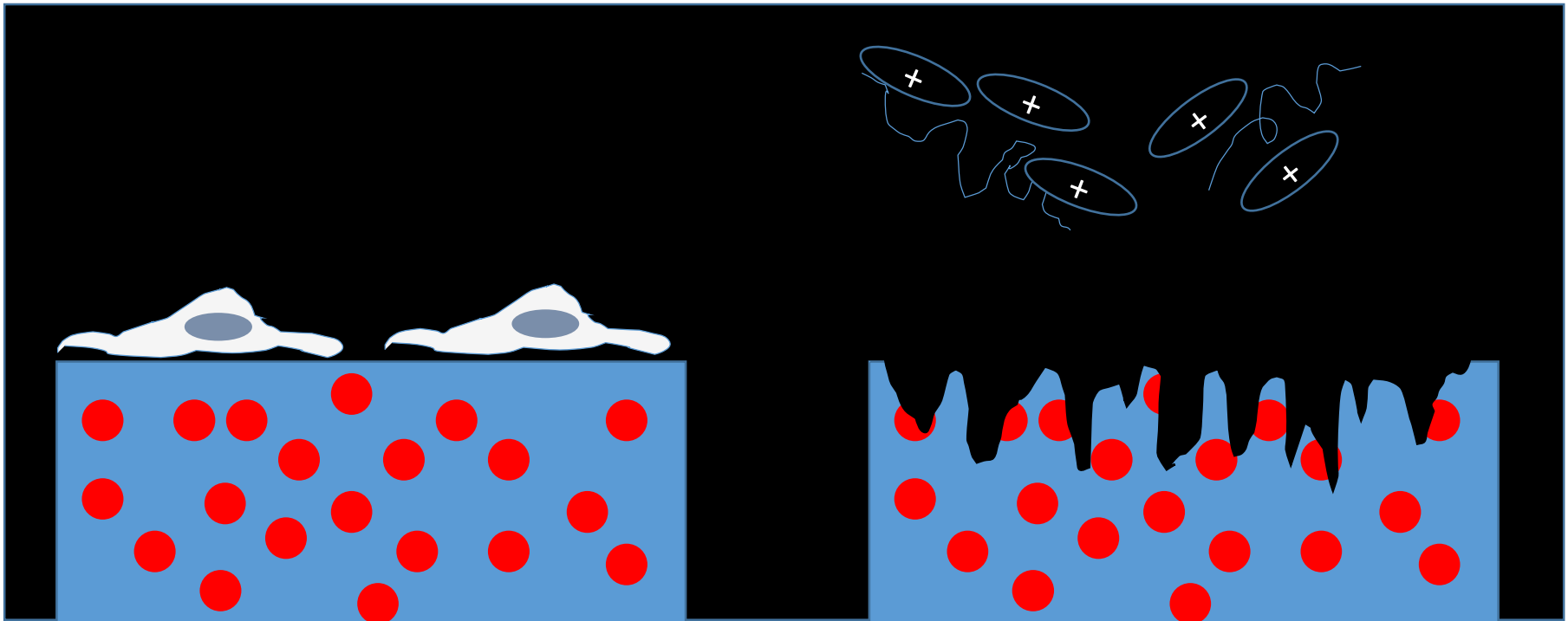


Acknowledgement

The research was financially supported by the Project no. 2016/23/B/ST8/01481 "Interdisciplinary methods of creating and functioning of biomimetic materials based on Animal origin extracellular matrix" of the Polish National Center of Science. Part of the work was co-financed by the **European Union from resources of the European Social Fund (Project No.WND-POWR.03.02.00-00-I043/16)**.

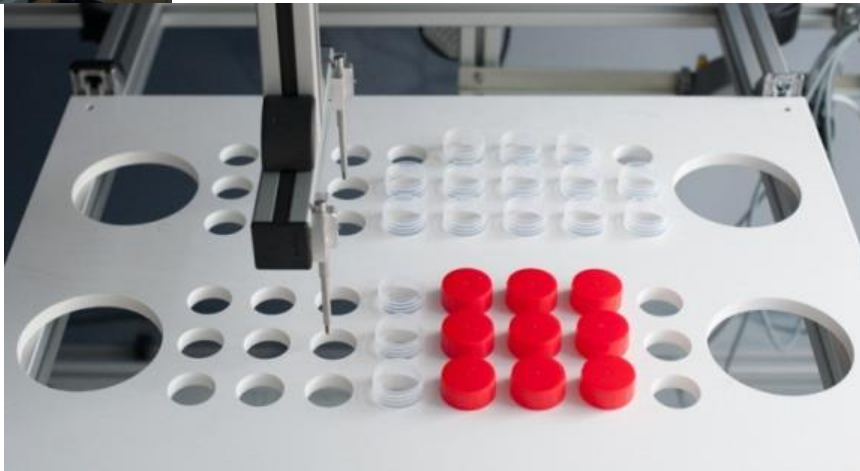


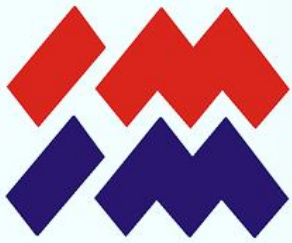
Analogi tkanki



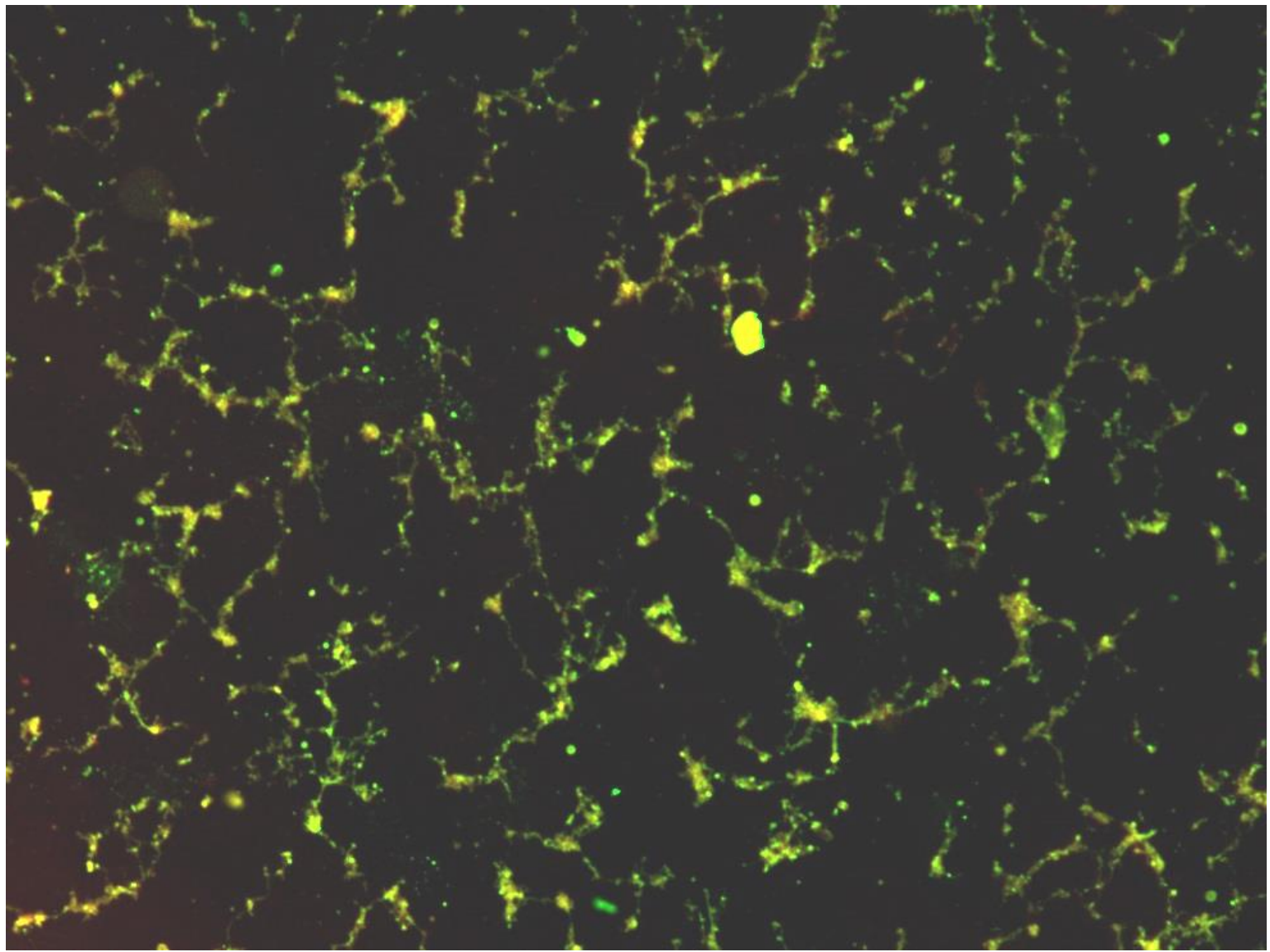
Bioaktywność poprzez kontakt

Bioaktywność poprzez degradację

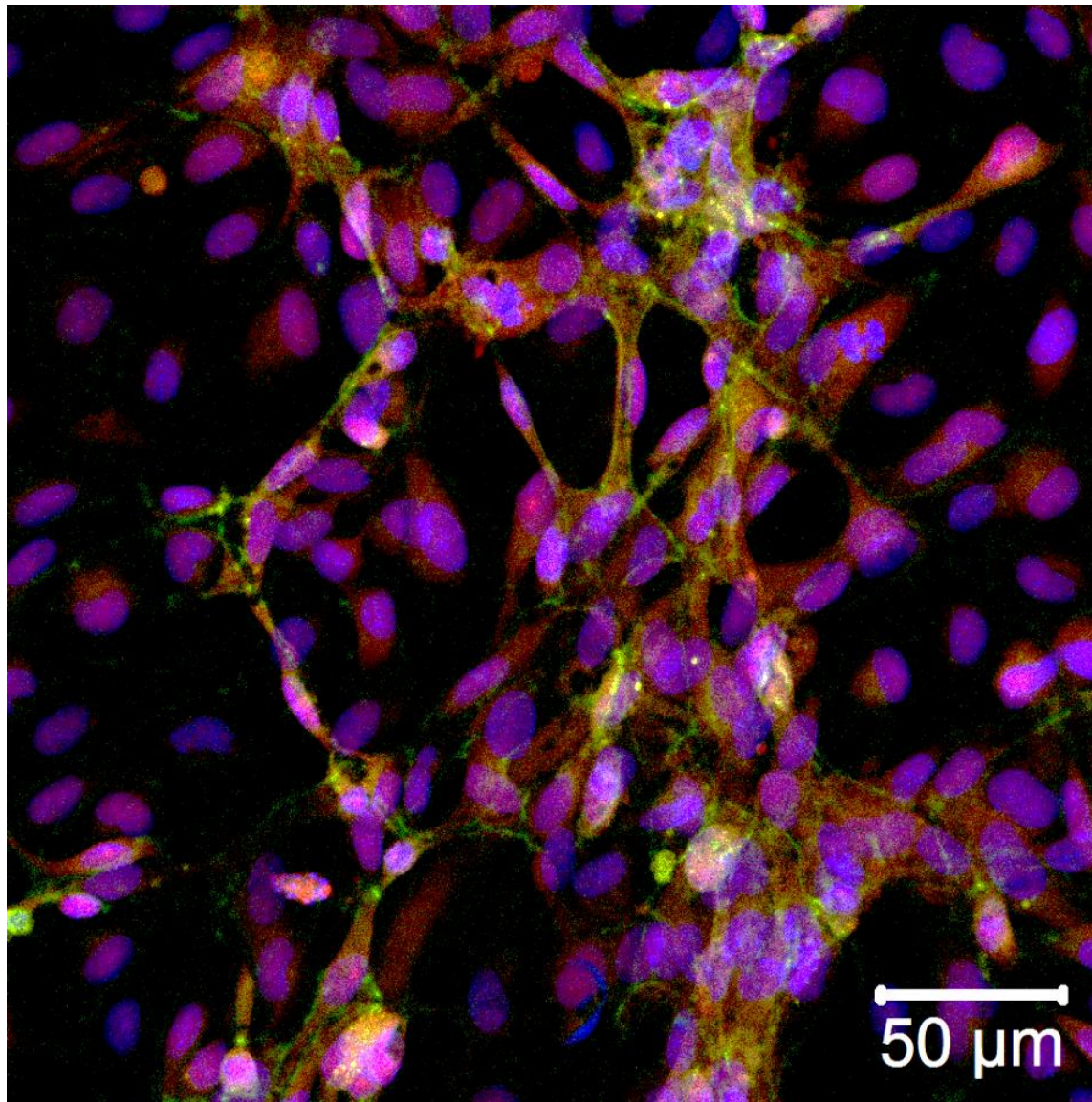




Polyelectrolytes



Differentiation

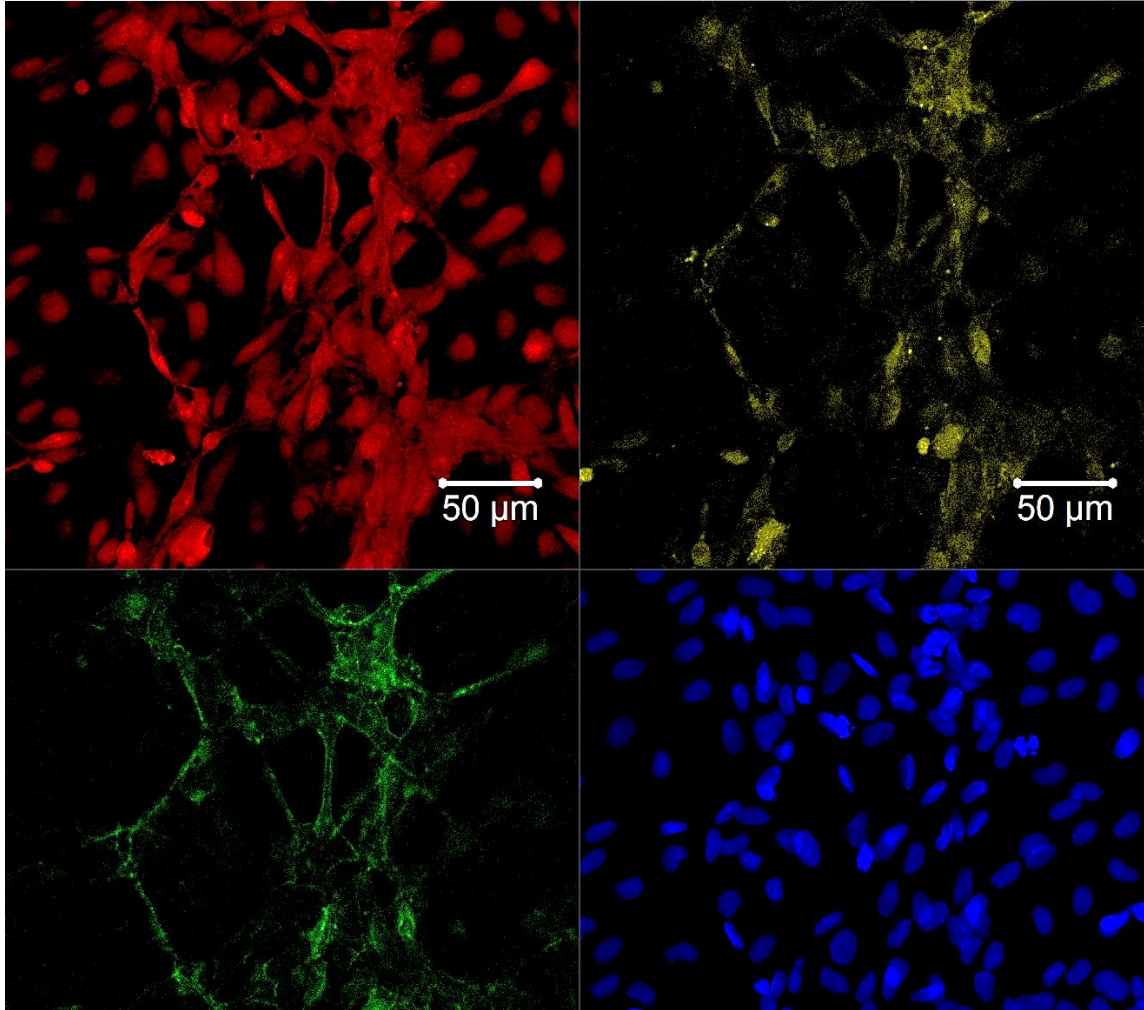


Red – PECAM-1
Yellow- selektin E
Green – tight junctions
Blue – nuclei

50 μm

Cells

Differentiation

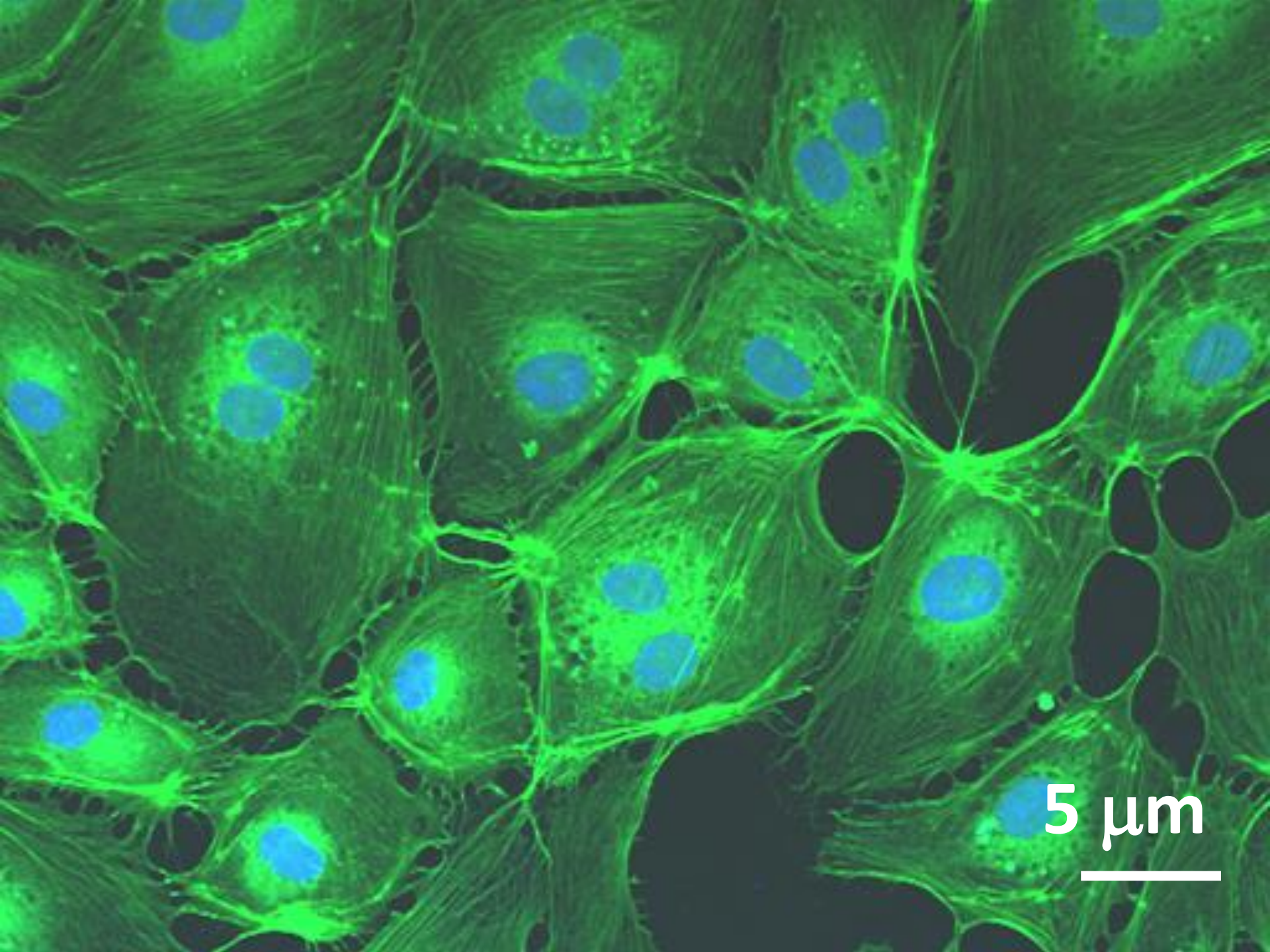


Red – PECAM-1

Yellow- selektin E

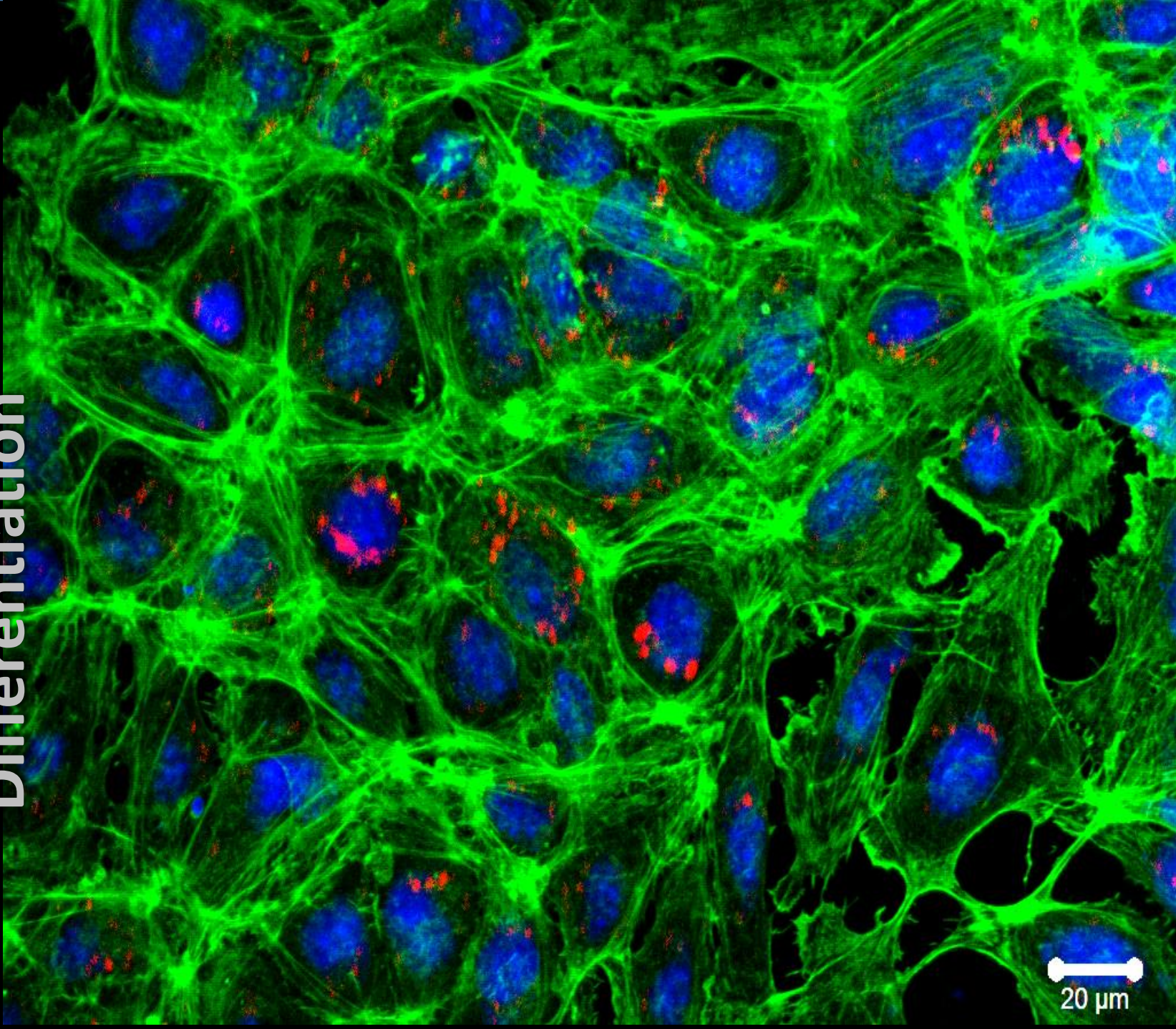
Green – tight junctions

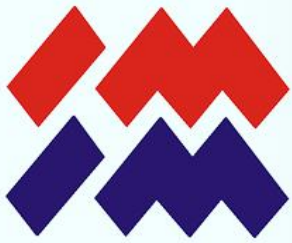
Blue – nuclei



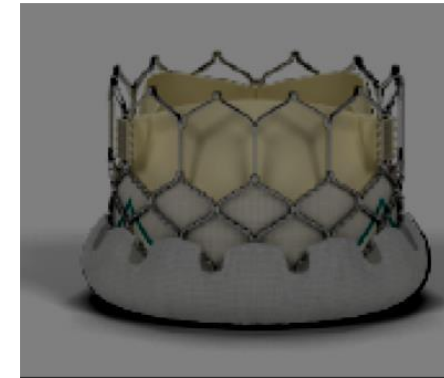
5 μ m

Differentiation

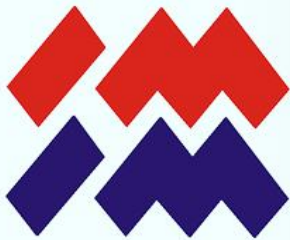




Coating



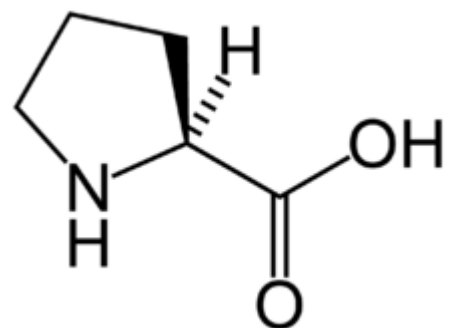
New cooperation and tasks

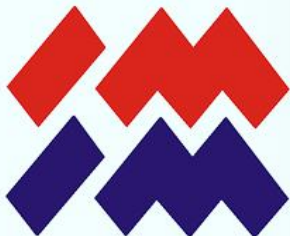


ProSAM- novel oligopropylene

Pro6 (Ac-Cys-(Pro)₆-CONH₂)

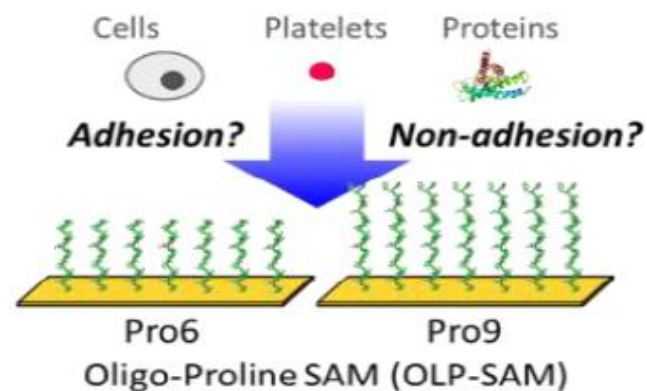
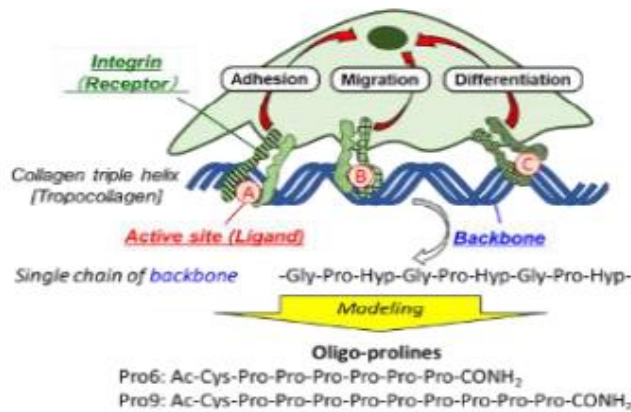
Pro9 (Ac-Cys-(Pro)₉-CONH₂)



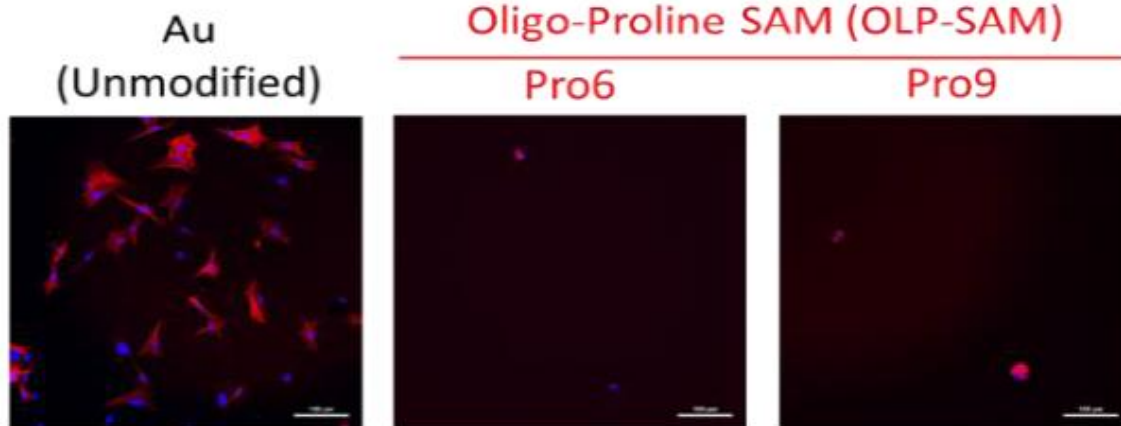


ProSAM

(A)



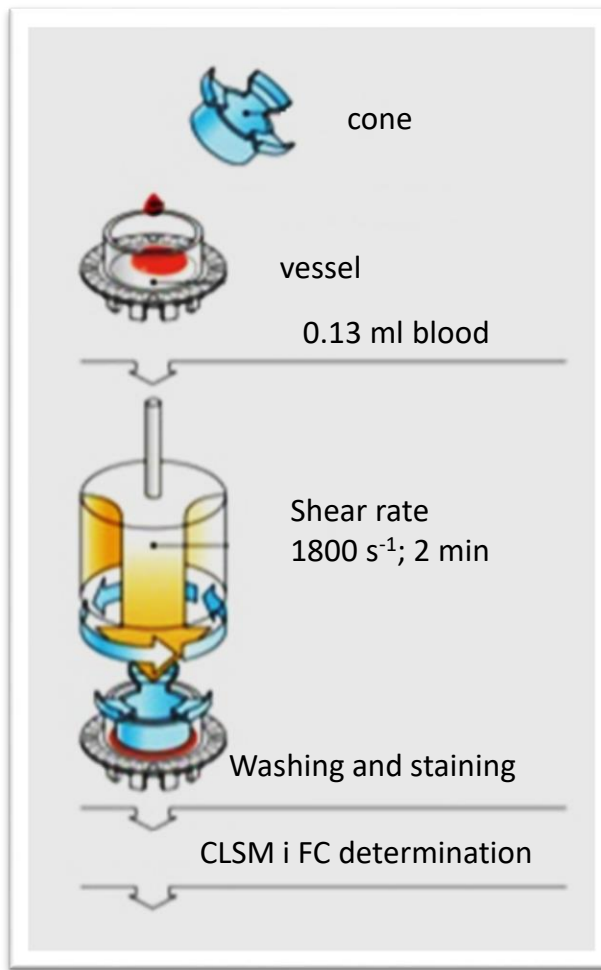
(B)





ProSAM

ProSAM interaction with blood



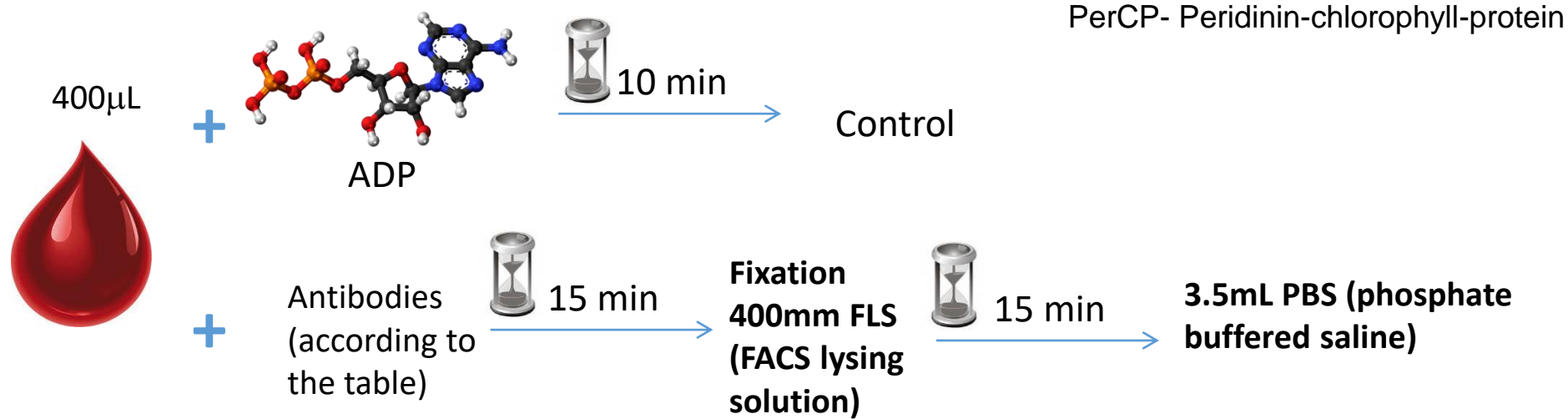
Impact R test

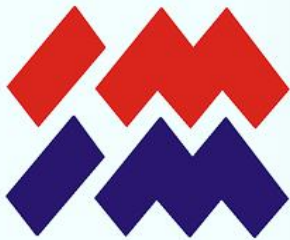




ProSAM

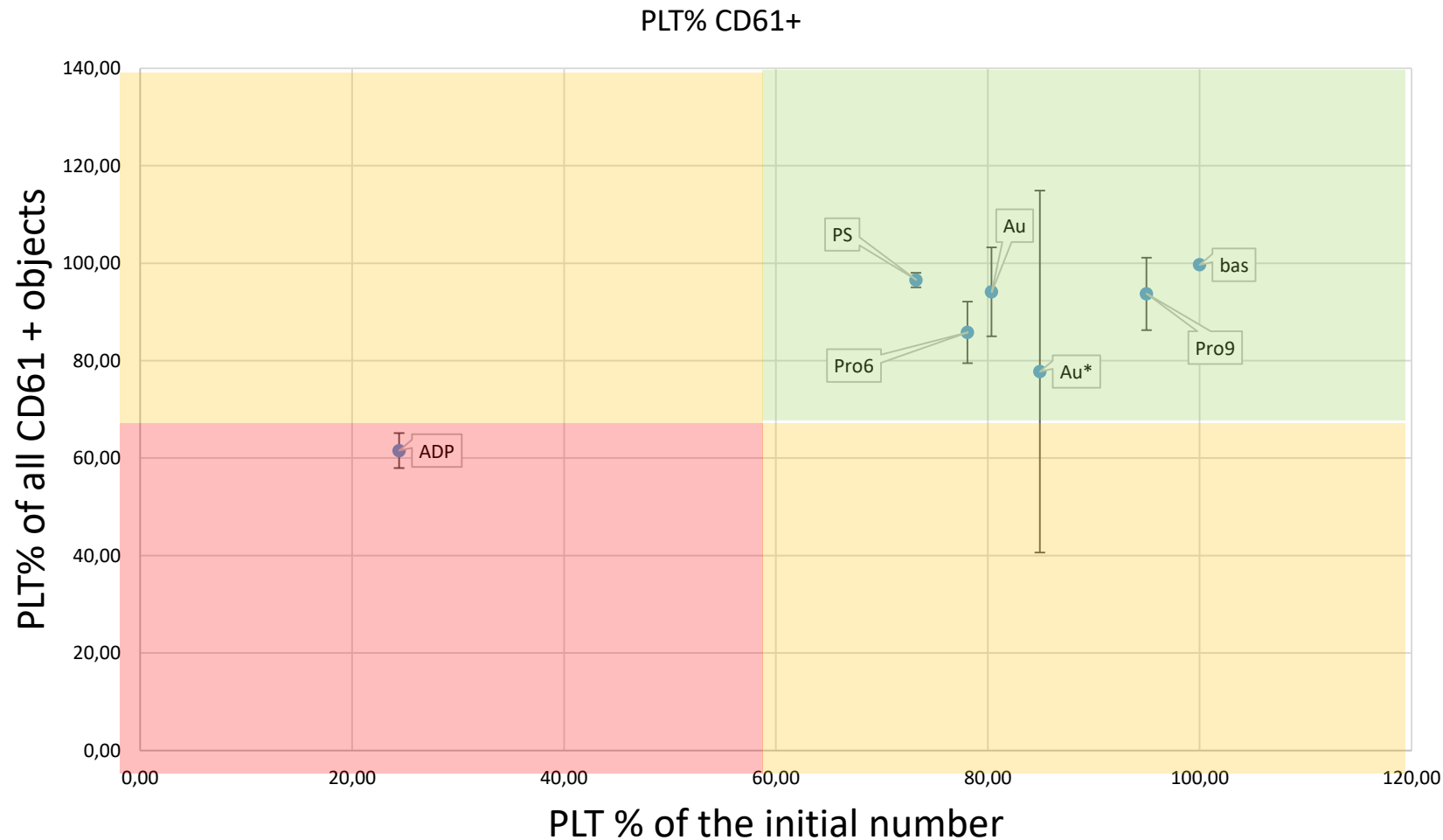
Name	Composition	Application
M	CD61-PerCP, CD62P, PAC-1	evaluation of activation in terms of contact with the material (+ control)
A	CD61-PerCP, CD62P, PAC-1	assessment of platelet activation using ADP
ADP 1	ADP 0.4mM	Positive control

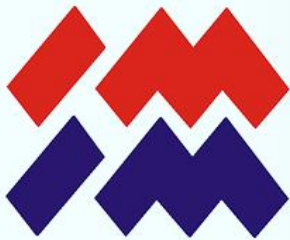




ProSAM

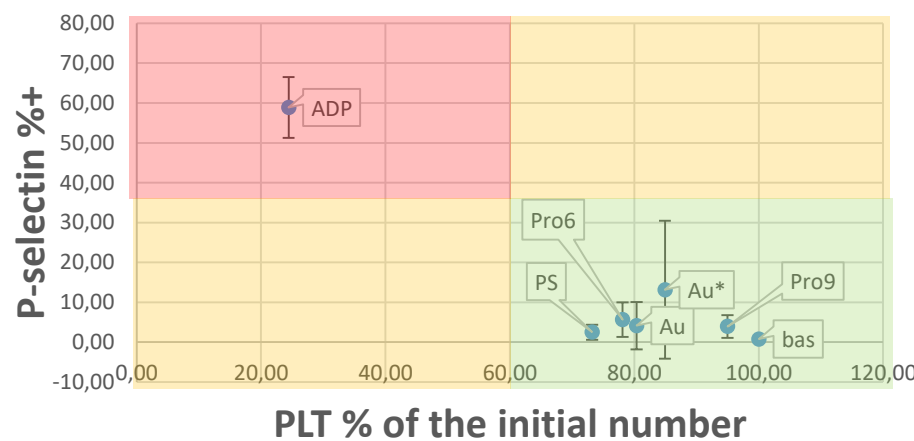
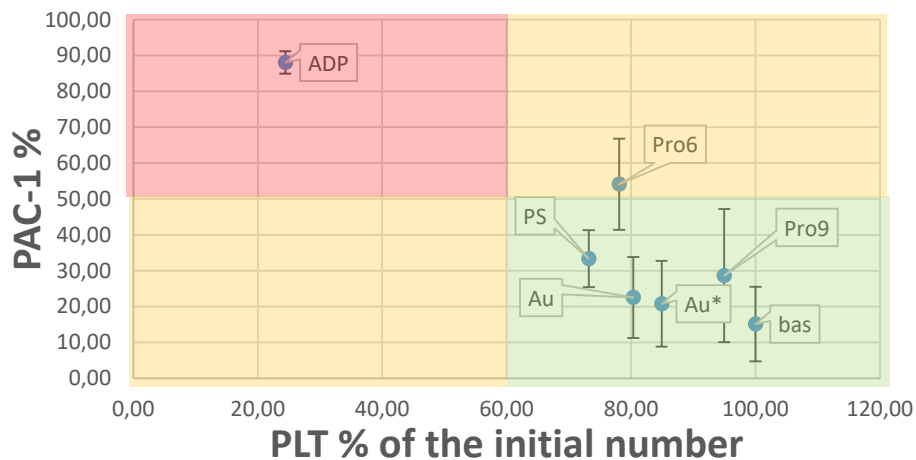
Impact-R test- PLT consumtion

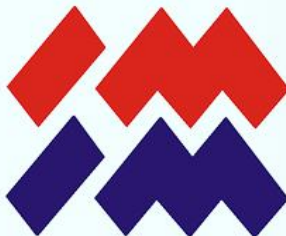




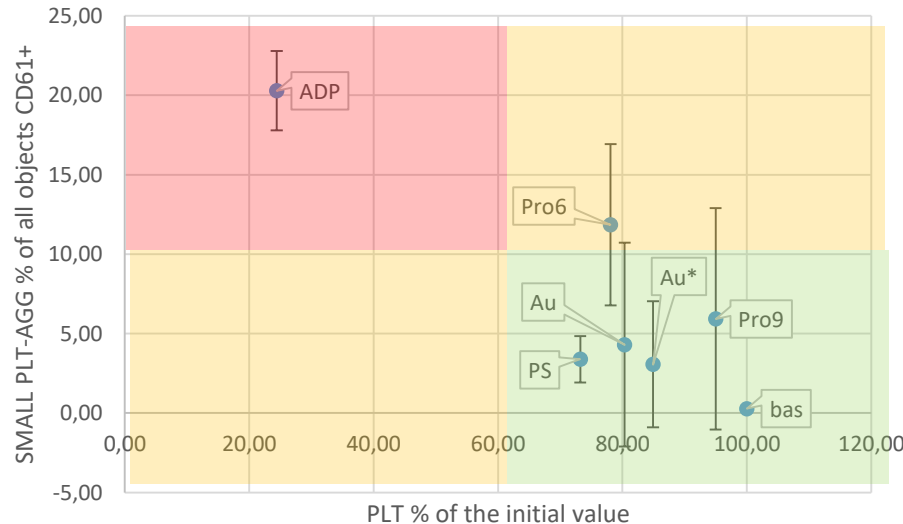
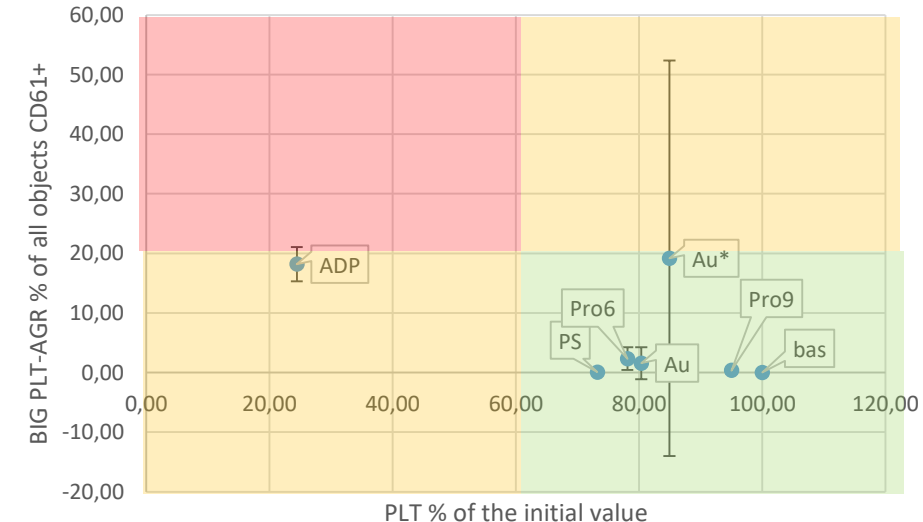
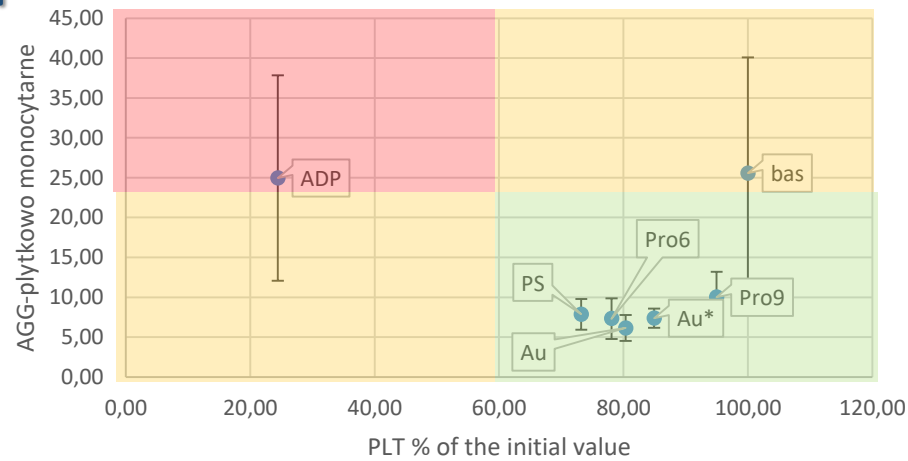
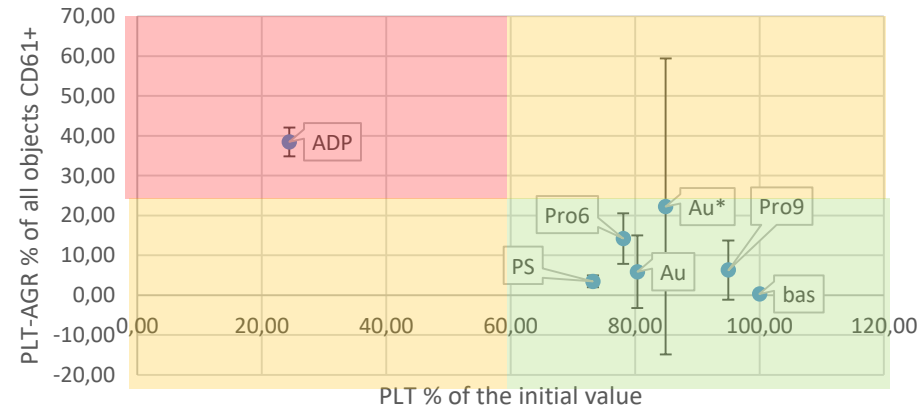
ProSAM

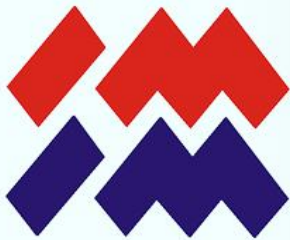
Impact-R test- PLT activation



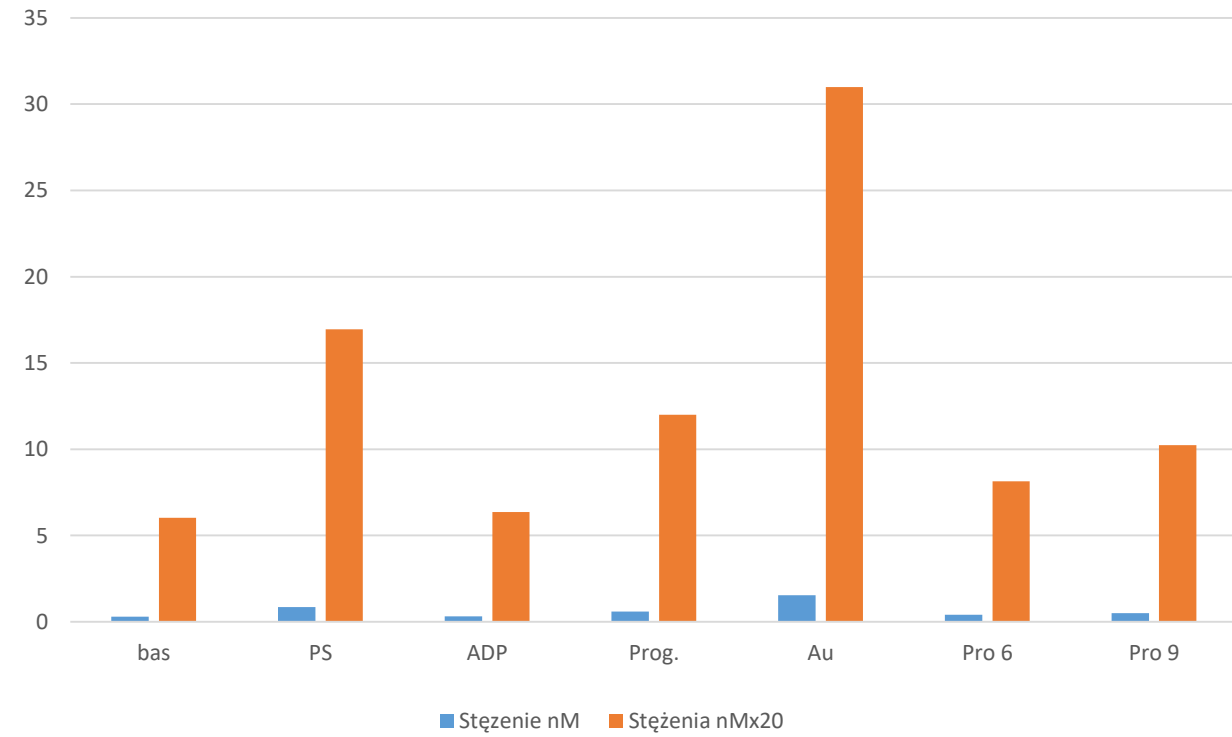
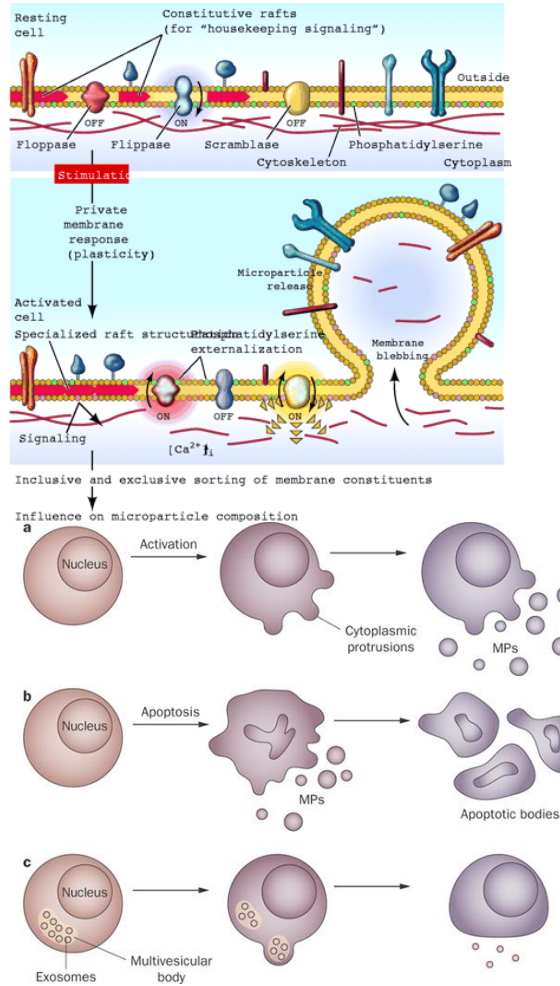


Impact-R test- PLT activation

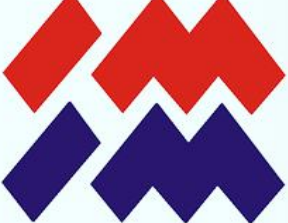




Impact-R test- PLT microparticles



■ Stężenie nM ■ Stężenia nM \times 20

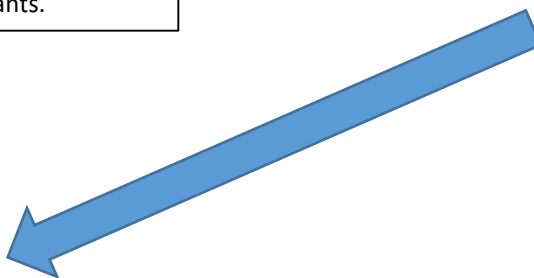


ProSAM

The first challenge of the research will concern synthesis of oligopeptides library that contains sequences without specific functionality and with variable chain length and secondary structure (especially polyproline-II helix) depends on the single substitutions in the amino acid sequence preserved among all library variants.



In the next step, all oligopeptide variants will be immobilized on the surface of polyurethane materials previously modified with thin carbon based ceramic coating in order to correlate oligopeptides secondary structure, chain length and spatial orientation with number, type, aggregation range and lateral interactions of proteins adsorbed from blood serum.



The oligopeptides will be deposited and characterized regarding to the physicochemical properties, the endothelial cells response as well as the *in vitro* hemocompatibility under dynamic conditions.



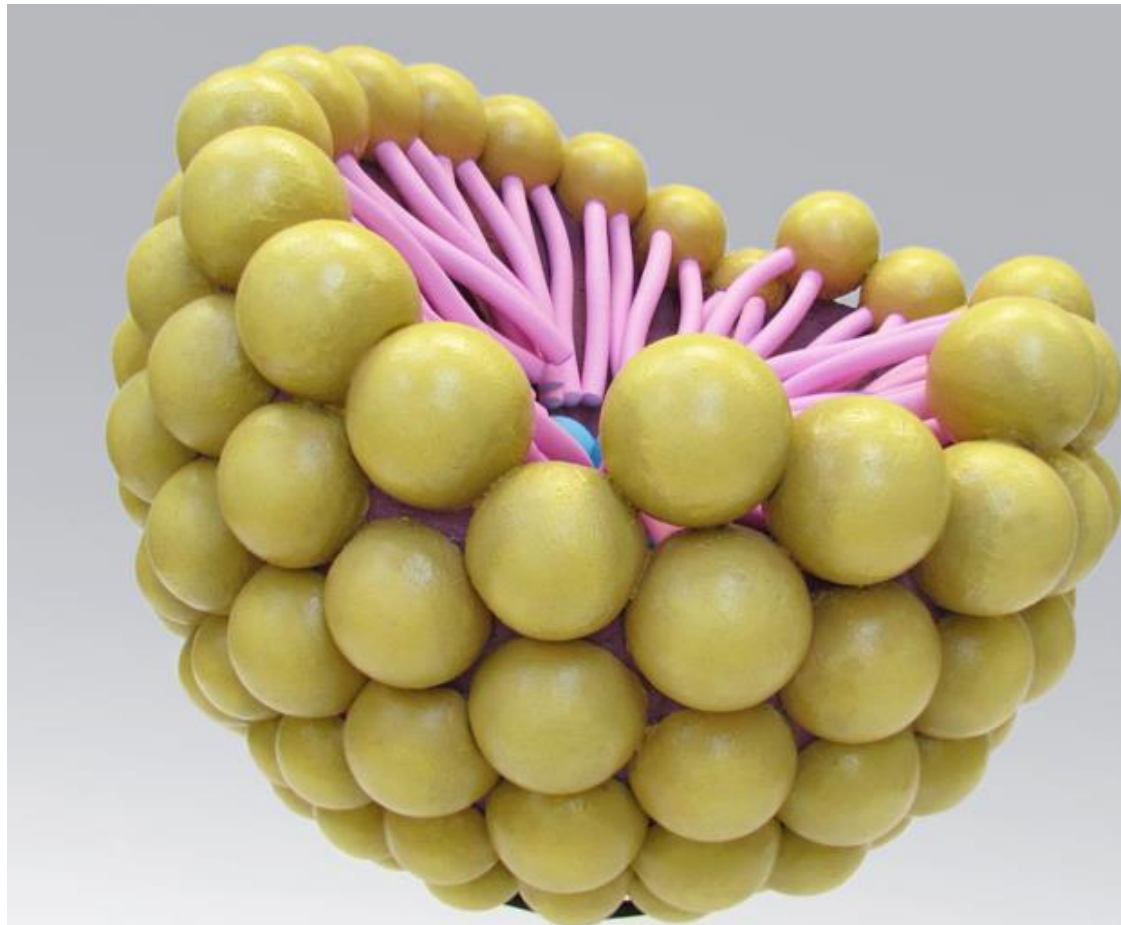
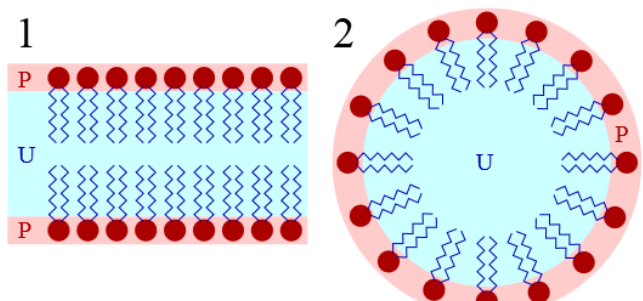
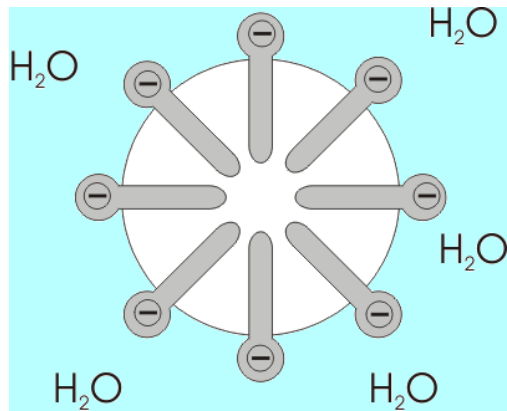
The project will result in phenomenological description of the influence of surface-immobilized oligopeptides secondary structure, mobility, backbone stiffness on their biological activity evaluated based on interaction with serum proteins, blood morphotic elements and endothelial cells under flow conditions.



This will decide about final design of peptide-based SAM coating that may be successfully applied to functionalize surface of the heart assist device.

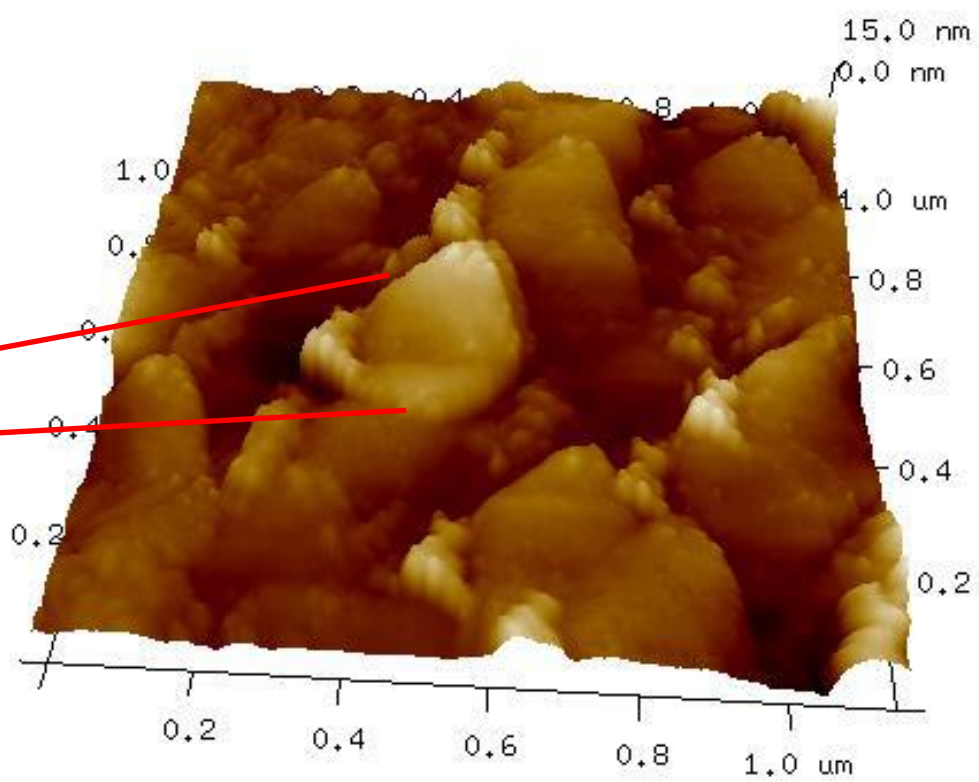
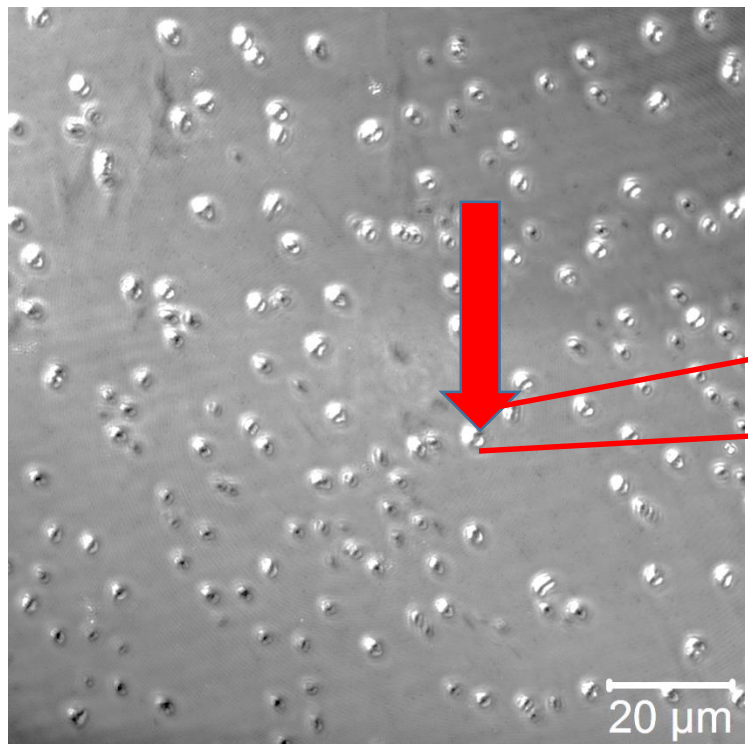


Micelles



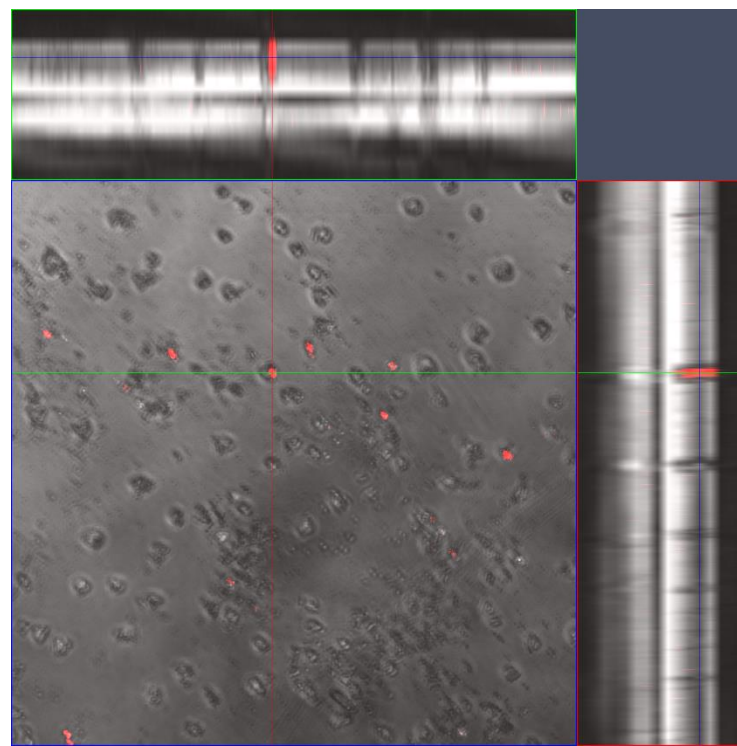
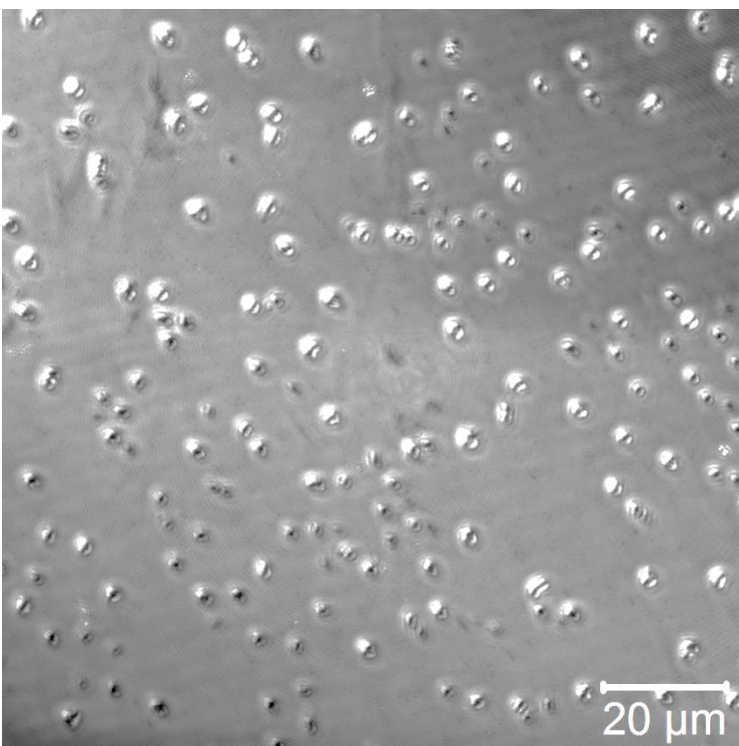
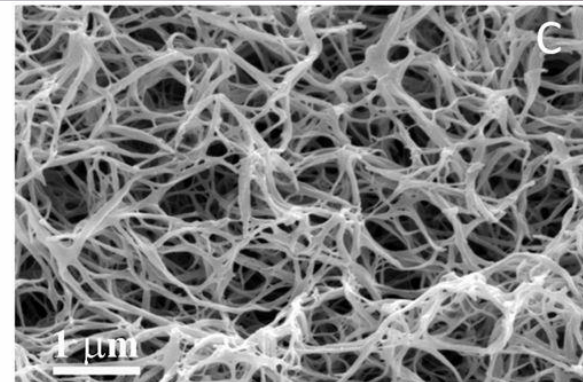
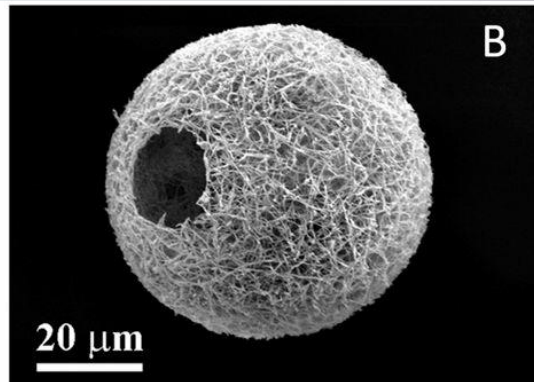
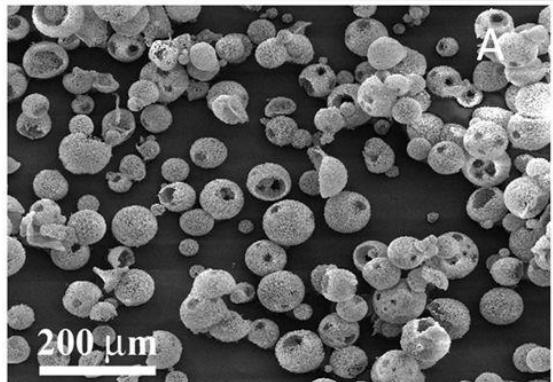


Micelles





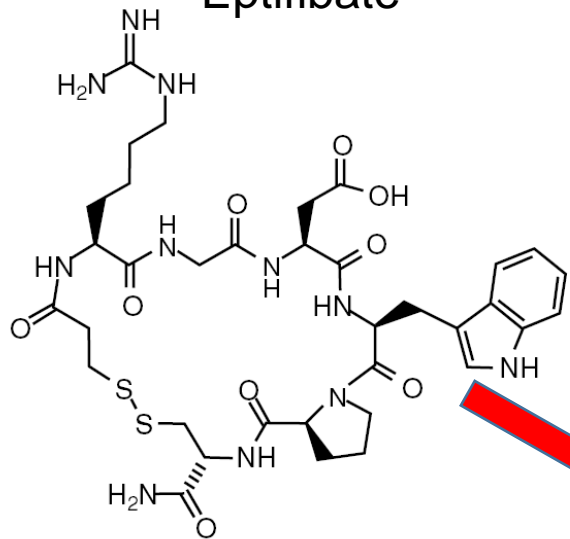
Micelles



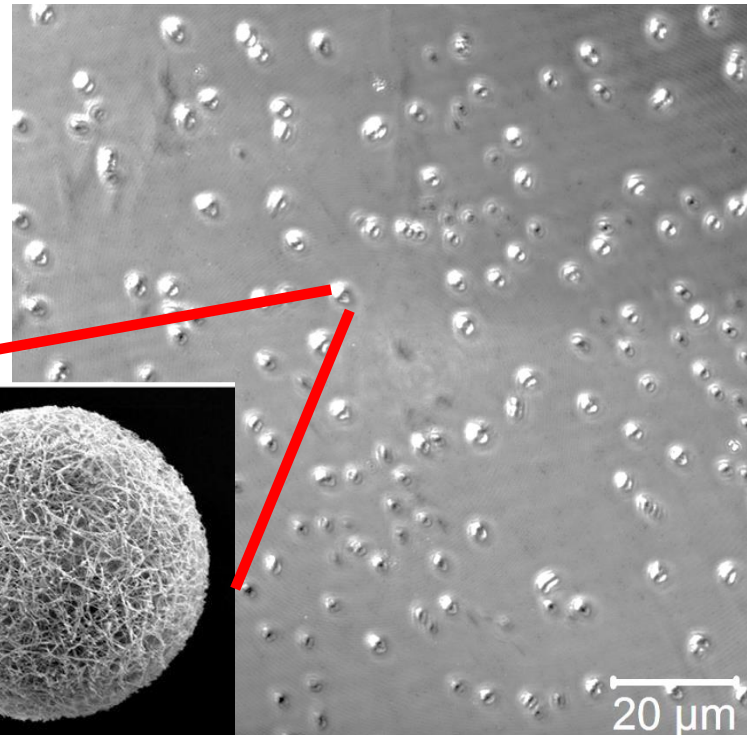
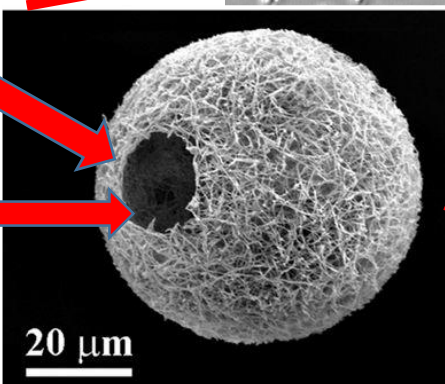
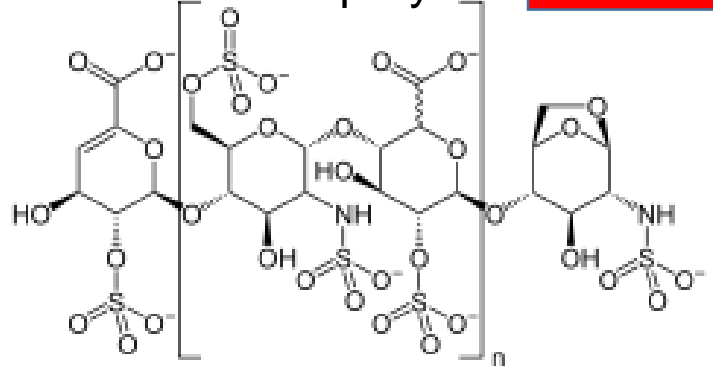


Micelles

Eptifibate



Enoksaparyna





Micelles

Chitosan (CS)

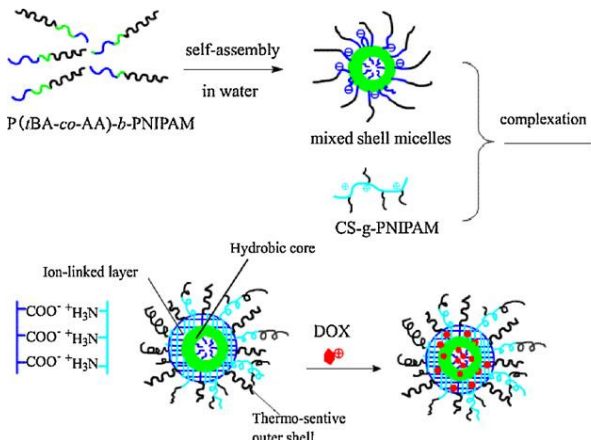
Carboxymethyl cellulose (CMC)

N-Isopropylacrylamide (NIPAM)

Cerium ammonium nitrate (CAN) (ini)

glutaraldehyde (GA)

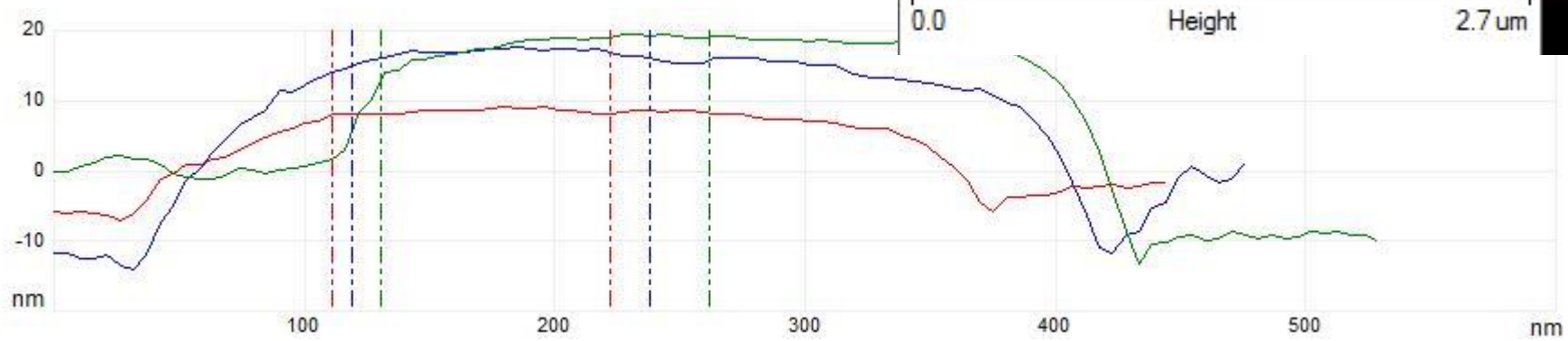
1. Chitozan m.cz. 100,000-300,000 /ACROS 349051000
2. ACRS34905-030-100
3. Karboksymetyloceluloza sól sodowa śr. M.W. 90000 (DS=0.7) /ACROS 332601000/
4. 4. N-Izopropyloakrylamid stab., czysty, 99% /ACROS 412780250/ ACRS41278-030-25
5. Amonu ceru(IV) azotan do analizy, 99.5% /ACROS 201441000/
6. Glutarowy aldehyd , roztwór 50 % /ACROS 410960
7. Kwas octowy 99,5%--99,9% CZDA
8. Aceton CZDA, ODCZ. FP
9. Metanol CZDA, ODCZ. FP





Micelles

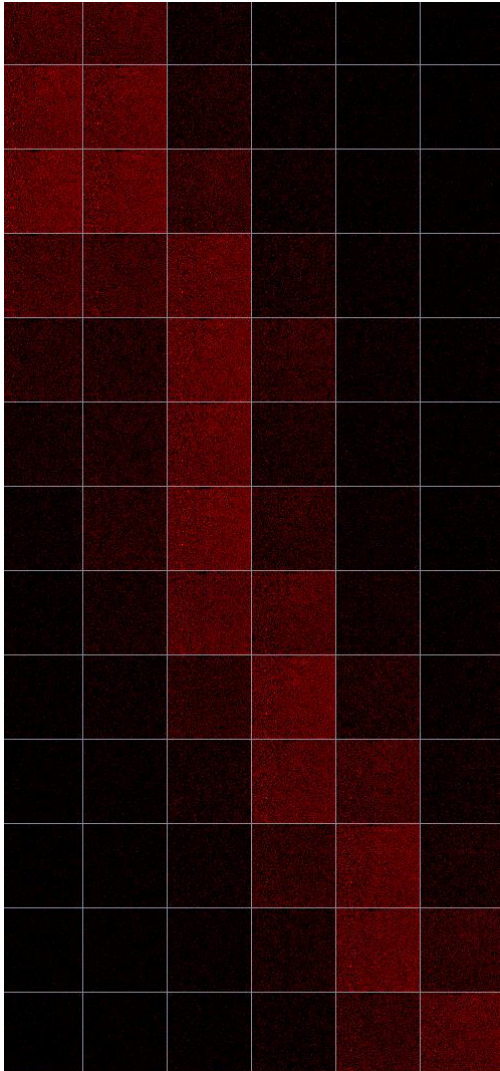
$d = 327,9 \pm 45 \text{ nm}$
 $h = 31 \pm 9 \text{ nm}$



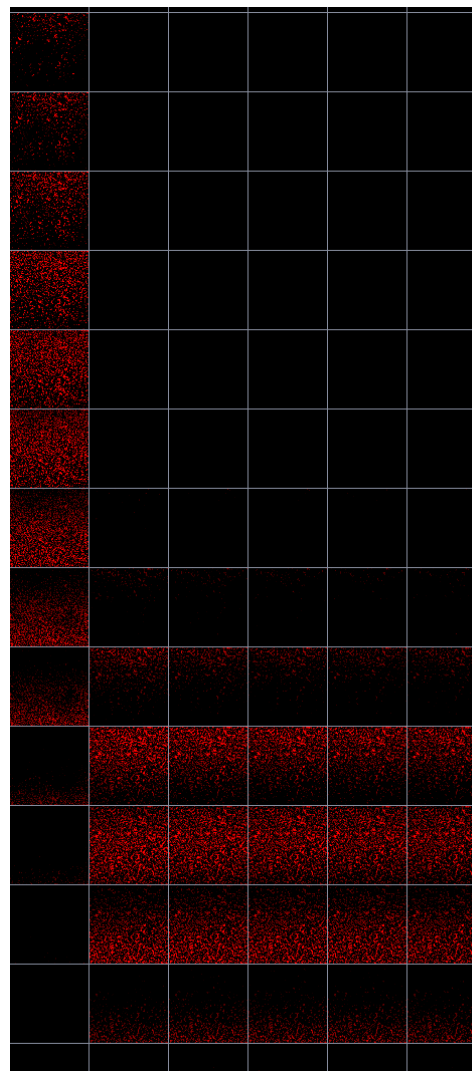


Micelles

Non cross linked



Cross linked





Micelles

Poliuretan



Integrilin 1 day

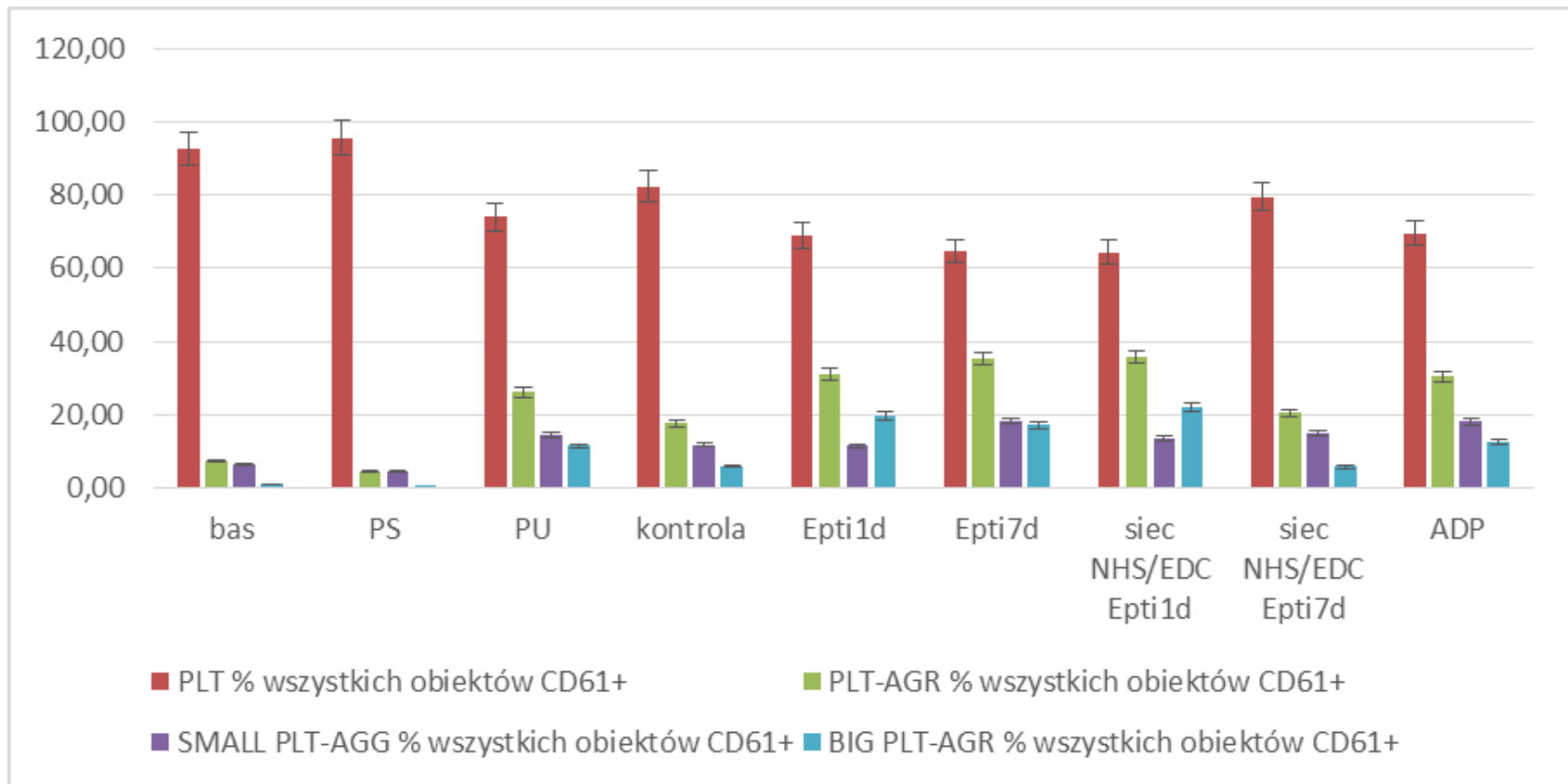


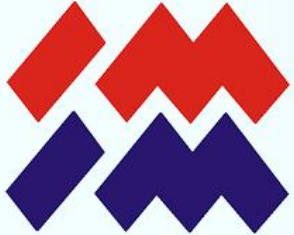
Integrilin 7 days



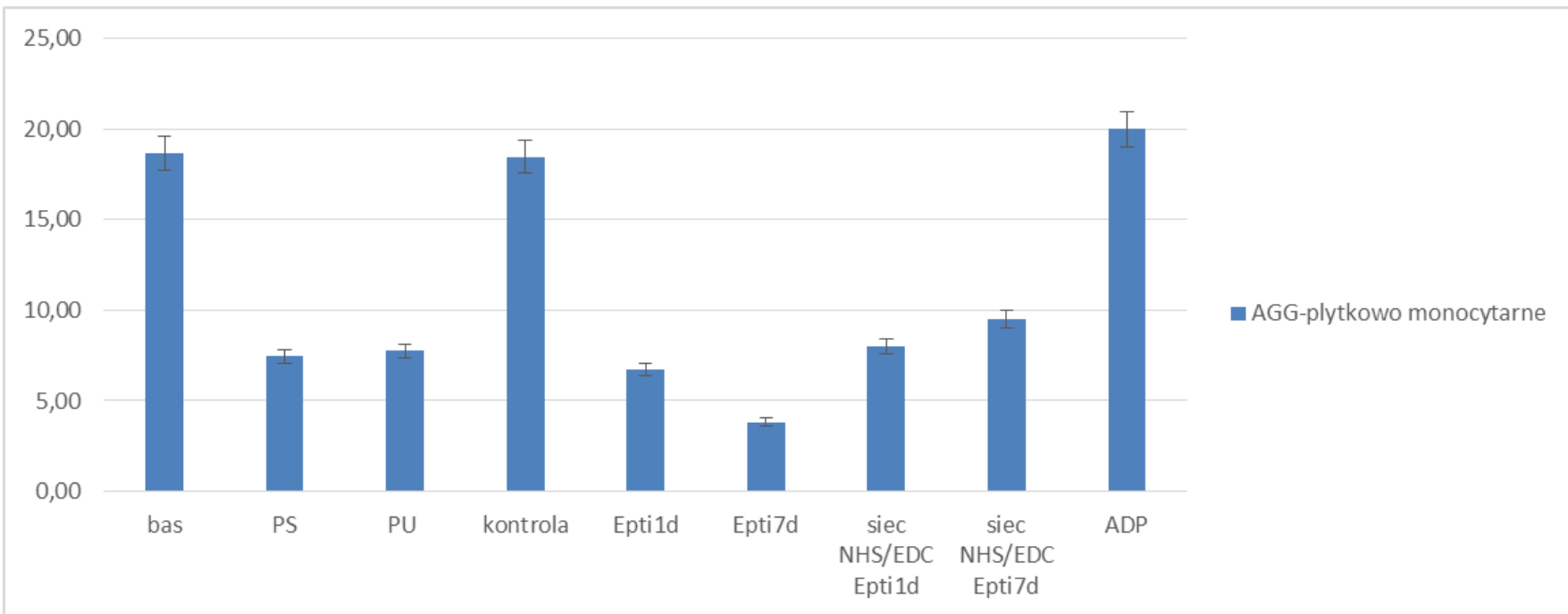


Micelles



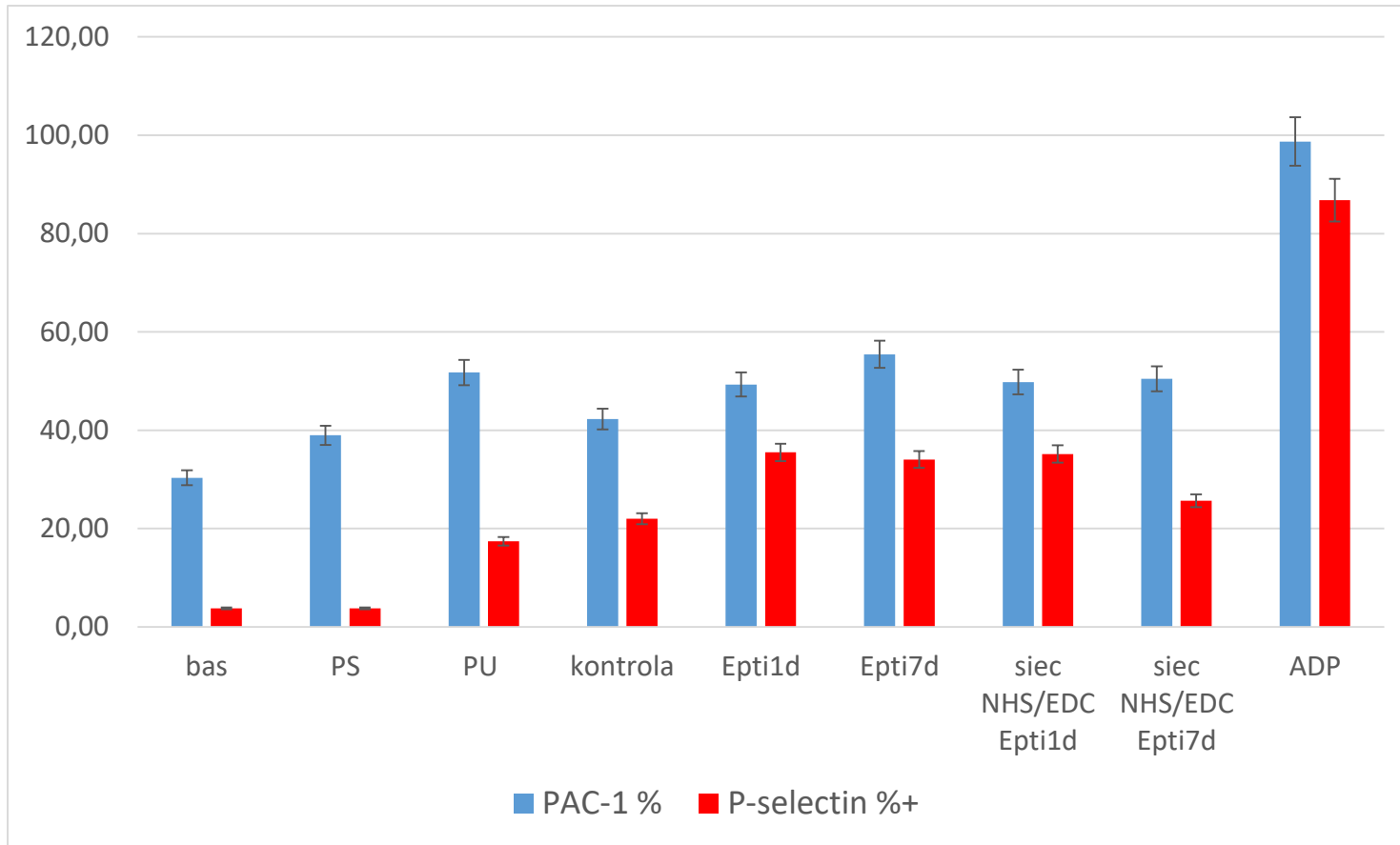


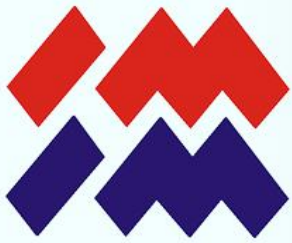
Micelles





Micelles



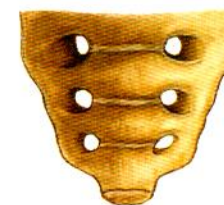
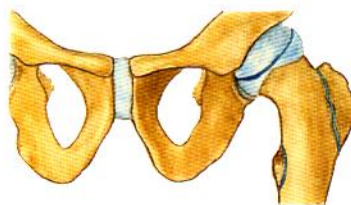
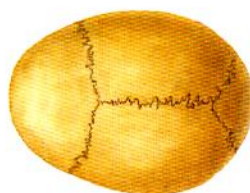
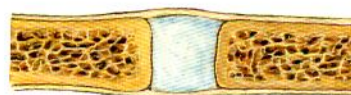
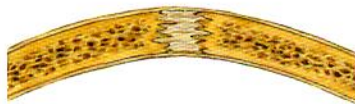


Part 3

Regeneration of the bone and joint system



The bone-joint system



Ryc. 15 Więzozrost, *articulatio fibrosa*, na przykładzie szwów czaszki.

Ryc. 16 Chrząstkozrost, *articulatio cartilaginea*, na przykładzie spojenia łonowego.

Ryc. 17 Kościozrost, *articulatio ossea*, na przykładzie kości krzyżowej.

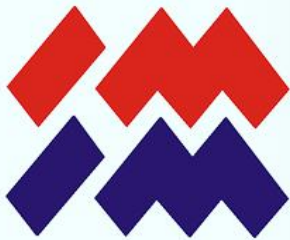
Strict (immovable)- Ścisłe (nieruchome)

Więzozrosty (syndesmosis)

Chrząstkozrosty (synchondrosis)

Kościozrosty (synostosis)

Free (mobile) or joints (articulatio)- Wolne (ruchome) czyli stawy (articulatio)



Joints

Selection

Zawiasowy (ginglymus)

Obrotowy (trochoidea)

Śrubowy (cochlearis)

Elipsoidalny (elipsoidea)

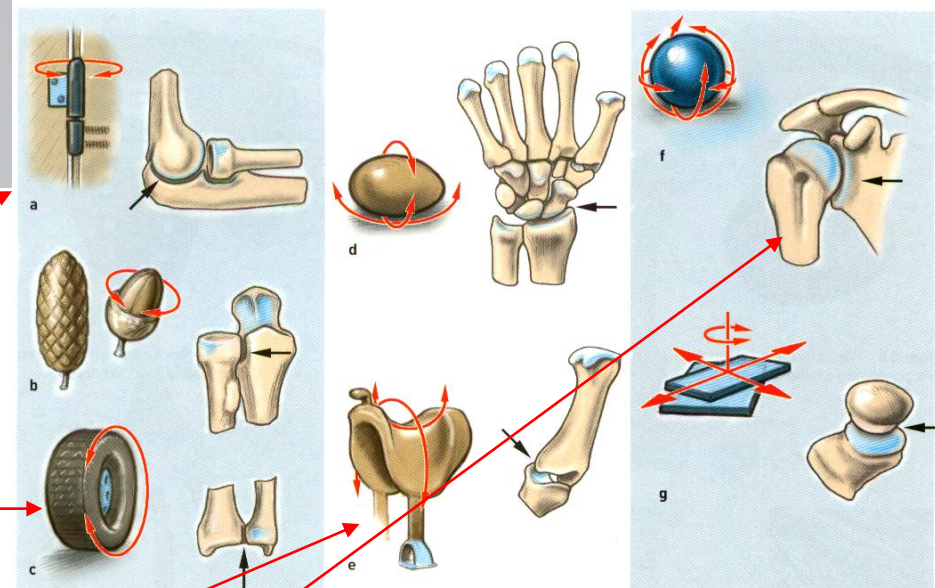
Siodełkowaty (sellaris)

Kulisty wolny (spheroidea)

Kulisty panewkowy (cotylica)

Nieregularny

Płaski



Ryc. 19 a-g Stawy, *articulae synoviae*.

a staw zawiasowy, *articulatio cylindrica*

b staw stożkowy, *articulatio conoidea*

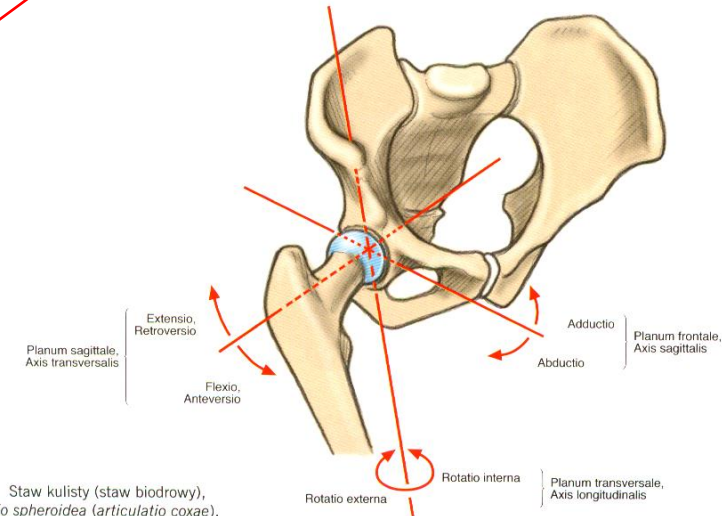
c staw obrotowy, *articulatio trochoidea*

d staw owalny, *articulatio ovoidea*

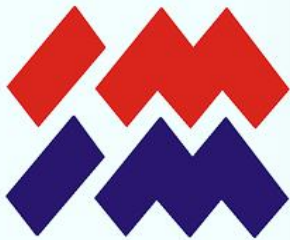
e staw siodełkowy, *articulatio sellaris*

f staw kulisty, *articulatio sphaeroidea*

g staw płaski, *articulatio plana*



Ryc. 20 Staw kulisty (staw biodrowy),
articulatio spheroidea (*articulatio coxae*).



Skull

Kość czołowa (os frontale)

Kość klinowa (os sphenoidale)

Kość ciemieniowa (os parietale)

Kość skroniowa (os temporale)

Kość sitowa (os ethmoidale)

Kość potyliczna (os occipitale)

Żuchwa (os mandibule)

Szczęka (os maxillare)

Kość jarzmowa (os zygomaticum)

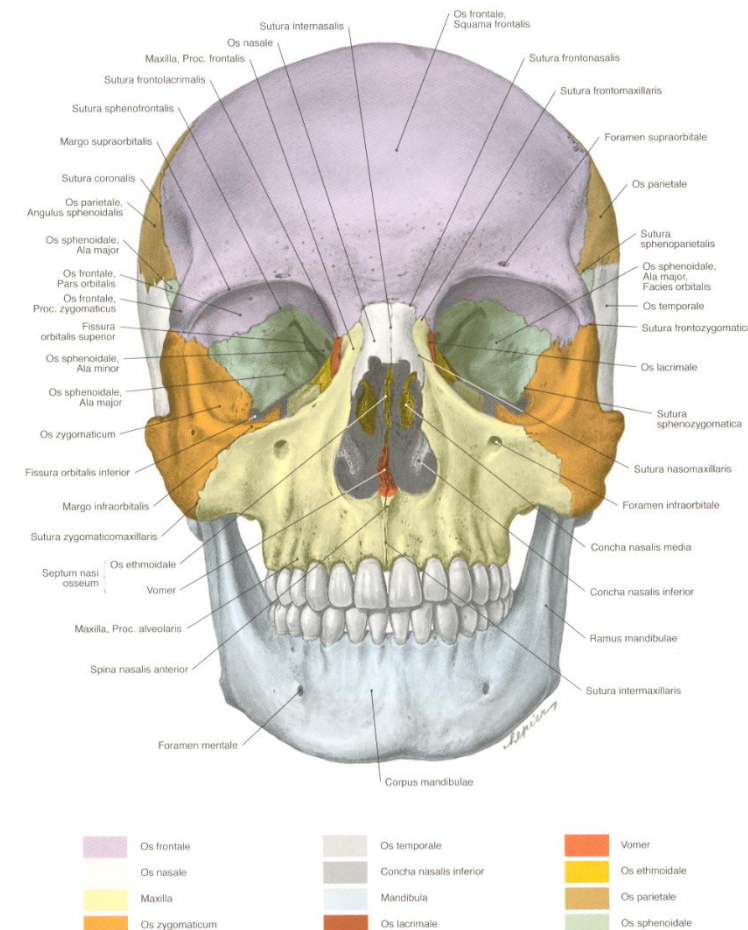
Kość nosowa (os nasale)

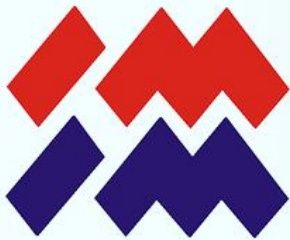
Kość łzowa (os lacrimale)

Lemiesz (vomer)

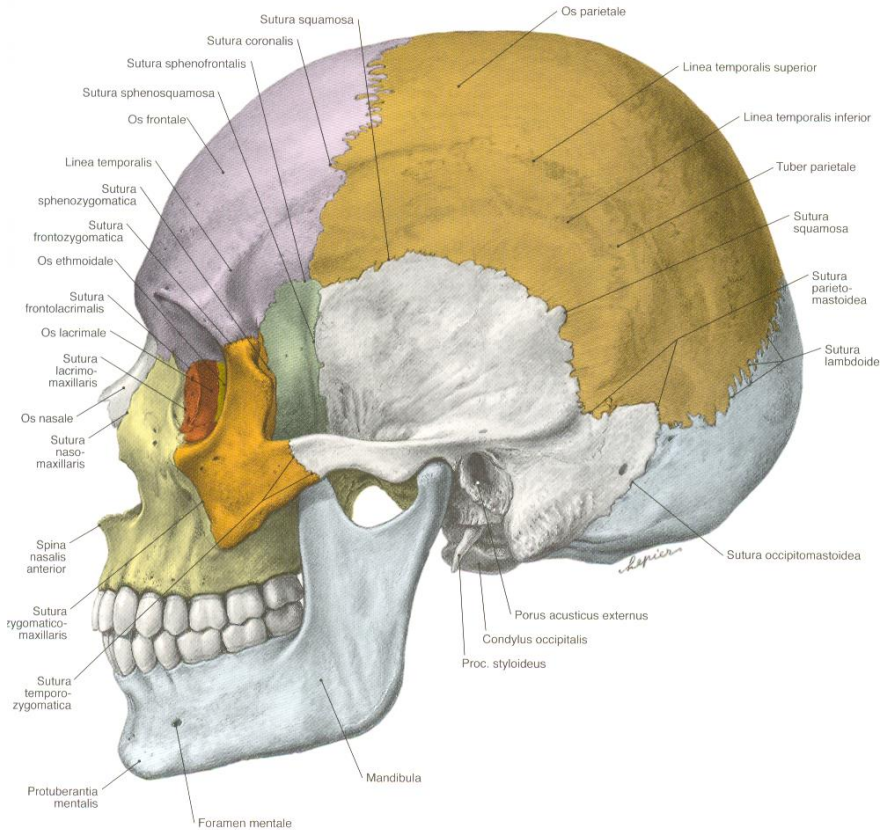
Kość podniebienna (os palatinum)

Mażowina nosowa dolna (concha nasalis inferior)





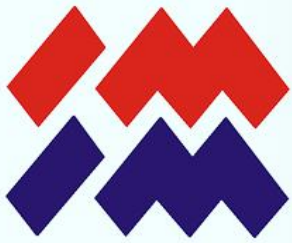
Skull



Os frontale
Os parietale
Os occipitale
Os nasale

Os lacrimale
Os zygomaticum
Os sphenoidale
Os ethmoidale

Os temporale
Maxilla
Mandibula



M-ERA.NET Transnational Call 2016

Full Proposal

Project Acronym:

jawMPLANT

Project Coordinator:

(Organisation and country):

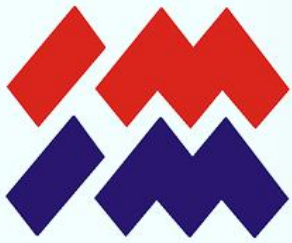
***JOANNEUM RESEARCH Forschungsges.m.b.H., Institute
for Surface Technologies and Photonics***



Part 3.1

Executed projects

The bone-joint system



M-ERA.NET Transnational Call 2016

Full Proposal

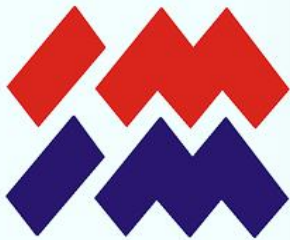
Project Acronym:

jawMPLANT

Project Coordinator:

(Organisation and country):

***JOANNEUM RESEARCH Forschungsges.m.b.H., Institute
for Surface Technologies and Photonics***



Bioactive, antimicrobial 3D printed implants for large jawbone defects after tumour resection



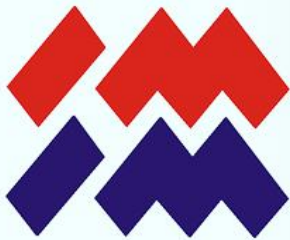
Roman Major¹, Marcin Surmiak², Juergen M. Lackner³, Michal Charkiewicz⁵

1 Institute of Metallurgy and Materials Science, Polish Academy of Sciences, Reymonta St. 25, Crakow, PL.

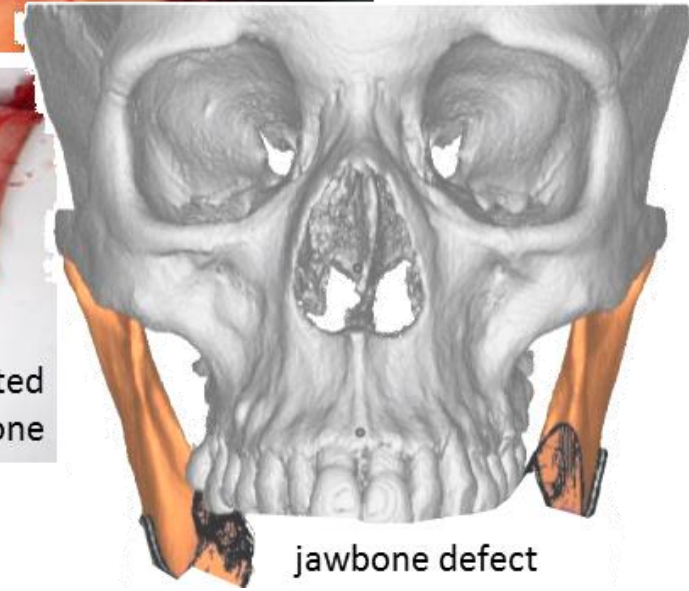
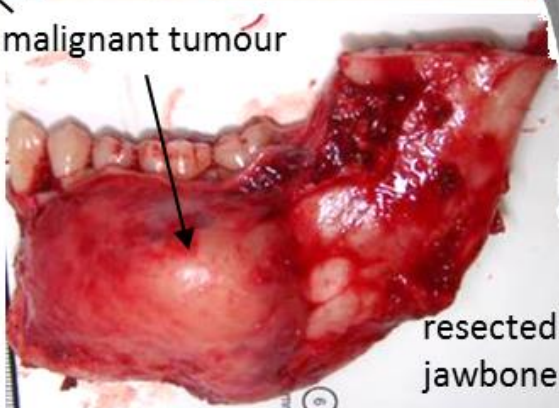
2 Department of Medicine, Jagiellonian University Medical College, 8 Skawinska Street, 31-066 Cracow, PL.

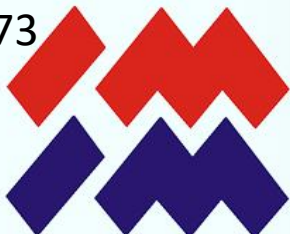
3 JOANNEUM RESEARCH Forschungsgesellschaft mbH MATERIALS - Institute of Surface Technologies and Photonics Functional Surfaces Leobner Straße 94 A-8712 Niklasdorf A

4 ChM sp. z.o.o. Lewickie 3B 16-061 Juchnowiec Koscielny PL



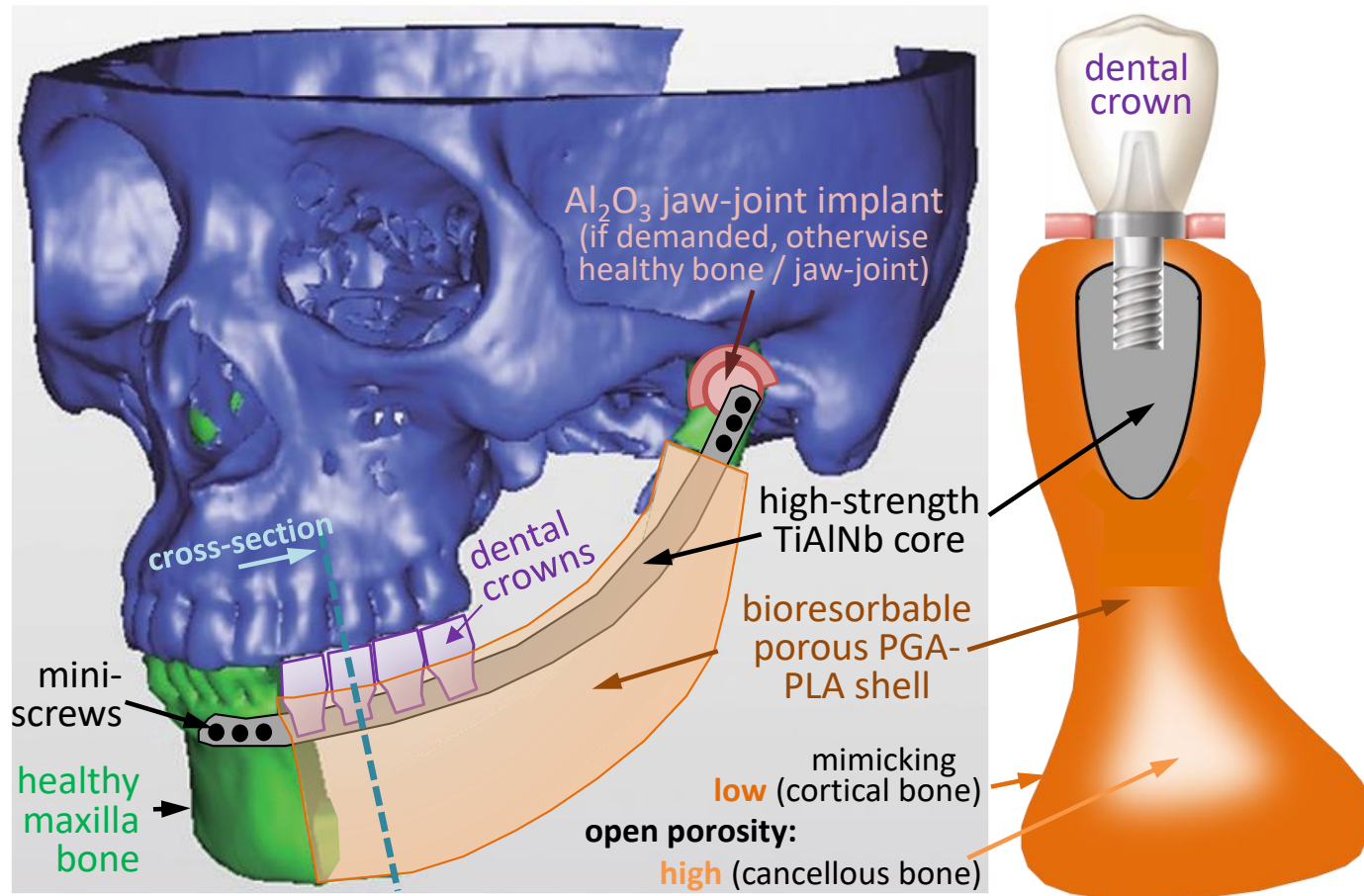
Introduction

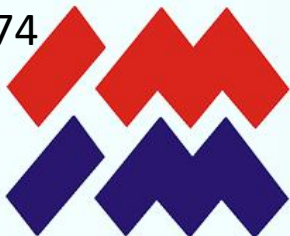




Introduction

Concept of the patient-specific metal-core, polymer-shell maxillofacial implant with artificial jaw-joint





Project partners

- JOANNEUM Research Forschungsgesellschaft m.b.H., Materials, Institute for Surface Technologies and Photonics (JR)
- ChM Sp. z.o.o. (ChM)
- Lithoz GmbH (Lithoz)
- Haratech GmbH (HT)
- Alphacam Austria GmbH (aC)
- Medical University of Vienna, Department of Cranio-, Maxillofacial and Oral Surgery (VMU)
- Warsaw University of Technology, Faculty of Chemical and Process Engineering (WUT)
- Polish Academy of Sciences, Institute of Metallurgy and Material Sciences (IMIM)



Materials

Med. 610 meshes 1mm

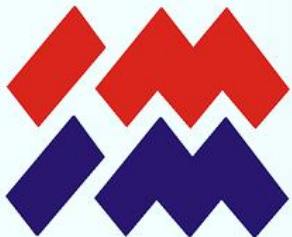
Med. 610 meshes 2mm

Med. 610

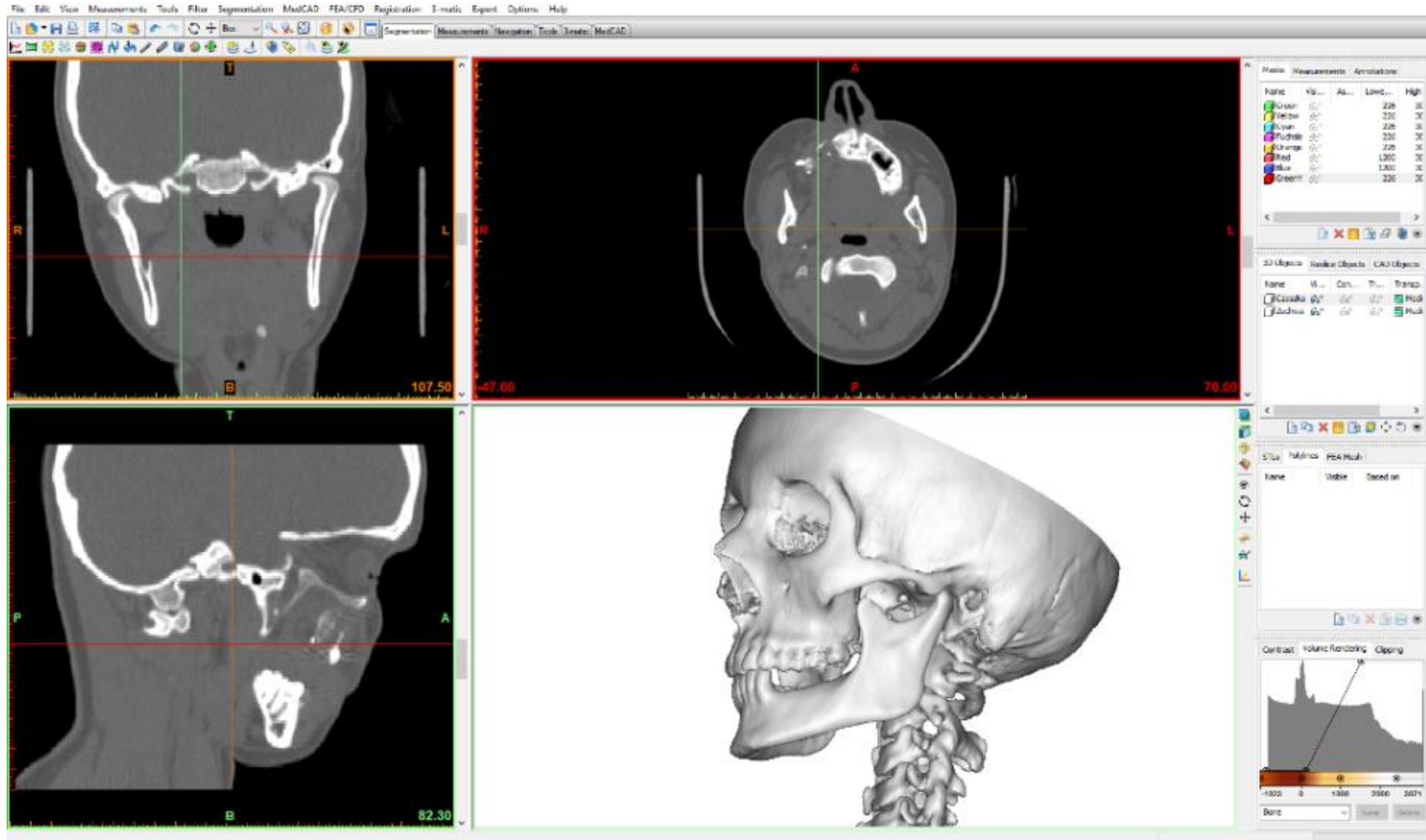
Zirconia LithaCon 3Y230 ZTA10 (Zirconia)

Alumina LithaLox 350D

ChM nonporous ChM 0.5 porosity



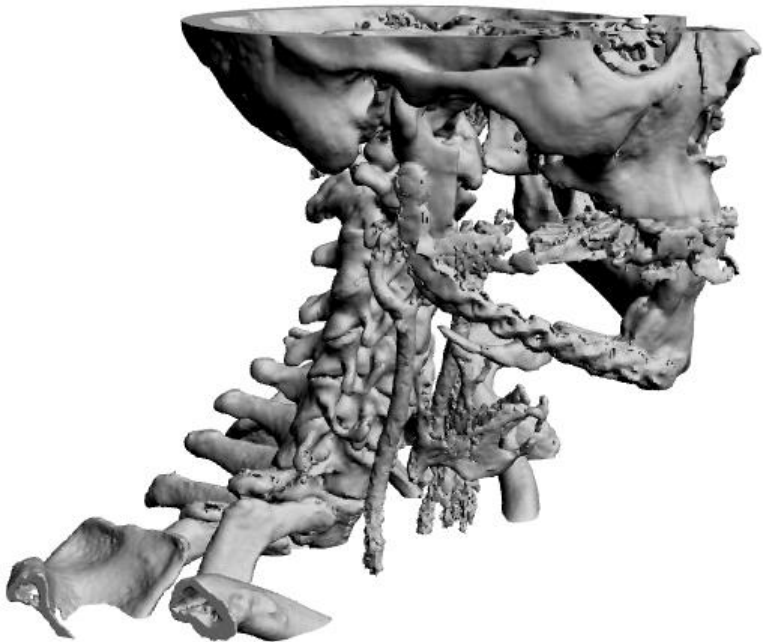
Introduction



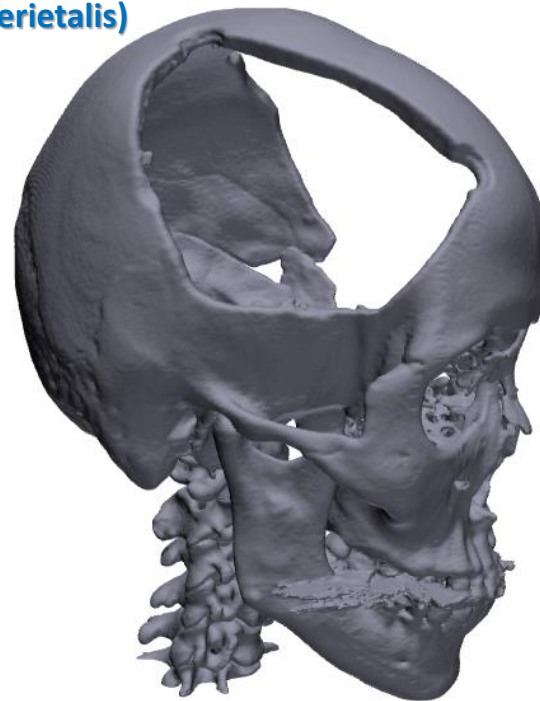


Cases

Case 1: Mandibula



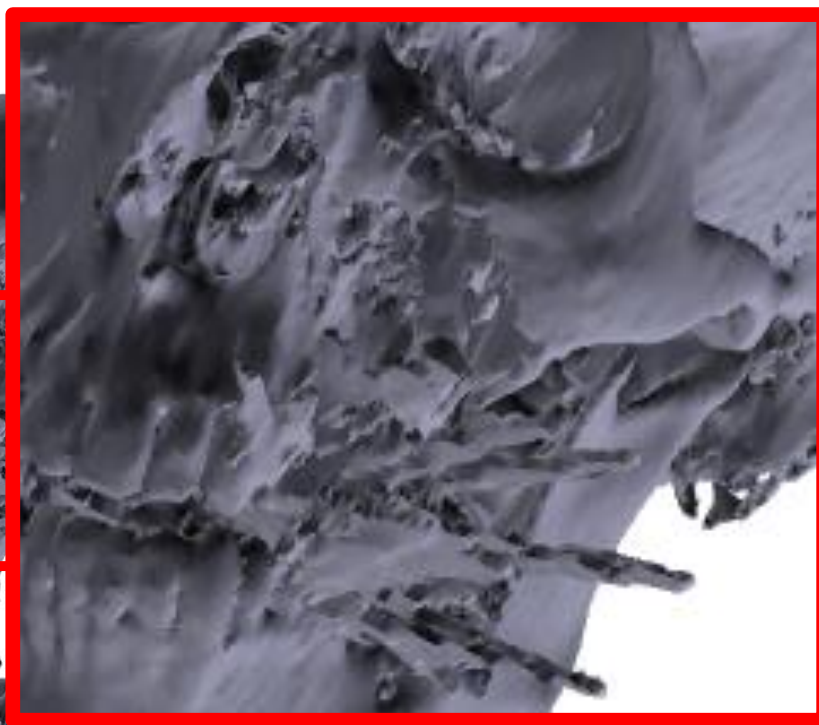
Case 3: Skullcup (perietalis)





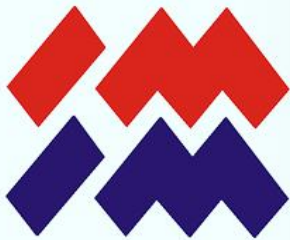
Cases

Case 4 Nasofrontal



Case 5: Upper anterior tooth





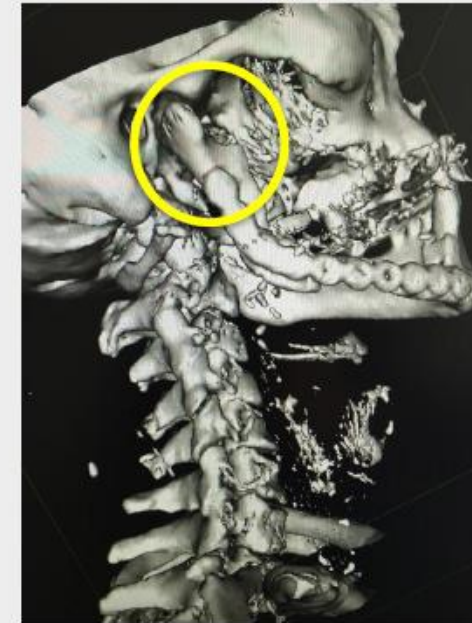
Case 1

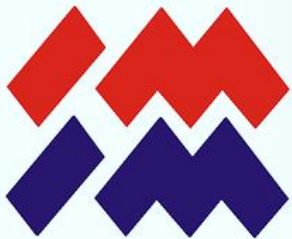
CASE 01 MANDIBULA

LITHOZ

Original data

Software: InVesalius 3.1





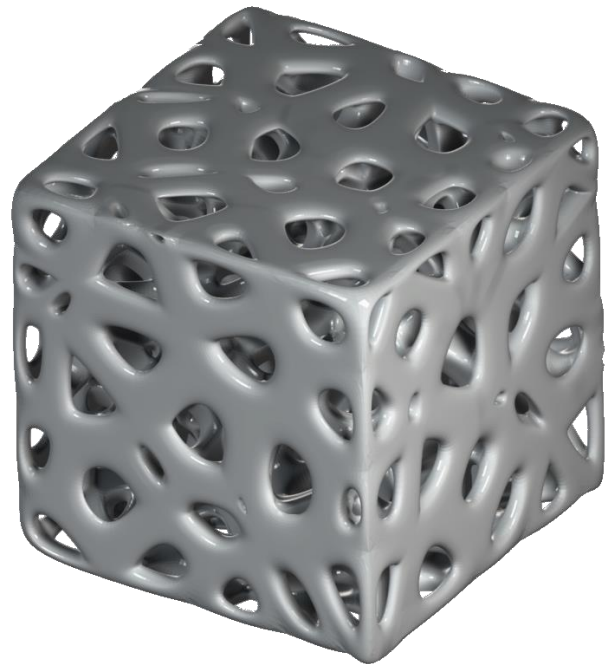
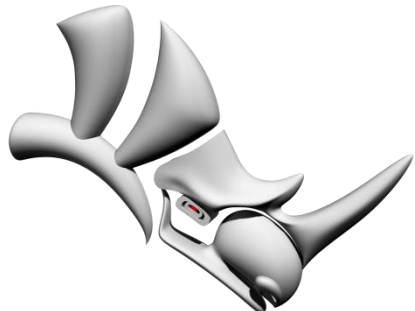
The idea

Report by Guillaume CLÉMENT, Haratech GmbH

T +43 (0) 732 287070-65

guillaume.clement@haratech.at

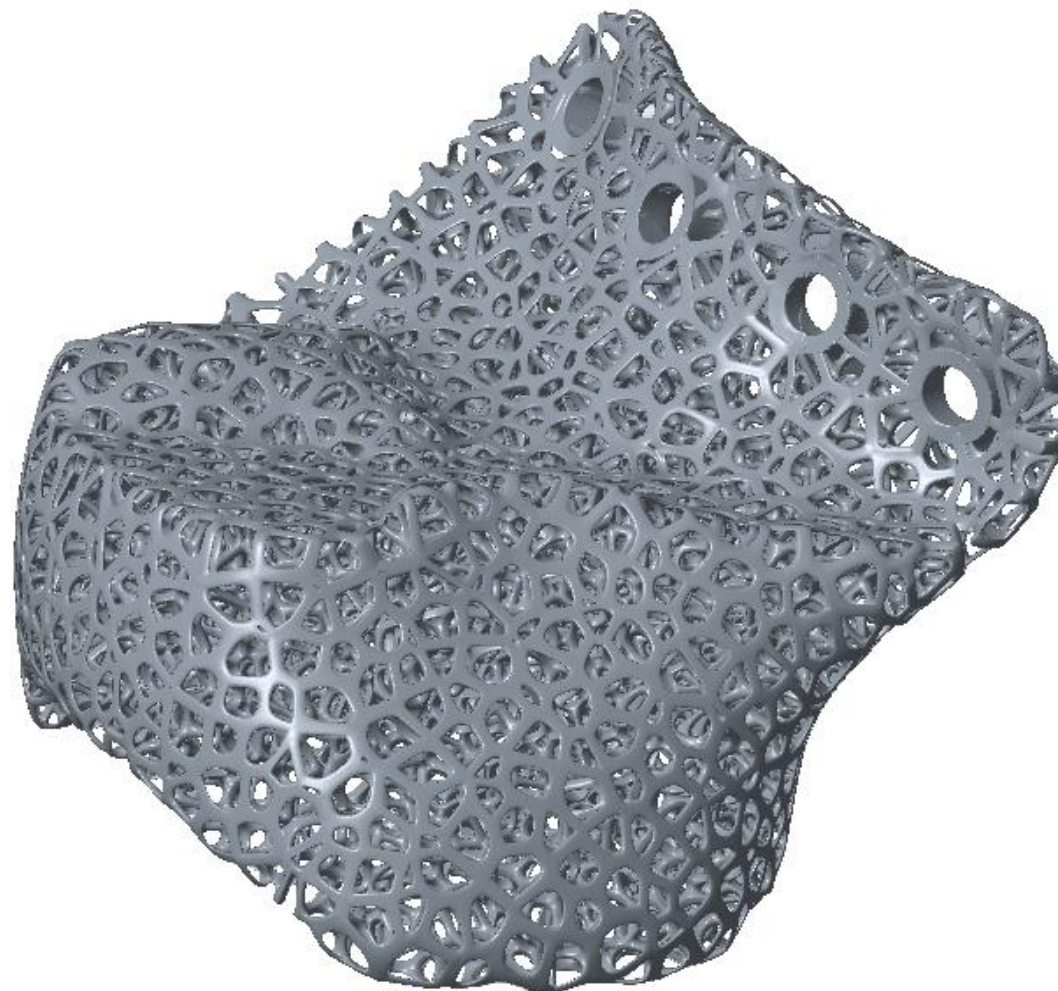
www.haratech.at

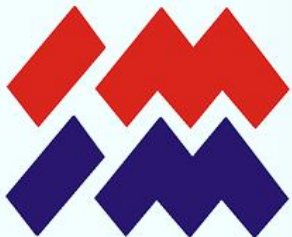




The idea

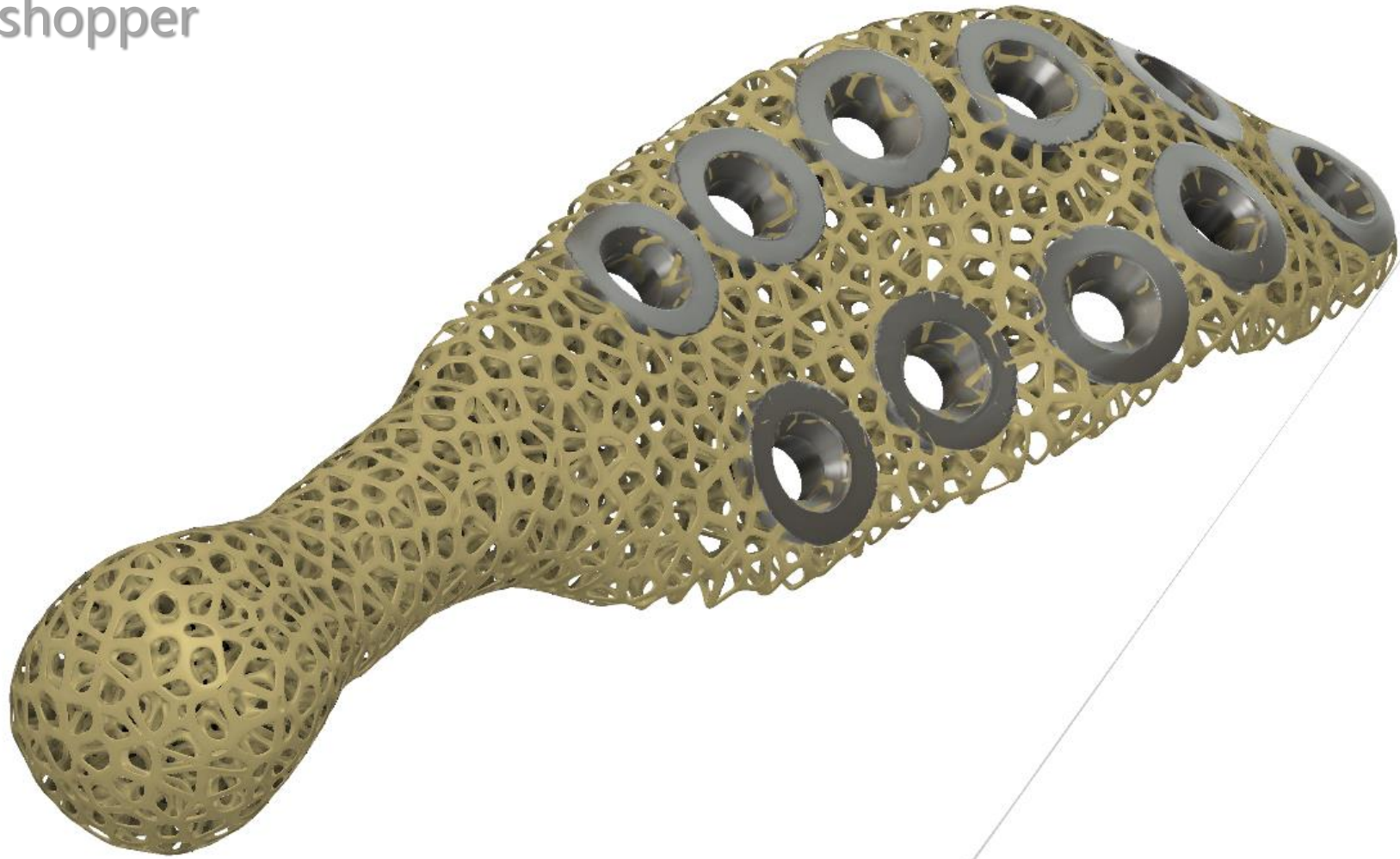
Grasshopper

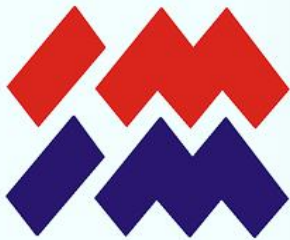




The idea

Grasshopper





The idea

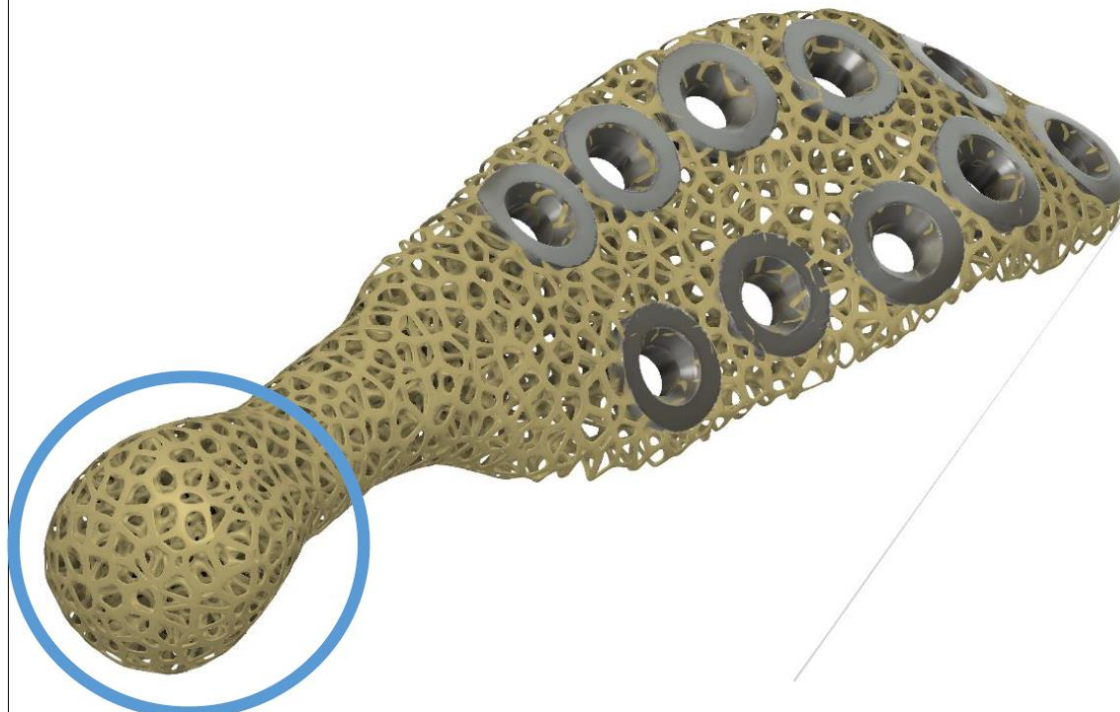
Grasshopper

Constituent materials – slender bone

The ball joint (blue circle on the next image) shall be made of ceramics.

The rest of the implant should be composed of (sorted by decreasing priority):

1. Non-resorbable polymer only
1. Titanium alloy only (equal priority)
2. A titanium alloy core (incl. the screw threads), incased in non-resorbable polymer
3. A resorbable polymer core, incased in titanium alloy (incl. the screw threads)
4. One half made of titanium alloy (on the exterior side) and one half made of resorbable/non-resorbable polymer (on the interior side)

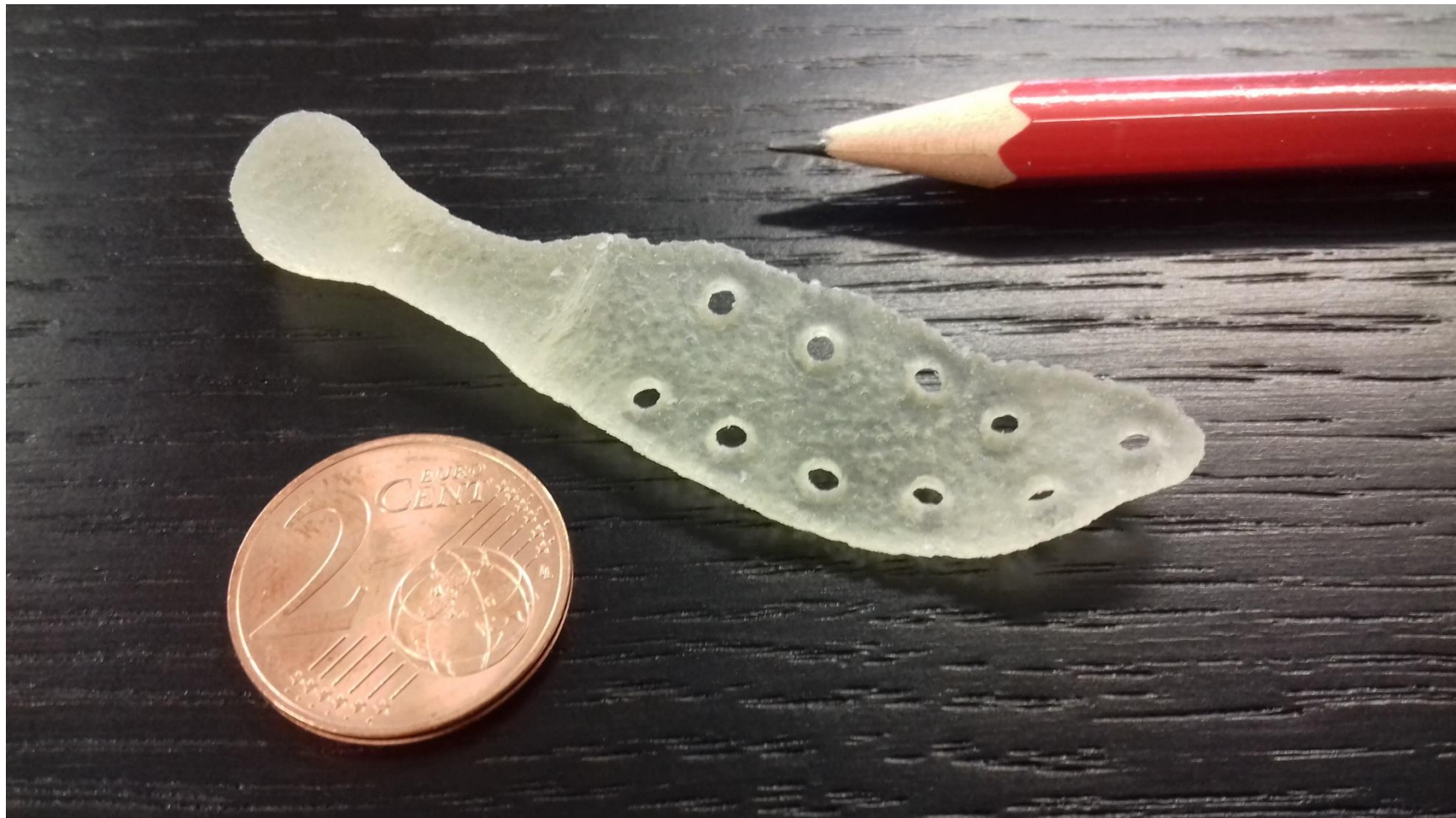


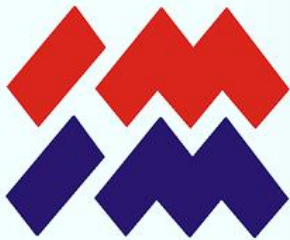


The idea

Grasshopper

Quick print trial with a Objet Eden 350V
Half scale!

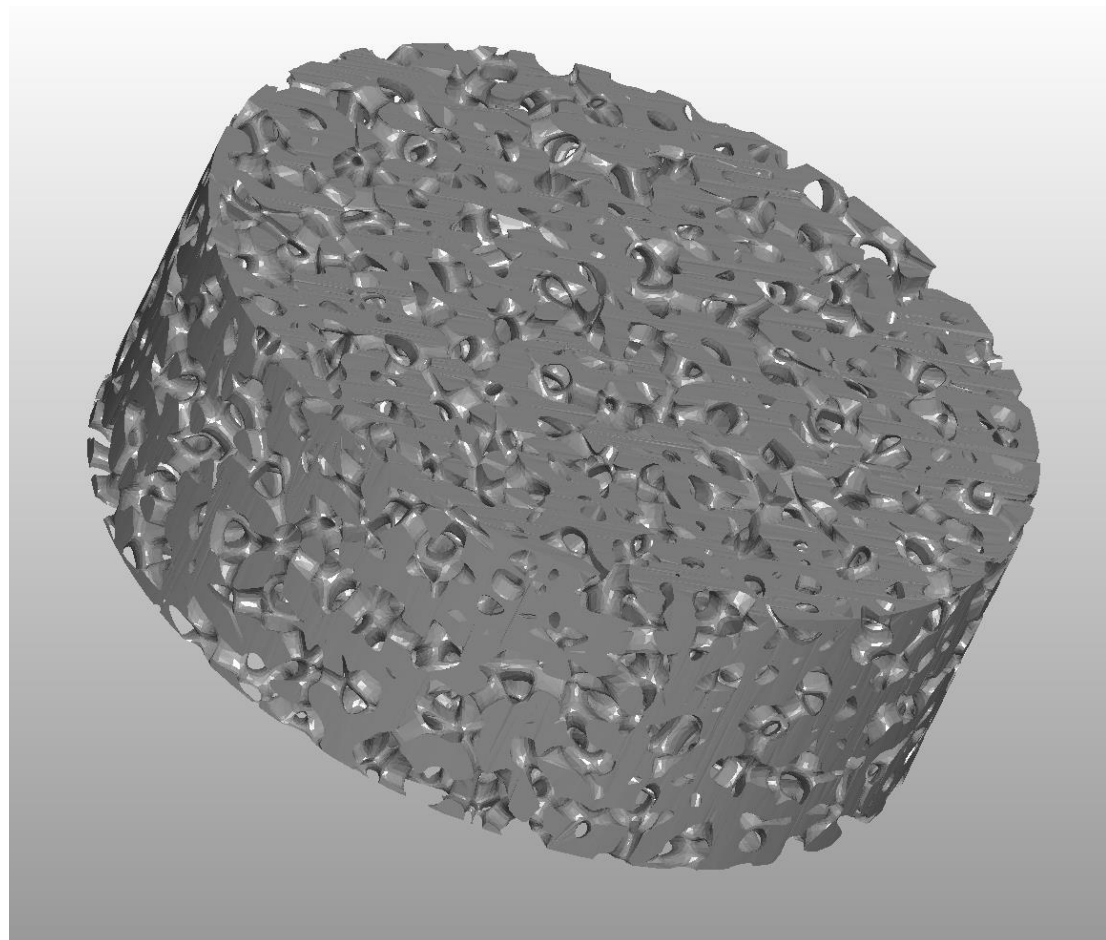




The idea

Grasshopper

Sample stl-file: diameter 13.7mm, height 5mm, main pore diameter 1mm



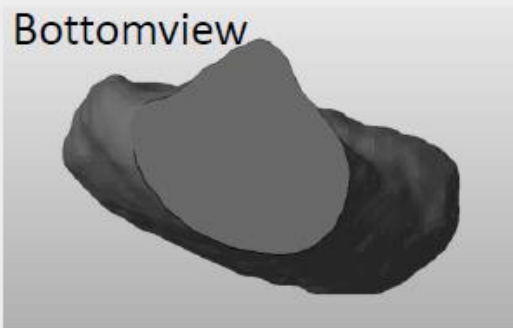


Case 1

CASE 01 MANDIBULA

LITHOZ

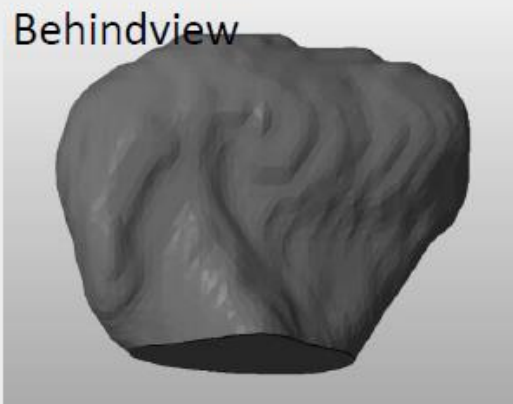
Bottomview



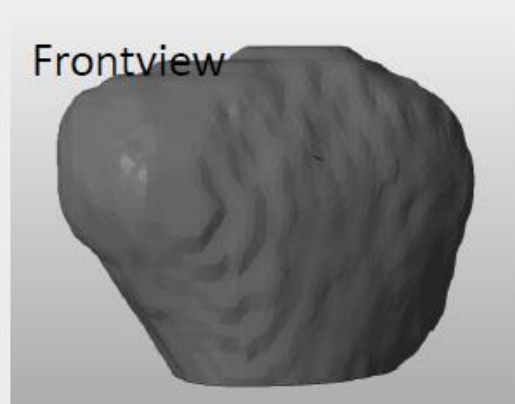
Topview



Behindview



Frontview



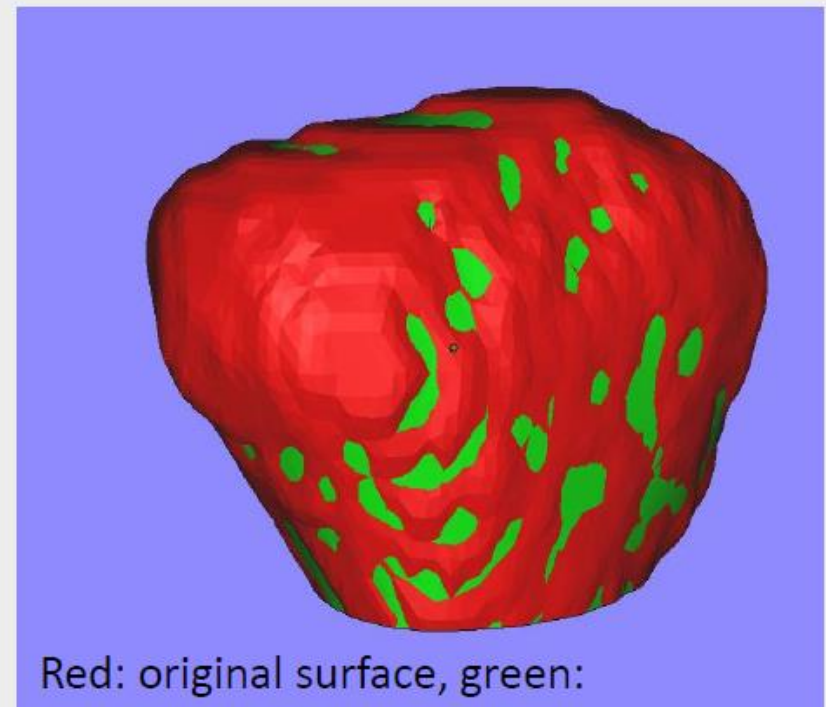
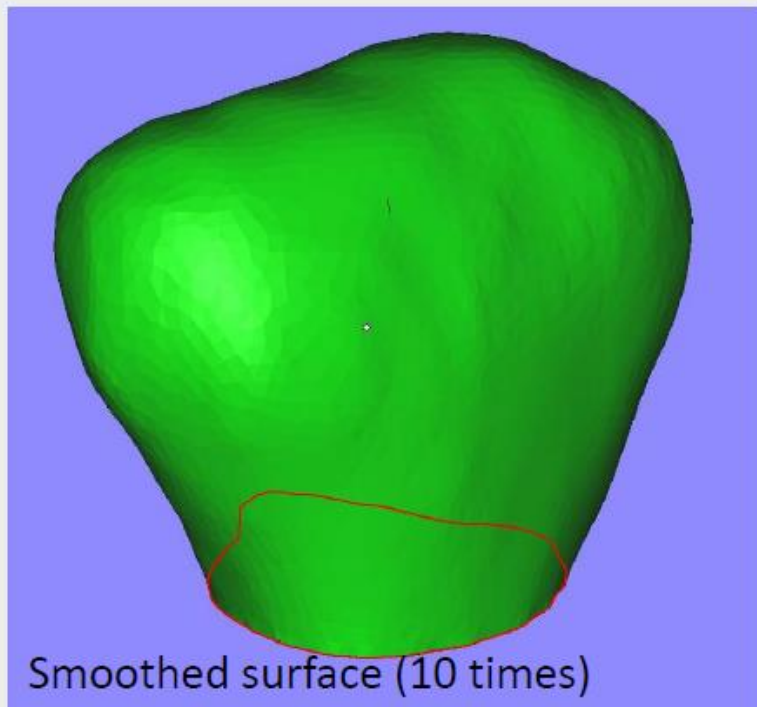


Case 1

Mandibula

Smoothening

LITHOZ



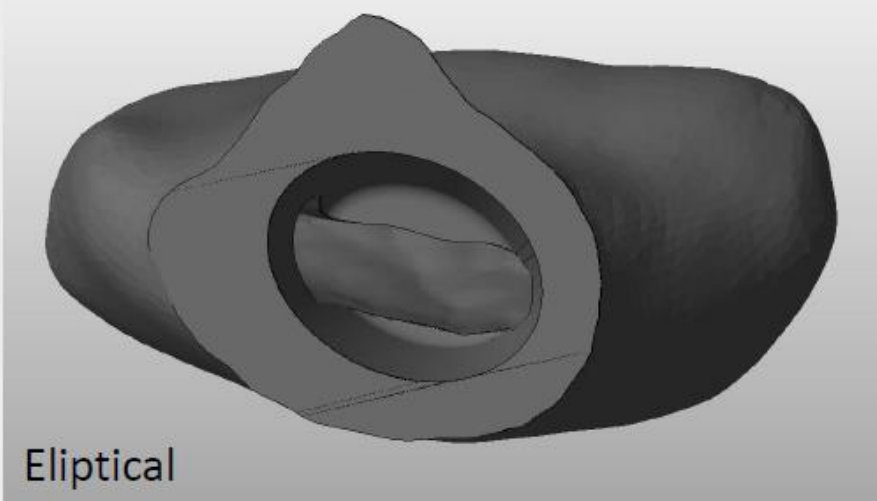


Case 1

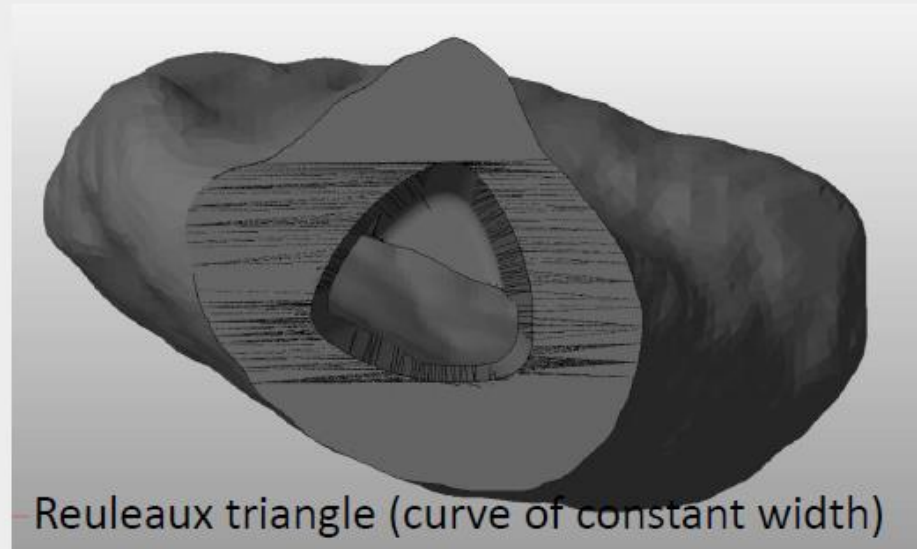
Mandibula

Connections – 2 options

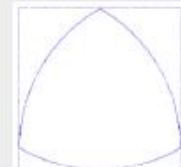
LITHOZ



Elliptical



Reuleaux triangle (curve of constant width)



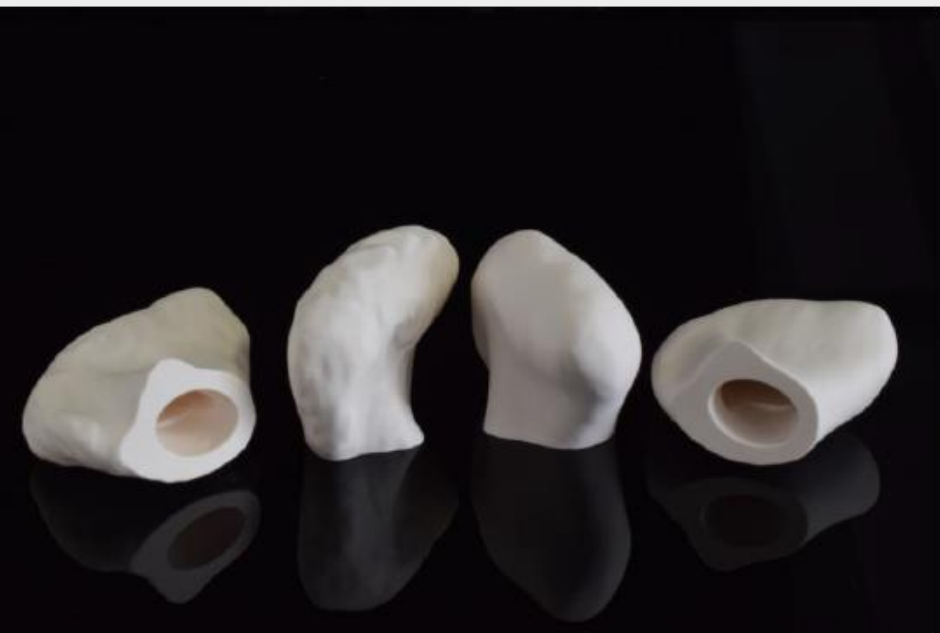


Case 1

Mandibula

Pictures of green parts

LITHOZ



Overview



Surface comparison



Case 1

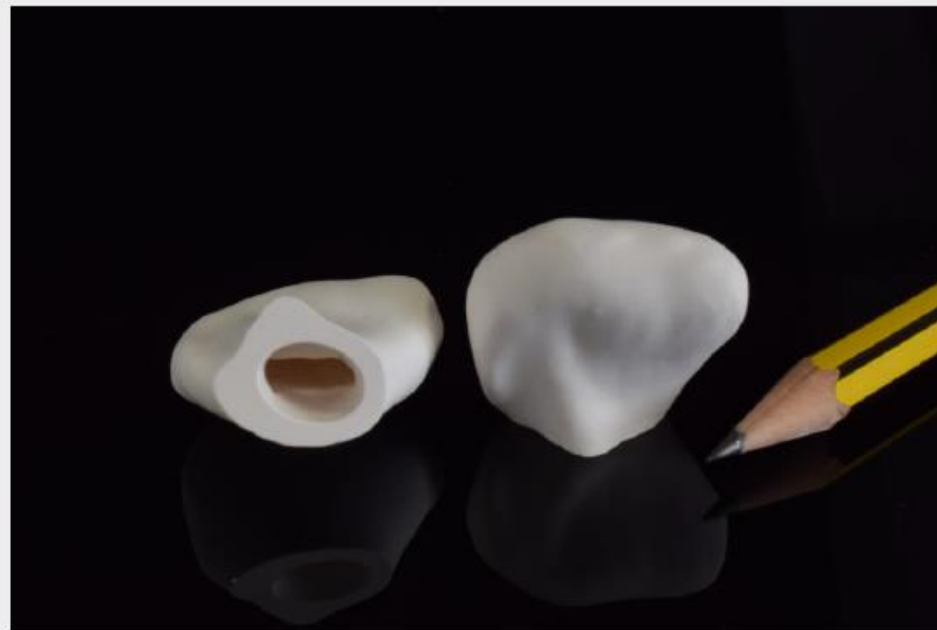
Mandibula

Photos - connections

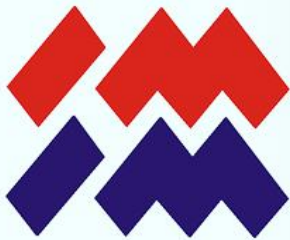
LITHOZ



Original surface – elliptic connection



Smoothened surface – elliptic connection



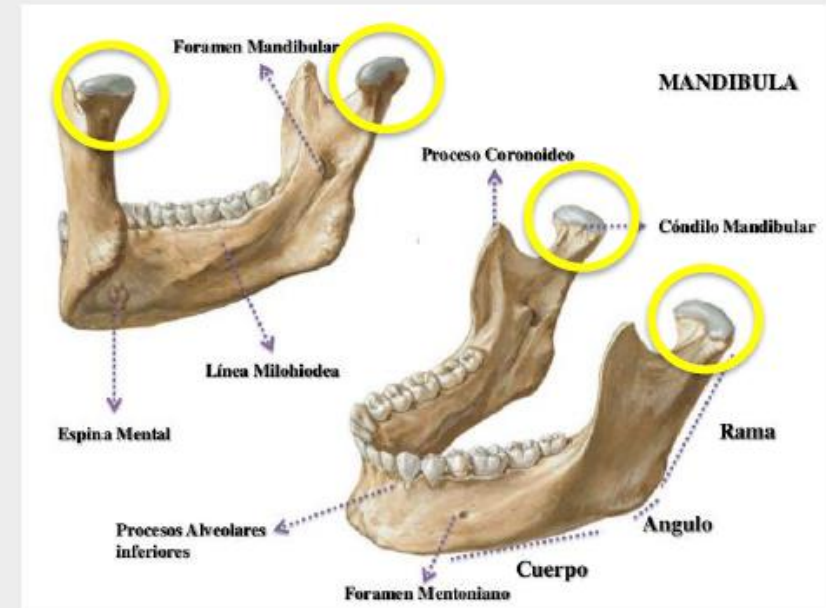
Case 1

Mandibula

Articulating surfaces

LITHOZ

How to determine the roughness?





Case 1

MECHANICAL DISCONNECTION OF THE TITANIUM-CERAMIC PARTS

- The titanium shank was patterned with an oval shaped seat of two fit types:
fine fit – T-C/5,68,
clearance fit – T-C/6,17.
- Dental quick-setting phosphate cement Agatos S was purchased on this purpose.

Sample name	Maximum force [N]	
	smooth	groove 0,5
T-C/5,68/1	444	601
T-C/5,68/2	442	790
T-C/6,17/1	692	537
T-C/6,17/2	443	637

SAMPLES AFTER THE TEST

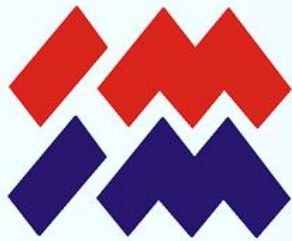


smooth

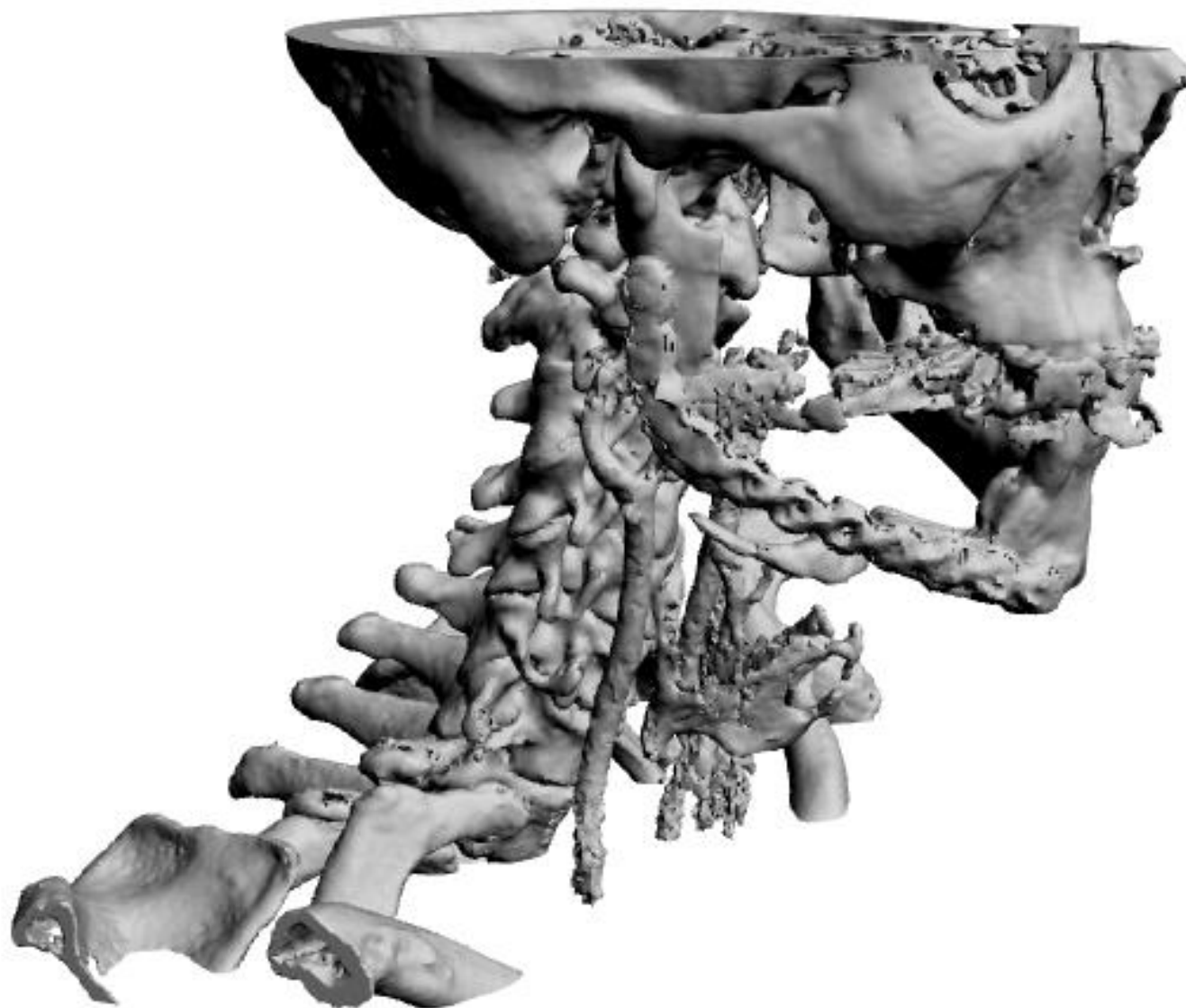


groove





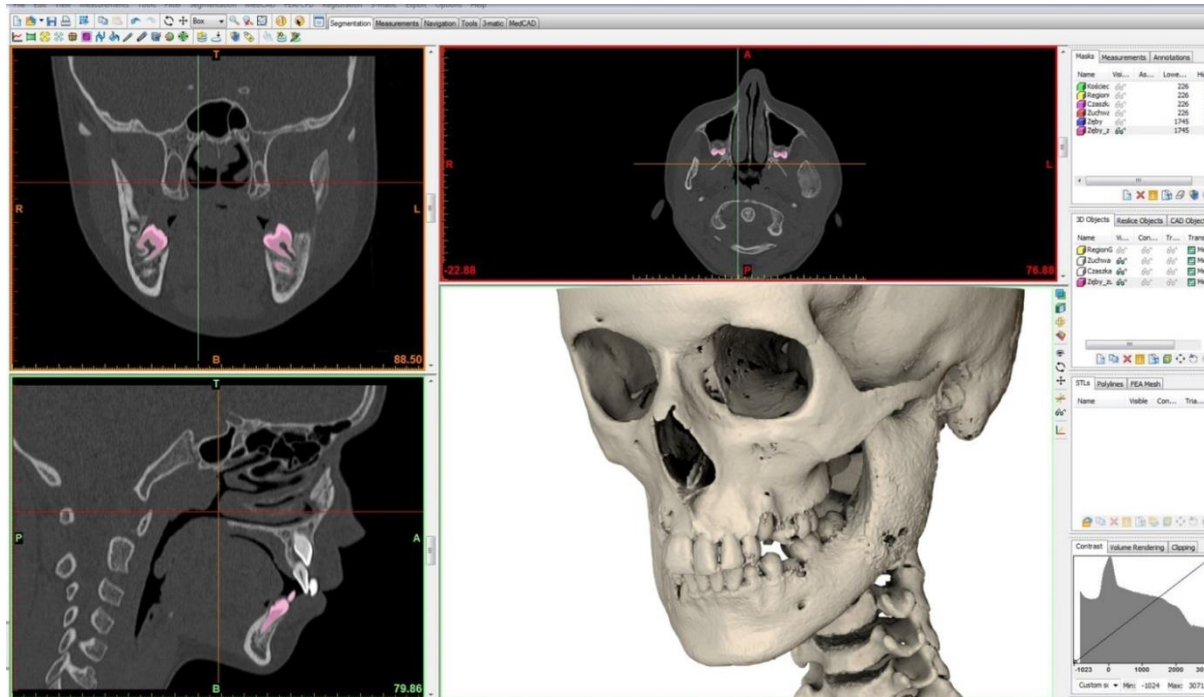
Case 2



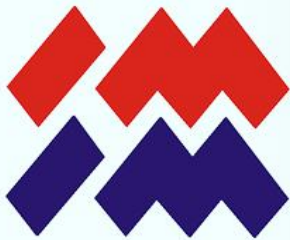


State of the art

CT image transformation

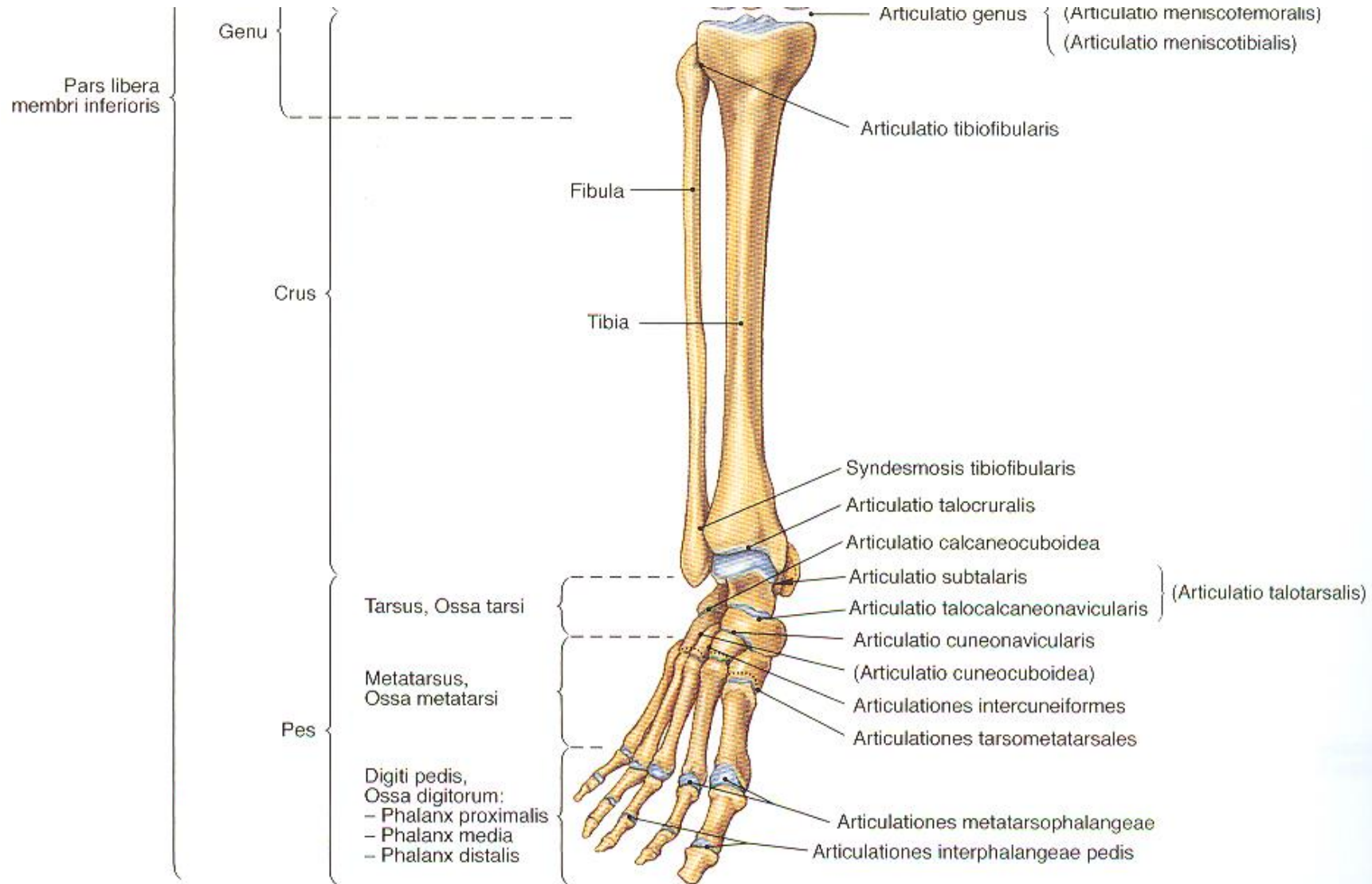


The first work on the development of procedures for the removal of neoplastic hard tissues and adjustment of the desired shape of the jaw and mandible bones based on healthy, undamaged bones ("Side mirroring", the position of the teeth on the opposite side to the removed tissue) and face features were also carried out:



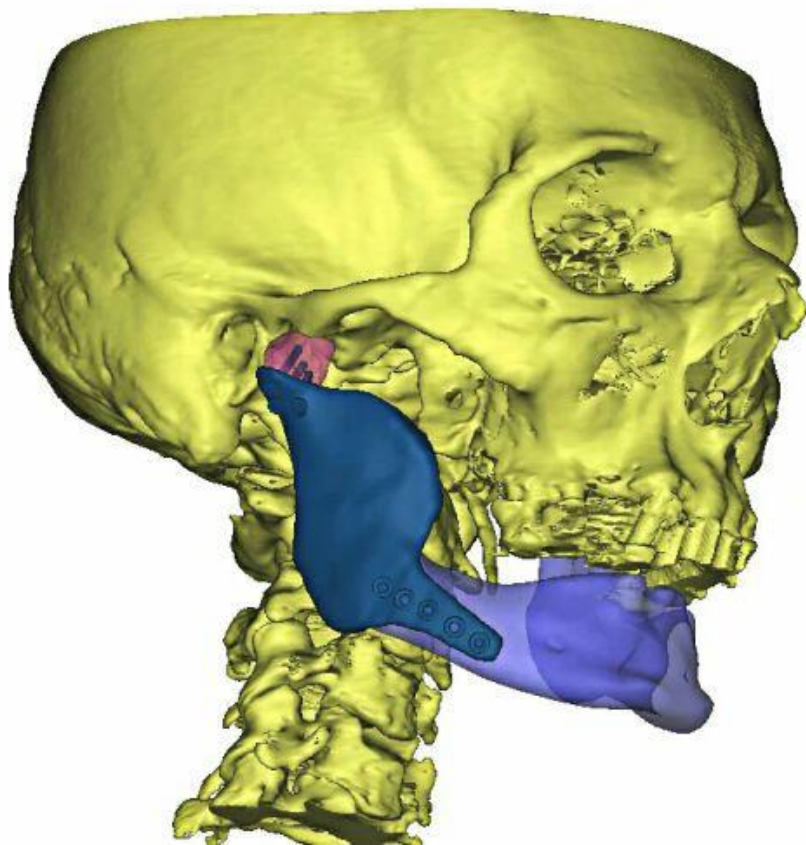
State of the art

(membrum inferius)



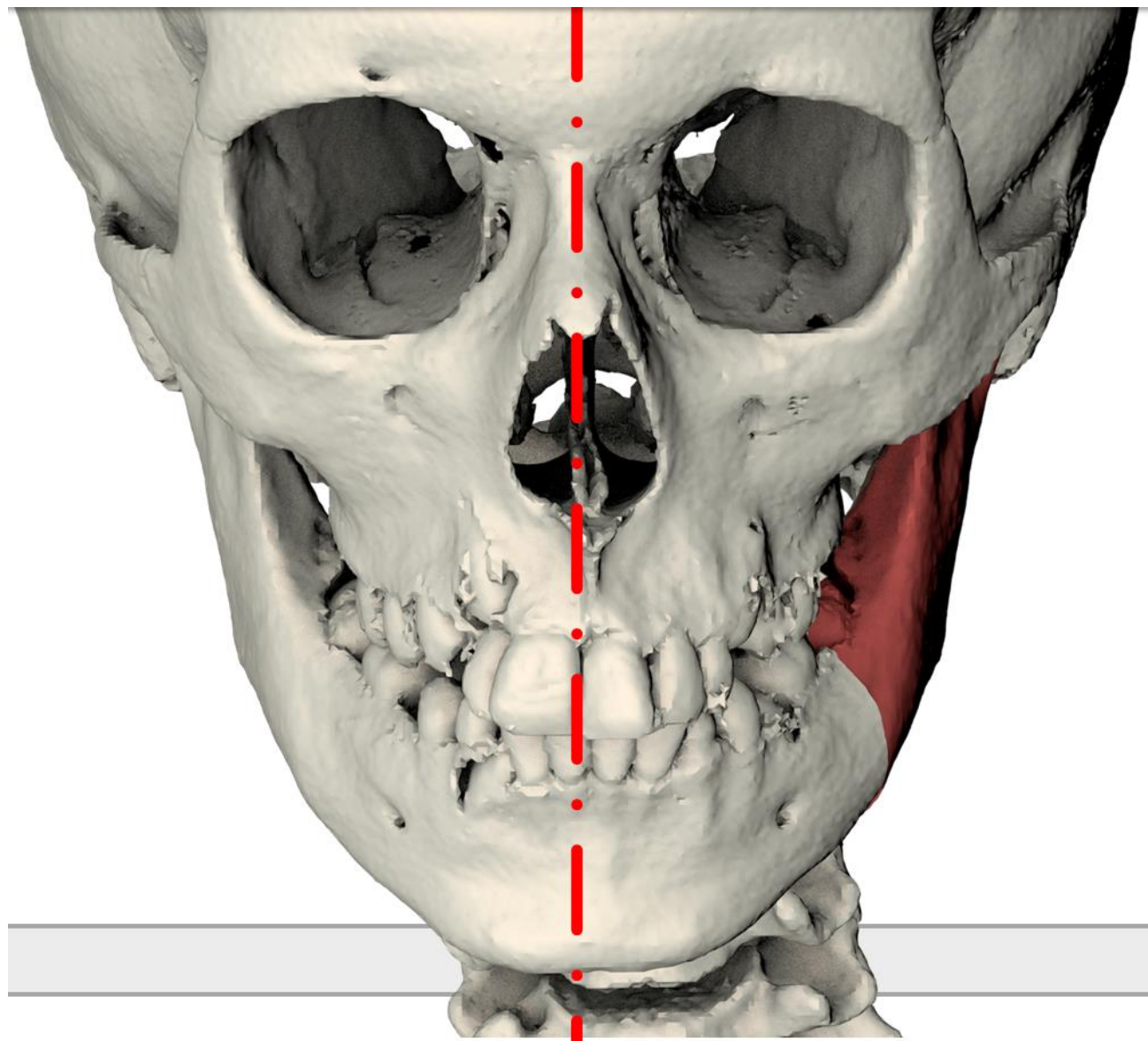


State of the art





CT image transformation: side mirroring



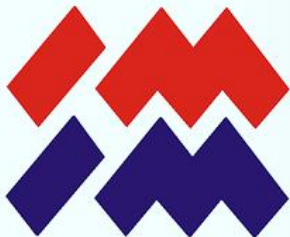
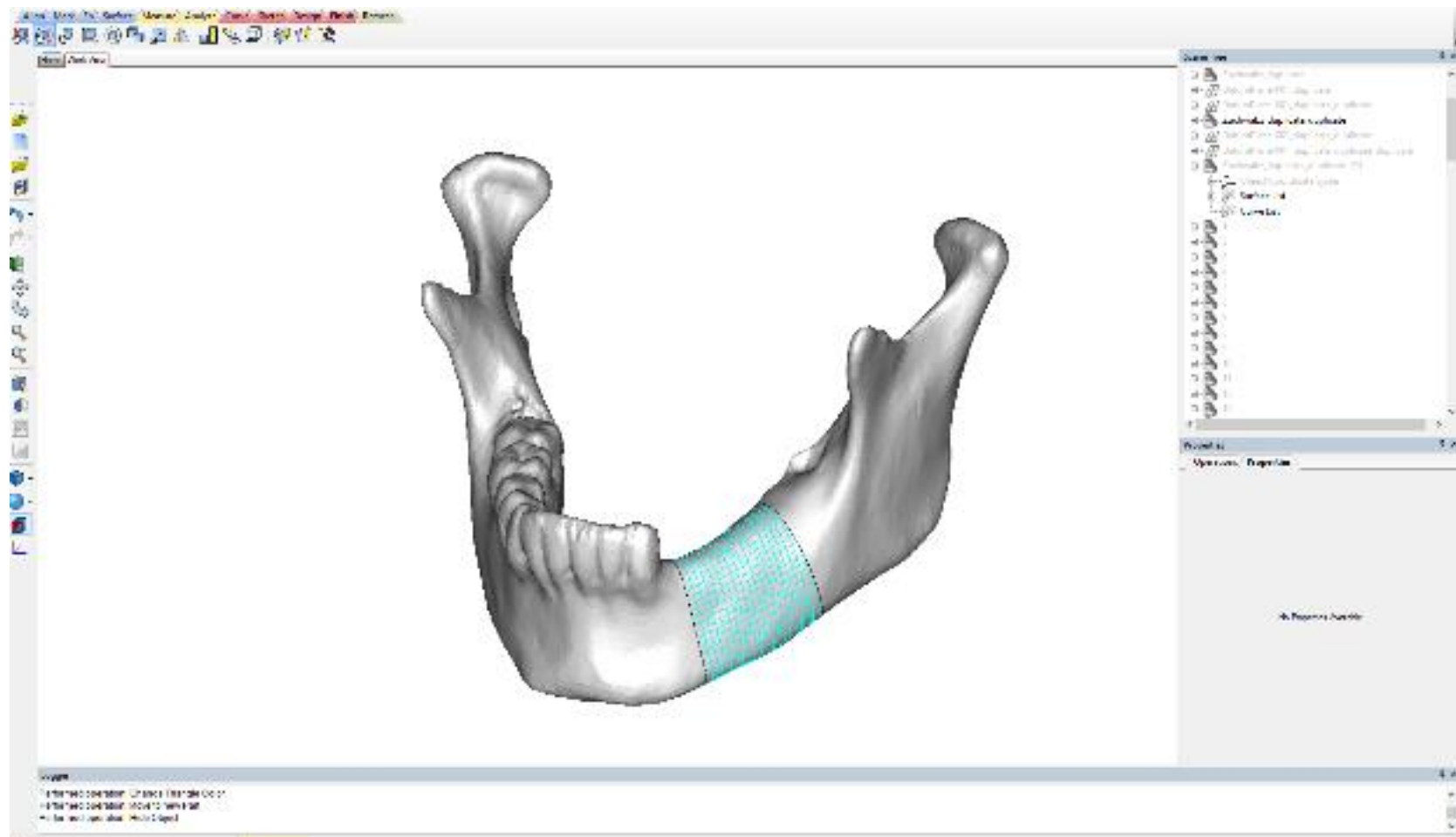


Image transformation: side mirroring

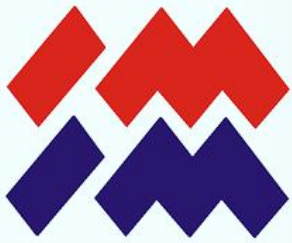
The bone of the mandible was isolated from the obtained skull bone model. It is on the prepared model that marks the section of bone that has been replaced with an implant made of titanium alloy.





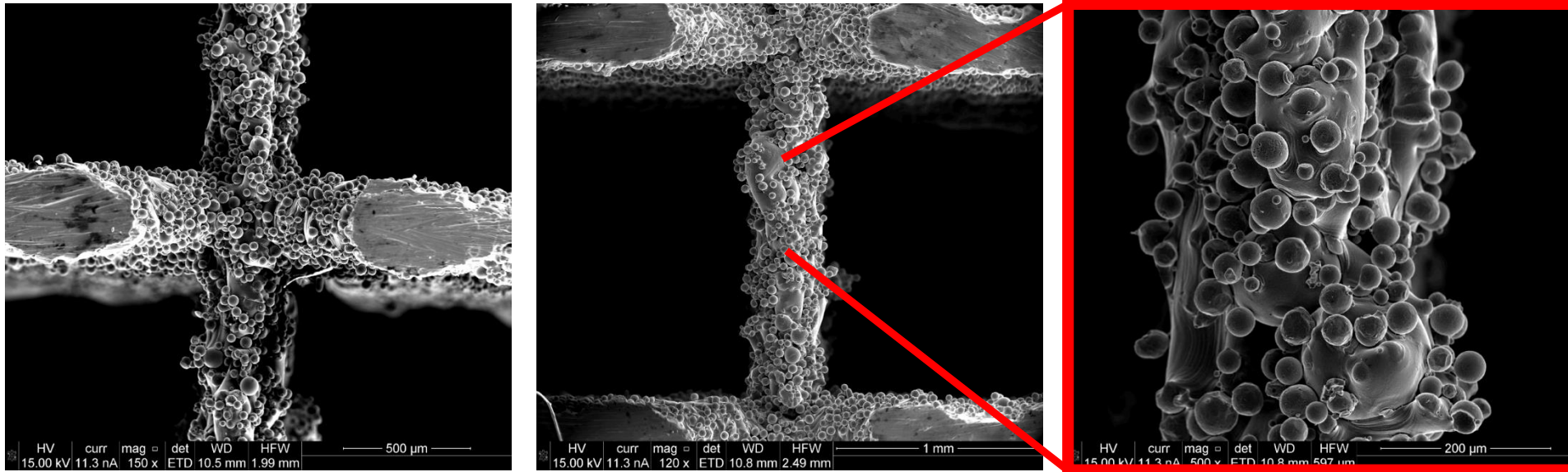
Final design

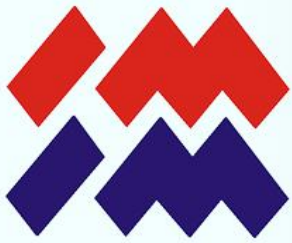




Template designs of maxillofacial implants and requirements of surgical instruments

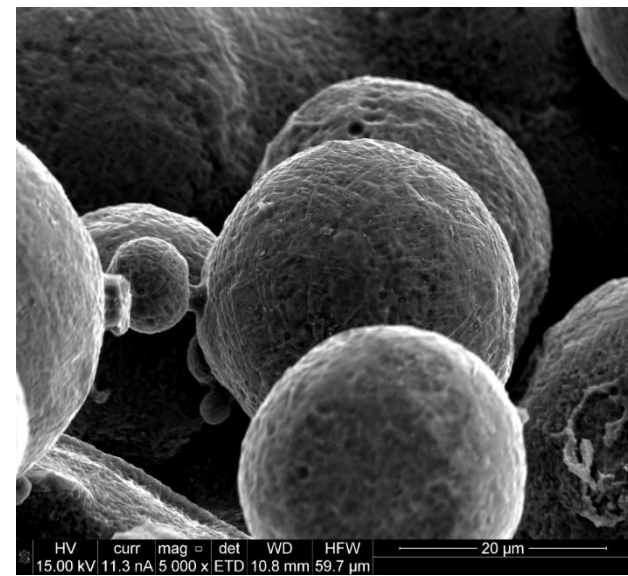
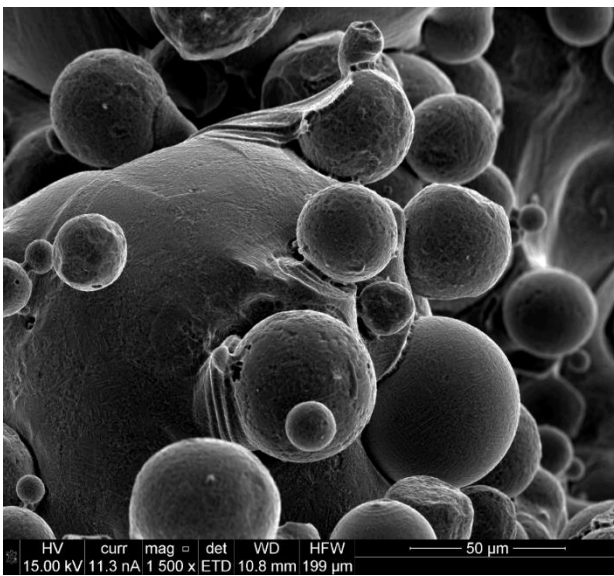
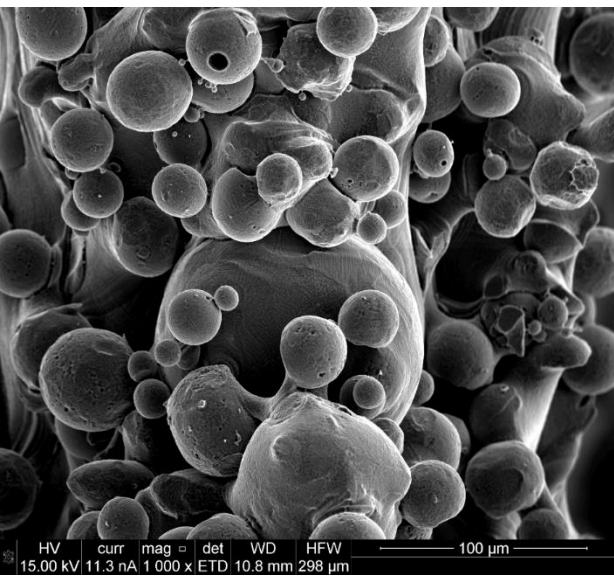
Scanning Electron Microscopy

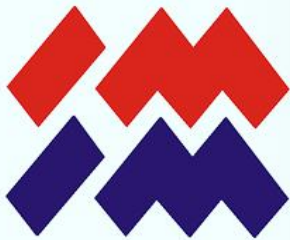




Template designs of maxillofacial implants and requirements of surgical instruments

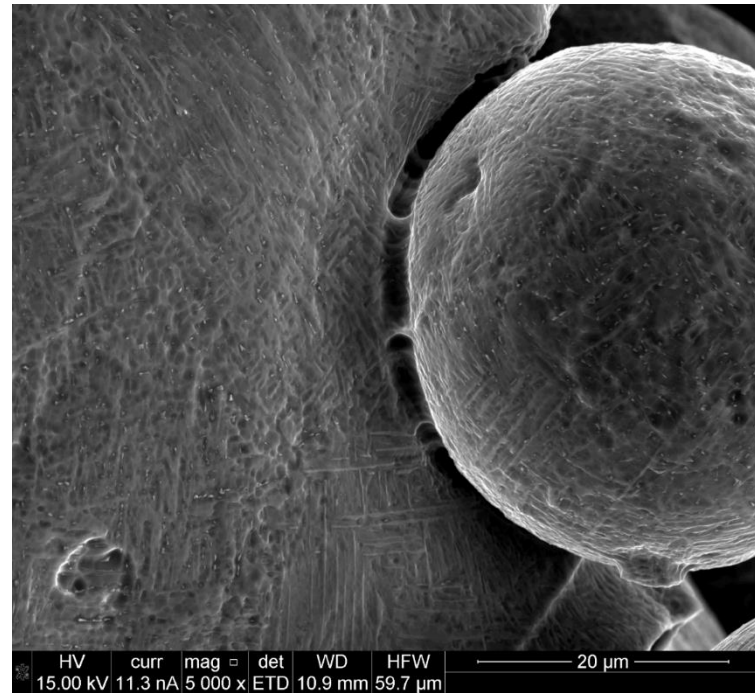
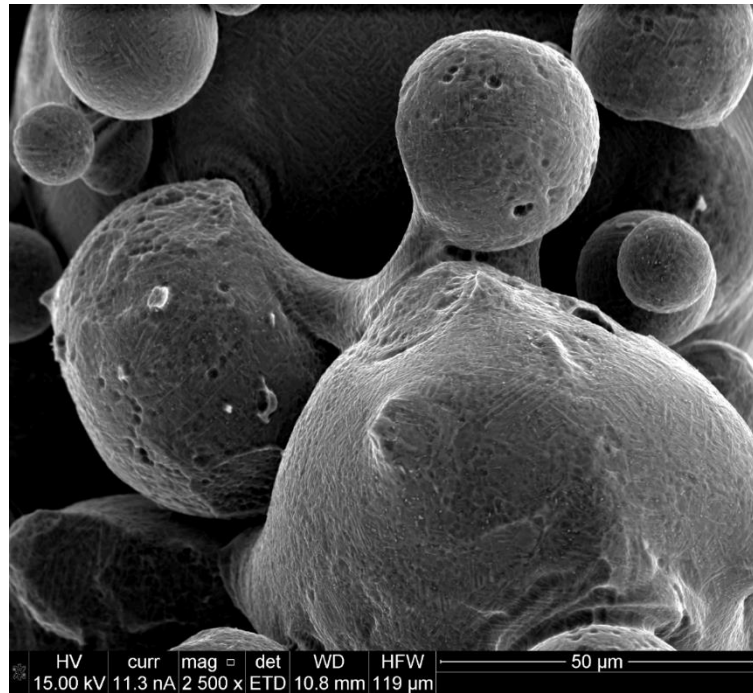
Scanning Electron Microscopy





Template designs of maxillofacial implants and requirements of surgical instruments

Scanning Electron Microscopy

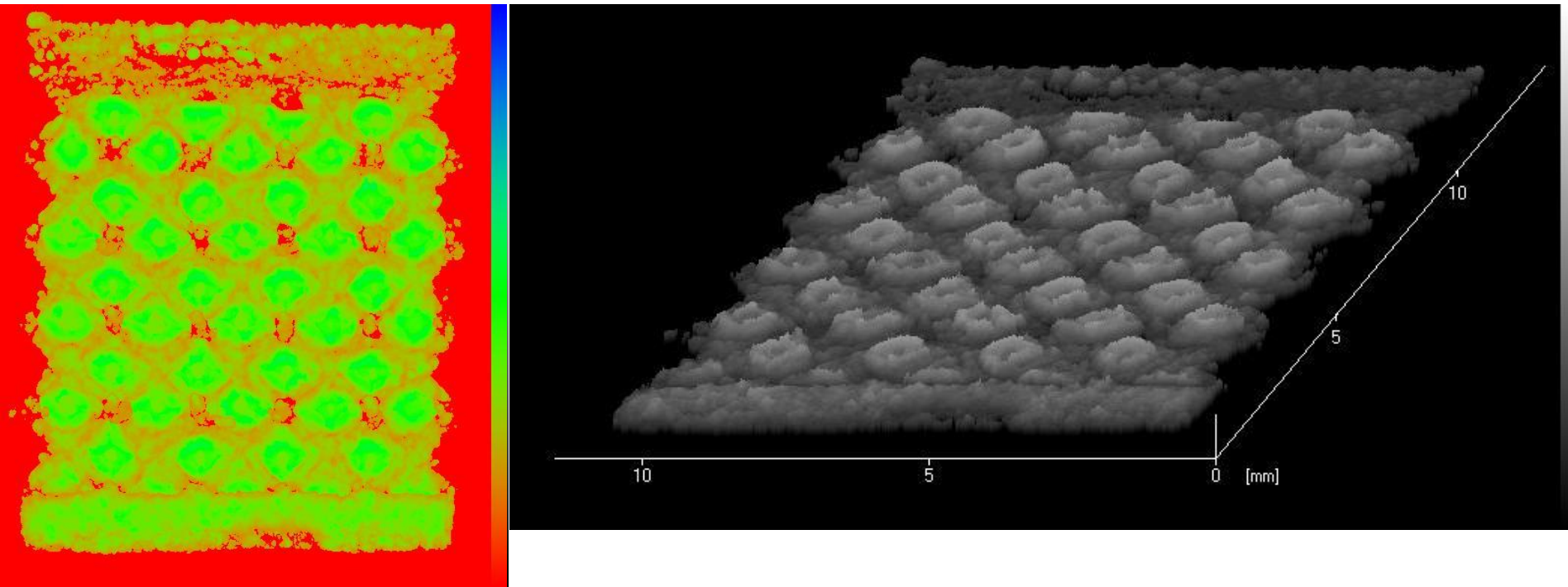


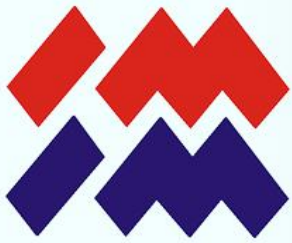


Template designs of maxillofacial implants and requirements of surgical instruments

Scanning Acoustic Microscopy

Mesh 2.0 not deformed

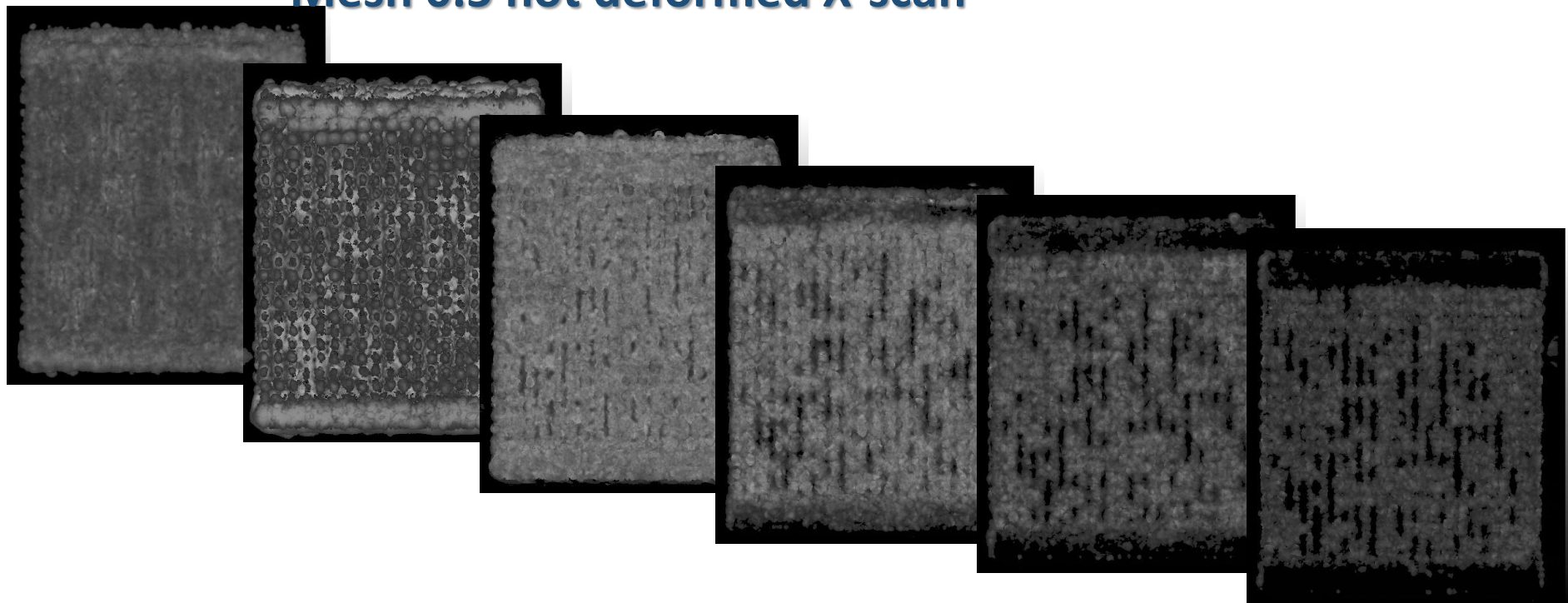


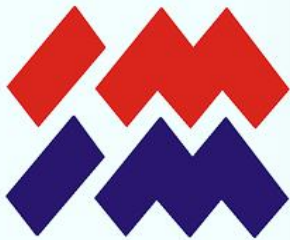


Template designs of maxillofacial implants and requirements of surgical instruments

Scanning Acoustic Microscopy

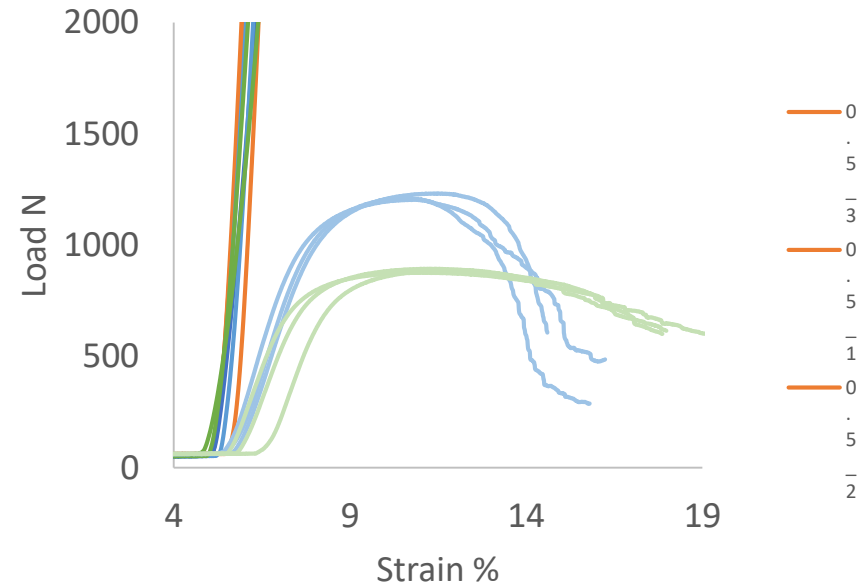
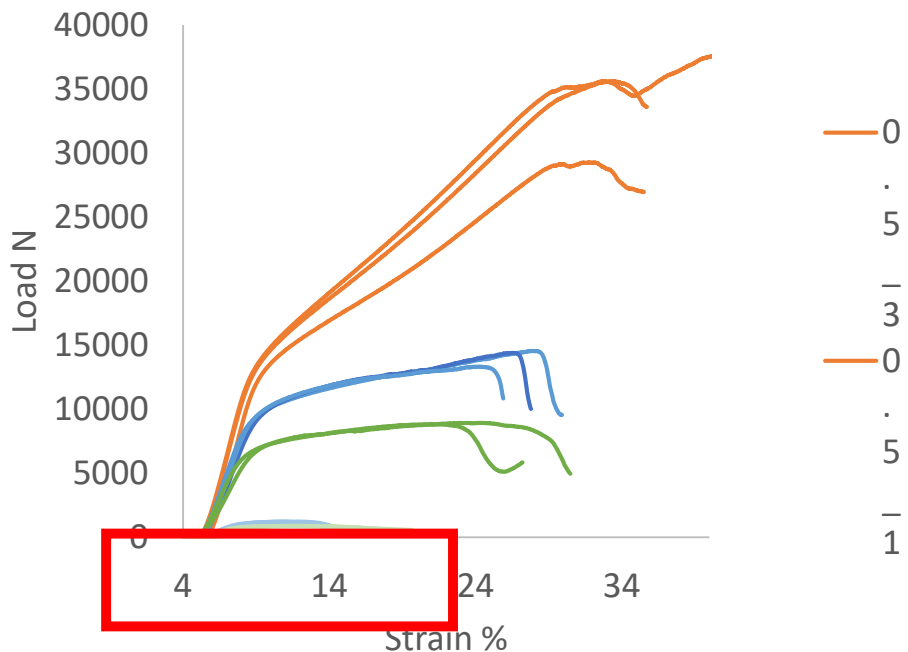
Mesh 0.5 not deformed X-scan

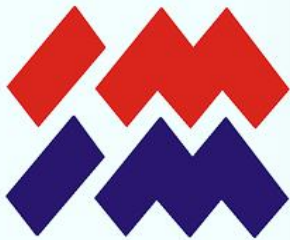




Template designs of maxillofacial implants and requirements of surgical instruments

Tensile Test

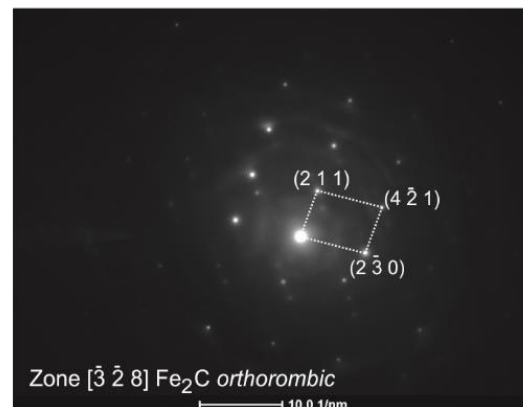
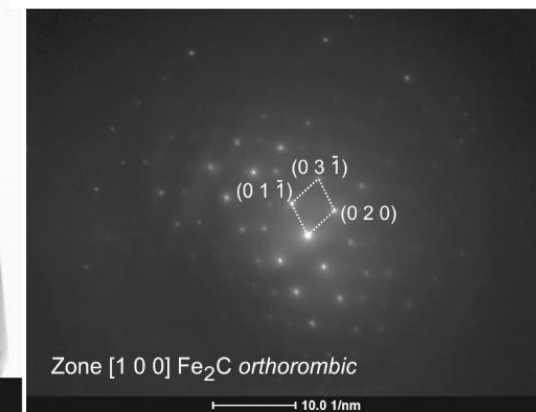
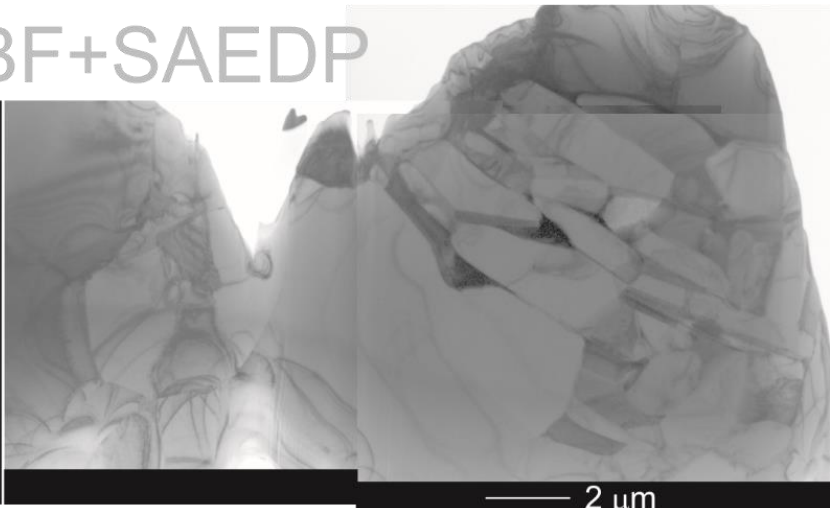
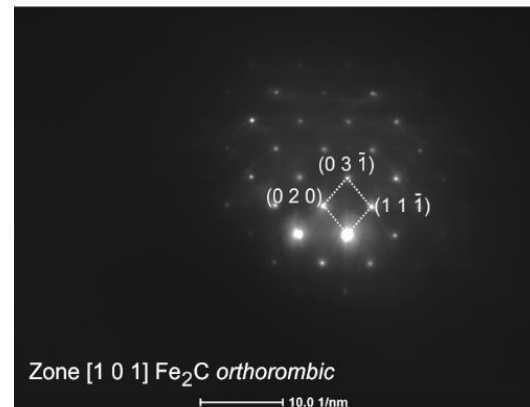


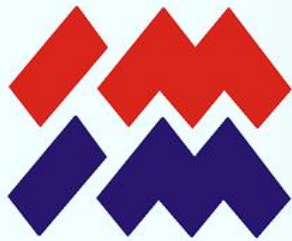


Template designs of maxillofacial implants and requirements of surgical instruments

Transmission Electron Microscopy

TEM BF+SAEDP

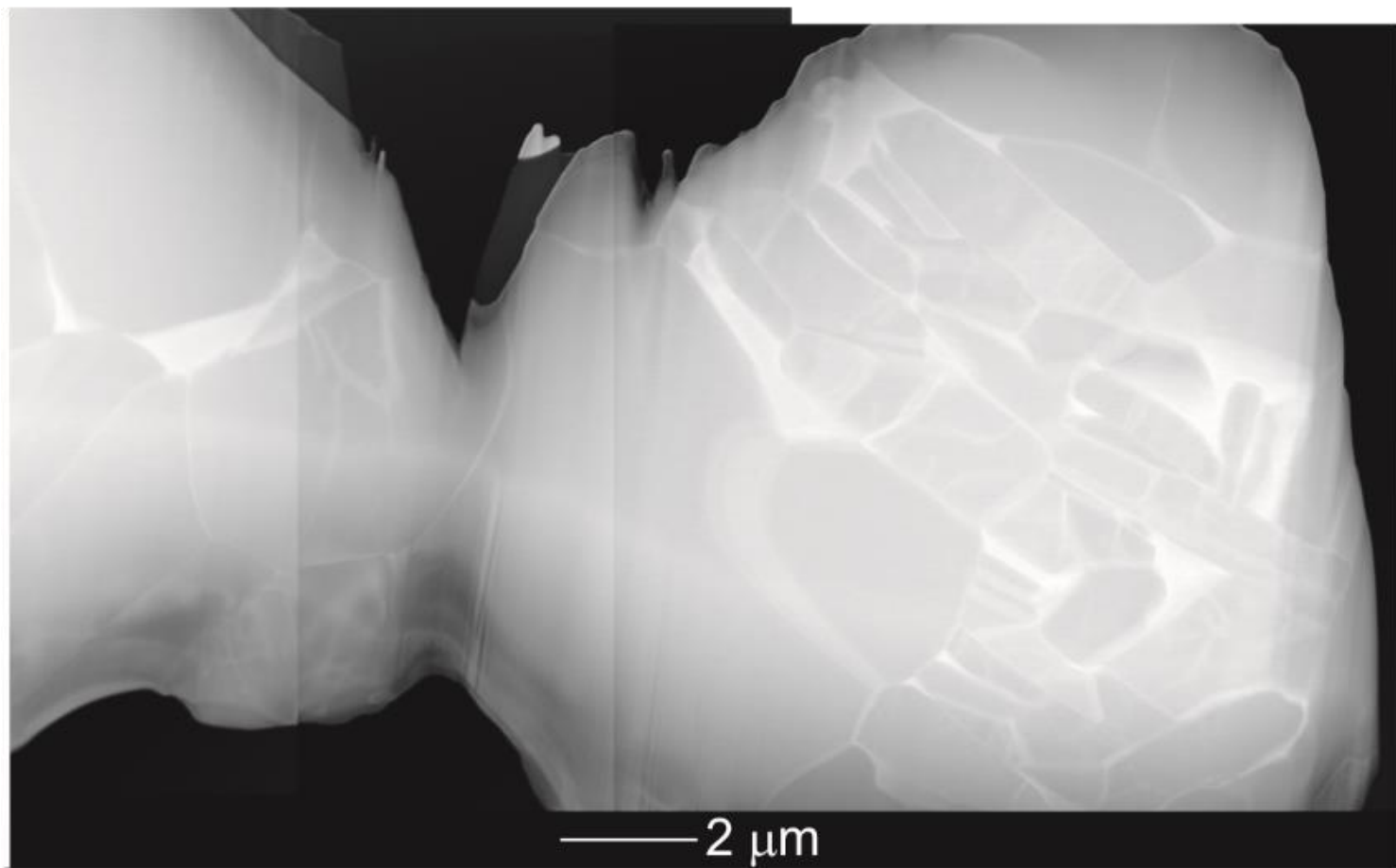


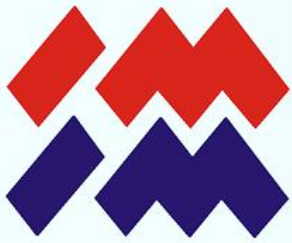


Template designs of maxillofacial implants and requirements of surgical instruments

Transmission Electron Microscopy

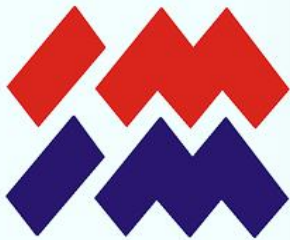
STEM





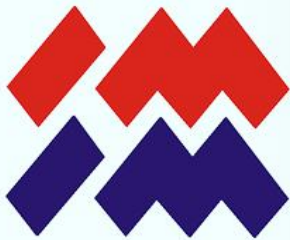
Bacteriology

**Pseudomonas aeruginosa;
Streptococci; Candida albicans**



Bacteriology

1. The examined biomaterials were incubated respectively: "cubes" 15 ml 24-hour cultures of Pseudomonas aeruginosa, Streptococcus pyogenes, Candida albicans and "circles" 4 ml 24-hour culture of Pseudomonas aeruginosa, Streptococcus pyogenes, Candida albicans.
2. Before the incubation with biomaterials for all cultures of microorganisms, the optical density (OD) at 600 nm was determined.
3. After 24 and 48 hours, the OD was measured again at 600 nm.
4. Subsequently, the biomaterials were rinsed with a 3.5% paraformaldehyde aqueous solution.
5. Conclusions: in all examined cultures with biomaterial the OD value increased, which may indicate the growth of microorganisms and indirectly testify to the fact that the biomaterial does not have bactericidal properties.



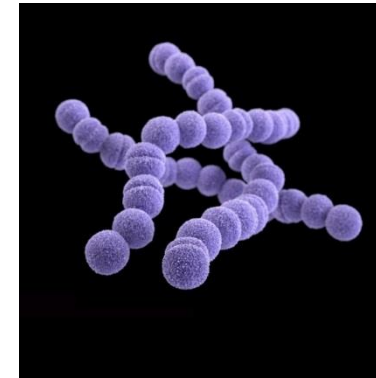
Bacteriology



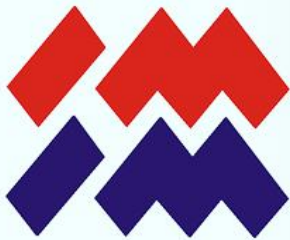
Pseudomonas aeruginosa is a common Gram-negative, rod-shaped bacterium that can cause disease in plants and animals, including humans. A species of considerable medical importance, *P. aeruginosa* is a multidrug resistant pathogen recognized for its ubiquity, its intrinsically advanced antibiotic resistance mechanisms, and its association with serious illnesses – hospital-acquired infections such as ventilator-associated pneumonia and various sepsis syndromes.

The organism is considered opportunistic insofar as serious infection often occurs during existing diseases or conditions – most notably cystic fibrosis and traumatic burns. It is also found generally in the immunocompromised but can infect the immunocompetent as in hot tub folliculitis. Treatment of *P. aeruginosa* infections can be difficult due to its natural resistance to antibiotics. When more advanced antibiotic drug regimens are needed adverse effects may result.

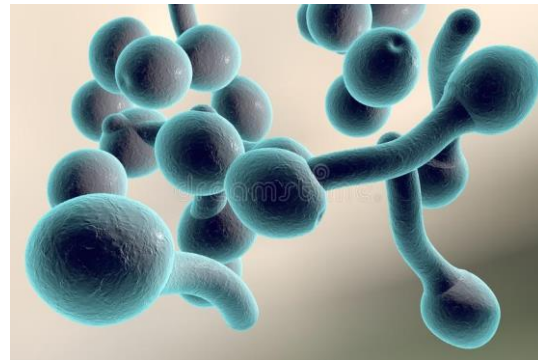
It is citrate, catalase, and oxidase positive. It is found in soil, water, skin flora, and most man-made environments throughout the world. It thrives not only in normal atmospheres, but also in low-oxygen atmospheres, thus has colonized many natural and artificial environments. It uses a wide range of organic material for food; in animals, its versatility enables the organism to infect damaged tissues or those with reduced immunity. The symptoms of such infections are generalized inflammation and sepsis. If such colonizations occur in critical body organs, such as the lungs, the urinary tract, and kidneys, the results can be fatal.^[1] Because it thrives on moist surfaces, this bacterium is also found on and in medical equipment, including catheters, causing cross-infections in hospitals and clinics. It is also able to decompose hydrocarbons and has been used to break down tarballs and oil from oil spills.^[2] *P. aeruginosa* is not extremely virulent in comparison with other major pathogenic bacterial species – for example *Staphylococcus aureus* and *Streptococcus pyogenes* – though *P. aeruginosa* is capable of extensive colonization, and can aggregate into enduring biofilms.^[3]



Streptococci and staphylococci constitute the main groups of medically important gram-positive cocci. Streptococci are gram-positive, nonmotile, and catalase negative. Clinically important genera include *Streptococcus* and *Enterococcus*. They are ovoid to spherical in shape and occur as pairs or chains. Most are aerotolerant anaerobes because they grow fermentatively even in the presence of oxygen. Because of their complex nutritional requirements, blood enriched medium is generally used for their isolation. Diseases caused by this group of organisms include acute infections of the throat and skin caused by group A streptococci (*Streptococcus pyogenes*); female genital tract colonization, resulting in neonatal sepsis caused by group B streptococci (*Streptococcus agalactiae*); pneumonia, otitis media, and meningitis caused by *Streptococcus pneumoniae*; and endocarditis caused by the viridans group of streptococci.

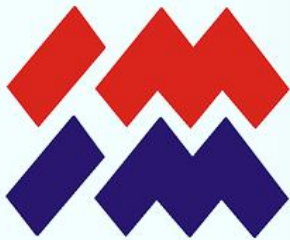


Bacteriology



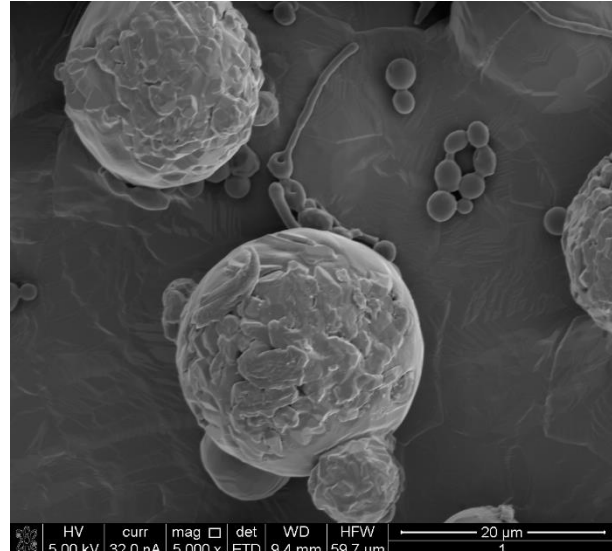
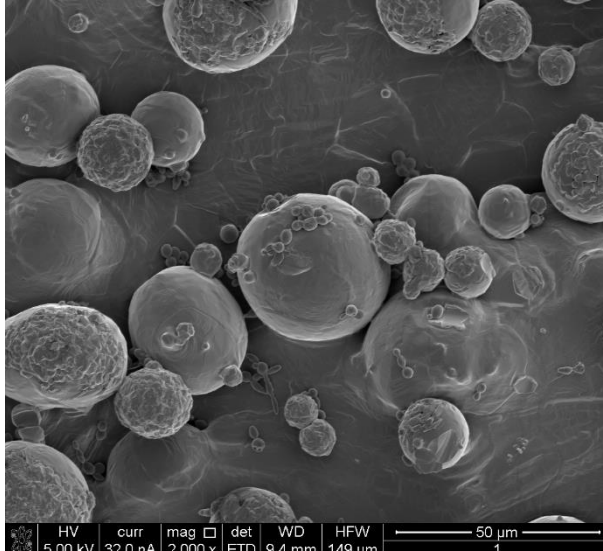
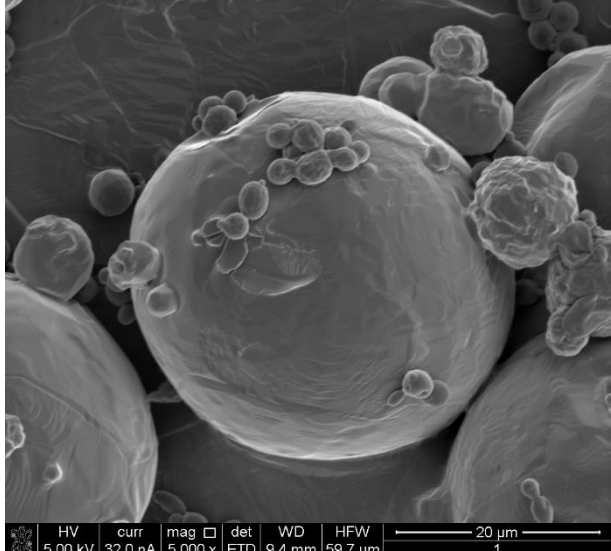
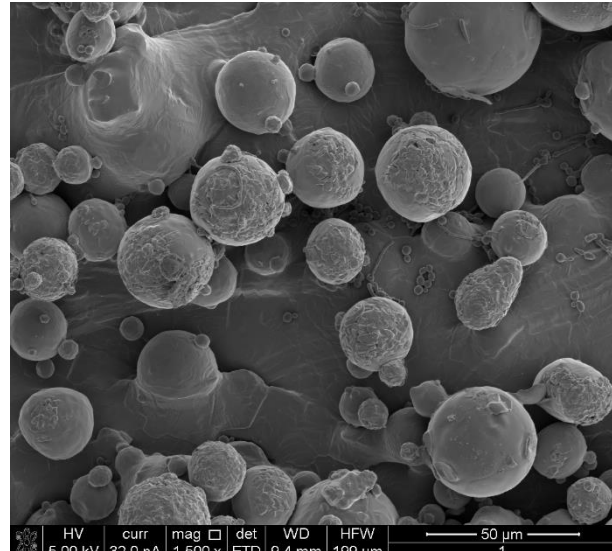
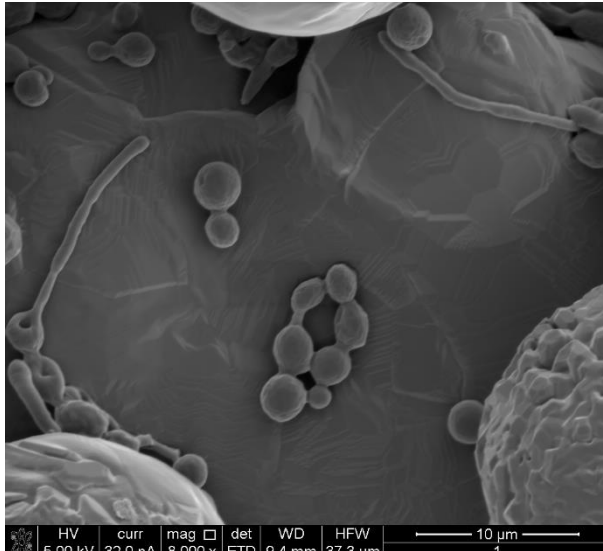
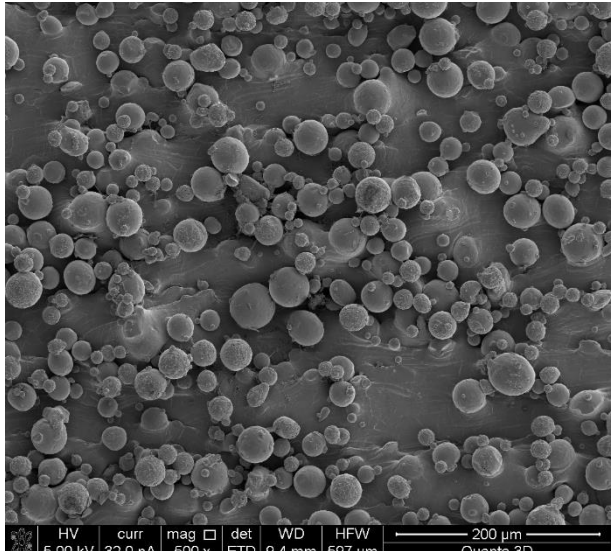
Candida albicans is an opportunistic pathogenic yeast[4] that is a common member of the human gut flora. It does not proliferate outside the human body.[5] It is detected in the gastrointestinal tract and mouth in 40–60% of healthy adults.[6][7] It is usually a commensal organism, but can become pathogenic in immunocompromised individuals under a variety of conditions.[7][8] It is one of the few species of the genus Candida that causes the human infection candidiasis, which results from an overgrowth of the fungus.[7][8] Candidiasis is for example often observed in HIV-infected patients.[9] C. albicans is the most common fungal species isolated from biofilms either formed on (permanent) implanted medical devices or on human tissue.[10][11] C. albicans, C. tropicalis, C. parapsilosis, and C. glabrata are together responsible for 50–90% of all cases of candidiasis in humans.[8][12][13] A mortality rate of 40% has been reported for patients with systemic candidiasis due to C. albicans.[14] By one estimate, invasive candidiasis contracted in a hospital causes 2800 to 11200 deaths yearly in the US.[15]

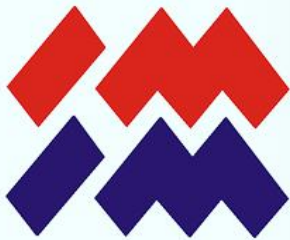
C. albicans is commonly used as a model organism for biology. It is generally referred to as a dimorphic fungus since it grows both as yeast and filamentous cells. However it has several different morphological phenotypes. C. albicans was for a long time considered an obligate diploid organism without a haploid stage. This is however not the case. Next to a haploid stage C. albicans can also exist in a tetraploid stage. The latter is formed when diploid C. albicans cells mate when they are in the opaque form.[16] The diploid genome size is approximately 29 Mb, and up to 70% of the protein coding genes have not yet been characterized.[17] C. albicans is easily cultured in the lab and can be studied both in vivo and in vitro. Depending on the media different studies can be done as the media influences the morphological state of C. albicans. A special type of medium is CHROMagar™ Candida which can be used to identify different species of candida.[18][19]



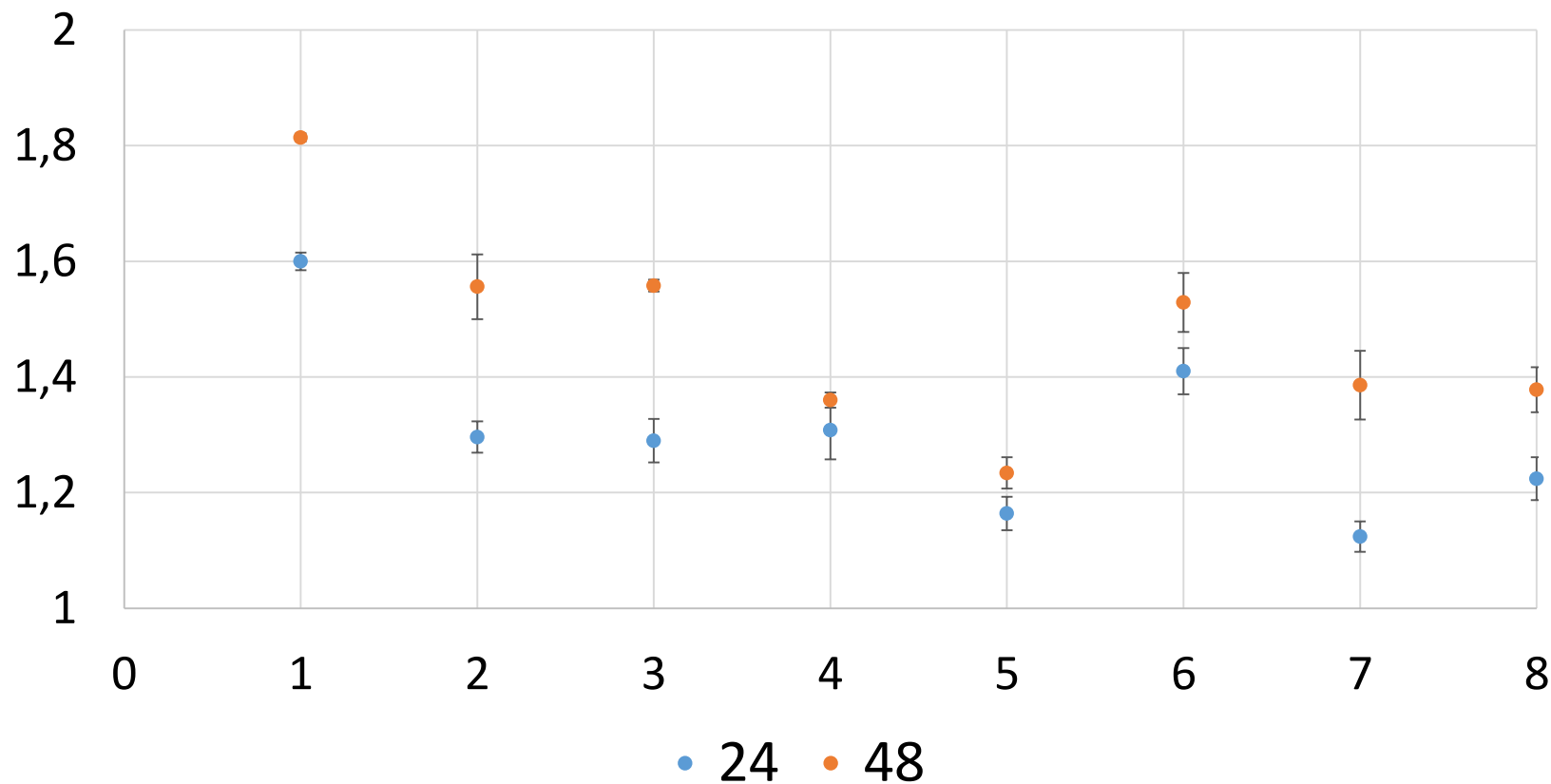
P.aeruginosa

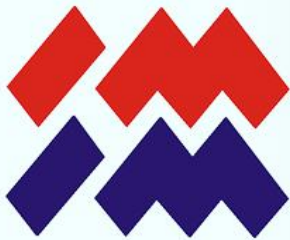
Bacteriology



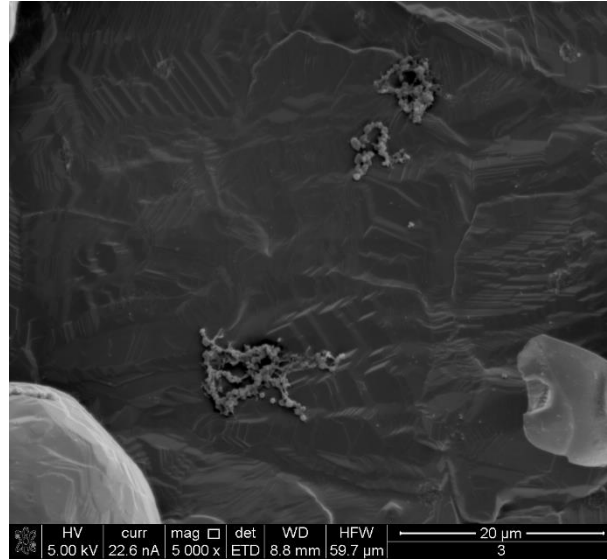
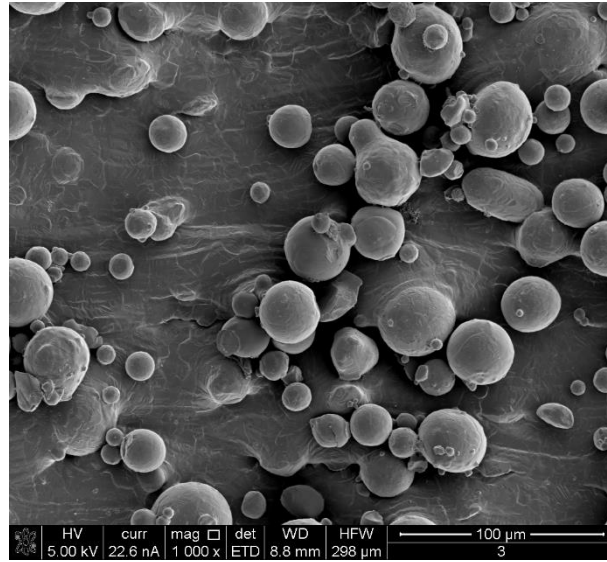
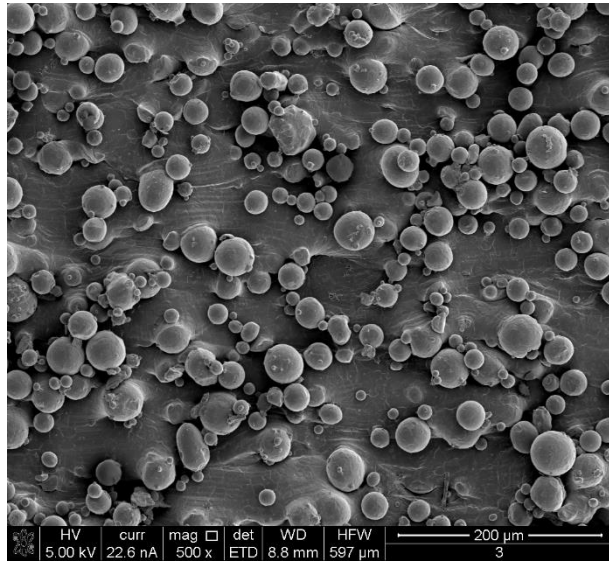
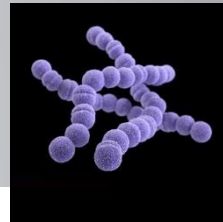


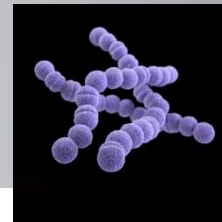
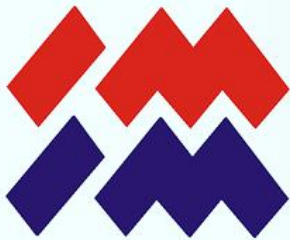
Pseudomonas aureginosa



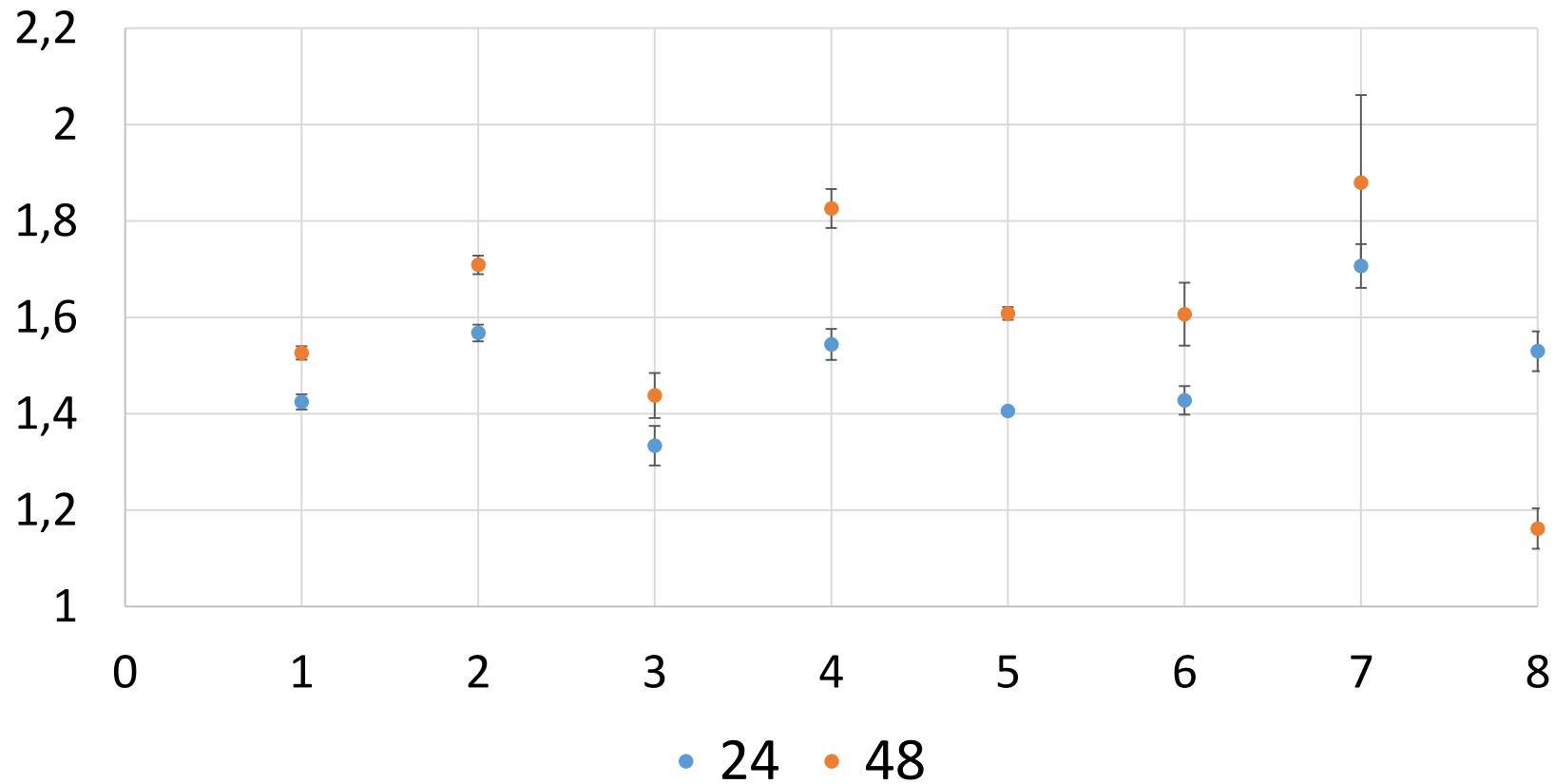


Bacteriology





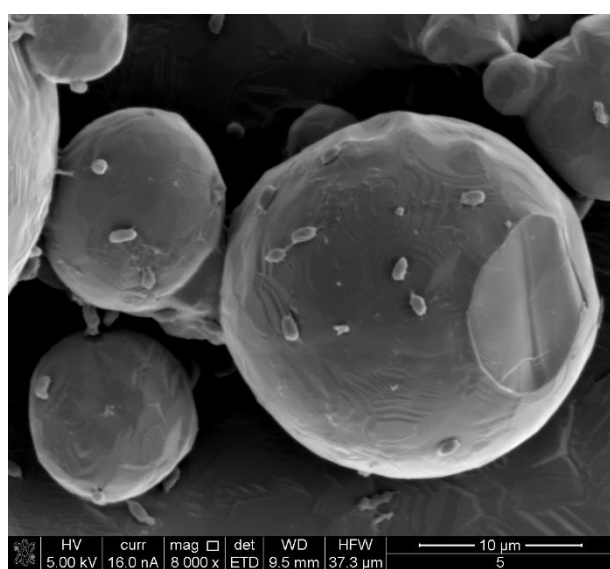
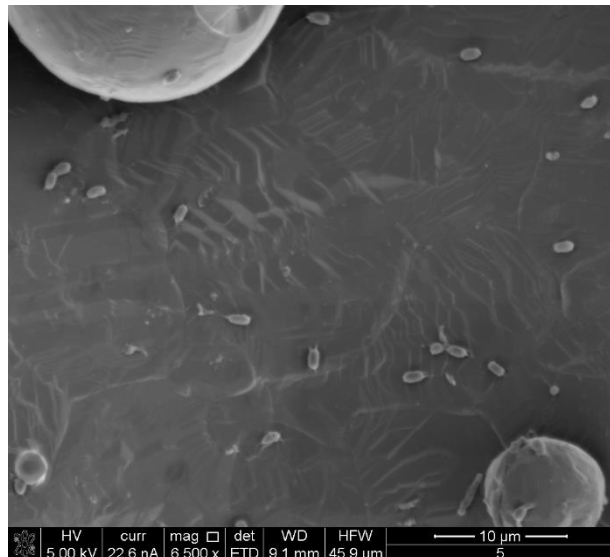
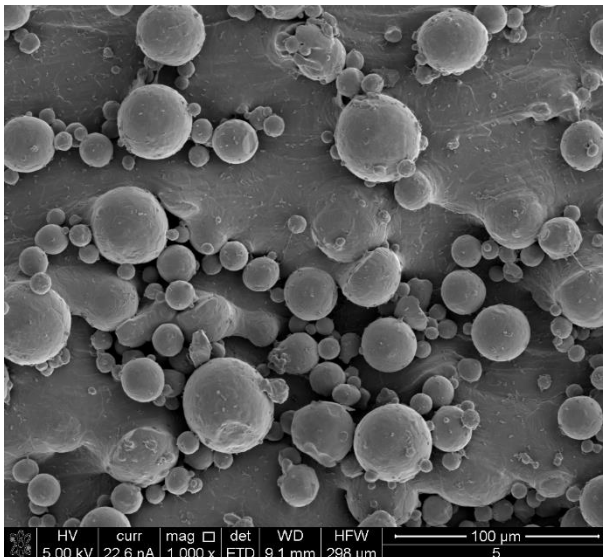
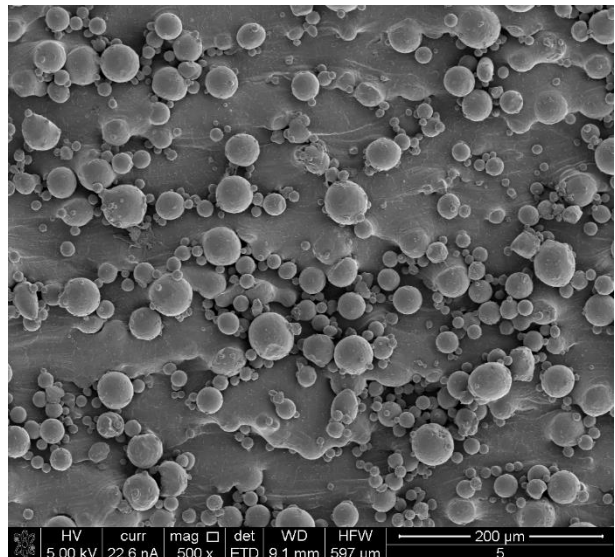
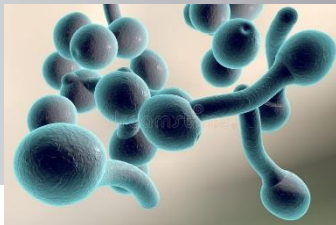
Streptococcus pyogenes

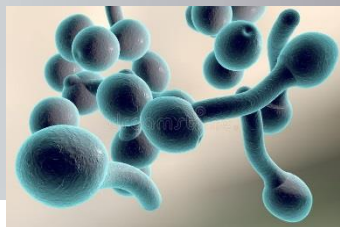
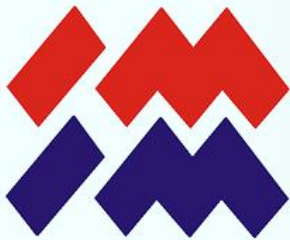




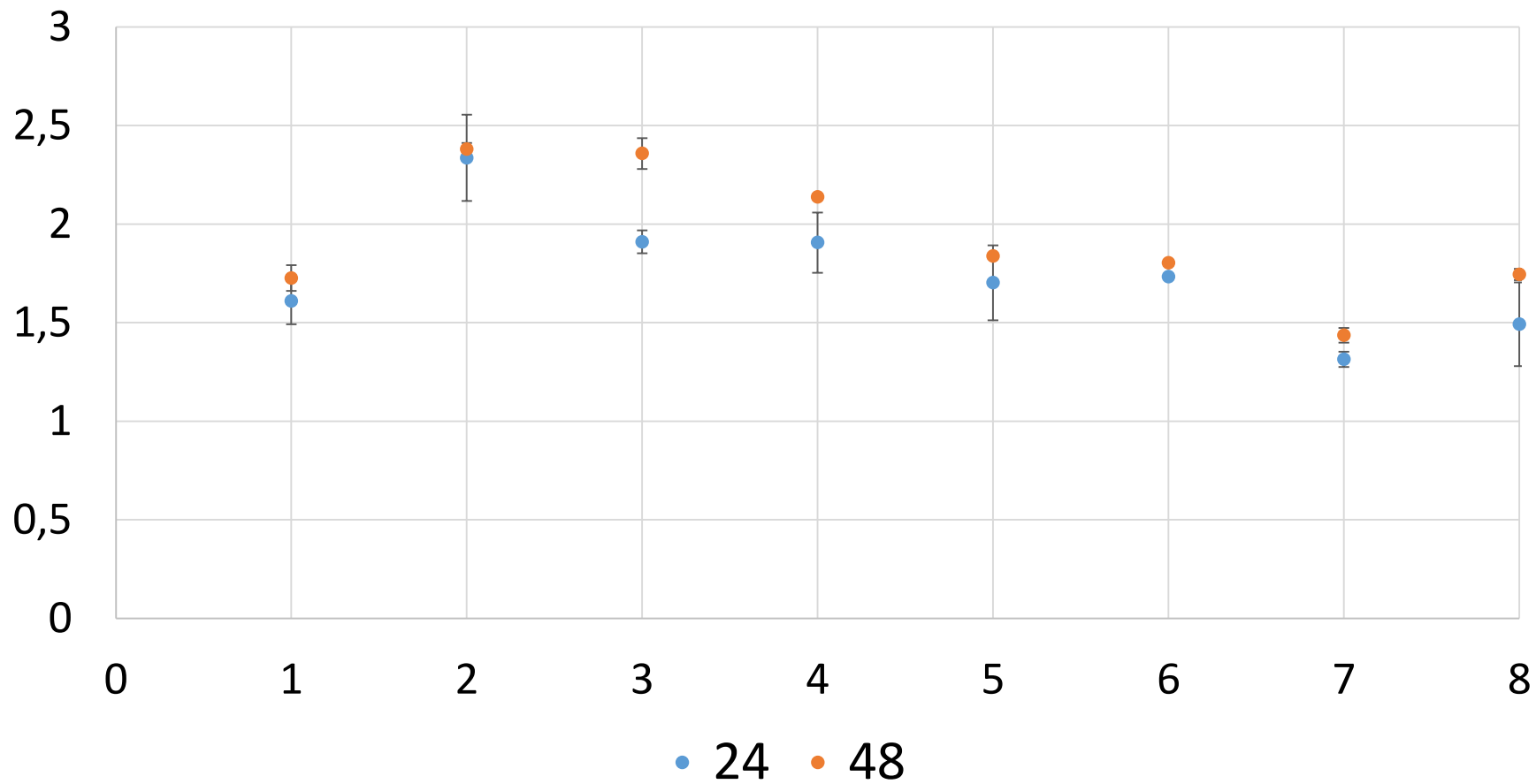
Candida albicans

Bacteriology



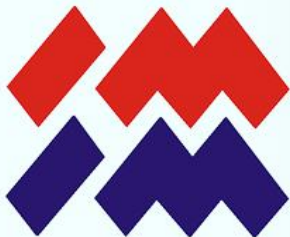


Candida albicans



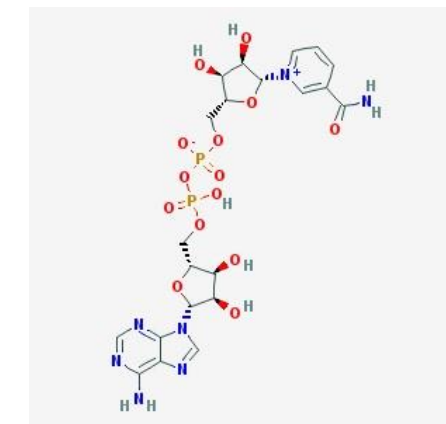
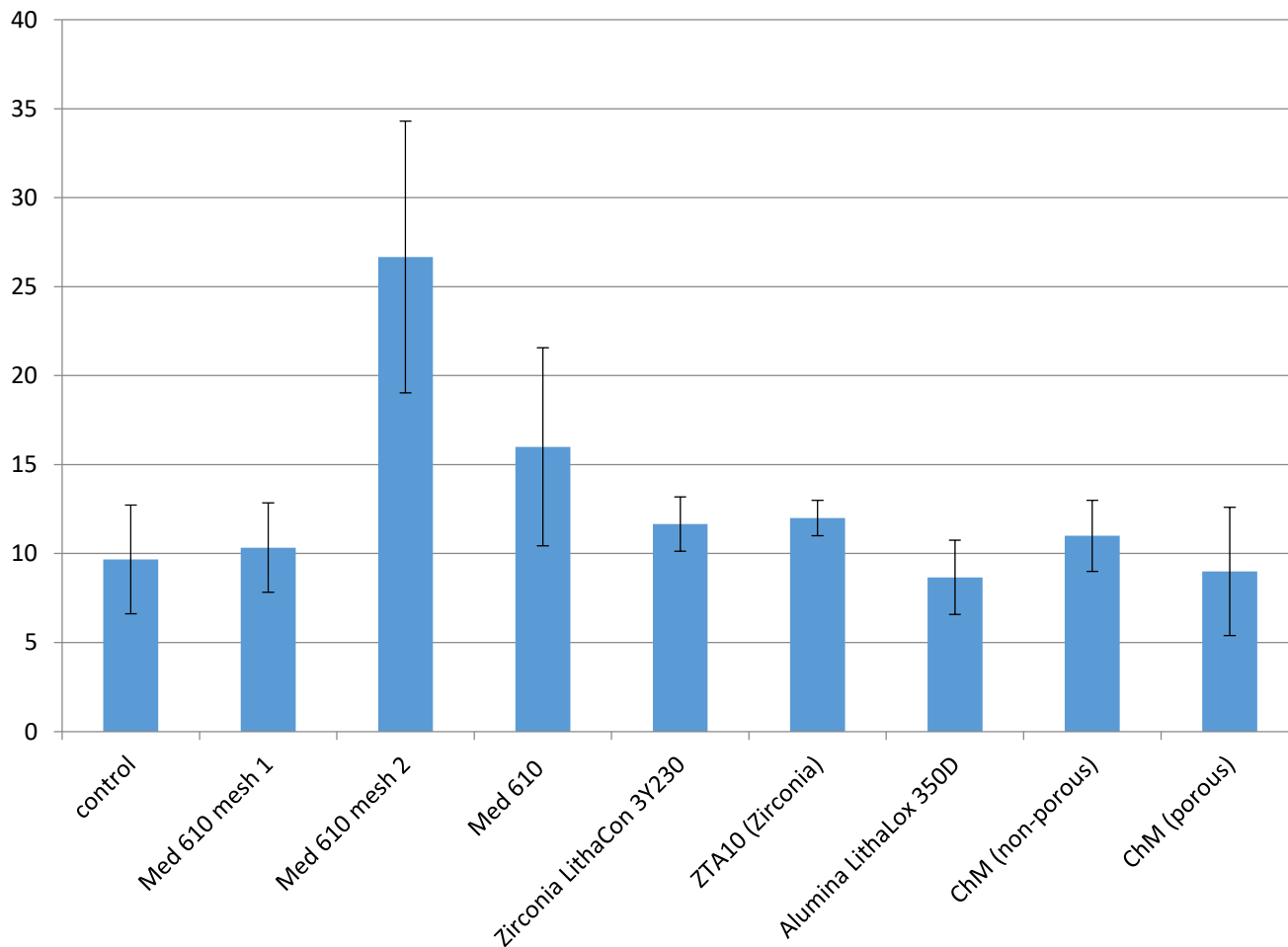


Cytotoxicity



Genotoxicity

Lactate dehydrogenase (LDH): study



Construction of NAD

The basis of LDH test

LACTATE → PYRUVATE

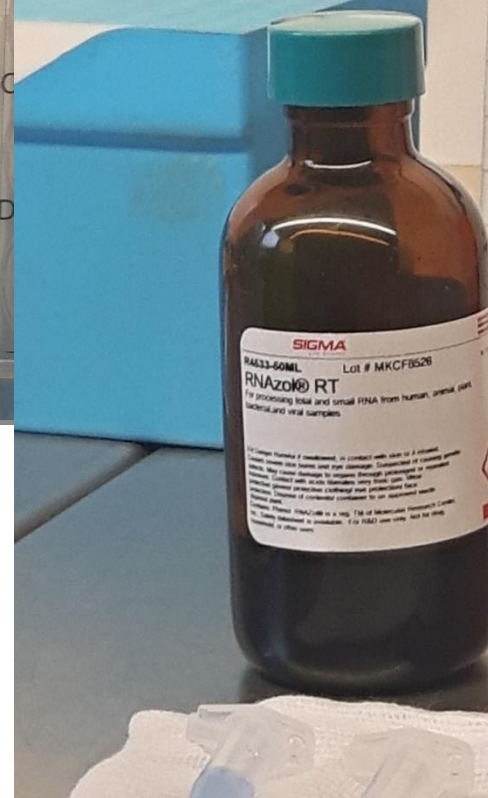
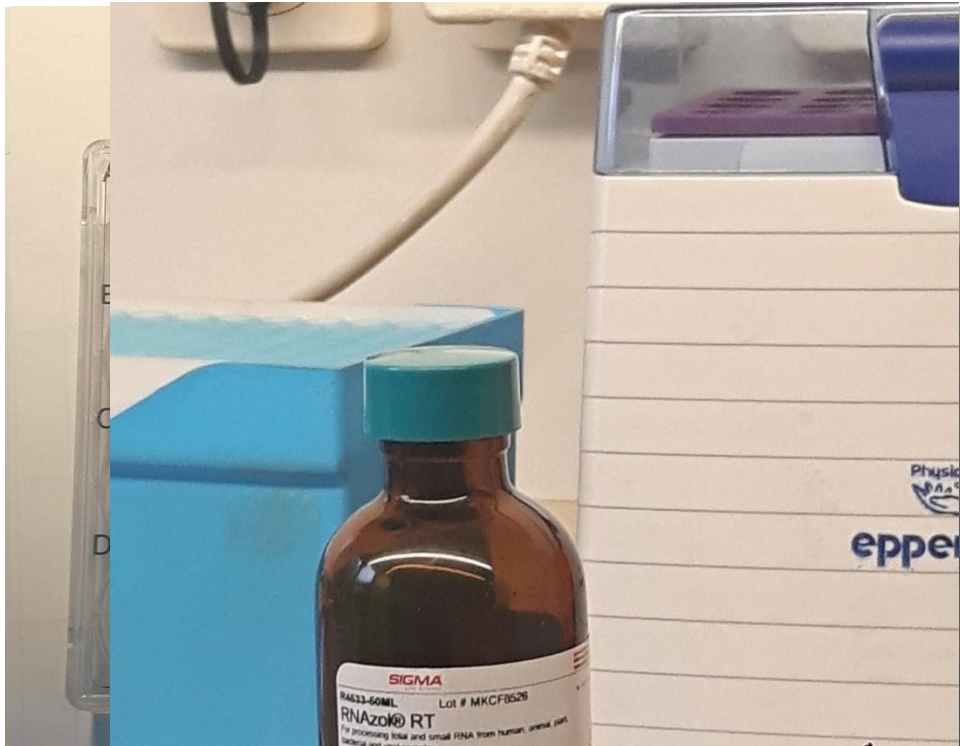
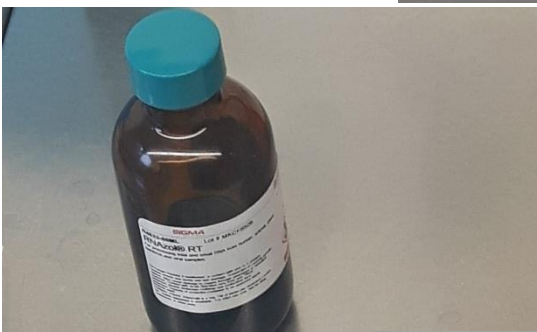
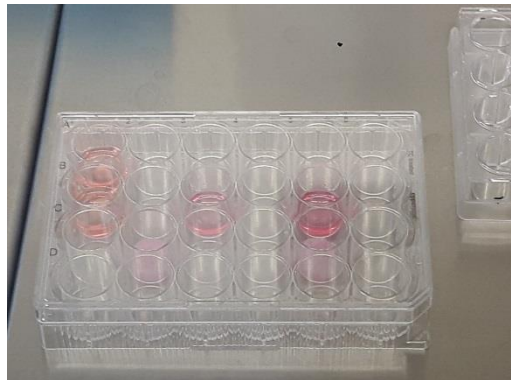
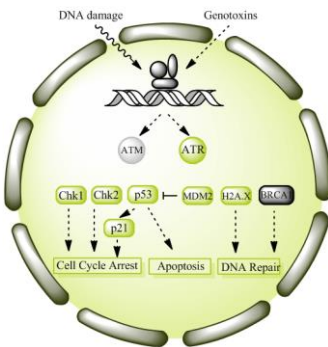
NAD+ → NAPDH+H+

TETRAZOLIN → FORMAZAN

Diaphoresis

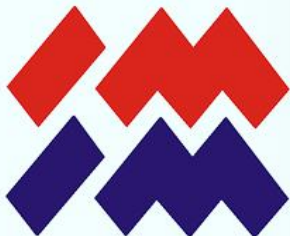


Genotoxicity





Genotoxicity

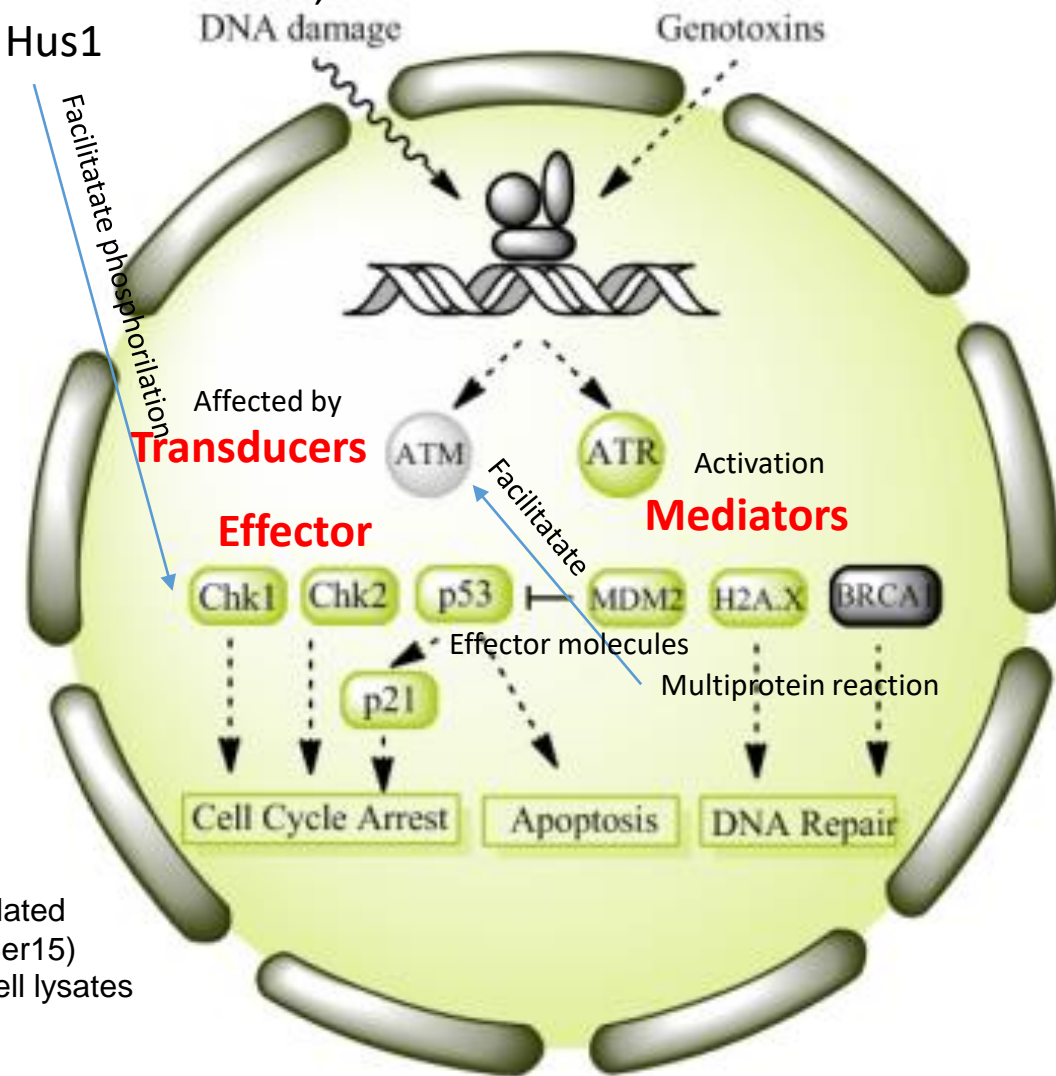


Genotoxicity

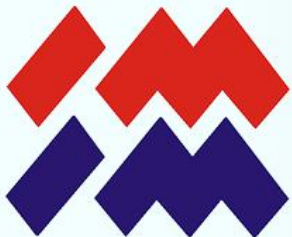
Sensor proteins like Rad9,
Rad1 and Hus1

Traditional genotoxicity

assays detect gain or loss of function mutations, but provide little or no mechanistic data as to how this DNA damage may have occurred. Protein expression and phosphorylation detection of multiple proteins involved in DNA damage or genotoxicity provides a faster and more accurate assessment of the status of the cell for researchers exposing cells to potentially genotoxic compounds or researching DNA damage and repair mechanisms.



The MILLIPLEX® MAP 7-plex DNA Damage/Genotoxicity Magnetic Bead kit is used to detect changes in phosphorylated Chk1 (Ser345), Chk2 (Thr68), H2A.X (Ser139) and p53 (Ser15) as well as total protein levels of ATR, MDM2 and p21 in cell lysates



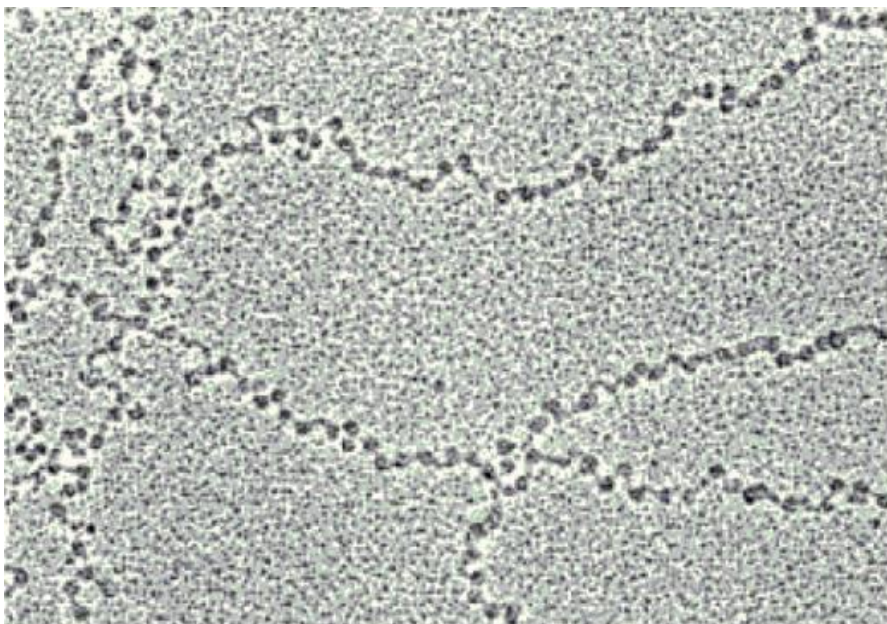
Micronucleus test

Chromatin- DNA complex
with proteins found
in the cell nucleus

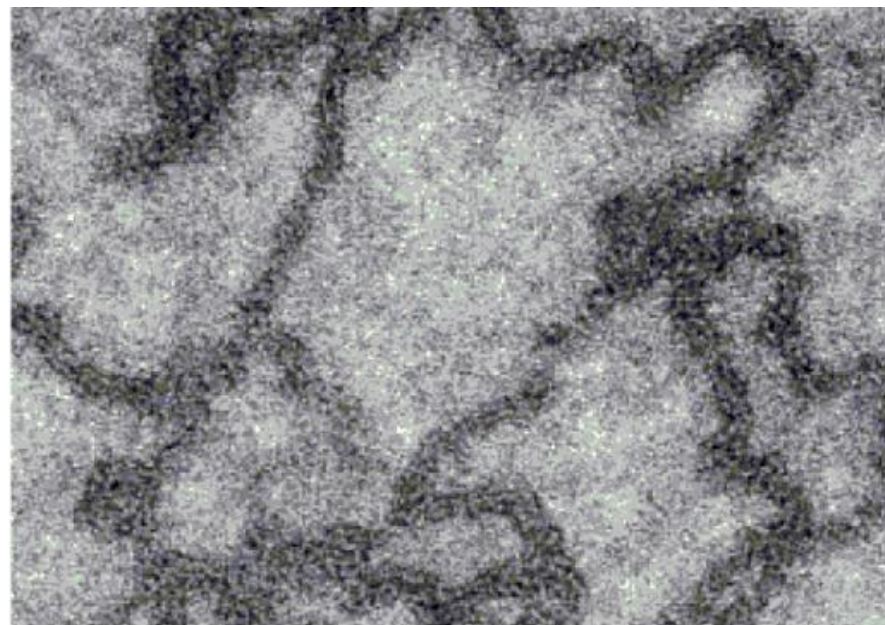


Micronucleus test

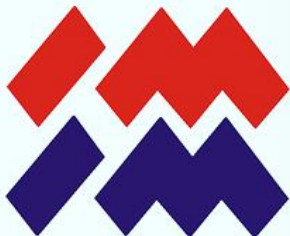
Chromatin occurs in the form of stretched or condensed fibers



struktura „sznura koralików”



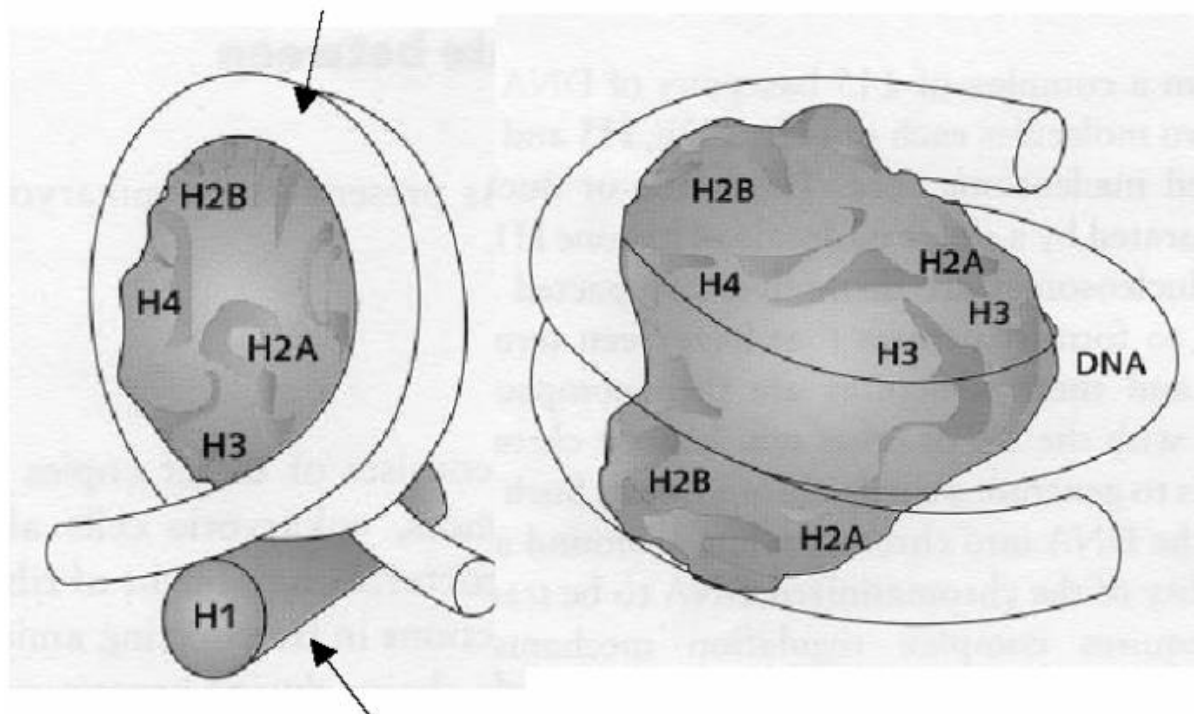
struktura włókna 30 nm



Micronucleus test

„Coral“ chromatin structure (OKTAMER)

146bp DNA



Linker histone

Compaction

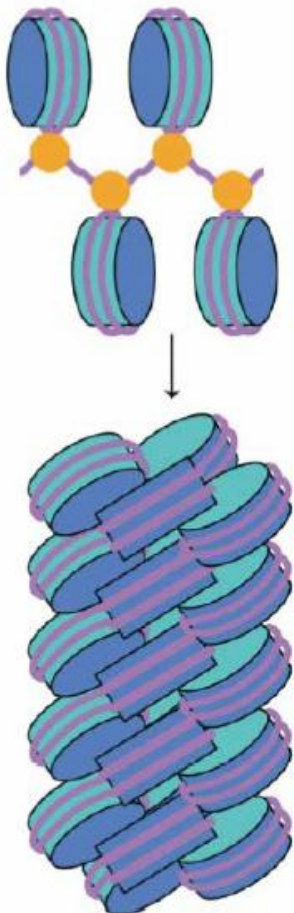
* 10 nm → 30 nm

Histone octamer:
H2A-H2B dimers
 $H3_2$ - $H4_2$ tetramers

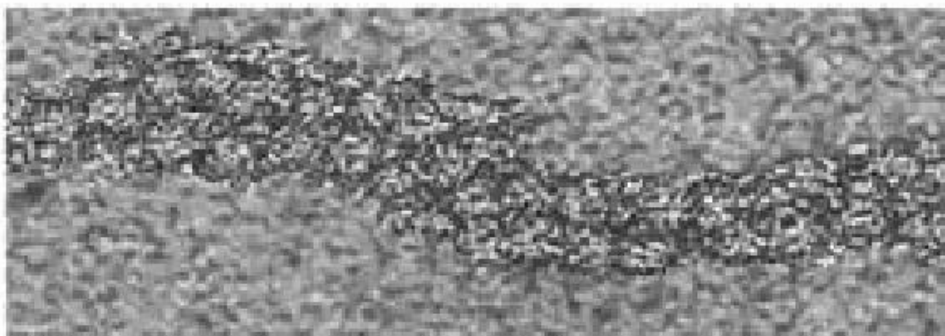
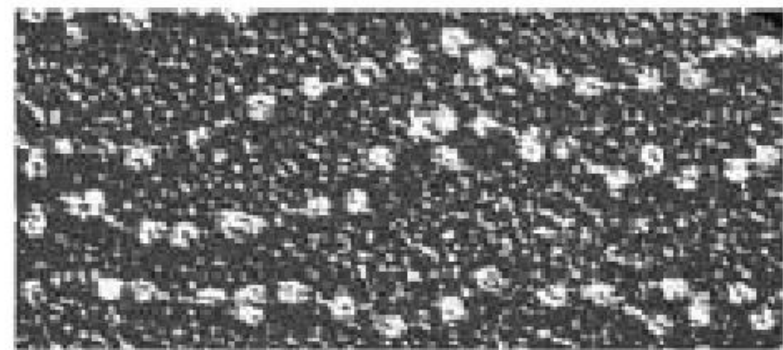
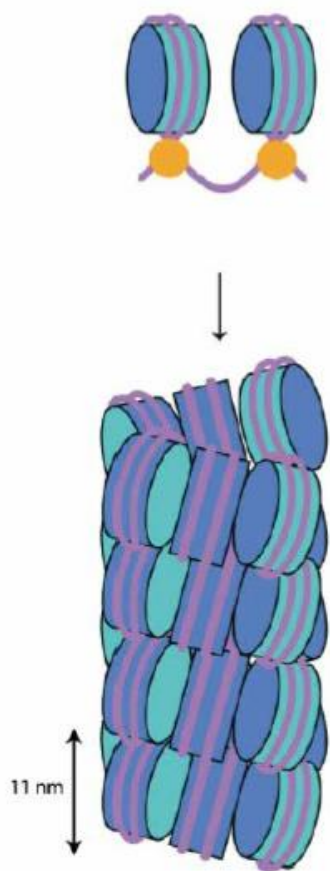


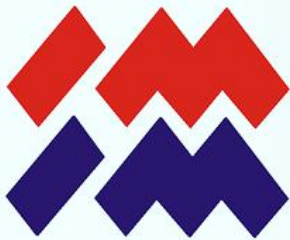
Micronucleus test

A Zigzag



B Solenoid

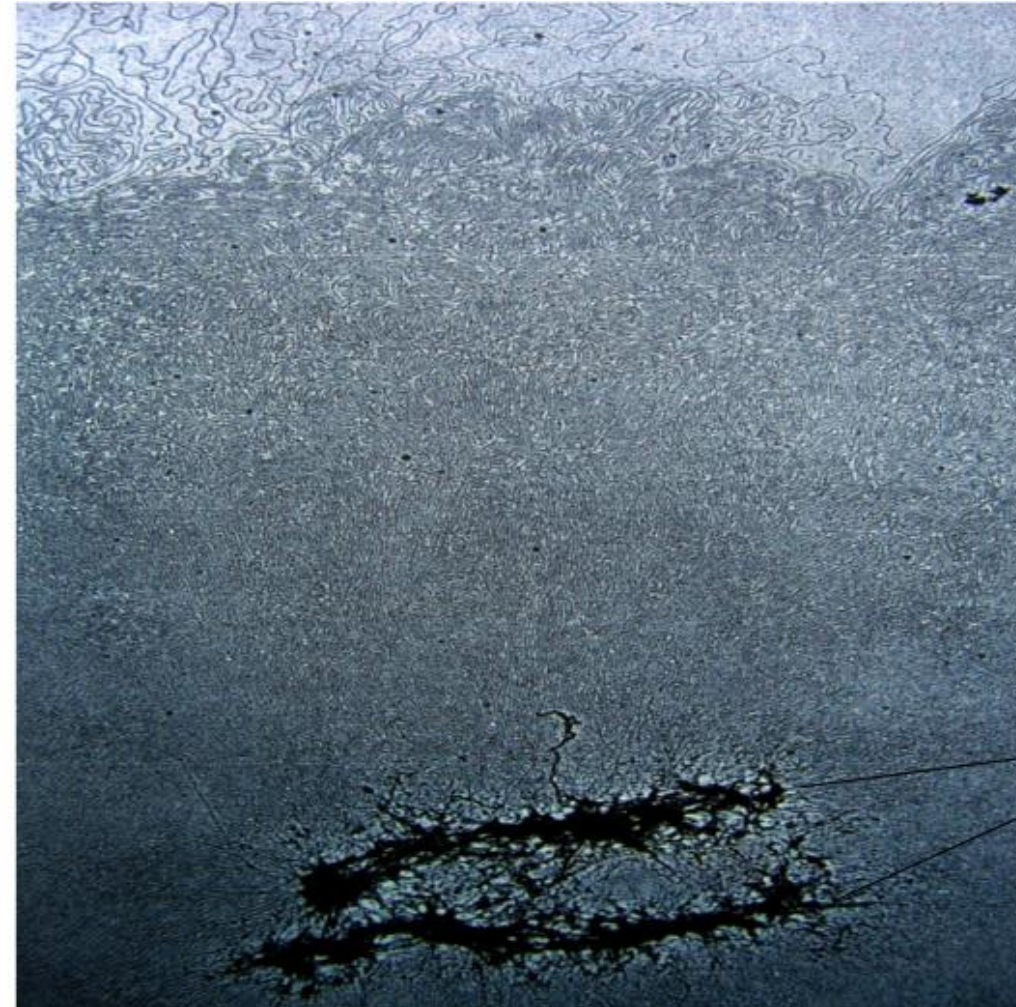




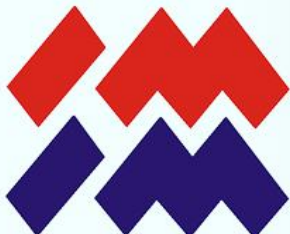
Micronucleus test

Non-histone proteins form a scaffold for long chromatin loops

pętle

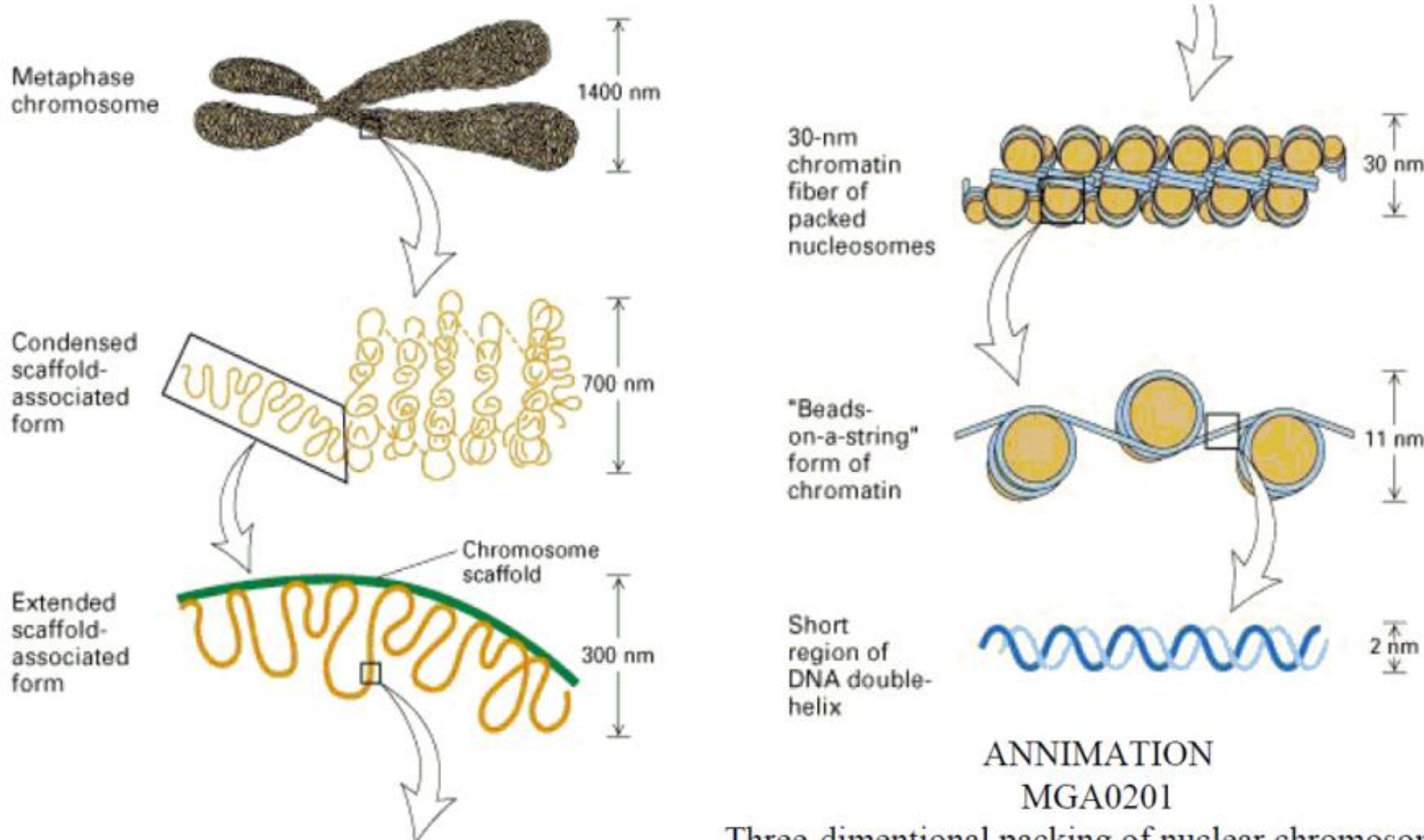


Rusztowanie
białkowe



Micronucleus test

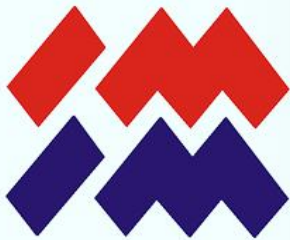
Model of chromatin packing in metaphase chromosomes



ANIMATION
MGA0201

Three-dimentional packing of nuclear chromosomes

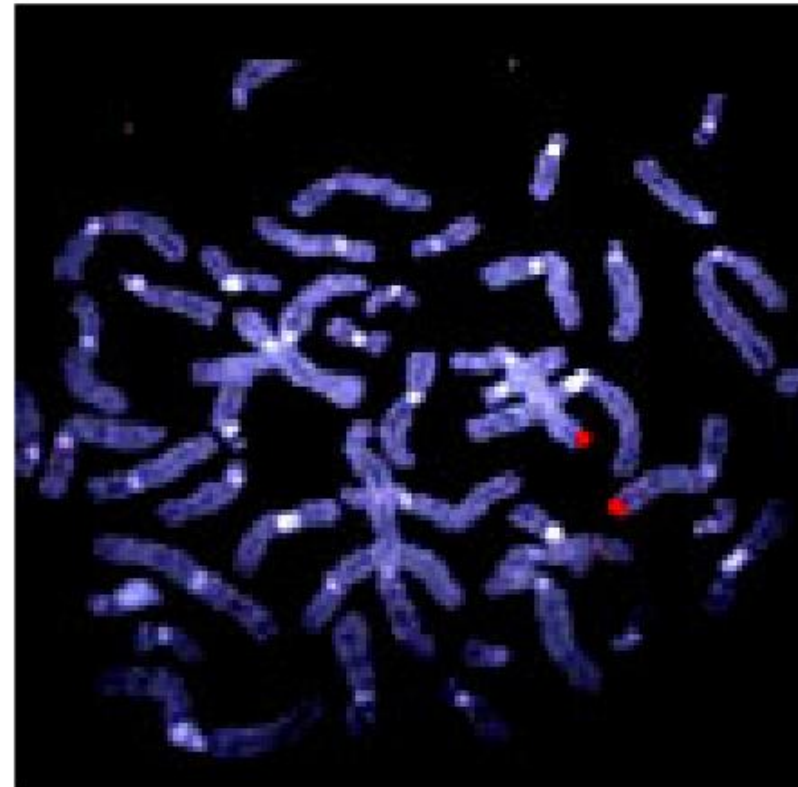
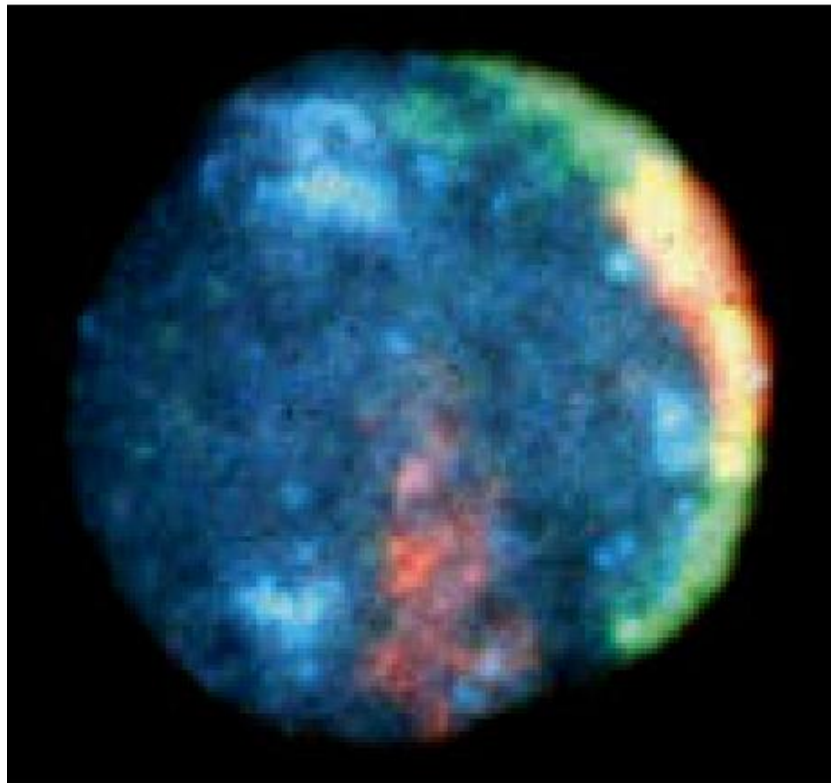
Na skutek upakowania cząsteczki DNA w chromosom mitotyczny jej długość skraca się 50 000 razy.

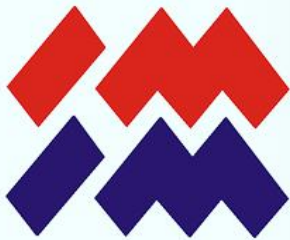


Micronucleus test

The cell nucleus

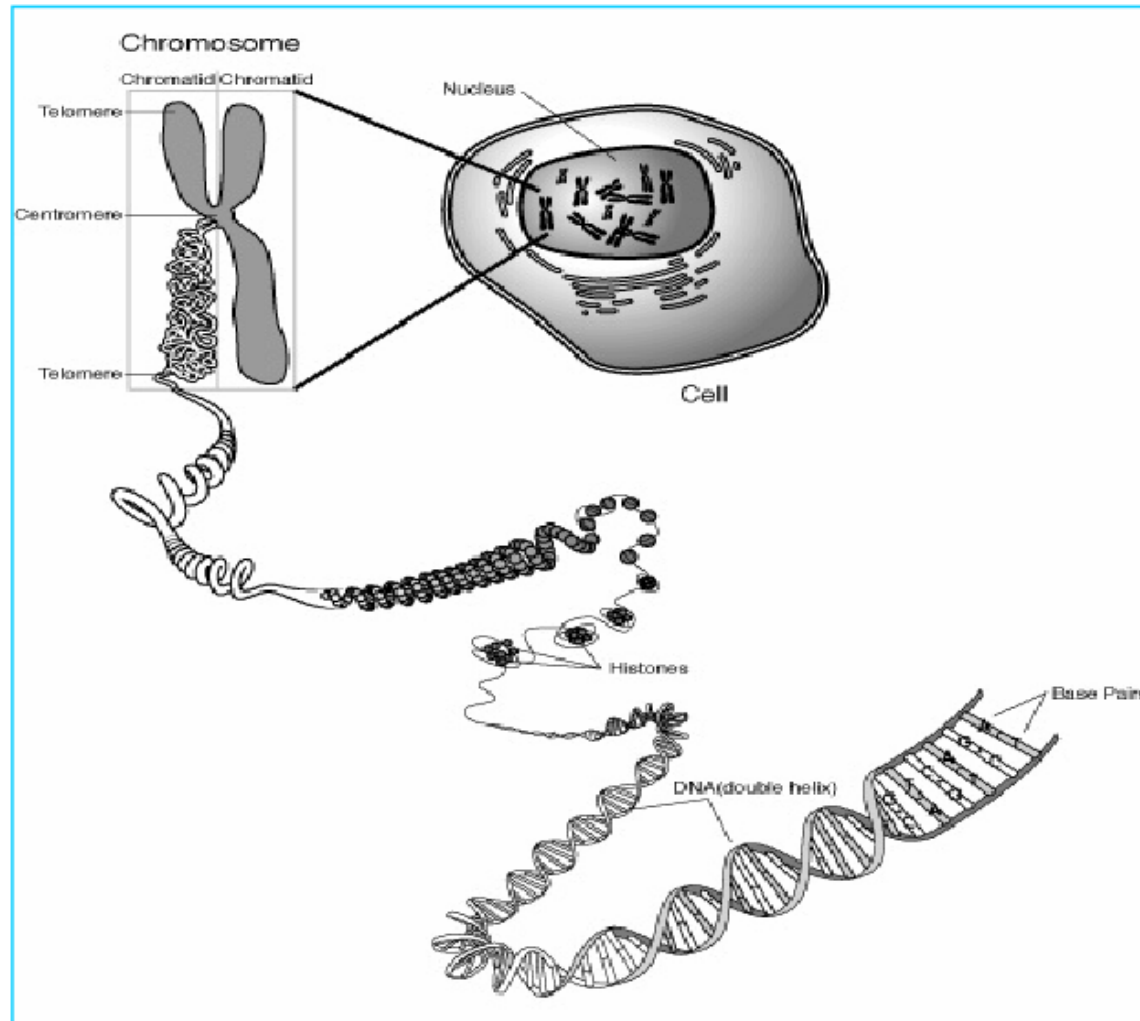
There is a cell nucleus in every human cell. In the cellular nucleus there is genetic information packed into structures called chromosomes





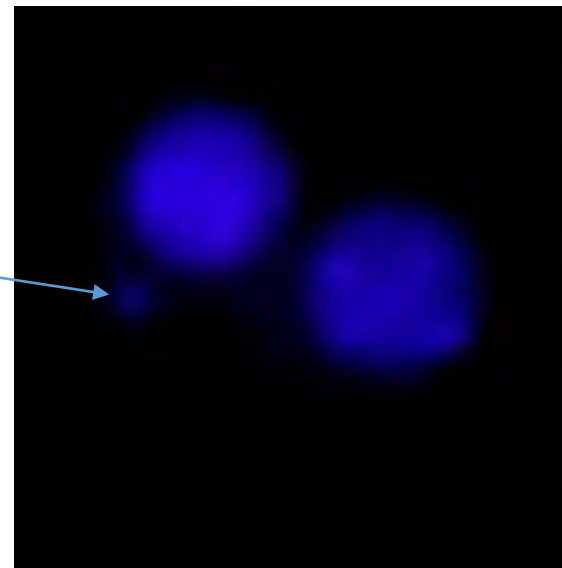
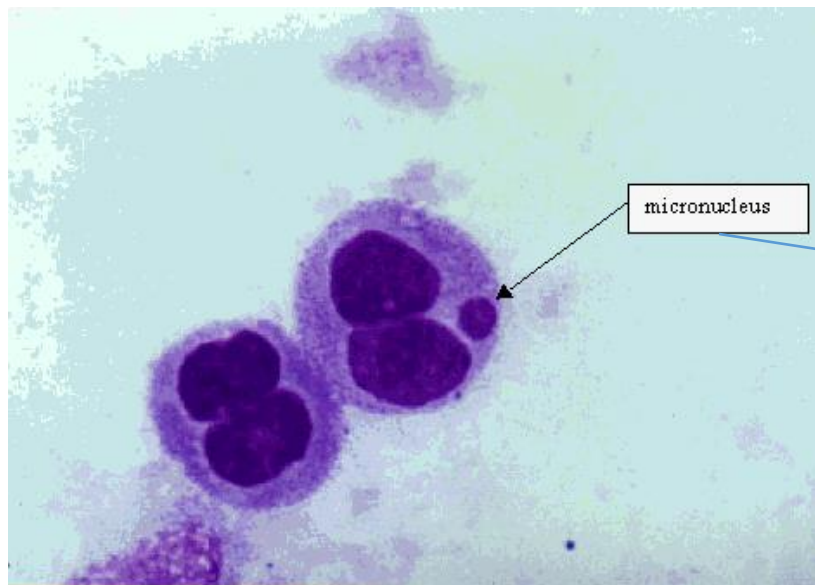
Micronucleus test

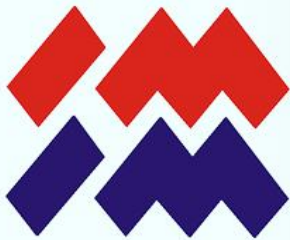
DNA in a eukaryotic cell





Micronucleus test





Micronucleus test

Chromatin- ordered complex of DNA and chromosomal proteins

Metaphase chromosome

- the highest level of chromatin packing
- formed only during cell divisions

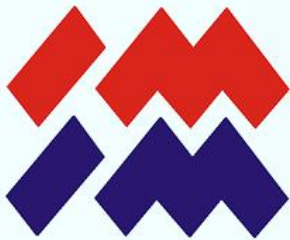
After cell division

disappear metaphase chromosomes - interphase chromosomes
the packing level is reduced
chromatin appears in the form of euchromatin and heterochromatin



Research protocole

- Chromosome damage test - micronucleus test
- Evaluation of the expression of selected genes associated with activation of the genotoxicity / DNA damage pathway
- The determinations will be made in an in vitro model using test substrates provided by the contracting authority and two cell lines: with the use of human osteoblasts and osteoblast-like tumor cells - SaOS-2.
- The assessment of the potential genotoxicity of the tested substrates will be based on the analysis of the expression of selected genes associated with the genotoxicity / DNA damage pathway. The proposed panel includes the following genes: ATR, MDM2, TP53, PPIA, ATM, CHEK1, CHEK2, and CDKN1A. Evaluation of the expression of selected genes will be made using the Real-time PCR method using molecular probes of the TaqMan type.



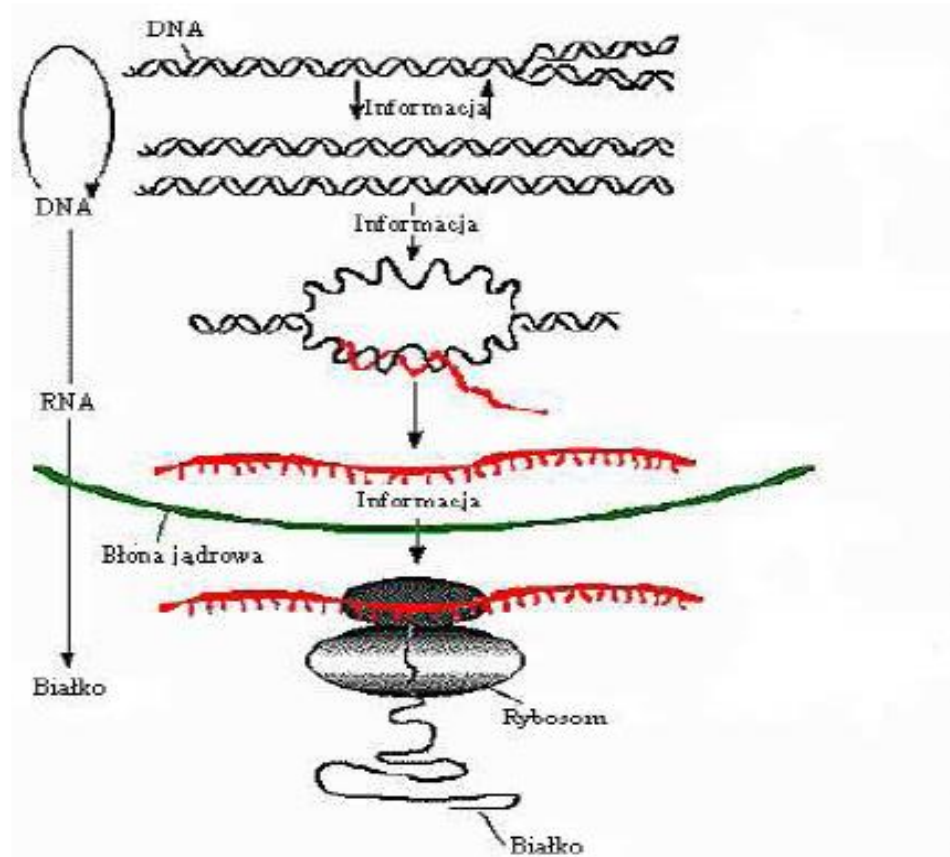
Genotoxicity

Dogma of molecular biology

Replication

Transcription

Translation

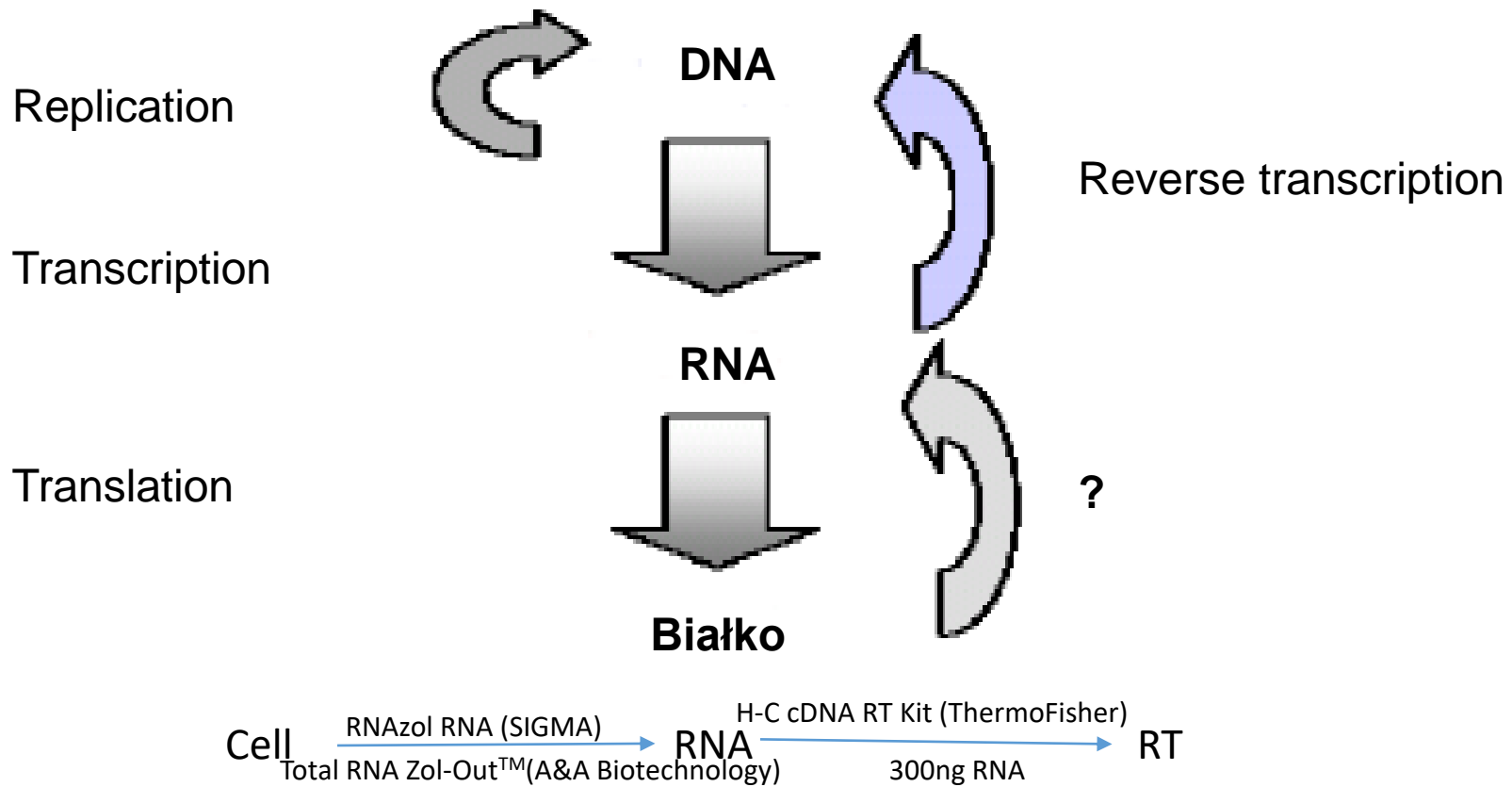


**The flow of genetic information takes place in the direction of
DNA -> RNA-> protein**

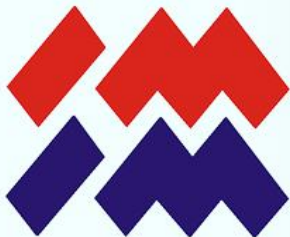


Genotoxicity

Upgrade of the molecular biology dogma



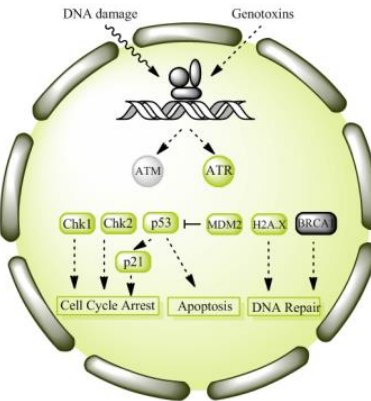
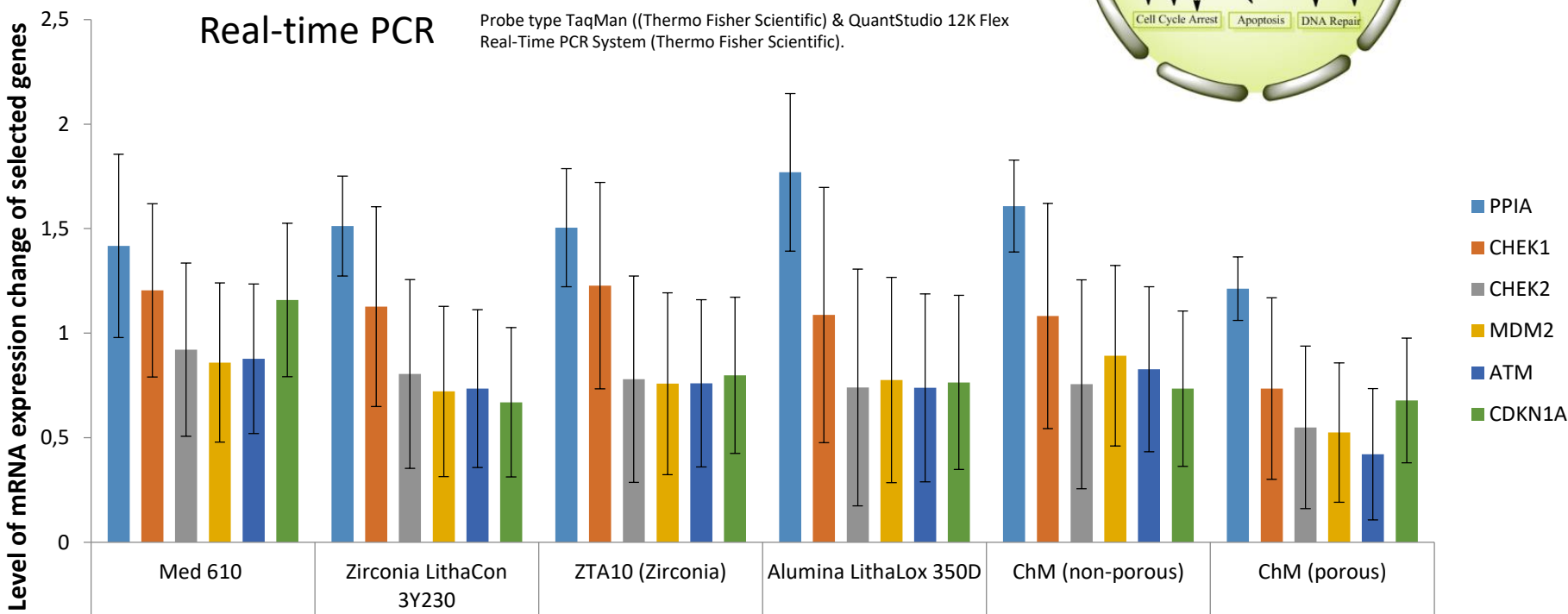
The flow of genetic information takes place in the direction of nucleic acid -> protein

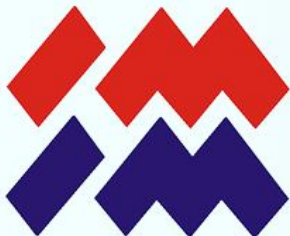


Genotoxicity

Expression of the selected genes evaluation involved in the genotoxic stress pathway

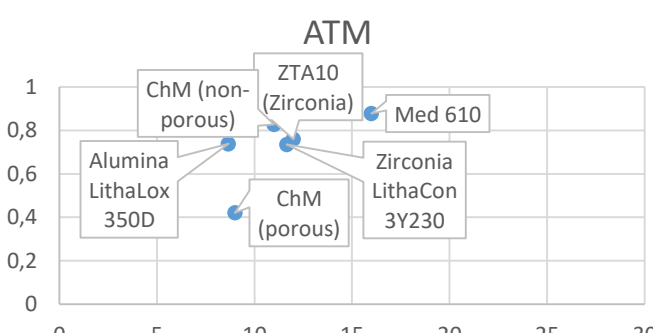
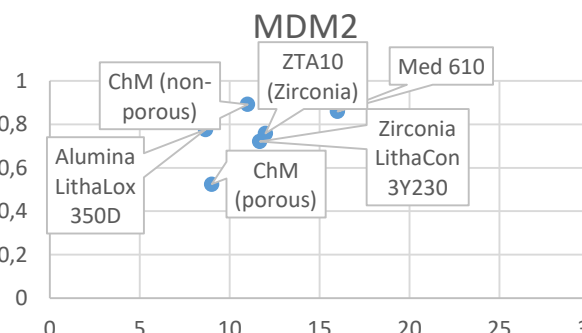
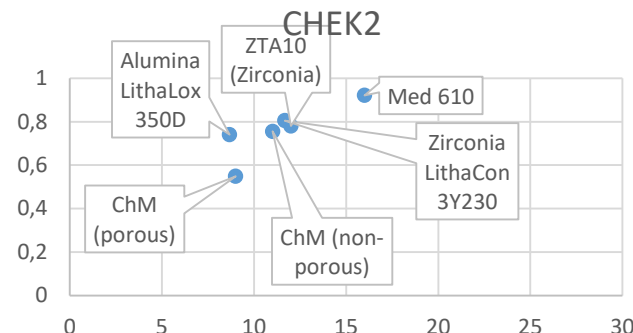
FOCAL CHANGE



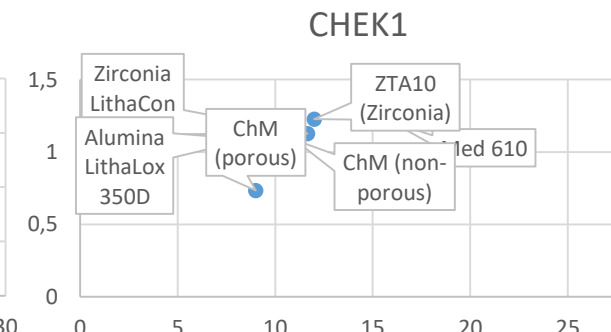
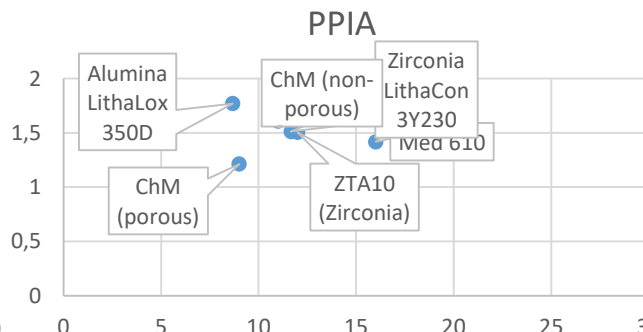
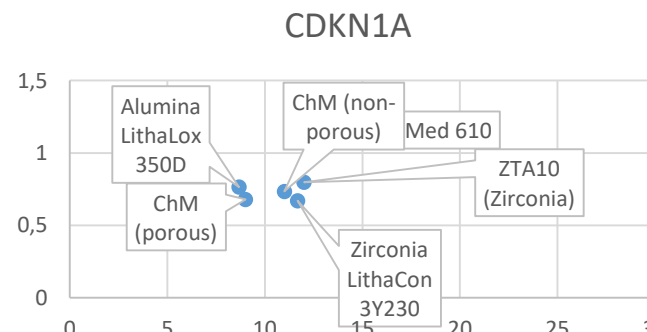


Genotoxicity

Expression of the selected genes evaluation involved in the genotoxic stress pathway



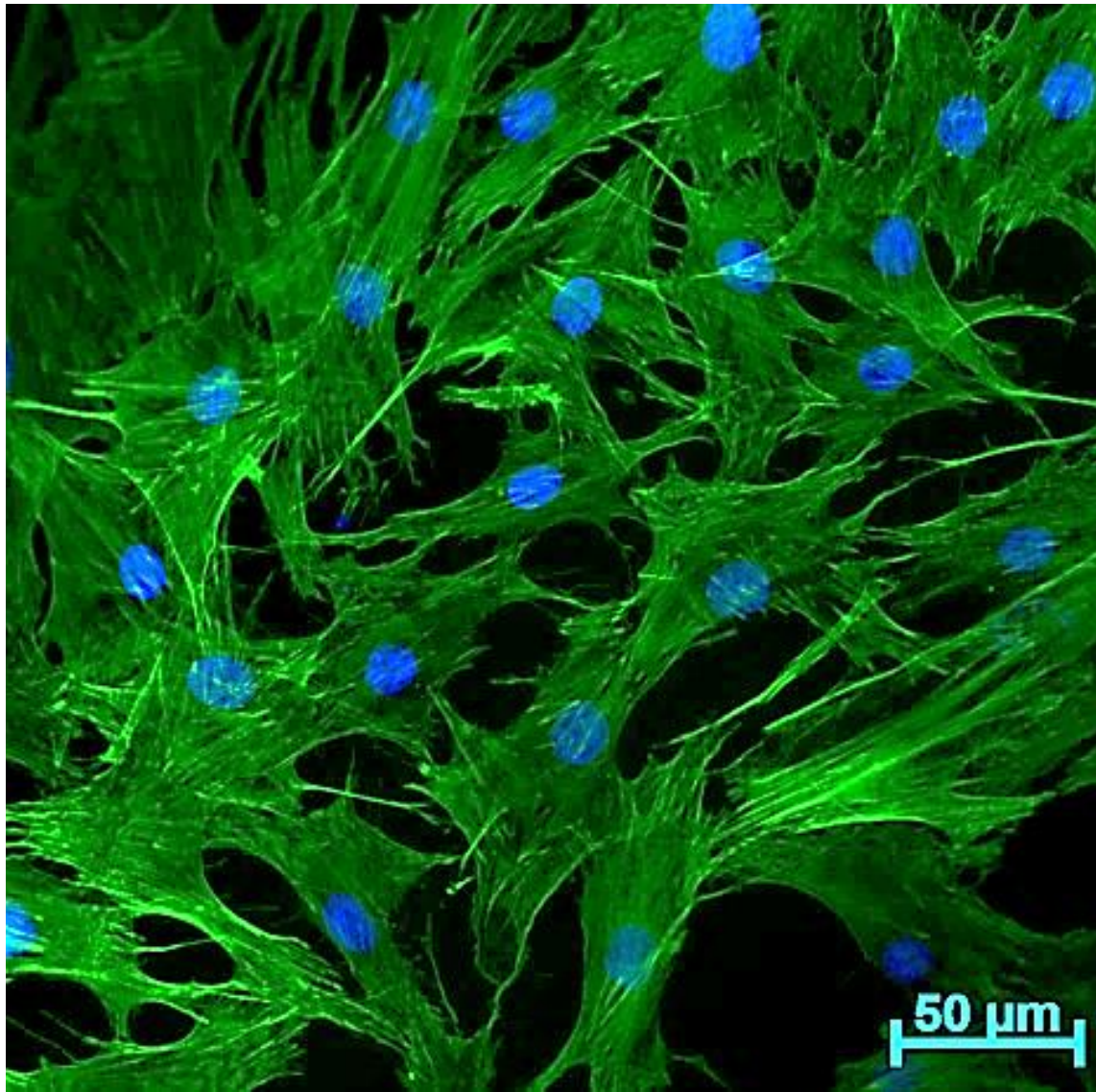
Lactate dehydrogenase (LDH)

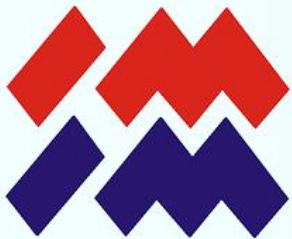


Lactate dehydrogenase (LDH)



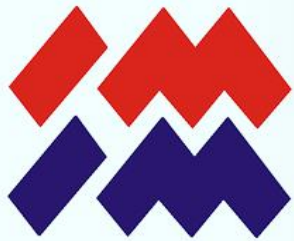
Cell-material interaction



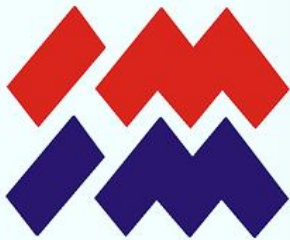


Printed implant prototype





Initial results of the drug release from the surface modified capsules

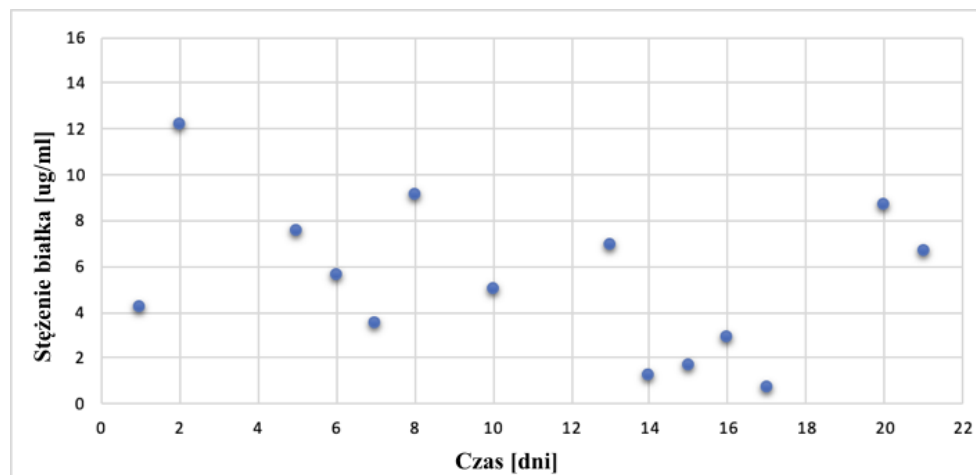


On going futher steps

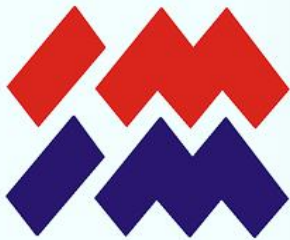
First attempts to release protein from microcapsules (membrane method) - UV-VIS

- The first attempts to load proteins into microparticles were made. Albumin was added to the aqueous solution, which is also a non-solvent for the polymer used. The amount of released protein was measured using the BCA test (Bicinchoninic Acid Kit, Sigma-Aldrich)

The amount of protein released from PLA microparticles within 21 days (the amount of protein released was measured every two days, each point corresponds to the protein released over these two days).



The albumin concentration in the experiment changed irregularly. During incubation the pH of the solution was constant and was 7.39. There was no apparent dependence showing the kinetics of protein release over time, so this technique was considered unsuitable. For this reason, the first attempts were made to load the protein into microparticles using the Schiff base - through a covalent bond.



Acknowlegement

The work is supported by the project M-ERA.NET-2016/232/2017 “jawIMPLANT” financed by National Center of Science and Development



M-ERA.NET Transnational Call 2016

Project Acronym:

jawMPLANT

Project Coordinator:

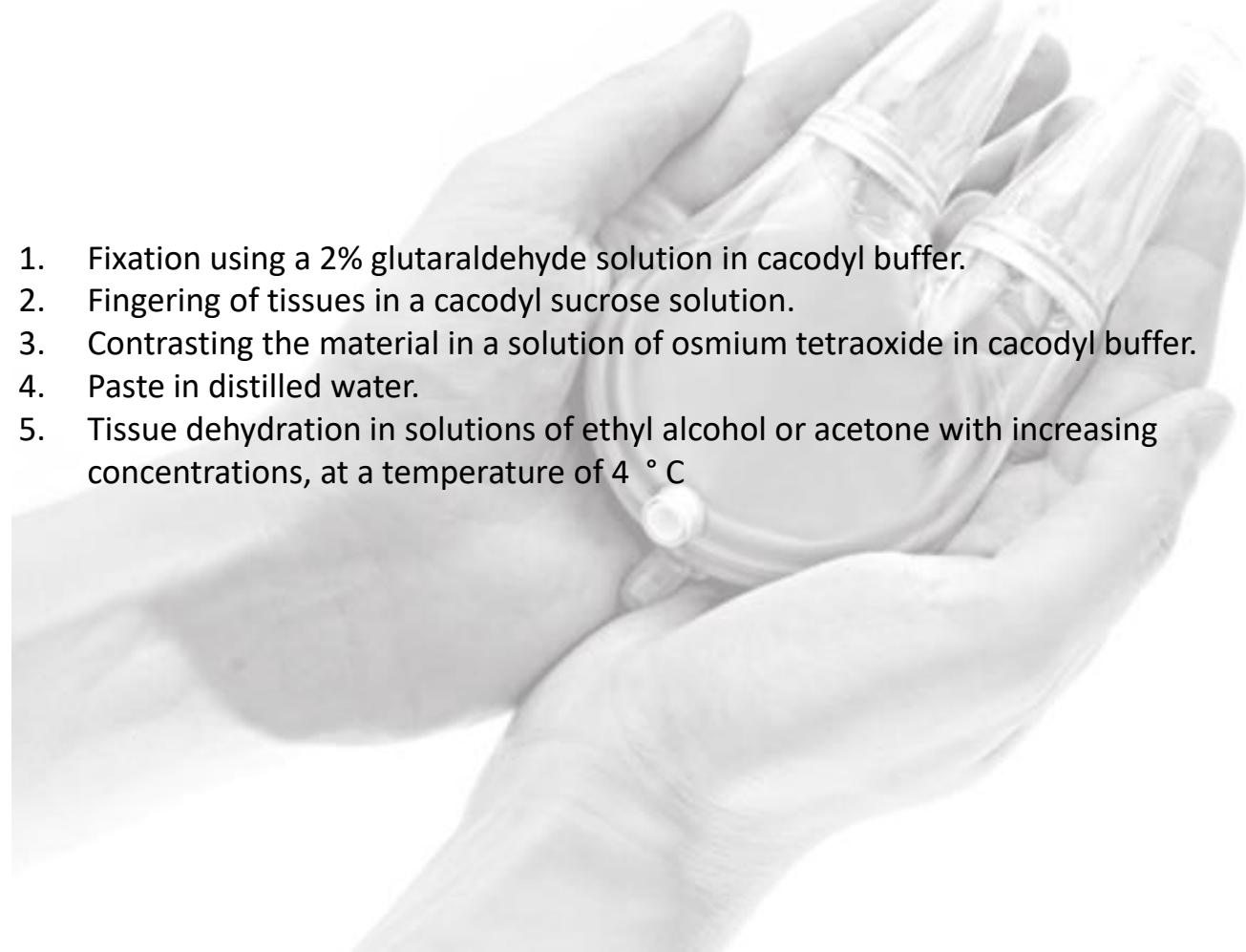
(Organisation and country):

***JOANNEUM RESEARCH Forschungsges.m.b.H., Institute
for Surface Technologies and Photonics***



Protocol

Development of a protocol for the preparation of thin films for tissue testing using the transmission electron microscopy technique

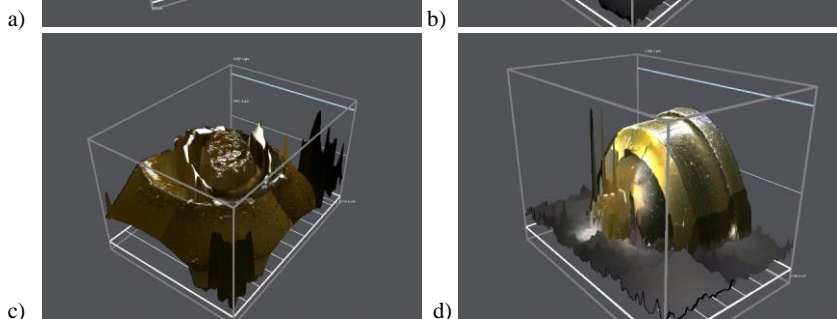
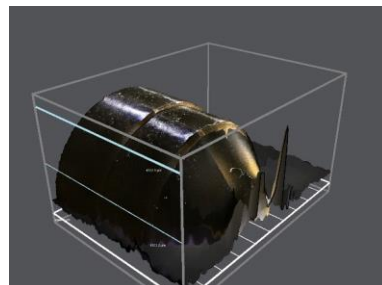
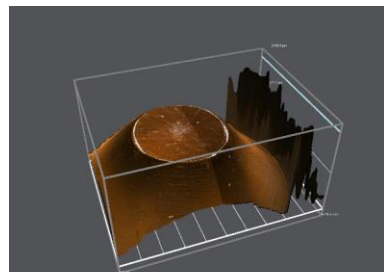
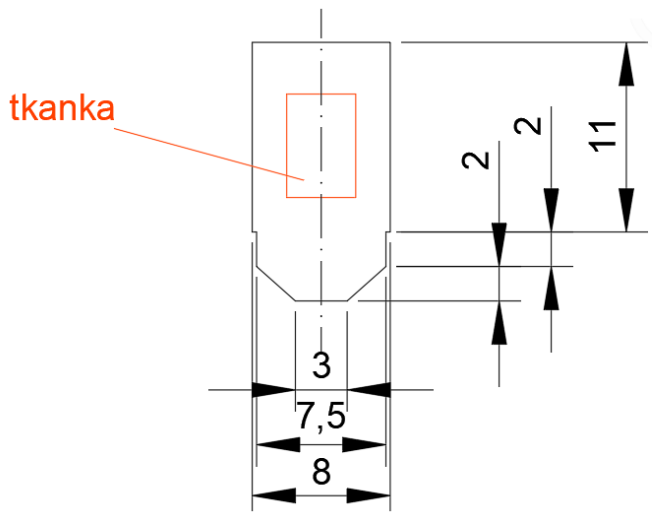


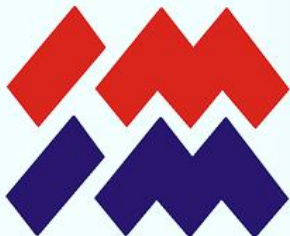
1. Fixation using a 2% glutaraldehyde solution in cacodyl buffer.
2. Fingering of tissues in a cacodyl sucrose solution.
3. Contrasting the material in a solution of osmium tetroxide in cacodyl buffer.
4. Paste in distilled water.
5. Tissue dehydration in solutions of ethyl alcohol or acetone with increasing concentrations, at a temperature of 4 °C

1. Utrwalenie przy użyciu 2-procentowego roztworu aldehydu glutarowego w buforze kakodylowym.
2. Płukanie tkanki w roztworze sacharozy w kakodylowym.
3. Kontrastowanie materiału w roztworze czterotlenku osmu w buforze kakodylowym.
4. Płukanie w wodzie destylowanej.
5. Odwadnianie tkanki w roztworach alkoholu etylowego lub acetonu o wzrastających stężeniach, w temperaturze 4 °C



Protocol





Optimal Positioning of the Optical Head

The Eucentric Movement of the Leica EM UC7 viewing system allows examination of sections, even with a lowered water level e.g. for Lowycryls and dry sections.

The patented defined position marks of the eucentric movement provide maximum approach accuracy either for glass or diamond knife approach.

For accurate approach of the knife towards the specimen with the backlight, the viewing angle must be set according to the type of knife in use.



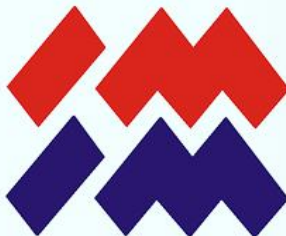
Section observation with lowered water level without eucentrically moveable stereomicroscope.



Section observation with lowered water level with eucentrically moveable stereomicroscope.



Diamond knife approach as seen through the Leica M80 stereomicroscope with backlight illumination.



Advanced Features

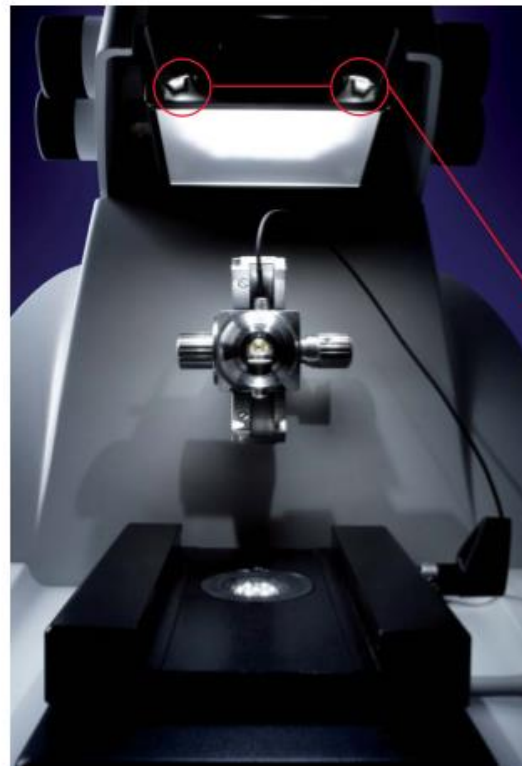
Motorized knife stage

Motorized North-South movement of the knife stage is a unique feature of Leica ultramicrotomes. The additional implementation of motorized East-West movement of the Leica EM UC6 was a logical step forward. Additionally, the E-W quick adjustment buttons on the Leica UC7 controller allow efficient traversing of the knife.

Motorization of the stage has also allowed many useful features to develop hand in hand with it, for example the patented Autotrim mode, E-W measuring function and the automatic approach of the selected knife segment (patent applied).

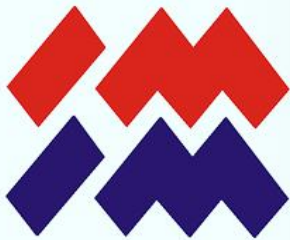
Brightness-controlled LED illumination

LED light sources provide outstanding illumination for top light, back-light, and transmitted illumination. All illumination modes are independently brightness-controlled for the best visual clarity. The additional spot illumination enhances the optical performance of the Leica EM UC7 and provides superior visibility while cleaning the knife edge or trimming the block face, for example.



Knife edge with particles visible under spot light illumination.

Site-specific trimming with spot illumination.



Advanced Cryo-section Collection



Leica EM CRION ionizer and micromanipulator

Especially for frozen hydrated sectioning or the Tokuyasu method, the Leica EM CRION with electrostatic discharge and charge mode used with the micromanipulator provides outstanding cryo sectioning performance.

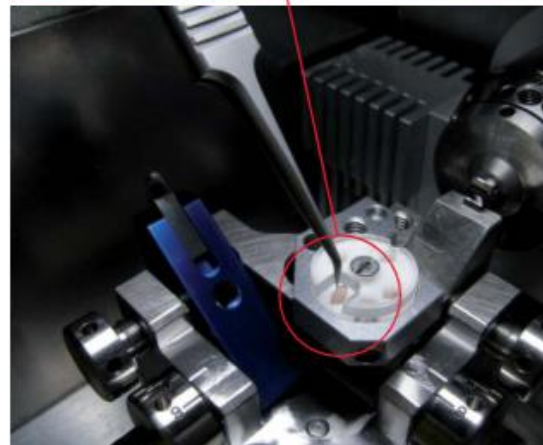
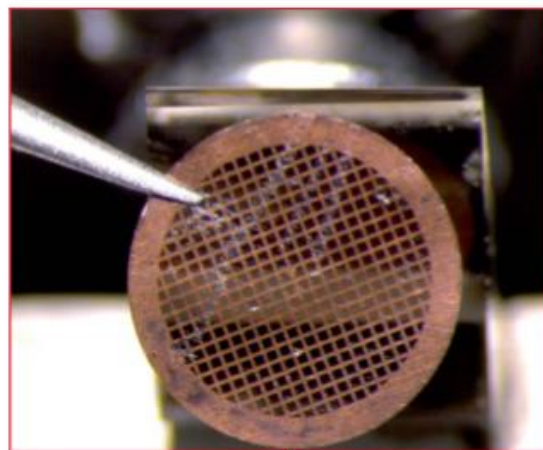
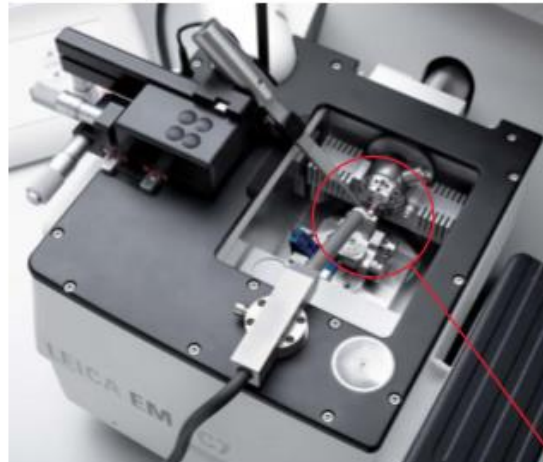
The micromanipulator easily attaches to the Leica EM FC7 cryo chamber, which allows the grid to be exactly positioned close to the knife edge using the micrometer gauges. Once these positions are defined, fast retraction of the grid can be performed manually prior to sectioning to prevent possible influence of the grid on the ionizer. The Leica EM CRION is used in discharge mode in order to reduce electrostatic charging while sectioning.

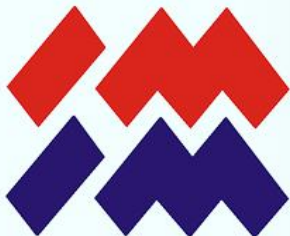
When the section ribbon needs to be placed on the grid, return to the pre-set grid position can be quickly performed. The ribbon is then attached to the grid using the charge mode of the Leica EM CRION, which is operated by a footswitch. Thus, the specimen adheres to the grid without the need for a section press.

As a grid box can be placed near the knife, the micromanipulator can be used to easily place the grid into its storage position.



Protocol

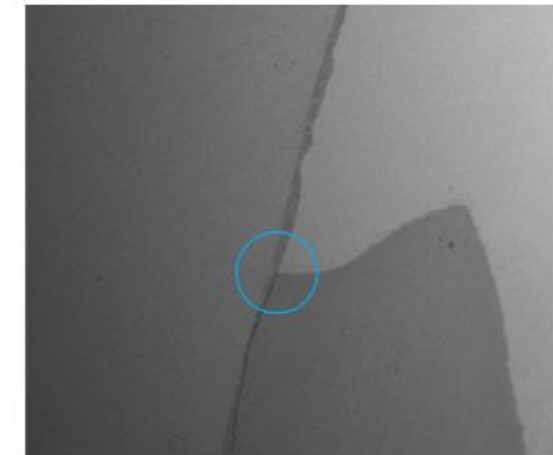




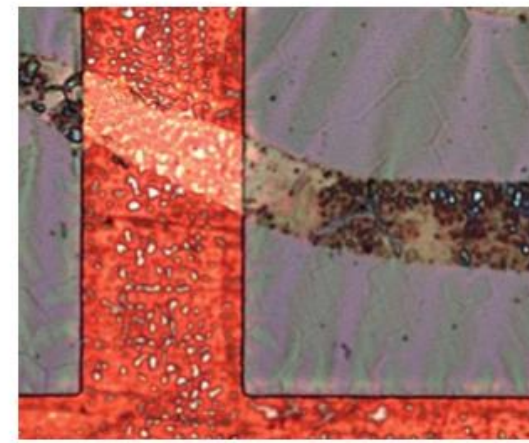
Preparing Specimens for Ultramicrotomy

All specimens need to be prepared prior to sectioning. The size and shape of the specimen have a profound effect on sectioning characteristics. Trimming soft specimens can be performed with the Leica EM TRIM2 or EM RAPID using a milling tool. Alternatively, with the versatile Leica EM TXP, even hard and brittle material can be trimmed using grinding and

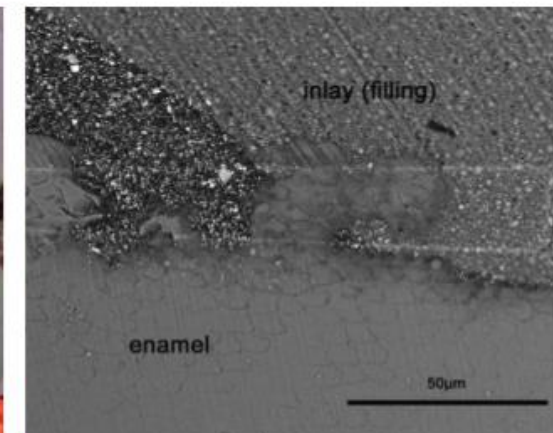
polishing abrasives. The perfectly shaped block face with sharp edges has a considerable influence on the section quality of hard and brittle materials.



Cross section of a tooth with inlay (filling) prepared with the Leica EM TXP (area of interest marked blue).

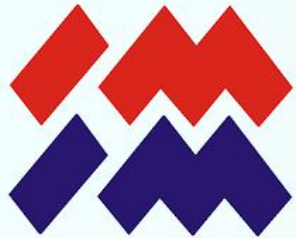


50 nm sections on the grid



Block face after sectioning

	odwadnianie	Szereg alkoholowy (50%,70%,80%,96%,100% x 2)	Czas: 15 minut
1	przepajanie	Tlenek propylenu + żywica (2:1 obj.) Tlenek propylenu + żywica (1:1 obj.) Tlenek propylenu + żywica (1:2 obj.) 100% żywica	Czas: 2 h Czas: 2 h Czas: 3h Czas: overnight
2	odwadnianie	Szereg alkoholowy (50%,70%,80%,96%,100% x 2)	Czas: 30 minut
	przepajanie	Tlenek propylenu + żywica (2:1 obj.) Tlenek propylenu + żywica (1:1 obj.) Tlenek propylenu + żywica (1:2 obj.) 100% żywica	Czas: 2 h Czas: 2 h Czas: 3h Czas: overnight
3	odwadnianie	Szereg acetony (50%,70%,80%,96%,100% x 2)	Czas: 30 minut
	przepajanie	Tlenek propylenu + żywica (2:1 obj.) Tlenek propylenu + żywica (1:1 obj.) Tlenek propylenu + żywica (1:2 obj.) 100% żywica	Czas: 2 h Czas: 2 h Czas: 3 h Czas: overnight
4	odwadnianie	Szereg alkoholowy (30 %, 50%, 60%, 70%, 80%, 90%, 96%, 100% x 2)	Czas: 30 minut
	przepajanie	Tlenek propylenu + żywica (2:1 obj.) Tlenek propylenu + żywica (1:1 obj.) Tlenek propylenu + żywica (1:2 obj.) 100% żywica	Czas: 2 h Czas: 2 h Czas: 4 h Czas: overnight
5	odwadnianie	Szereg alkoholowy (50%,70%,80%,96%,100% x 2)	Czas: 45 minut
	przepajanie	Tlenek propylenu + żywica (2:1 obj.) Tlenek propylenu + żywica (1:1 obj.) Tlenek propylenu + żywica (1:2 obj.) 100% żywica	Czas: 2 h Czas: 2 h Czas: overnight Czas: overnight
6	odwadnianie	Szereg alkoholowy (50%,70%,80%,96%,100% x 2)	Czas: 1 h
	przepajanie	Tlenek propylenu + żywica (2:1 obj.) Tlenek propylenu + żywica (1:1 obj.) Tlenek propylenu + żywica (1:2 obj.) 100% żywica	Czas: 2 h Czas: 2 h Czas: overnight Czas: overnight
7	odwadnianie	Szereg alkoholowy (50%,70%,80%,96%,100% x 2)	Czas: 1 h
	przepajanie	Tlenek propylenu + żywica (2:1 obj.) Tlenek propylenu + żywica (1:1 obj.) Tlenek propylenu + żywica (1:2 obj.) 100% żywica x 2	Czas: 2 h Czas: 2 h Czas: overnight Czas: overnight + 2h
8	odwadnianie	Szereg acetony (50%,70%,80%,96%,100% x 2)	Czas: 1 h
	przepajanie	Tlenek propylenu + żywica (2:1 obj.) Tlenek propylenu + żywica (1:1 obj.) Tlenek propylenu + żywica (1:2 obj.) 100% żywica x 2	Czas: 2 h Czas: 2 h Czas: overnight Czas: overnight + 2h
9	odwadnianie	Szereg alkoholowy (30 %, 50%, 60%, 70%, 80%, 90%, 96%, 100% x 2)	Czas: 1 h
	przepajanie	Tlenek propylenu + żywica (2:1 obj.) Tlenek propylenu + żywica (1:1 obj.) Tlenek propylenu + żywica (1:2 obj.) 100% żywica x 2	Czas: 2 h Czas: overnight Czas: overnight Czas: overnight + 2h



Cellula

„The key to solve the problems with biomaterials one should find in the cell”
E.B. Wilson, (1925)

